Interleukin-1 in brain haemorrhage and ischaemia

A thesis submitted to The University of Manchester for the degree of Doctor of Philosophy in the Faculty of Biology, Medicine and Health

2019

Jack Barrington

School of Medical Sciences

Division of Cardiovascular Sciences

Table of Contents

Word count: 44,405

Table of Figures

Table of Tables

Abbreviations

AIM	Absent in melanoma
AMPA	α-amino-3-hydroxy-5-methyl-4-isoxazole propionic acid
APP	Amyloid precursor protein
ASC	Apoptosis-associated speck-like protein containing a caspase recruitment domain
ATP	Adenosine triphosphate
Aβ	Amyloid-β
BBB	Blood brain barrier
BP	Blood pressure
CAA	Cerebral amyloid angiopathy
CANTOS	Cardiovascular Risk Reduction Study (Reduction in Recurrent Major CV Disease Events)
CARD	Caspase recruitment domain
CBF	Cerebral blood flow
CCA	Common carotid artery
CCL	C-C motif ligand
CG	Cathepsin-G
CNS	Central nervous system
COL4A1	Collagen type IV alpha 1 protein
COX	Cyclooxygenase
CRP	C-reactive protein
CSF	Colony stimulating factor
CT	Computed tomography
CVD	Cerebrovascular disease
CXCL	C-X-C motif ligand
DALYs	Disability-adjusted life years
dMCAO	Distal middle cerebral artery occlusion
ER	Endoplasmic reticulum
GSDM	Gasdermin
Hb	Haemoglobin

HIC	High-income country
HIF	Hypoxia-inducible factor
Hm	Haem
HMGB	High mobility group box protein
Hp	Haptoglobin
HS	Haemorrhagic stroke
IAT	Intrarterial thrombectomy
ICAM	Intercellular adhesion molecule
ICH	Intracerebral haemorrhage
ICP	Intracranial pressure
IFN	Interferon
Ig	Immunoglobulin
IKK	inhibitor of nuclear factor kappa-light-chain-enhancer of activated B cells kinase
IL	Interleukin
IL-1R1	Type 1 interleukin-1 receptor
IL-1RA	Interleukin-1 receptor antagonist
IL-1RAcP	Interleukin-1 receptor accessory protein
IMPROVE	Ischaemia Models: Procedural Refinements Of in Vivo Experiments
IRAK	Interleukin-1 receptor-associated kinase
IS	Ischaemic stroke
JNK	c-Jun N-terminal kinase
LAA	Large artery atherosclerosis
LFA	Lymphocyte function-associated antigen
LMIC	Low- to middle-income country
LPC	Lysophosphatidylcholine
LPS	Lipopolysaccharide
LRR	Leucine rich repeat
MAC-1	Macrophage-1 antigen
MAPK	Mitogen-activated protein kinase
MCA	Middle cerebral artery
MCAO	Middle cerebral artery occlusion
MDM	Monocyte-derived macrophage

MEKKK	Mitogen-activated protein kinase kinase kinase
MLKL	Mixed lineage kinase domain-like
MMP	Matrix metalloproteinase
MyD88	Myeloid differentiation primary response gene 88
NADPH	Nicotinamide adenine dinucleotide phosphate
NE	Neutrophil elastase
NEMO	nuclear factor kappa-light-chain-enhancer of activated B cells essential modulator
NF-κB	nuclear factor kappa-light-chain-enhancer of activated B cells
NHS	National Health Service
NK	Natural killer
NLR	Nucleotide-binding oligomerisation domain -like receptor
NLRC	Nucleotide-binding oligomerisation domain -like receptor containing a caspase recruitment domain
NLRP	Nucleotide-binding oligomerisation domain -like receptor containing a pyrin domain
NMDA	N-methyl-d-aspartic acid
NOD	Nucleotide-binding oligomerisation domain
OxLDL	Oxidised low-density lipids
PAMP	Pathogen associated molecular pattern
PAR	Protease activated receptor
PGE_2	Prostaglandin E_2
PLA_2	Phospholipase A_2
PYD	Pyrin domain
RAGE	Receptor for advanced glycation end products
RBC	Red blood cell
RIPK	Receptor interacting protein kinase
ROS	Reactive oxygen species
SAH	Subarachnoid haemorrhage
SMC	Smooth muscle cell
spSHRs	Spontaneously hypertensive stroke-prone rats
TAB	Transforming growth factor-activated protein kinase-binding protein
TAK	Transforming growth factor-activated protein kinase

TGF	Transforming growth factor
TIR	Toll-interleukin-1 resistance
TLR	Toll-like receptor
TNF	Tumour necrosis factor
TNFR	TNF receptor
TOAST	Trial of Org 10172 in Acute Stroke Treatment
TRAF	Tumour necrosis factor–associated factor
Tregs	Regulatory T cells
TREM	Triggering receptor expressed on myeloid cells
UK	United Kingdom
VCAM	Vascular cell adhesion molecule
VLA	Very late antigen

Abstract

Stroke is a major global health burden with limited therapeutic options. Two major subtypes of stroke exist, ischaemic stroke (IS) and intracerebral haemorrhage (ICH). IS occurs following cerebrovascular occlusion, whereas ICH occurs when a vessel bursts and blood enters parenchymal brain tissue. The acute inflammatory response to both of these subtypes is thought to exacerbate neuronal injury and contribute to poor patient outcomes. The prototypical cytokine interleukin-1 (IL-1) sits at the apex of many inflammatory processes and a substantial amount of preclinical evidence strongly implicates IL-1 in IS pathogenesis. However, despite this, it is currently unclear whether IL-1 contributes to ICH pathophysiology. Thus, the primary aim of this doctoral thesis was to determine the contribution of IL-1 to ICH. Further, the canonical IL-1 family is composed of two distinct proteins, IL-1α and IL-1β, which require proteolytic processing to activate the IL-1 receptor. Therefore, the secondary aim of this doctoral thesis was to further our understanding of the active IL-1 proteolytic processing pathways in IS and ICH. Initial work carried out for this thesis refined the collagenase-induced mouse model of ICH to reduce animal usage and suffering. This refined model was subsequently used to uncover novel dichotomous actions of IL-1 in ICH. Using RNA sequencing, IL-1 was revealed as the major upstream regulator of cerebral inflammation that controlled harmful monocyte trafficking to the haemorrhaged brain. However, inhibition of IL-1 actually worsened neuromotor injury following ICH by preventing an IL-1-dependent increase in cerebral blood flow to the affected hemisphere. IL-1β was the predominant IL-1 molecule produced in ICH, but inhibition of the IL-1β processing enzyme, caspase-1, showed this pathway was not necessary for immune recruitment. Similarly, pharmacological and genetic targeting of the NLRP3 inflammasome, which sits upstream of caspase-1 activation, did not affect inflammation or lesion size in a clot-induced mouse model of IS. Overall this thesis exposes novel actions of IL-1 in ICH. Whilst IL-1 appears to be a major upstream regulator of harmful immune recruitment in both IS and ICH, it may also positively regulate cerebral blood flow in ICH. Therefore, future work should build upon the findings in this thesis and segregate the downstream molecular mechanisms governing IL-1s beneficial and harmful effects, in order to provide novel therapeutic targets for both stroke subtypes.

Declaration

I declare that no portion of the work referred to in the thesis has been submitted in support of an application for another degree or qualification of this or any other university or other institute of learning.

Jack Barrington

26th September 2019

Copyright Statement

I. The author of this thesis (including any appendices and/or schedules to this thesis) owns certain copyright or related rights in it (the "Copyright") and he has given The University of Manchester certain rights to use such Copyright, including for administrative purposes.

II. Copies of this thesis, either in full or in extracts and whether in hard or electronic copy, may be made **only** in accordance with the Copyright, Designs and Patents Act 1988 (as amended) and regulations issued under it or, where appropriate, in accordance with licensing agreements which the University has from time to time. This page must form part of any such copies made.

III. The ownership of certain Copyright, patents, designs, trademarks and other intellectual property (the "Intellectual Property") and any reproductions of copyright works in the thesis, for example graphs and tables ("Reproductions"), which may be described in this thesis, may not be owned by the author and may be owned by third parties. Such Intellectual Property and Reproductions cannot and must not be made available for use without the prior written permission of the owner(s) of the relevant Intellectual Property and/or Reproductions.

IV. Further information on the conditions under which disclosure, publication and commercialisation of this thesis, the Copyright and any Intellectual Property and/or Reproductions described in it may take place is available in the University IP Policy (see http://documents.manchester.ac.uk/DocuInfo.aspx?DocID=2442 0), in any relevant Thesis restriction declarations deposited in the University Library, The University Library's regulations (see http://www.library.manchester.ac.uk/about/regulations/) and in The University's policy on Presentation of Theses

Journal Format Submission

This thesis has been submitted in the journal format to include published work and manuscripts due to be submitted. The format consists of a general introduction, three results chapters presented in research paper format, a general discussion, bibliography, and an appendix.

Acknowledgements

This page represents the most important piece of writing of this whole thesis. For without the people I am about to mention, there would not be a thesis altogether. I often hear of the difficulties fledgling scientists face during their PhDs and how the feeling of isolation can make the lows reach the depths of despair. I feel extremely privileged to have spent the last four years surrounded by the most intelligent, welcoming, kind and inspirational people I have ever met (I'm yet to leave my hometown so make of that what you will). Every single person who has been as lucky as me to become part of the Brain Inflammation Group has contributed to the best four years of my life and, in doing so, has improved me as a scientist and as a person.

First of all I would like to thank my supervisors, each of whom have a unique trait that all of us should look to adopt; Stuart, whose enthusiasm to help others benefits all of those who meet him; Dave, whose enthusiasm for new data fuels the inspirational energy in his lab; and Adrian, who is making a huge difference to the lives of ICH patients. Whilst Stuart, Dave and Adrian have given me the guidance needed to make the discoveries found in this thesis, I have also had some of the best peer mentors who inspire me on a daily basis.

I am very fortunate to have met Patrick Strangward in the first year of my PhD who has, alongside becoming a good friend and making the most significant contributions to my development, introduced me to nearly every new technique I know; tyramide, brain FACs, sectioning spheroids into the dead of night, drinking 4 Costas a day, developing a powerlifters gut in the absence of powerlifting, laying sophisticated traps, etc… I was also very lucky to have joined the lab when the whirlwind genius Jack (Rocky) Rivers-Auty had just started. I have seen Jack inspire everybody around him and watched in awe as he became a monster all-round scientist who, in the process, has been extremely generous with his time, especially with his teachings from the holy statistical scripture. I am also lucky to have started around the same time as Eloise, who first introduced me to *in vivo* work and gave me all the tools and support I needed to get going with my PhD. I am thankful to Jack G, who had to endure being my desk neighbour for the longest period; I had a great time and learned a lot! To Kieron, it has been short, but sweet, and I look forward to reading about all the great science you are doing!

I also want to thank all of my fellow PhD students that have joined me on this rollercoaster, from the original Brewtopians: Claire, Conor, Sid, and Amy, to the Broughers of Brough bay: Tess, Chris, Arthur and James, To Sabrina who has made some excellent contributions to this thesis, through to my daily distractions: Hannah and Ohud, and the biggest distraction over the past year: Bali! You have all kept me sane and all of the good times we have had, inside and outside the lab, would never fit on this page, but the memories will stay with me forever.

I am extremely grateful to Adam Denes, Niki Lenart, and Rebecca Fekete who all made me feel extremely welcome in Budapest and facilitated one of the best experiences of my whole PhD. It is clear to me that Adam has carried the energy and ethos of BIG to his own lab.

Most of all, I want to thank my family. To my Mum and sisters, Emma and Leanne, whose love and support has allowed me to get this far. To the Rea's, who have given our little family all the support we need during a tough four years. To my cousins, Steven and Mark, and the rest of the Glasto gang, who have given me great memories outside the lab. To my soulmate Marissa who has made more sacrifices than I have during this PhD; this is all for you. Last but by no means least, to my children Bobby, Rudy, and Olive, who shine with the brightest of lights to keep the darkness away and fill me with pride every minute of every day.

I also want to acknowledge my funders the MRC and the Natalie Kate Moss Trust, the latter of which is doing inspirational work for brain haemorrhage research in Manchester.

Chapter 1: Introduction

1.1 Cerebrovascular disease

Cerebrovascular disease (CVD) is the term used to refer to a collection of medical conditions that affect the vasculature supplying blood to the brain. Stroke is the most common clinical presentation of CVD and may result in large catastrophic haemorrhagic or ischaemic brain lesions (Feigin et al., 2019). CVD can also present more insidiously as a form of dementia, termed vascular dementia, where small vessel changes lead to haemorrhagic and ischaemic lesions on the microscale (Wardlaw et al., 2019). Thus, whilst this thesis focusses on understanding the role of inflammation during stroke, it is important to appreciate that much of the immunopathology described may also occur on the microscale in cases of vascular dementia.

1.2 Stroke

Stroke is the devastating clinical consequence of acute disruption to cerebral blood supply that affects cerebral function and leaves two thirds of patients either dead or disabled (Corbyn, 2014). There are two distinct subtypes of stroke defined by their pathology. Ischaemic stroke (IS) is the result of a vascular occlusion causing brain infarction and is responsible for 67 % of cases world-wide (Feigin et al., 2017). Haemorrhagic stroke (HS) is responsible for the remainder and occurs when a cerebral vessel ruptures and blood enters parenchymal (intracerebral haemorrhage; ICH) or subarachnoid (subarachnoid haemorrhage; SAH) compartments (Feigin et al., 2017). Although age-standardised incidence rates of stroke have declined over the past 25 years, 6.5 million lives and 113 million disability-adjusted life years (DALYs) were lost to stroke in 2013 alone (Feigin et al., 2017). This places stroke as the second most common cause of death worldwide, responsible for 12 % of total deaths, and the third most common cause of disability (Feigin et al., 2017, 2019). In the United Kingdom (UK) – a high-income country (HIC) – there is around one stroke every 5 minutes and the economic impact of this is enormous (Stroke Association, 2018). It is estimated that stroke alone costs the UK economy around £26 billion a year with the National Health Service (NHS) footing 13 % of that bill (Patel et al., 2017). Worldwide, there are roughly 32 million new stroke cases per year with around 70 % occurring in low- to middle-income countries (LMICs) (Feigin et al., 2014, 2017; Johnson et al., 2016). It is difficult to estimate the economic burden of stroke in LMICs, but with stroke severity being the best predictor of cost, and these countries having greater

stroke severity; it will be an outlay much larger than the UK's (Evers et al., 2004; Kaur et al., 2014).

1.2.1 Stroke aetiology

Stroke is a heterogeneous disease and this is in part due to the variety of factors that can trigger its onset. Whilst age, sex, ethnicity, and genetics represent important non-modifiable risk factors, it is estimated that the majority of worldwide stroke burden can be attributed to just ten modifiable risk factors (O'Donnell et al., 2016), seven of which are shared between both stroke subtypes (Table 1).

Table 1. Modifiable risk factors associated with stroke subtypes

Risk Factor	Ischaemic Stroke	Haemorrhagic Stroke
Hypertension	+	++
Current smoking	++	
Waist-to-hip ratio	+	+
Diet	+	+
Physical inactivity	+	+
Alcohol consumption	+	+
Apolipoprotein B to A1 ratio	++	
Diabetes mellitus	++	
Psychosocial factors	+	+
Cardiac causes	++	+

Data taken from (O'Donnell et al., 2016). ++ indicates risk factors with significantly stronger association to the relative stroke subtype.

IS aetiology

There are a number of IS classification systems to categorise cases based on their aetiology but the Trial of Org 10172 in Acute Stroke Treatment (TOAST) criteria are the most widely used (Adams et al., 1993). TOAST classifies IS into the following 5 categories (i) large artery atherosclerosis (LAA) (23%), (ii) cardioembolism (22%), (iii) small vessel occlusion (22%), (iv) other determined aetiology i.e. rare causes of IS (3%), and (v) indeterminate aetiology (26%), although the proportion of these subtypes changes dependent on age, race, ethnicity, and geographical location (Adams et al., 1993; Ornello et al., 2018).

The exact pathogenesis leading up to clot formation is unknown but in general clots are formed either locally or proximal to the site of infarction. Patients with LAA present with an occlusion in a major brain artery, or a branch cortical artery, caused by locally formed plaques that develop over decades in a well-defined process (Lusis, 2000). Atherosclerosis is first triggered by oxidation of low-density lipids (OxLDL) within the arterial wall. OxLDL initiates an immune response that leads to white blood cell infiltration, lipid deposition, smooth muscle cell proliferation, and cellular necrosis. Together these pathological changes to the vasculature result in the formation of a lipid rich fibrous scar known as an atheroma. Over time, circulating LDLs expand the atheroma until clinical complications arise through thrombus formation or complete luminal stenosis (Banerjee and Chimowitz, 2017).

In contrast to *in situ* formed thrombi, emboli can travel to the brain from a proximal site of origin. Cardioembolic strokes therefore have a multifaceted and heterogenous pathogenesis but cause large artery occlusion and thus result in comparable clinical features as LAAs (Kamel and Healey, 2017). Risk factors for cardioembolic stroke include atrial fibrillation, systolic heart failure, myocardial infarction and patent foramen ovale. Each of these conditions is linked to a hypercoagulable state and clots removed from cardioembolic stroke patients tend to have a greater density of platelets and fibrin (Sporns et al., 2017). In fact, the clot composition of cardioembolic stroke patients is similar in many ways to the clots retrieved from cryptogenic stroke patients and it is now estimated that many of these cryptogenic strokes could be of cardioembolic origin (Kamel and Healey, 2017; Sporns et al., 2017).

ICH aetiology

Spontaneous non-traumatic ICH is often subclassified into primary (presenting independently of other insults), or secondary to underlying morbidities or anticoagulant therapy (Qureshi et al., 2009). More recently ICH has been categorised as hypertensive (47%), cerebral amyloid angiopathy (CAA) related (20%), anticoagulant (9%), and structural (6%) (Rannikmäe et al., 2016). Hypertension, leading to hypertensive vasculopathy, and CAA are the 2 predominant aetiologies for ICH and are linked to bleeds in basal and lobar brain regions respectively.

Alongside its propensity to promote LAA, malignant hypertension induces lipohyalinosis in the penetrating arteries and arterioles in the brain (Lammie, 2002). Lipohyalinosis

(fibrinoid necrosis) is characterised by abnormal vessel wall architecture, collagenous sclerosis and lipid-laden mural cells and is often found in cerebral small vessel disease. Such changes render the affected arterioles susceptible to rupture, particularly those in close proximity to the high pressure circle of Willis. In hypertension-associated ICH, bleeding can indeed be traced to multiple deep-seated vessels in regions such as the basal ganglia, thalamus, cerebellum and pons (Fisher, 1971; Jackson and Sudlow, 2006; Sutherland and Auer, 2006).

Most studies refer to CAA as the main cause of ICH in aged individuals, although, one study found hypertension is apparent in >40 % of these individuals and CAA was present in less than 50% of those with ICH (Attems et al., 2008). It is clear, however, that lobar ICH has a stronger association with CAA and age than with hypertension (Kremer et al., 2015). In line with this, Amyloid-β (Aβ) accumulates over time within the perivascular space of the white matter and cortical regions of the brain (Yamada, 2015). The Aβ peptide first presents in the outer basement membrane of cerebral arteries and arterioles in the form of amyloid fibrils (Yamaguchi et al., 1992). These fibrils then begin to congregate around smooth muscle cells of the media, causing degeneration of the smooth muscle and subsequent structural abnormalities in the capillaries, arterioles and arteries (Qureshi et al., 2009; Yamada, 2015). The vasculopathological changes brought on by Aβ include lipohyalinosis, hyaline degeneration, microaneurysmal dilatation, amongst others, which lead to vessel instability.

1.2.2 Current acute stroke interventions

Due to the rapidly progressing nature of stroke injury; “time is brain”. The recommended course of action is, therefore, heavily dependent on subtype and speed of diagnosis.

There are currently no licensed acute therapies for ICH and thus current treatments aim to return body physiology back to homeostasis. Anticoagulant reversal, intensive blood pressure lowering and surgical interventions are indicated for subsets of acute ICH patients and can dramatically improve patient survival if rapidly implemented (Parry-Jones et al., 2019). Large haematomas are associated with extremely poor outcome and haematoma aspiration via minimally invasive surgery was hypothesised to improve functional outcome in cases where haematomas were > 30 mL. However, despite a trend toward improvement, a recent multi-centre phase 3 clinical trial showed no benefit (Hanley et al., 2019). ICH therefore remains an area of unmet clinical need.

There are currently two approved therapies for IS and both aim to restore cerebral blood flow (CBF) by dislodging the occluding clot. Intravenous application of a thrombolytic (tissue plasminogen activator) that degrades the problematic clot is only efficacious within 4.5 h of stroke onset (Hacke et al., 2008). This 4.5 h time window is particularly narrow as patients must first reach hospital and undergo imaging to be subsequently diagnosed with IS prior to treatment. It is, therefore, estimated that only 12 % of UK IS patients are eligible for thrombolysis.

Intrarterial thrombectomy (IAT) is the most recently developed treatment for IS and is often coupled with thrombolysis to increase the 4.5 h time-window to at least 6 h for eligible patients (Goyal et al., 2016). In order to mechanically remove the blood clot, highly skilled interventional radiologists are required to guide specially-designed clot removal devices to the affected region from distal arteries. It is estimated that around 10 % of UK IS patients are eligible for IAT yet less than 1 % of patients received this treatment between April 2017 and March 2018 (McMeekin et al., 2017; Royal College of Physicians, 2019). The reason for this poor uptake of IAT in the UK is due to a lack of skilled operators. However, the impressive benefit shown by IAT (Figure 1.1) has motivated the NHS to commission the procedure (NHS England, 2018).

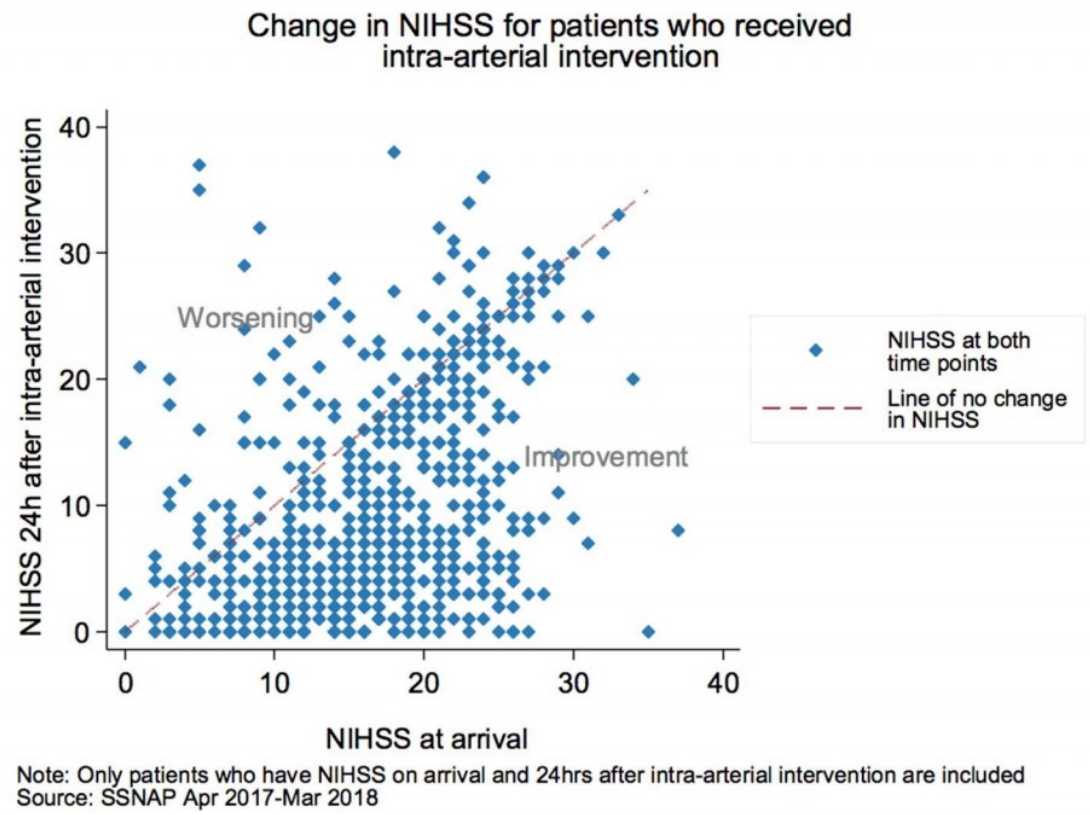

Figure 1.1 Intra-arterial intervention (IAT) reduces acute ischaemic stroke severity.
Patients presenting at UK stroke centres were scored on the National Institutes of Health Stroke Scale (NIHSS) on arrival (x axis) and 24 h following IAT (y axis). Graph taken from (Royal College of Physicians, 2019).

Acute treatment options for stroke patients are clearly limited but progress has been made to improve medical management in HICs, which in return has improved patient outcome. Thus, stroke related mortality and morbidity rates are highest in LMICs (Feigin et al., 2014; Johnson et al., 2016). Current acute stroke treatment guidelines are based on HIC data and it is clear that these guidelines are not optimal for cases in LMICs. For example, it is critical to identify the stroke subtype to inform treatment strategies and this is done using computed tomography (CT) scans. CT scanners are often unavailable or unaffordable in LMICs and clinicians must therefore make decisions in the absence of subtype diagnoses (Johnson et al., 2016). On top of this, higher HS rates in LMICs (34 % vs 9 %) compound the difficulties in subtype diagnosis and, due to the diametrically opposed pathophysiology of IS and HS, increase the chances of starting contraindicated therapies (Johnson et al., 2016; Feigin et al., 2019).

If all eligible patients were to undergo licensed procedures to reduce acute stroke damage, roughly 90 % of IS and 100 % of ICH patients remain without a licensed treatment option in the UK. The logistics, expense and complexities of current licensed procedures make it

difficult for LMICs to incorporate even these limited options. There is, therefore, a need to fully understand the pathophysiology of stroke to design therapies that are easier to apply and that can be implemented on a global scale.

1.3 Animal models of stroke

The inaccessible nature of human brain tissue and ethical barriers to human experimentation make it difficult to evaluate stroke pathophysiology without model systems. Moreover, the complex interactions of multiple biological systems, which occur following stroke, are currently impossible to mimic *in vitro*. Animal models have, therefore, been essential in dissecting stroke pathophysiology and differentiating between correlation and causation in pathological processes.

1.3.1 Spontaneous models of stroke

Spontaneous models of stroke are useful in modelling the heterogeneity of the human condition. Hypertension is the predominant risk factor for both IS and ICH and can be induced to promote spontaneous stroke in rodents. Spontaneously hypertensive stroke-prone rats (spSHRs) are a genetic breed of rat that develop malignant hypertension when fed a high salt diet (Bailey et al., 2011). By 20 weeks of age spSHRs develop symptomatic ischaemic and haemorrhagic lesions in the cortex due to hypertension induced vascular changes (Bailey et al., 2011). There are also two mouse models that induce malignant hypertension pharmacologically with or without transgenic overexpression of human renin and angiotensin (Iida et al., 2005; Wakisaka et al., 2010). However, these hypertensive mouse models of spontaneous stroke only induce haemorrhagic lesions.

Mutations to the gene encoding the collagen type IV alpha 1 protein (COL4A1) that cause reductions in protein secretion are linked to ICH in patients (Weng et al., 2012). A transgenic mouse line with Col4a1 mutations, causing intracellular accumulation of the protein, has severe developmental issues, including cerebral haemorrhage (Jeanne et al., 2015). When expressed specifically in adulthood these mice consistently develop sporadic ICH.

CAA occurs during aging and in humans is linked to lobar bleeds in older individuals. Dogs and non-human primates are also prone to develop CAA during aging and microbleeds are evident in extreme cases (Alharbi et al., 2016). Five transgenic mouse models incorporate rare familial mutations of the human amyloid precursor protein (APP)

gene on neuronal promoters to induce CAA, which results in development of microbleeds (Alharbi et al., 2016). The best characterised are the APP23 mice that overexpress human APP751 with the Swedish double mutation on a Thy-1 promoter (Winkler et al., 2001). Haemorrhages in these mice develop exponentially from 19 months of age but are mostly below 100 μm in size (Reuter et al., 2016).

Although these spontaneous models of stroke are useful tools to investigate mechanisms of onset and thus develop prophylactic therapies, there are a number of limitations to their use in understanding post-stroke pathophysiology. Prolonged treatment with hypertensives and aging of transgenic models incur significant time and financial costs to researchers. Moreover, the sporadic nature of the models leads to large variation in time of onset and size of lesion. These limitations are compounded by the models generating microlesions which may not contribute to behavioural alterations (Alharbi et al., 2016; Sommer, 2017). Inducible models of stroke have therefore been developed to discriminate between causative and symptomatic pathological pathways post-stroke.

1.3.2 Inducible models of ischaemic stroke

Emboli, photothrombotic dyes and endothelin-1 can be used to induce ischaemic lesions in rodents (Sommer, 2017). However, the most widely used models of IS are those that produce focal ischaemic lesions by occluding the middle cerebral artery (MCA). Around 50 % of IS patients present with occlusion to the MCA territories and there are 2 main approaches to model this in rodents (Ng et al., 2007). The MCA can be occluded at its origin by intraluminal filament insertion or at its distal branch following craniotomy.

1.3.3 Intraluminal filament middle cerebral artery occlusion

To occlude the MCA at its origin, a monofilament is introduced into the carotid artery and advanced until it reaches the MCA. This method was first developed for use in rats by Koizumi *et al.* (1986) and then later refined for use in mice. In the Koizumi method the filament is inserted through the common carotid artery (CCA) and consequently requires the surgeon to permanently ligate one CCA. A second intraluminal filament method was developed by Longa *et al.* (1989) wherein the filament is introduced through the external carotid artery, thus negating the requirement to permanently ligate a CCA. Once occluded, the monofilament is left in place for a period of time before being withdrawn. Following filament withdrawal, striatal or striato-cortical lesions develop over time which results in profound quantitative behavioural phenotypes (Howells et al., 2010). The Longa method

allows greater reperfusion than the Koizumi method, although, there are questions to the clinical relevance of this reperfusion (Morris et al., 2016). Patients with spontaneous reperfusion and those that are thrombolysed experience protracted reperfusion in comparison to the rapid reperfusion following filament removal. It is argued that the nature of injury following protracted vs rapid reperfusion is distinct and this mismatch directly harms translatability of findings from filament models (Hossmann, 2012). Moreover, due to the natural anatomical variation in vascular collateralisation of inbred mice strains, lesion sizes can be extremely variable and attrition rates high in filament models of MCA occlusion (MCAO) (McColl et al., 2004; Howells et al., 2010). Each of these limitations can be nullified by performing MCAO at a distal branch of the MCA.

1.3.4 Distal middle cerebral artery occlusion

Distal MCAO (dMCAO) requires an initial craniotomy be performed in order to expose the distal branches of the MCA. Once exposed, the MCA can be occluded via photothrombosis (Labat-gest and Tomasi, 2013), electrocoagulation (Llovera et al., 2014) or by applying chemicals to induce clot formation. Histopathological examination of IAT-retrieved thrombi has revealed that patient clots are heterogeneous but composed mainly of various proportions of red blood cells (RBCs), leukocytes, platelets and fibrin (Kim et al., 2015). Thrombin or $FeCl_3$ can be applied to the dMCA to induce formation of crosslinked fibrin or platelet rich clots respectively (Orset et al., 2007; Karatas et al., 2011). This ability to form clinically relevant thrombi in the MCA region separates dMCAO from other models of IS and permits study of *in vivo* clot biology in stroke. Moreover, these dMCAO models produce consistent cortical lesions and detectable behavioural phenotypes without overt mortality issues. However, surgical exposure of the brain does result in a number of limitations in the dMCAO model. Craniotomy can be technically challenging and cause accidental trauma to the brain, surgery-induced meningeal and brain inflammation, and perturbed intracerebral pressure.

1.3.5 Inducible models of intracerebral haemorrhage

As with IS, there are a number of inducible preclinical models of ICH. Intracerebral injection and subsequent inflation of a micro-balloon has been used to model the space-occupying effect of an intracerebral haematoma (Ma et al., 2011). Whereas, laser-induced and, more recently, transgenic mouse models exist which produce microbleeds with limited surgical intervention (Rosidi et al., 2011; Li et al., 2018). Patients with focal haematomas in deep brain regions have worse prognosis and are therefore most likely to

benefit from targeted interventions (Samarasekera et al., 2015). Autologous blood or collagenase can be injected into deep brain regions to model deep focal ICH and these two methods represent the most commonly used preclinical ICH models.

1.3.6 Autologous blood injection

Blood injection models were first established in rats by aspirating blood from a donor and injecting a set amount into the caudate nucleus of a subject (Ropper and Zervas, 1982). The model has since undergone multiple iterations to improve infusion pressures and reduce variability in haematoma location and spread (Ma et al., 2011). One key issue with blood injection models is the predilection for blood to reflux up the needle tract. Deinsberger *et al.* (1996) overcame this reflux issue by performing double injection rather than the standard single injection of blood. For the double injection method, a small amount of blood is injected and allowed to coagulate along the needle tract prior to injection of the remaining blood volume. Another notable modification of the model was the switch to using autologous blood rather than donor blood. Autologous blood is often taken via cannulisation of the femoral artery of the subject animal and thus requires femoral artery ligation. As focal ICH induces hemiparesis, femoral artery ligation can complicate interpretation of behavioural phenotypes. Sansing *et al.* (2011) have since modified the model for use in mice whereby tail vein blood is used and thus nullifies femoral artery ligation issues. When performed correctly the autologous blood injection model deposits a large RBC mass within the striatum. The resultant haematoma recapitulates many features of ICH including raised intracranial pressure, cerebral hypoperfusion, RBC toxicity, inflammation, and detectable neuromotor deficits. The autologous blood model does not mimic persistent bleeding from *in situ* vessels however.

1.3.7 Collagenase injection

To promote ICH from *in situ* vessels Rosenberg *et al.* (1990) generated the collagenase injection model. Collagenases are proteolytic enzymes that digest the extracellular matrix protein collagen. In the brain, collagen is predominantly deposited in the basement membrane of capillaries and postcapillary venules (Baeten and Akassoglou, 2011). Collagenase injection therefore causes breakdown of supporting structures and subsequent bleeding from capillaries and postcapillary venules. Similar to the clinical condition, this model produces a bleed that progresses over a 24 hour period and is said to mimic the bleeding-rebleeding phenomenon (Kirkman et al., 2011). Due to dependence on collagenase dose, haematoma volume in this model is also easily controlled and is not

susceptible to reflux up the needle tract. In comparison to the autologous blood injection model, collagenase injection recapitulates the same clinical features but produces less mass effect due to the progressive nature of the bleed. However, collagenase injection promotes small vessel rupture, as seen in the human disease, and thus allows study of active bleeding and coagulation during ICH. This model can therefore be deemed the most clinically relevant model of ICH. It must be noted, however, that collagenase is obtained from bacteria and is said to induce a greater inflammatory response and may be directly neurotoxic, though both of these points have been debated more recently (Kirkman et al., 2011).

1.4 Pathophysiology of acute cerebrovascular events

Experimental models of stroke are unable to recapitulate the enormous heterogeneity of the human condition. However, despite their limitations, the models discussed thus far, along with basic *in vitro* findings, have contributed enormously toward the understanding of the pathophysiological consequences of each stroke subtype.

1.4.1 Cerebral infarction

Once a cerebral artery is occluded, the territory supplied by the artery becomes hypoperfused and subsequently deficient of vital oxygen and glucose. However, the degree of hypoperfusion varies in this territory due to the many collaterals in neurovascular architecture (Hossmann, 1994). In regions with poor collateral flow, where CBF falls below 12 mL 100 g^{-1} per minute, cells die rapidly and create a core of unsalvageable infarcted tissue. Surrounding the infarcted core however, where greater collateral flow sees CBF levels fall between 12 – 22 mL 100 g^{-1} per minute, cells become metabolically compromised and functionally dormant yet remain salvageable (Heiss, 2000). This area of compromised yet viable tissue is known as the ischaemic penumbra and is central to efforts to limit damage following IS. Over the course of hours to days the ischaemic cascade induces cell death within penumbral tissue and subsequently expands the infarct core.

1.4.2 The ischaemic cascade

The ischaemic cascade is a complex sequence of events (depicted in Figure 1.2) with intricate interplay and multiple directions of evolution which result in permanent cell death following infarction. During ischaemia, metabolic failure and breakdown of ion

homeostasis trigger lipolysis, proteolysis, and rapid cellular necrosis and apoptosis (Brouns and De Deyn, 2009). Depletion of cellular adenosine triphosphate (ATP) quickly leads to failure of energy dependent ion pumps and the subsequent depolarisation of cells. Cell depolarisation causes activation of voltage dependent Ca^{2+} channels leading to the release of excitatory neurotransmitters such as glutamate. Extracellular concentrations of glutamate rise further due to the inactivation of energy dependent reuptake processes and induce a pathological neuronal cell death termed excitotoxicity. Glutamate accumulation triggers the overstimulation of α-amino-3-hydroxy-5-methyl-4-isoxazole propionic acid (AMPA) and N-methyl-d-aspartic acid (NMDA)-type glutamate receptors on nearby neurones. Activation of these receptors results in the influx and intracellular accumulation of Na^{+}, Cl^{-} and Ca^{2+} ions which, via osmosis, bring water and trigger cytotoxic oedema. At the same time, Ca^{2+}, as the universal second messenger, induces activation of proteases, lipases and nucleases which destroy cell integrity. In addition, Ca^{2+} contributes to oxidative and nitrosative stress through activation of enzymes that produce nitric oxide, arachidonic acid and superoxide. Alongside Ca^{2+} dependent oxidative and nitrosative stress, excitotoxic NMDA receptor activation leads to nicotinamide adenine dinucleotide phosphate (NADPH) oxidase-generated free radicals (Brennan et al., 2009). In turn, NADPH-generated free radicals are hypothesised to promote mitochondrial uncoupling and release of further free radicals (Moskowitz et al., 2010). Free radicals are short lived molecules that induce a plethora of detrimental cellular effects once levels rise above antioxidant defences (Lo et al., 2003). During ischaemia, free radicals cause enzyme inactivation, release of intracellular Ca^{2+} stores, protein and lipid destruction, and damage to the cytoskeleton and DNA. In the presence of ATP the aforementioned cell damage induces a programmed cell death termed apoptosis, whereas, in the absence of ATP this cell damage results in cellular necrosis, with the latter being the most dominant form of cell death following ischaemia (Lo et al., 2003; Moskowitz et al., 2010). This energy failure, ionic imbalance, excitotoxicity and free radical generation are all intrinsically linked and persist within the ischaemic region until the core engulfs the penumbra. One important process that mediates the speed at which the ischaemic cascade engulfs the penumbra is inflammation.

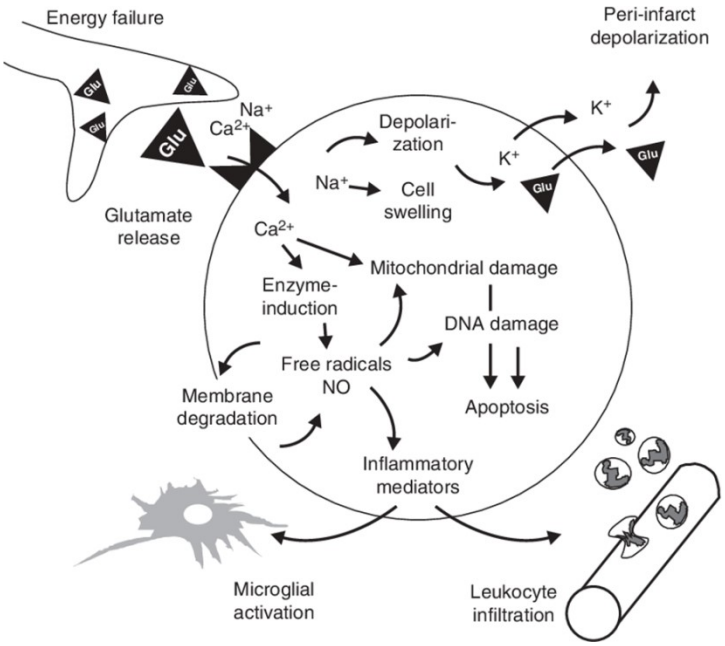

Figure 1.2 Pathophysiology of Ischaemic Stroke.
Starving the brain of blood supply triggers the ischaemic cascade that progressively kills neurones. Energy depletion leads to the release of excitatory neurotransmitters, such as glutamate, which activate downstream receptors leading to ionic imbalances. Greater amounts of Ca^{2+} and Na^{+} cause cell swelling and trigger intracellular signalling pathways leading to mitochondrial damage, enzyme activation and DNA damage, which in turn promote membrane damage, cell death and inflammation. The release of K^{+} ions also propagates waves of spreading depolarisations through actions on neighbouring neurones. Schematic taken from (Dirnagl et al., 1999)

1.4.3 Cerebral haemorrhage

The precise mechanisms underpinning neuronal damage following ICH remain elusive, though current evidence suggests two distinct pathways exist that are summarised in Figure 1.3. Primary brain injury occurs immediately upon rupture of a cerebral vessel due to the mass effect of blood accumulating within parenchymal tissue (Qureshi et al., 2009). This mechanical space occupying effect of the haematoma results in raised intracranial pressure (ICP) and instant neuronal death (Sinar et al., 1987; Fernandes et al., 2000). Primary injury can also persist for longer in up to 30 % of patients who are subject to substantial (> 33 %) haematoma expansion in the first 24 hours (S. M. Davis et al., 2006). At the same time, cytotoxic oedema and clot retraction produce an ionic gradient that rapidly results in the genesis of perihaematomal oedema, which further increases ICP and contributes to mass effect (Urday et al., 2015). Although CBF drops following ICH, there is no evidence to suggest this reduction is adequate enough to promote ischaemia within or around the haematoma, though patients are susceptible to delayed ischaemic events (Zazulia et al., 2001; Menon et al., 2012). It is currently unclear if excitotoxicity features during ICH, as it does during IS, but glutamate is known to accumulate within the interstitial fluid and could be a contributing factor in cytotoxic oedema (Urday et al.,

2015). During this acute primary injury phase, a secondary injury begins and progresses within hours to days of ICH onset and is characterised by RBC- and haemostasis-related toxicity, the onset of inflammation and vasogenic oedema.

1.4.4 Secondary injury after intracerebral haemorrhage

The serine protease thrombin has dichotomous effects following ICH. Thrombin cleaves fibrinogen into fibrin monomers that are subsequently processed into cross-linked fibrin clots to stem further bleeding. However, thrombin can also directly open the blood brain barrier, exacerbate neuronal death, and activate protease activated receptors (PARs) on cells to trigger inflammation (Cunningham, 1997; Lee et al., 1997; Xi et al., 2003).

RBC components are major contributors to the damage seen after ICH. RBC lysis is proposed to occur 24 hours after ICH and leads to the release of haemoglobin (Hb), haem (Hm), Fe, biliverdin, and carbon monoxide . These components are released in a sequential manner, increasing reactive oxygen species (ROS), eliciting an immune response, and causing massive cell death (Aronowski and Zhao, 2011). A number of homeostatic mechanisms exist to reduce RBC toxicity by sequestering, or responding to, the various RBC breakdown products; Haptoglobin (Hp) binds and sequesters Hb, whereas hemopexin directly conjugates to Hm, and transferrin binds Fe (Smith and McCulloh, 2015). Injection of packed RBCs into the brains of rodents leads to functional deficits and oedema over several days, whereas, RBC lysate injection invokes BBB disruption, oedema and DNA injury within 24 hours (Xi et al., 1998; Hua et al., 2002). Thus indicating that RBC components promote secondary injury as the homeostatic mechanisms are overloaded over several days post-ICH.

RBC lysis is postulated to occur through the depletion of energy reserves and/or stimulation of the complement pathway, the former leading to necrosis and the latter leading to activation of the membrane attack complex (Ducruet et al., 2009; Keep et al., 2012). Upon lysis, RBCs release around 289 million molecules of Hb each, which equates to around 1.45×10^{18} molecules of Hb per ml of blood, far in excess of the amount of Hp (Smith and McCulloh, 2015). Hp is, however, synthesised in the brain by oligodendrocytes after ICH, causing a reduction in RBC based toxicity (Zhao et al., 2009).

Auto-oxidation of Hb occurs over several hours, producing ferric Hb and superoxide anion (O_2^-), whereas Hm is rapidly oxidised into hemin and O_2^- within seconds (Bonaventura et al., 2013). The highly oxidative environment of the haematoma is likely to accelerate

oxidation of Hb and Hm. The release of ferric Fe from Hm allows the Fenton reaction to commence, subsequently producing a large number of ROS. Oxidative Hb products overwhelm the natural anti-oxidant defence system, causing depletion of glutathione and leading to protein, lipid and DNA damage (Zhou et al., 2014).

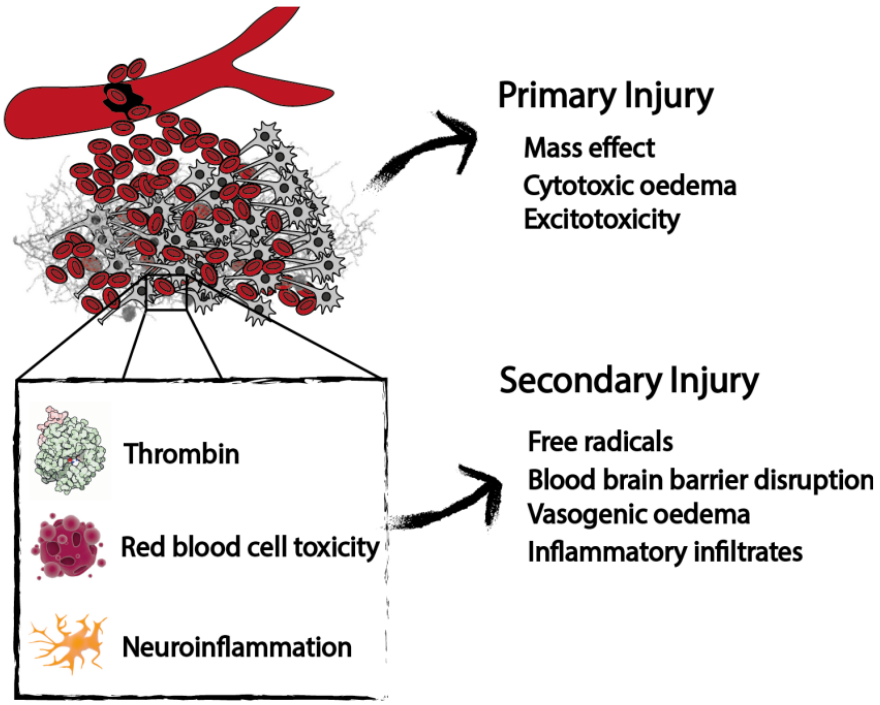

Figure 1.3 Pathophysiology of Intracerebral Haemorrhage.
Intraparenchymal blood accumulation results in primary injury triggered by mass effect, whereas, a secondary injury progresses over days and is characterised by thrombin, red blood cell toxicity and the onset of neuroinflammation.

1.5 Inflammation

In its purest sense inflammation is an essential biological process that guards organisms from disease and maintains a state of tissue homeostasis. An inflammatory response occurs upon recognition of harmful stimuli of both endogenous and exogenous origin. Acute infection or acute trauma result therefore in virtually identical biological features. Rubor (redness), tumor (swelling), calor (heat) and dolor (pain) constitute the four cardinal signs of inflammation and have been documented since the 1st century observations of Celsus. Since then, our understanding of the systemic, cellular and molecular basis of inflammation has improved tremendously. We have also discovered that, whilst these inflammatory processes are of paramount importance for host survival during infection, they also contribute directly to tissue damage during acute sterile inflammation (inflammation that occurs in the absence of infection). This section will discuss the complex role of inflammation in the pathogenesis of stroke.

1.5.1 Post-stroke inflammation

Host cells harbour intracellular molecules that have important functions during homeostasis but have evolved secondary pro-inflammatory functions. Damage associated molecular patterns (DAMPs) is the collective term used to describe such molecules as ATP, DNA and s100 proteins, which are concealed from the extracellular environment under steady state conditions but are expelled during necrosis (Janeway Jr. and Medzhitov, 2002; Kono and Rock, 2008). Following stroke, dying cells release DAMPs into the extracellular milieu which activate pattern recognition receptors (PRRs) on nearby cells such as microglia (the resident macrophages of the brain), astrocytes and endothelial cells to induce local production of cytokines (such as tumour necrosis factor (TNF)-α, interleukin (IL)-1 and IL-6), adhesion molecules, vasoactive substances, and chemokines, which all act to amplify the inflammatory response (Savage et al., 2012; Anrather and Iadecola, 2016; Askenase and Sansing, 2016).

Chemokines such as CXCL1 and CCL2 are released following PRR activation and create a concentration gradient through which first responder immune cells can hone to the site of injury. Consequently, circulating neutrophils and monocytes arrive in the vascular territory of the stroke lesion and transmigrate into the brain in a well-defined process that requires interactions between upregulated endothelial adhesion molecules - such as selectins, intercellular adhesion molecule (ICAM)-1 and vascular cell adhesion molecule (VCAM)-1 - and activated leukocyte adhesion molecules - such as lymphocyte function-associated antigen 1 (LFA)-1, macrophage-1 antigen (MAC-1) and very late antigen (VLA)-4 (Ley et al., 2007). At this point during sterile inflammation in peripheral tissues, vasoactive substances such as histamine, nitric oxide and eicosanoids are produced by the expanding immune cell repertoire and trigger vasodilation of nearby arterioles and capillaries (Pober and Sessa, 2015). The subsequent increase in blood flow signals the arrival of 2 of the cardinal signs of inflammation; rubor and calor. Following stroke however, it is hypothesised that vascular injury limits the effects of vasoactive substances (Hu et al., 2017). Nevertheless, during the vascular phase of post-stroke inflammation, factors are released from resident and trafficking immune cells which facilitate breakdown of the blood brain barrier (BBB) and promote vasogenic oedema.

Cytokines can signal directly to endothelial cells to trigger BBB breakdown through downregulation of important tight junction proteins such as claudin-5 (Holmin and Mathiesen, 2000; Aslam et al., 2012). Activated immune cells also produce ROS,

complement proteins, and extracellular matrix-degrading enzymes termed matrix metalloproteinases (MMPs), to further contribute toward BBB breakdown. (Yong et al., 2001; Anrather and Iadecola, 2016). Breakdown of the BBB compounds brain damage following stroke by further exposing the brain to circulating pro-inflammatory molecules, neurotoxic substances and proteases, and causing the influx of water, which, in the case of ICH can contribute directly to mass effect. Oedema volume tracks well with inflammatory biomarkers and both correlate with outcome following stroke. Inflammation thus exacerbates injury during the acute phase of stroke, however during sub-acute and chronic phases the immune response helps the brain recover through mechanisms that are only now being revealed. The dichotomous nature of post-stroke inflammation makes targeting its processes for therapeutic intervention challenging, yet much has been learned by studying the innate immune response at the cellular level.

1.5.2 Microglia, monocytes and macrophages

Once described as an immune-privileged organ, it is now evident the brain and meninges contain a diverse repertoire of immune cells with a particularly heterogeneous macrophage population (Mrdjen et al., 2018; Van Hove et al., 2019). Nevertheless, the compartmentalisation of the brain parenchyma behind the BBB has resulted in the evolution of a brain specific macrophage population, termed microglia, which are the only parenchyma-resident immune cells.

Under steady state, microglia readily survey their environment with dynamic outstretched processes (in a 'ramified' morphology) that perform important non-inflammatory functions, including the synaptic pruning of neuronal pathways (Nimmerjahn et al., 2005; Schafer et al., 2012). Microglia are seeded from the yolk sac and, under homeostasis, self-renew (Ginhoux et al., 2010). In order to self-renew, microglia rely on IL-34 and colony stimulating factor (CSF)-1-dependent activation of CSF-1 receptor. Inhibition of this pathway therefore specifically depletes microglia (Elmore et al., 2014; Spangenberg et al., 2019). Within hours of stroke, microglia rapidly obtain an activated 'amoeboid' morphology and begin to express inflammatory proteins (Schilling et al., 2003; Luheshi et al., 2011). It was for this reason that microglia were believed to be at the apex of the acute immune response and orchestrated all downstream detrimental effects. However, recent microglia depletion studies have revealed that these cells limit acute brain injury following IS (Szalay et al., 2016; Jin et al., 2017). In the first of these studies microglia are shown to protect neurones from excitotoxic death through direct interactions which regulate calcium

signalling. Whilst in the second study microglia are shown to protect the brain from an exaggerated inflammatory response. As with most immune cells, microglia have a high level of plasticity and can react to many insults with a tailored response. Recent research from the preclinical ICH field indicates that microglia contribute to acute brain injury by exacerbating the immune response (Li et al., 2017). The mechanisms by which microglia generate bespoke reactions to specific niches is an open question and the answers may reveal important insights for the stroke field. In acute phases of stroke however, microglia are joined by equally plastic macrophage progenitor cells known as monocytes.

Monocytes are circulating myeloid cells that exist in two subsets. Ly6Chi monocytes, sometimes called classical or pro-inflammatory monocytes, are recruited to sites of inflammation where they undergo differentiation into macrophages or dendritic cells. Ly6Clo monocytes, often referred to as non-classical or vascular patrolling monocytes, primarily crawl along the luminal surface of endothelial cells to patrol the vascular system but can also mount an immune response to tissue injury (Auffray et al., 2007). In models of ICH, preventing Ly6Chi monocyte entry into the brain has consistently been shown to reduce haematoma volume and improve outcome at acute time-points through a mechanism that is, as of yet, undefined (Hammond *et al.*, 2014; Hammond *et al.*, 2014; Chang *et al.*, 2018). Similarly, inhibition of monocyte entry reduces acute lesion volume in experimental IS (Dimitrijevic et al., 2007), though others have failed to replicate these findings (Schmidt et al., 2017). In the days following stroke, monocytes differentiate into macrophages which engraft within the brain and become morphologically indistinguishable from activated microglia (Gelderblom et al., 2009). It is becoming increasingly apparent however, that alongside microglia, these monocyte-derived macrophages (MDMs) contribute to tissue repair and resolution in chronic phases.

As part of the immune response to sterile injury, an initial burst of damaging inflammation is followed by a period of tissue remodelling and regeneration. Microglia and MDMs have the capacity to produce pro-inflammatory and pro-reparative factors and thus have important roles in both acute and chronic phases of inflammation (Lan et al., 2017). Significant research has been conducted on the premise that macrophages polarise into pro-inflammatory and anti-inflammatory phenotypes, however this is doubted by many, and recent evidence suggests that individual macrophages express markers of both 'phenotypes' *in vivo* (Ransohoff, 2016; Locatelli et al., 2018). Nonetheless, the study from Locatelli *et al.*, (2018) did show that, in a mouse model of multiple sclerosis, the

macrophage population swings from an initial pro-inflammatory majority at acute time-points toward an anti-inflammatory majority in chronic phases. In ICH, microglial production of repair factors is governed by transforming growth factor (TGF)-β and functional recovery is improved by addition of exogenous TGF-β (Taylor et al., 2017). The mechanisms underpinning microglia/MDM dependent tissue repair remain elusive. However, one study noted that MDMs prevent delayed haemorrhagic transformation of ischaemic brain injury by quelling microvascular injury, and this was also TGF-β dependent (Gliem et al., 2012). Therefore, microglia/MDMs may dampen injury and promote stability of the cerebrovascular system post-stroke, although, it is likely that these cells perform many pleiotropic functions.

Macrophages are professional phagocytes and are said to clear cellular debris in chronic phases of inflammation. Triggering receptor expressed on myeloid cells (TREM)-2 is a lipid receptor that is highly expressed on microglia and has important actions in Alzheimer's disease and metabolic homeostasis (Wang et al., 2015; Jaitin et al., 2019). Microglial expression of TREM-2 is required for effective functional recovery in the dMCAO model but is yet to be investigated in ICH (Kurisu et al., 2018). RBCs present a unique challenge to the brain following ICH as they begin to lyse and release neurotoxic compounds in the days post-ictus. The clearance of toxic RBCs is now known to be a crucial feature of MDMs and, importantly, contributes to functional recovery in experimental models of ICH (Chang et al., 2018). In 2007 Denes *et al.*, also hypothesised that microglia may prevent exaggerated and persistent inflammation in stroke by phagocytosing damaging neutrophils. It has recently been shown that microglia do indeed prevent brain neutrophil accumulation in chronic phases of ischaemic stroke through phagocytic clearance (Otxoa-de-Amezaga et al., 2019). It remains to be seen if the same event occurs in ICH and if microglial clearance of neutrophils would be beneficial at all in this setting.

1.5.3 Neutrophils

Neutrophils are a class of granulocytes that circulate within the vasculature at higher numbers than any other cell type and act as first responder cells during inflammation. Neutrophils, like mononuclear phagocytes, have the ability to act as phagocytic cells, yet unlike mononuclear phagocytes, neutrophils store intracellular granules containing lytic enzymes and readily produce ROS. Neutrophils are one of the first cell types to traffic to the brain following stroke. In ICH models, neutrophils can be found in the brain within 4

hours, although, temporal dynamics are slower in IS, where they are not found within the parenchyma until 24 hours (Wang and Tsirka, 2005; Perez-de-Puig et al., 2015). Neutrophils can directly contribute to ischaemia by mechanically occluding capillaries during IS; a pathway that has also been shown to occur in Alzheimer's disease (del Zoppo et al., 1991; Cruz Hernández et al., 2019). Alongside this, neutrophils promote post-stroke BBB breakdown, haemorrhagic transformation and neurotoxicity by releasing toxic factors such as MMPs and ROS (Mracsko and Veltkamp, 2014; Anrather and Iadecola, 2016). Neutrophil depletion improves outcome in acute models of ICH and IS (Lauren H Sansing et al., 2011; Moxon-Emre and Schlichter, 2011; Neumann et al., 2015).

Neutrophils can expel nuclear contents in a process called 'netosis', which ensnares bacterial pathogens and kills them (Brinkmann et al., 2004). Netosis also contributes to coagulation and neutrophil nets have been seen in IS patient thrombi and may impair efficient reperfusion (Martinod and Wagner, 2014; Laridan et al., 2017; Ducroux et al., 2018). Neutrophil nets can be found within the parenchyma following experimental stroke, are directly neurotoxic, and have been shown to contribute to injury in a permanent MCAO model of IS (Allen et al., 2012; Kim et al., 2019). To-date, no published studies have investigated netosis in ICH, although, with netosis contributing to coagulation and larger bleeds producing greater injury in ICH, preventing netosis may worsen outcome in this setting. Whilst neutrophils can exacerbate injury in the acute phase of stroke in a multitude of ways, much like macrophages, neutrophils can also adopt a pro-reparative role in chronic phases of stroke.

Neutrophils enter the brain in greatest numbers from day 3 onwards in experimental stroke models (Gelderblom et al., 2009; Mracsko et al., 2014). At these later time-points neutrophils express canonical markers of tissue repair such as CD206 (mannose receptor) and Ym-1 (chitinase 3-like 3, Chi3l3). Promoting neutrophil upregulation of these molecules through pharmacological intervention is neuroprotective in acute MCAO models (Cuartero et al., 2013; Cai et al., 2019). However, microglial clearance of these pro-reparative neutrophils has hampered study into their effects in chronic phases of IS (Cai et al., 2019). In ICH models however, the cytokine IL-27 has been used to modify neutrophil behaviour (Zhao et al., 2017). As part of their anti-microbial arsenal, neutrophil granules contain important iron-scavenging molecules such as lactoferrin and haptoglobin. In rodents, IL-27 injection polarises bone marrow neutrophils to a phenotype where lactoferrin is upregulated and MMPs and ROS are downregulated. Thus, in the autologous

blood model of ICH, IL-27 stimulated neutrophils improve functional recovery by dampening inflammation and reducing iron toxicity (Zhao et al., 2017).

1.5.4 Lymphocytes

Cells of the adaptive arm of the immune system have beneficial and detrimental roles in post-stroke inflammation too. The humoral response to injury requires a latency period where antigen presentation fine-tunes T and B cell functions. However, cytotoxic lymphocytes can act irrespective of this latency period and have been implicated in acute IS injury. A series of studies found interferon (IFN)-γ producing T cells, IL-17 producing γδT cells, and natural killer (NK) T cells potentiate acute ischaemic injury in rodent models (Yilmaz et al., 2006; Shichita et al., 2009; Kleinschnitz et al., 2010; Liesz, Zhou, et al., 2011). However, regulatory T cells (Tregs) have been shown to accumulate in the brain at later time-points and promote resolution of tissue injury through IL-10 secretion (Liesz et al., 2009). Regulatory B cells have also been shown to offer neuroprotection by secreting IL-10, yet others have found evidence that B cell follicles form in the parenchyma following IS and the secreted immunoglobulins contribute to post-stroke cognitive decline (Ren et al., 2011; Doyle et al., 2015). Very little is known about lymphocyte activity following ICH. In one study, CD4+ T cells were found to be the predominant immune cell population in the brain within 24 hours of experimental ICH, however, T cells do not appear in the parenchyma until 48 – 96 hours in the majority of studies (Xue and Del Bigio, 2000, 2003; Hammond *et al.*, 2014; Mracsko *et al.*, 2014). Nevertheless, there is evidence that T cells contribute to BBB breakdown and mediate repair following ICH, as they do in IS (Zhang et al., 2017; Zhou et al., 2017). To-date, no studies have assessed B cell functions in the setting of ICH.

The inflammatory response to stroke proceeds in a stochastic fashion and has dichotomous influences on injury progression. Overall, the innate immune reaction, which triggers the acute immune response to stroke, is seen to be detrimental and, in the brain, the cytokine IL-1 is the most potent mediator of this response (Giles et al., 2015). IL-1, however, also has a very complex biology.

1.6 Interleukin 1

First discovered as an endogenous pyrogen, the prototypical cytokine IL-1 has been at the forefront of many important discoveries in the field of inflammation. The complex pleiotropic nature of cytokine biology and its importance in resistance to infection was first revealed by researchers studying IL-1 (Reviewed in Garlanda et al., 2013). Alongside this, investigations into IL-1 also exposed the intricacies of highly conserved intracellular pro-inflammatory signalling networks. Since then, the IL-1 superfamily has been revealed consisting of 11 soluble ligands and 10 receptors (Rivers-Auty et al., 2018). IL-1 family ligands can be further subdivided into 7 pro-inflammatory cytokines (IL-1α, IL-1β, IL-18, IL-33, IL-36α, IL-36β, and IL-36γ), 1 anti-inflammatory cytokine (IL-37), and 3 receptor antagonists (IL-1RA, IL-36RA, and IL-38) (Garlanda et al., 2013; Rivers-Auty et al., 2018). The most studied and best characterised of the IL-1 superfamily are IL-1α and IL-1β which both act through the type 1 IL-1 receptor (IL-1R1).

1.6.1 Type 1 interleukin 1 receptor signalling

IL-1R1 is a membrane-bound receptor consisting of 3 extracellular immunoglobulin (Ig) domains and an intracellular Toll-IL-1 resistance (TIR) signalling domain. The binding of IL-1α or IL-1β to IL-1R1 induces a conformational change in the first Ig domain that results in recruitment of the IL-1 receptor accessory protein (IL-1RAcP) (Weber et al., 2010). An IL-1R1/IL-1RAcP complex dimerises through homotypic intracellular TIR interaction and recruits a third TIR domain containing molecule called myeloid differentiation primary response gene 88 (MyD88). MyD88 acts as a signalling adaptor molecule to recruit the serine-threonine kinase IL-1R-associated kinase 4 (IRAK4), which, in turn, autophosphorylates and activates IRAK1 and IRAK2. The activated IRAK complex subsequently recruits and oligomerises the ubiquitin E3 ligase TNF–associated factor 6 (TRAF6) which amplifies the previously receptor-proximal signalling into a whole cell event.

TRAF6 polyubiquitinates a number of secondary messenger molecules including TGF-β–activated protein kinase (TAK) 1 and TAK–binding protein (TAB) 2 and 3. The ubiquitination of TAK1 promotes the formation of a TRAF6-TAK1-Mitogen-activated protein kinase kinase kinase (MEKK)-3 complex which subsequently activates c-Jun N-terminal kinase (JNK), and p38 Mitogen-activated protein kinases (MAPK) pathways. These two pathways amplify and thus facilitate efficient activation of the main output of

IL-1R1; the major pro-inflammatory transcription factor nuclear factor kappa-light-chain-enhancer of activated B cells (NF-κB) (Huang et al., 2004).

To activate NF-κB, the TAK1/TAB2/TAB3 complex binds and phosphorylates the inhibitor of NF-κB kinase (IKK) complex, which consists of IKKα, IKKβ and NF-κB essential modulator (NEMO). Activated IKK phosphorylates IκBα leading to K48 ubiquitination and its resulting proteasomal degradation. IκBα degradation then releases the p65 NF-κB subunit which translocates to the nucleus to act as a transcription factor for a plethora of genes including cytokines (IL-6), chemokines (CXCL1 or IL-8), eicosanoids (prostaglandin E), adhesion molecules (ICAM1 and VCAM1), and even IL-1 in a positive feedback loop (Libermann and Baltimore, 1990; Lévesque et al., 2016; Mantovani et al., 2019). There are also reported interactions between IL-1 and sphingolipids that can enhance its downstream signalling and in some circumstances act in a non-transcriptional manner (Ballou *et al.*, 1992; Masamune, Igarashi and Hakomori, 1996; Davis *et al.*, 2006). In fact, the downstream signalling of IL-1R1 is so potent, 2 distinct regulatory mechanisms evolved to prevent its activation . A receptor antagonist, IL-1RA, evolved from a gene duplication of IL-1β to bind IL-1R1 without triggering its activation, whereas a decoy receptor, IL-1R2, evolved through gene duplication of IL-1R1 to bind IL-1 without transmitting intracellular signals (Rivers-Auty et al., 2018). On top of this, IL-1 signalling is also tightly regulated at the genetic and protein level of the ligand.

1.6.2 Interleukin 1 expression

Under basal conditions few cells, if any, express the IL-1β protein but there are data to suggest IL-1β mRNA is expressed at very low levels in brain regions such as the hippocampus, hypothalamus and cortex, and may be under control of circadian rhythms (Vitkovic et al., 2000). In contrast however, the IL-1α protein is said to be constitutively expressed in keratinocytes, platelets and fibroblasts where it has important functions in barrier immunology (Kong et al., 2006; Daniels and Brough, 2017; Daniels et al., 2017). During acute inflammation IL-1 is produced by cells of the myeloid lineage such as neutrophils, monocytes and 'sentinel' macrophages. Thus IL-1 must be induced in myeloid cells to perform its main function during inflammation (Martin, 2016).

The most common way to induce IL-1 expression in the laboratory setting is via incubation of myeloid cells with the bacterial pathogen associated molecular pattern (PAMP) lipopolysaccharide (LPS). LPS binds and activates a canonical PRR named Toll-

like receptor (TLR) 4 which, using many overlapping signalling networks with IL-1R1, triggers JNK, MAPK and NF-κB activation. Downstream signalling of TLR-4 converges on the transcription factors NF-κB, PU.1, C/EBPβ and AP-1 which bind and activate the IL-1 promoter (Hiscott et al., 1993; Shirakawa et al., 1993; Tsukada et al., 1994; Kominato et al., 1995; Roman et al., 2000). More recently, it has been shown that IL-1β expression is also under control of a cellular metabolic switch (Tannahill et al., 2013). Following TLR-4 activation, cellular respiration moves from oxidative phosphorylation to aerobic glycolysis, wherein, the metabolite succinate accumulates and triggers the stabilisation of hypoxia-inducible factor-1α (HIF-1α). HIF-1α subsequently binds to a region upstream of the IL-1β transcriptional start site where it facilitates gene transcription. IL-1α, on the other hand, has its own unique mechanism regulating its expression in mice. An inducible stretch of long non-coding RNA on the antisense strand of the gene, similar in sequence to IL-1α itself, is required for the recruitment of transcriptional machinery to the IL-1α promoter (Chan et al., 2015). As mentioned earlier, these extensive details of IL-1 expression have been revealed with the use of LPS. However, IL-1 has important functions in sterile inflammatory settings where myeloid cells would not be exposed to such PAMPs. Endogenous molecules must therefore exist that activate the signalling networks revealed by LPS.

DAMPs are often intracellular molecules which are released upon cell death to alert nearby immune cells to danger. Notable DAMPs include high mobility group box protein (HMGB) 1, S100 proteins, DNA, and RBC breakdown products such as Hm and oxidised Hb. Although many of these DAMPs have been shown to trigger TLR-4 dependent IL-1 expression, there are concerns that endotoxin contamination may have contributed to observed effects (Erridge, 2010). One notable example of the misinterpretation of pro-inflammatory effects of a protein due to LPS contamination is that seen in the literature surrounding the serine-protease thrombin. It is suggested that thrombin promotes NF-κB signalling during coagulation by activating TLR-4 and PARs on nearby macrophages (Mracsko and Veltkamp, 2014; Foley and Conway, 2016). However, Chang *et al.*, (2018) showed that this NF-κB activity was due to LPS contamination as an ultrapure thrombin preparation had no effect. This finding is especially pertinent to the field of ICH as it is currently hypothesised that thrombin is one of the main factors driving inflammation post-stroke (Keep et al., 2014). In fact, many published studies have used thrombin injection to model ICH in rodents (Masada et al., 2001; Cui et al., 2011). The findings from these

studies may, therefore, be driven by endotoxin contamination rather than thrombin. Thrombin is known to activate innate immune cells through PARs, however, so more research is required to separate thrombin from endotoxin effects in current ICH literature.

Due to the considerable evidence that TLRs have non-redundant functions in sterile disease, it is undeniable that there are endogenous activators of TLRs (Cook et al., 2004). Therefore, many of the aforementioned DAMPs are likely to promote IL-1 production through TLR activation. There are also non-TLR mechanisms of IL-1 transcription. HMGB1, s100 proteins and Aβ bind to a second type of PRR termed receptor for advanced glycation end products (RAGE). RAGE activates 3 of the core IL-1 transcription factors, NF-κB, CREB, and Sp1 (Rouhiainen et al., 2013). Cytokines such as TNF-α and even IL-1 can also facilitate the expression of IL-1 (Franchi et al., 2009).

Not only is IL-1 tightly regulated by complex mechanisms at the genetic level but its actions are also controlled by post-translational modification.

1.6.3 Interleukin 1 processing

IL-1α and IL-1β both lack leader sequences to facilitate their secretion from the cell through the canonical ER-Golgi secretory pathway. Consequently, once the proteins are synthesised they become sequestered within the cytosol. The release of both molecules is therefore heavily linked to loss of membrane integrity. In fact, both IL-1 molecules are produced as 31 kDa proteins containing protease cleavage sites that a number of serine and aspartate proteases linked to cell death can bind. The proteolytic cleavage of pro-IL-1β into a 17 kDa form is essential for its activation of IL-1R1. On the contrary, there is evidence that pro-IL-1α is biologically active, yet it to is often cleaved to a 17 kDa form with markedly increased potency (Mosley et al., 1987; Afonina et al., 2011). Interestingly, both molecules contain cleavage sites for a number of molecules associated with cells linked to the first response during inflammation.

Pro-IL-1α and pro-IL-1β contain cleavage sites for the neutrophil granule proteases neutrophil elastase (NE) and cathepsin-G (CG), and the mast cell-derived protease chymase. Early studies indicated that NE and CG cleavage of pro-IL-1β resulted in an active IL-1β molecule with low efficacy, however, a more recent study linked NE and CG cleavage to inactivation of IL-1β and activation of IL-1α (Afonina et al., 2015; Clancy et al., 2018). Chymase cleavage on the other hand, results in biologically active IL-1α and IL-1β (Mizutani et al., 1991; Afonina et al., 2011). Pro-IL-1α also contains a cleavage site

for the NK cell-derived cytotoxic granule protease granzyme-B, and cleavage at this site has also been shown to result in active IL-1α (Afonina et al., 2011). The significance of these findings is currently unclear but it is possible that these proteases are released by first responder cells to promote the activation and release of IL-1 from cell types which lack the canonical IL-1 processing machinery (As depicted in Figure 1.4 for IL-1α). In endothelial cells for example, the secretion of biologically active IL-1 cannot be triggered by stimuli used on myeloid cells, yet it can be triggered by NE (Wilson et al., 2007; Alfaidi et al., 2015). It is also possible that cellular necrosis, or pathogen inhibition of intracellular cleavage enzymes, causes deposition of pro-IL-1 within the extracellular milieu where first responder-derived proteases can process the molecules. Conversely, these protease cleavage sites might bind IL-1 to specific actions of each cell type. It has recently been uncovered, for example, that IL-1α contains a thrombin cleavage site which results in a biologically active 18 kDa IL-1α molecule which is important in coagulation (Burzynski et al., 2019). Further studies are clearly required to elucidate the actions of first responder proteases on IL-1 biology. On the contrary, great progress has been made studying the actions of specific enzymes for each pro-IL-1 molecule which links each to particular cell death processes.

IL-1α release in necrosis and necroptosis

IL-1α is closely linked to necrotic cell death and a type of programmed necrotic cell death termed necroptosis. Due to biological activity in the pro-form, IL-1α does not require further energy-dependent intracellular signals for activity. Thus, once produced, IL-1α can act independently of host cell survival. It then follows that under biological stresses, which lead to necrotic cell death, IL-1α can act as a proto-typical DAMP, sometimes referred to as 'alarmins'. Three groups have now shown this function of IL-1α *in vivo*. Chen et al. (2007) first showed that the immune response to necrotic cells was dependent on IL-1α, whilst a separate group showed that necrotic cell extracts contained IL-1α that binds to IL-1R1 on mesothelial cells to mediate its effects (Eigenbrod et al., 2008). Cohen *et al.*, (2010) investigated this further and highlighted a unique trait of pro-IL-1α that packages the protein within the nucleus and contributes to its release during necrosis. Unlike pro-IL-1β, pro-IL-1α contains a nuclear localisation sequence that transports the protein to the nucleus where a large proportion is retained (Luheshi et al., 2009). It is said that nuclear IL-1α can bind to chromatin and act as a transcription factor for some pro-inflammatory genes, although, in a diametrically opposed line of thinking, it has been suggested that

nuclear compartmentalisation may act as a further safeguard in preventing IL-1α release and is thus anti-inflammatory in nature (Buryskova et al., 2004; Werman et al., 2004; Luheshi et al., 2009). Either way, Cohen *et al.*, (2010) showed that release of nuclear IL-1α is the key signal that discriminates necrotic cell death from apoptotic cell death to stimulate an inflammatory response. It is now apparent that what the aforementioned groups believed was necrosis could actually have been a programmed cell death termed necroptosis.

Necroptosis is a rapid cell death pathway that occurs as a consequence of receptor interacting protein kinase (RIPK) 3 and mixed lineage kinase domain-like (MLKL) activation. Under normal conditions, binding of TNF to TNF receptor 1 (TNFR1) activates RIPK1 that triggers an intracellular signalling cascade converging on caspase-8 activation to induce 'extrinsic' apoptosis (Elmore, 2007). In the presence of viral or synthetic caspase inhibitors however, RIPK1 can no longer induce apoptosis and instead activates RIPK3 which in turn phosphorylates and relocates the pore-forming MLKL molecule to the plasma membrane (Kearney and Martin, 2017). It is currently unclear exactly how MLKL promotes necroptosis but it has been shown that this pathway also results in IL-1α release that is partly dependent on a class of calcium-dependent cysteine proteases termed calpains (England et al., 2014). The calpain family is comprised of 14 proteins with calpain-1 and calpain-2 being the most studied. Both calpain-1 and -2 proteolytically cleave IL-1α, when intracellular levels of calcium rise, and facilitate its secretion through an unknown mechanism that is closely tied to, but independent of, cell death (Groß et al., 2012; Tapia et al., 2019). Little is known about IL-1α processing by calpains during necroptosis and the field will surely improve when specific calpain inhibitors become available. The processing of IL-1β, on the other hand, has been the subject of extensive study.

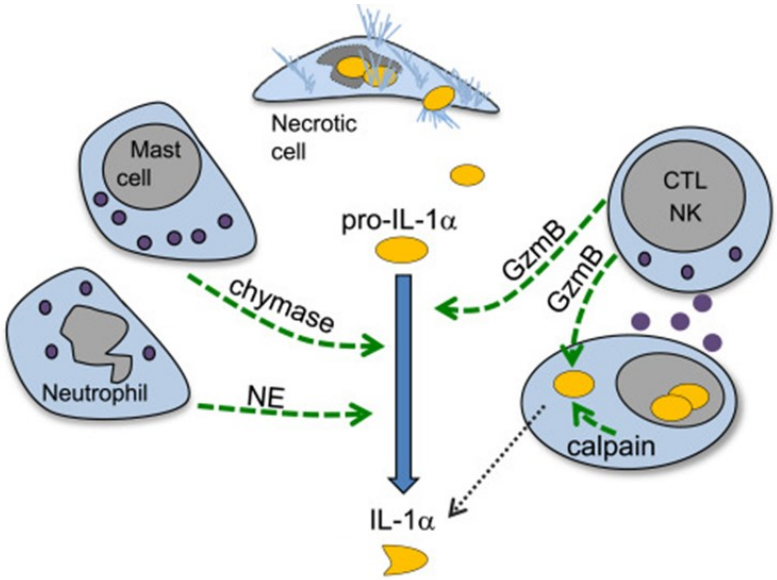

Figure 1.4 IL-1α cleavage mechanisms.
Cleavage and activation of the IL-1α molecule is closely linked to necrotic cell death through the calpain enzymes. IL-1α can also be released as an 'alarmin' and cleaved by enzymes of first responder cells such as neutrophil elastase (NE) from neutrophils, granzyme B (GzmB) from NK T cells, and chymase from mast cells. Schematic adapted from (Afonina et al., 2015).

IL-1β processing in pyroptosis

In macrophages, the activation and release of IL-1β is coupled to a second type of lytic programmed cell death known as pyroptosis. First described in 1992, the name pyroptosis was coined in 2001 following the observation that macrophages undergo rapid controlled necrotic-like cell death once infected with bacteria (Zychlinsky et al., 1992; Cookson and Brennan, 2001). Pyroptosis is derived from the Greek 'pyro', meaning fire or fever, and 'ptosis', denoting a falling, and the process is named as such due to the ensuing release of fever-inducing products such as IL-1β. Initially believed to be dependent on the enzyme that cleaves pro-IL-1β, it is now apparent that a number of enzymes of the same class can also induce pyroptosis (Kayagaki et al., 2011).

Caspases are cysteine-aspartyl-specific proteases (hence the name c-asp-ase) that cleave a broad spectrum of substrates which are important in programmed cell death and can be subdivided into apoptotic (caspase-2, 3 and 6-10) and pro-inflammatory (caspase-1, 4, 5, 11, 12) classes. First identified and named as the IL-1β converting enzyme (ICE) in cytosolic fractions of monocytes, caspase-1 is now known to cleave pro-IL-1β at two distinct sites to produce the active 17 kDa protein (Kostura et al., 1989; Thornberry et al.,

1992; Wilson et al., 1994). Caspase-1 itself is produced as a 45 kDa inactive zymogen that requires auto-cleavage for activity. Initially it was believed that auto-cleavage led to formation of an active tetrameric oligomer composed of two p20 and two p10 fragments, yet recently it was shown that this p20/p10 oligomer in fact represents a terminal inactive conformation (Wilson et al., 1994; Boucher et al., 2018). Instead, a transient p33/p10 species harbours greatest protease activity but incorporates a self-limiting mechanism through auto-cleavage to the terminal p20/p10 oligomer. Following activation, caspase-1 cleaves IL-1β and a constitutively expressed IL-1 family cytokine called IL-18. IL-18 is suggested to have no role in stroke (Wheeler et al., 2003), though this requires further investigation. Unlike caspase-1, caspase-11 (caspase-4 and -5 in human) cannot directly cleave IL-1β and instead has an important role in sensing intracellular LPS (Shi et al., 2014). Both caspase-1 and -11 can initiate pyroptosis but this finding took a while to establish due to the caspase-$1^{-/-}$ mice also being deficient in caspase-11 (Kayagaki et al., 2011). Therefore, many early studies attributed pyroptosis to caspase-1 alone.

In 2010, Agard, Maltby and Wells, published a study wherein they identified 82 caspase-1 substrates including a novel highly specific interaction with a poorly characterised protein named gasdermin-D (GSDMD). Upon analysis of expression patterns, which showed high levels of caspase-1 and GSDMD in immune cells, the group proposed GSDMD as a primary target of caspase-1 *in vivo*. It was not until 2015 however, that 3 independent research groups uncovered how both caspase-1 and -11 promote the secretion of active IL-1β during pyroptosis through cleavage of GSDMD (He et al., 2015; Kayagaki et al., 2015; Shi et al., 2015). It is now understood that caspase-mediated cleavage of GSDMD releases an N-terminal fragment that associates with the cell membrane to form 10 – 14 nm pores (Ding et al., 2016; Sborgi et al., 2016). It is likely that active IL-1β is released through these membrane pores, however, cell death occurs through poorly characterised GSDMD actions on ion flux, mitochondrial depolarisation and lysosomal leakage (de Vasconcelos et al., 2019).

Although pyroptosis can occur in its absence, caspase-1 activation is essential for release of the active 17 kDa IL-1β (Kayagaki et al., 2011). Caspase-1 is produced as an inactive zymogen that requires its own activation step. The process that governs caspase-1 activation rests on the formation of a large multi-molecular complex called an inflammasome.

1.6.4 Inflammasomes

Named in 2002 by Tschopp and colleagues, inflammasomes are an inducible high molecular weight complex typically composed of an intracellular PRR or seed molecule, an adaptor molecule and caspase-1 (Martinon et al., 2002). The majority of known inflammasome forming complexes sense activating stimuli via a PRR termed a nucleotide-binding oligomerisation domain (NOD)-like receptor (NLR). There are 22 NLR genes in the human genome and 34 in the mouse genome yet only a handful have been characterised to-date (Lamkanfi and Dixit, 2012). Each NLR contains a central NOD flanked by a C-terminal leucine rich repeat (LRR) and an N-terminal caspase recruitment domain (CARD) or pyrin domain (PYD) (Schroder and Tschopp, 2010). NLRs which contain an N-terminal PYD (NLRPs) require an adaptor molecule known as apoptosis-associated speck-like protein containing a CARD (ASC) in order to activate caspase-1. ASC is composed of a C-terminal CARD and an N-terminal PYD, hence its gene name *PYCARD*, and is thus able to associate with NLRPs and recruit caspase-1 through respective homotypic PYD-PYD and CARD-CARD interactions. NLRCs (those containing an N-terminal CARD) do not require ASC to activate caspase-1, although the recruitment of ASC has been shown to potentiate caspase activation (Mariathasan et al., 2004). Following NLR activation, ASC is recruited and rapidly assembles in a prion-like manner into filamentous speck structures reaching up to 2 μm in size (Hoss et al., 2017). These focal speck structures accumulate large numbers of caspase-1 molecules in close proximity and subsequently lead to its auto-activation. Therefore, inflammasome assembly (depicted in Figure 1.5) sits upstream of caspase-1 activation, pyroptosis and IL-1β release, and thus is tightly controlled.

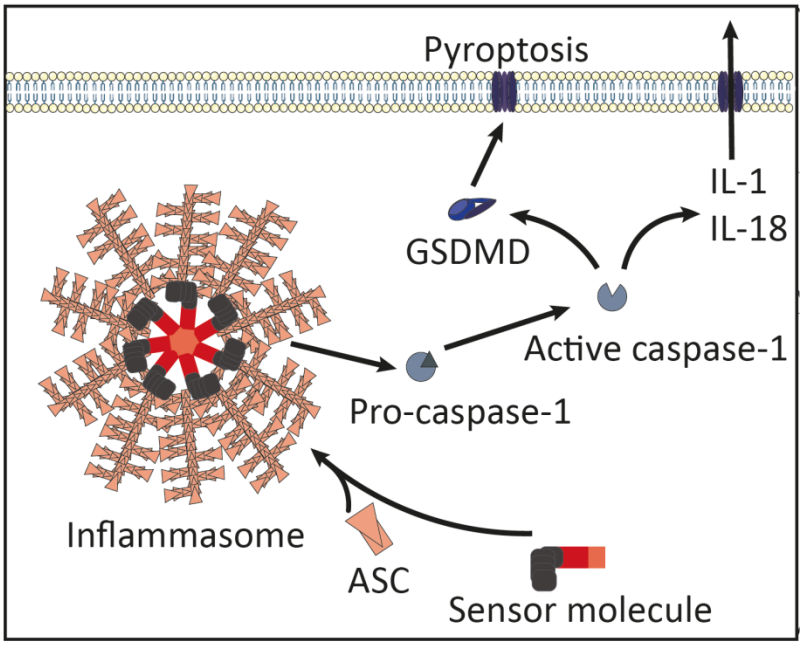

Figure 1.5 The mechanism of inflammasome activation.
Inflammasomes are multimolecular protein structures that form when a sensor molecule detects pathogen proteins or cell dyshomeostasis. In most cases, the adaptor molecule ASC (Apoptosis-associated speck-like protein containing a caspase recruitment domain) interacts with the activated sensor molecule through homotypic pyrin domain interactions and recruits caspase-1 to the complex through homotypic caspase recruitment domain interactions. In turn, the close proximity of caspase-1 molecules leads to autocleavage and subsequently activates gasdermin D (GSDMD), to induce a type of inflammatory cell death termed pyroptosis, and IL-1β.

NLRP3 activation

Inflammasomes can respond to a plethora of stimuli, including PAMPs such as flagellin and DAMPs such as ATP. The best characterised inflammasome is formed by the PRR NLRP3, which first came of interest following the finding that gain of function mutations caused familial autoinflammatory conditions known as cryopyin-associated periodic syndrome (Hoffman et al., 2001; Aganna et al., 2002; Aksentijevich et al., 2002). Since then, nearly 2 decades of research have uncovered important roles for NLRP3 in a wide variety of inflammatory diseases and revealed the intricate details of its activation (Mangan et al., 2018).

In macrophages NLRP3 appears to require a two-step activation process. The first step, often performed with LPS and known as 'priming', is required to upregulate expression of inflammasome components and downstream effectors such as IL-1β, caspase-1 and NLRP3 itself, and 'licence' the NLRP3 protein in a post-translationally modified pre-activated state (Swanson et al., 2019). Once primed, the second 'activation' step promotes inflammasome formation upon the sensing of NLRP3 activating ligands.

NLRP3 appears unique amongst inflammasomes because of its ability to respond to a diverse range of stimuli, and it is due to this ability that it is believed NLRP3 cannot directly interact with these ligands, but instead, is able to sense downstream cellular dysfunction. There is currently no unifying model of NLRP3 activation but it is thought to include non-mutually exclusive upstream signals including, ionic disturbance, lysosomal disruption, mitochondrial dysfunction and trans-Golgi network disassembly. Muñoz-Planillo *et al.*, (2013) showed that many known NLRP3 agonists converge on K^+ efflux, although more recently, Cl^- efflux, which is difficult to dissociate from K^+ efflux, has also been shown to be critical for efficient inflammasome activation (Green et al., 2018). It was initially believed that K^+ efflux was in fact an absolute requirement for NLRP3 activation, yet the discovery of K^+-independent agonists which may act through mitochondrial pathways has called that view into question (Groß et al., 2016; Wolf et al., 2016). It is currently unclear whether release of mitochondrial ROS, DNA or metabolic compounds triggers NLRP3 activation, or indeed whether NLRP3 oligomerisation is nucleated on the mitochondrial membrane itself (Zhou et al., 2011; Groß et al., 2016; Zhong et al., 2018). Recently however, Chen and Chen, (2018) discovered that NLRP3 activating stimuli cause dispersal of the trans-Golgi network (TGN) and it is here that NLRP3 oligomerisation is nucleated via an interaction with the phospholipid phosphatidylinositol-4-phosphate. This may prove to be a seminal finding in the field because dispersal of the TGN occurs independently of K^+ efflux, yet, K^+ efflux-dependent and –independent agonists require NLRP3-TGN association for activity. Current models of NLRP3 activation may therefore converge on TGN association.

The field of NLRP3 activation is flourishing and with each new study comes added complexity. Indeed, further and distinct NLRP3 activation pathways have been described; (i) the 'non-canonical inflammasome' is activated upon recognition of intracellular LPS by caspase-11 independent of TLR4, and (ii) a mechanism, specific to human and porcine monocytes, whereby an extended signal 1 stimulus facilitates 'alternative' NLRP3 activation independent of K^+ efflux, speck formation and pyroptosis (Kayagaki et al., 2011, 2013; Gaidt et al., 2016).

Other inflammasomes

Alongside NLRP3, there are another 4 known inflammasome forming proteins capable of responding to distinct stimuli and thus fine-tuning caspase-1 activation to specific scenarios. Activation mechanisms for NLRP1, NLRC4, and non NLR-inflammasome

members absent in melanoma (AIM) 2 and pyrin have been described. NLRP1 contains a C-terminal function-to-find domain (FIIND) that releases an active CARD subunit once the N-terminus has been cleaved by bacterial proteases (Sandstrom et al., 2019). NLRC4, on the other hand, becomes activated once a sensor molecule known as a NAIP (NLR family Apoptosis Inhibitory Protein) binds to bacterial flagellin and complexes with the NLRC4 protein (Kofoed and Vance, 2011). Thus it is currently unclear whether NLRP1 or NLRC4 have endogenous triggers. AIM2, however, is known to directly sense cytosolic double-stranded DNA, which can be of exogenous or endogenous origin, via a hematopoietic expression, interferon-inducible nature, nuclear localisation (HIN) domain (Hornung et al., 2009). Whereas, pyrin is activated following inhibition of the cytoskeletal-associated small GTPase RAS homologue gene family member A (RHOA), and thus, similar to NLRP3, can detect and respond to cellular dyshomeostasis (Park et al., 2016).

1.7 Interleukin 1 in the central nervous system

IL-1 is said to have important physiological and pathological functions within the central nervous system (CNS). As previously mentioned, IL-1β has been detected at low levels within the CNS where it acts as a neuromodulator. At low picomolar levels, IL-1β facilitates neuronal depolarisation, whereas, at higher concentrations (>10 picomolar), it hyperpolarises neurones to prevent firing. On top of this, IL-1 signals through a neurone-specific IL-1RAcP isoform that is unable to recruit MyD88 to the receptor complex and thus cannot activate NF-κB (Smith et al., 2009). Through these unique neuronal actions, IL-1 has adopted physiological CNS functions such as those contributing to sleep regulation, learning, and memory consolidation (Fang et al., 1998; Schneider et al., 1998; Vitkovic et al., 2000; Avital et al., 2003).

It was noted as early as 1985 that brain injury, in this case a stab wound, elicits production of supraphysiological levels of IL-1β which cause gliosis (Giulian and Lachman, 1985; Giulian et al., 1988). Following these findings, Perry and colleagues produced a series of studies presenting evidence that intraparenchymal high-dose IL-1 injection results in many of the multifaceted canonical features of brain inflammation, including BBB breakdown, neutrophil recruitment, cytokine and eicosanoid production, activation of endothelial adhesion molecules, vasodilation and raised CBF (Andersson et al., 1992; Anthony et al., 1997, 1998; Minghetti et al., 1999; Blamire et al., 2000; Bernardes-Silva et al., 2001). During this time, intraparenchymal IL-1β injection was also shown to cause death of

neurones, thus placing IL-1 at the bridge between brain injury and deleterious brain inflammation (Holmin and Mathiesen, 2000). Accordingly, IL-1 began to generate great interest in many fields of CNS disease. Pathological production of IL-1 is now known to contribute to sickness behaviour, neurodegeneration, multiple sclerosis, Parkinson's disease, epilepsy, traumatic brain injury, and not least; stroke (Allan et al., 2005).

1.7.1 Interleukin 1 in ischaemic stroke

Perhaps the most convincing evidence of a role for IL-1 in brain disease comes from the IS field. A cluster of IL-1 family genes are swiftly expressed in the brain following ischaemia and the IL-1α protein, in particular, is rapidly expressed by microglia in the period preceding immune infiltration (Luheshi et al., 2011). It was noted as early as 1992 that blocking IL-1 through administration of recombinant IL-1RA could protect the brain from ischaemic and excitotoxic damage (Relton and Rothwell, 1992). Since then, a vast number of studies have recapitulated these findings, not least, a multi-centre preclinical study evidencing the efficacy of IL-1RA in several IS models (Maysami et al., 2016; McCann et al., 2016). Central or peripheral administration of IL-1 also exacerbates neuronal loss in IS models and may have important clinical implications (Stroemer and Rothwell, 1998). Many common stroke comorbidities, such as hypertension and atherosclerosis, result in elevated levels of systemic inflammation which, when modelled in animals, exacerbates IS injury through IL-1 (McColl et al., 2007).

The cellular and molecular pathways underpinning the actions of IL-1 in IS are complex and remain somewhat a mystery. The use of transgenic mice has shown that IL-1α and IL-1β are not mutually exclusive and exacerbate IS injury in a semi-redundant fashion. Whereas, IL-1R1$^{-/-}$ mice are not protected from stroke, no longer benefit from IL-1RA treatment, but can still be exacerbated by IL-1β injection (Touzani et al., 2002). It is now believed that a truncated form of IL-1R1 driven from the IL-1R1 promoter could explain effects of IL-1R1$^{-/-}$ mice, but this is yet to be tested (Qian et al., 2012). Nevertheless, IL-1α/IL-1β double knockouts have a drastic 87% reduction in neuronal loss following IS (Boutin et al., 2001). Recently, IL-1 has been shown to promote neuroinflammation by two distinct routes and at least one of these routes is important in IS pathogenesis (Liu et al., 2019). Through conditional deletion of IL-1R1 in specific cell types, Wong *et al.*, (2019) identified brain endothelial cells and cholinergic neurons as the major downstream effectors of deleterious IL-1 signalling in IS. In this study, the authors were able to show that, alongside orchestrating the immune response, IL-1 acts on endothelial cells to reduce

CBF in the ischaemic hemisphere. Previous studies have also shown that IL-1 reduces blood flow following brain ischaemia through a mechanism that is unclear, but may include downstream endothelin-1 production and platelet aggregation in microvessels (Parry-Jones et al., 2008; Murray et al., 2014). Thus, alongside exacerbating neuroinflammation during IS, IL-1 may also be directly contributing to the no-reflow phenomenon. This would signal a unique action of IL-1 in ischaemia as injection of IL-1 into naïve brains increases CBF and, of course, one of the cardinal signs of inflammation is rubor (Blamire et al., 2000). Thus, IL-1-dependent CBF reduction is in contrast to the canonical model of inflammation and may hint at pleiotropic actions of IL-1 in diseased states. Nonetheless, whilst aspects of IL-1 biology in IS remain unsolved, the efficacy of IL-1RA in reducing preclinical IS injury has seen rapid implementation in clinical trials (Sobowale et al., 2016).

It is well documented that recombinant IL-1RA is safe and well tolerated in man following years of extensive research for its use in clinical rheumatoid arthritis (Mertens and Singh, 2009). A small phase II study measuring the effects of intravenous IL-1RA in acute IS patients echoed the findings of the arthritis field, in showing IL-1RA was well tolerated and was not attributed to any adverse events. Furthermore, the levels of IL-6 and C-reactive protein (CRP) (both biomarkers consistently linked to poor clinical outcome) were reduced in patients in the treatment arm of this study and 3-month clinical outcome trended toward improvement (Emsley et al., 2005). In a second phase II clinical trial using subcutaneous IL-1RA injections (which was required due to intravenous formulations no longer being manufactured), IL-1RA again reduced IL-6 and CRP levels but was not associated with better outcome (Smith et al., 2018). Mediation analysis suggested that, whilst subcutaneous IL-1RA reduced poor odds of outcome by reducing IL-6, there was an unknown residual increasing odds of poor outcome in the treatment arm. It is unclear what factor governed this unknown residual but the authors point toward a possible negative interaction of IL-1RA and thrombolytics, however, in preclinical models no such interaction was found (Maysami et al., 2016). Overall, these limited clinical trials have proven that IL-1RA reduces inflammation in clinical IS, as it does in preclinical models, but more experimental studies are warranted to elucidate possible pleiotropic actions of IL-1 in this setting.

1.7.2 Interleukin 1 in haemorrhagic stroke

In contrast to preclinical IS, very few studies have investigated IL-1 biology in experimental models of ICH. In rodents, IL-1β mRNA is rapidly expressed in the brain within 3 hours of collagenase-induced ICH and remains elevated for between 3 and 7 days (Liesz, Middelhoff, et al., 2011). Similar expression patterns are also found in porcine and rodent autologous blood injection models (Lu et al., 2006; Wagner et al., 2006; Wasserman et al., 2007). Microglia and astrocytes express IL-1β following ICH and the molecule is found at extremely low levels in patient serum and may rise over time (Wasserman et al., 2007; Li et al., 2017; Abid et al., 2018). No study to date has assayed for IL-1α in preclinical or clinical ICH and only one study has attempted to inhibit IL-1R1. In this study, Masada *et al.*, (2001) used an adenovirus to overexpress human IL-1RA in the brains of rats 5 days prior to autologous blood or thrombin injection. In the autologous blood model, overexpression of IL-1RA had no effect at day 1 but reduced oedema at day 3. IL-1RA also reduced neutrophil infiltration following thrombin injection, although, the thrombin formulation may have contained LPS contamination and thus inadequately modelled ICH. Nevertheless, what role IL-1 has in post-ICH inflammation remains an important open question. IL-1 expression has been found in the brain preceding detrimental immune recruitment, yet no study has attempted to fully ascertain its actions and measure functional outcome by inhibiting IL-1R1. IL-1RA has been given to ICH patients however.

Despite very little evidence pertaining to beneficial effects of IL-1RA in ICH, five ICH patients were entered into the first phase II study of IL-1RA in stroke (Emsley et al., 2005). Unfortunately, all five patients were randomised into the active arm of the study, by chance, and left interpretations of findings difficult. Of the five patients, one experienced neurological deterioration which was not deemed to be a result of treatment. There were, however, eight infectious episodes in the five patients treated with IL-1RA, which is high as previous studies indicate that only around 30% of ICH patients experience infection (Lord et al., 2014). Although it must be stressed that it is difficult to fully interpret these findings due to a lack of controls. A phase II clinical trial is currently ongoing to assess the effects of IL-1RA on perihaematomal oedema and is forecasted for completion in 2020 (NCT03737344).

1.7.3 Inflammasomes in stroke

In 2017, a clinical trial called the Cardiovascular Risk Reduction Study (Reduction in Recurrent Major CV Disease Events) (CANTOS) was published in the New England Journal of Medicine that has since had a profound impact on how we view inflammation in cardiovascular disease (Ridker et al., 2017). Prior to this trial, IL-1 had been implicated as a critical mediator in the pathogenesis of atherosclerosis and atherothrombosis (Duewell et al., 2010). The phase III CANTOS trial, conducted over four years with over 10,000 patients, showed that targeting IL-1β with a monoclonal antibody, termed canakinumab, significantly lowered rates of recurrent cardiovascular events, thereby proving IL-1β, and in all probability inflammasomes, significantly contribute to atherothrombosis. Interestingly, stroke rates were unaffected by canakinumab treatment but, with only 172 stroke cases, statistical power was extremely limited. There is however, evidence that IL-1β and inflammasomes do affect post-stroke inflammation.

Despite earlier reports suggesting IL-1α and IL-1β can act alone or in combination to potentiate ischaemic damage in the MCAO model, Liberale *et al.*, (2018) found that a murine-equivalent canakinumab antibody, administered at time of reperfusion, reduced infarct volume, oedema and improved neurological outcome. This latter report also built on the findings from a paper published in 1995, showing that intracerebroventricular administration of an anti-IL-1β antibody markedly reduced infarct volume in a rat model of MCAO (Yamasaki et al., 1995). These conflicting findings remain unexplained but answers may lie in the method of inhibition. One possibility is that genetic deletion of one IL-1 molecule may facilitate compensatory upregulation of another as has been seen for other molecules (El-Brolosy and Stainier, 2017). In any case, there are multiple preclinical reports implicating inflammasomes in post-stroke pathophysiology.

First evidence of a role for inflammasomes in IS pathogenesis came in 1997 when Friedlander *et al.*, generated a mouse line overexpressing a dominant negative caspase-1 mutant. Neurones from these mice were resistant to serum deprivation and the mice themselves were protected from ischaemic damage in the MCAO model. At the same time, Friedlander and colleagues contributed to a second paper highlighting the protective capacity of a specific caspase-1 inhibitor in IS models (Hara et al., 1997). The importance of caspase-1 activity in stroke was compounded the following year when Schielke *et al.*, (1998) presented evidence that caspase-1 deficient mice had a 52% smaller infarct following permanent MCAO. Since then, a number of published studies have described the

efficacy of several caspase-1 inhibitors in limiting IS damage in preclinical models (Rabuffetti et al., 2000; Ross et al., 2007). It was not until 2010 that caspase-1 inhibition was tested in an animal model of ICH however (Wu et al., 2010). In this study, the caspase-1 inhibitor Ac-YVAD-CMK was shown to reduce levels of BBB breakdown markers and improve neurological outcome in the collagenase-induced mouse model of ICH. Interestingly, caspase-1 activation in stroke may first occur in neurones and not immune cells.

Caspase-1 activation occurs within 30 minutes of MCAO, in a period preceding IL-1β production and immune infiltration (Benchoua et al., 2001; Gelderblom et al., 2009). Moreover, in their seminal study, Friedlander *et al.*, (1997) used a neurone-specific promoter to overexpress the dominant negative caspase-1 mutant that was found to be protective in IS. Caspase-1 may, therefore, mediate immediate neuronal death following IS. Interestingly, neurones may have a unique set of cell death processes that rely on the caspases but incorporate diverse downstream effectors. Neurones do not express GSDMD and caspase-1 activation in these cells promotes apoptotic cell death via caspase-3 activation (Zhang et al., 2003; Tsuchiya et al., 2019). Whether this is true apoptotic cell death or a secondary form of pyroptosis is unclear. Caspase-3 has recently been shown to induce pyroptosis by cleaving a second GSDM protein known as GSDME (or deafness, autosomal dominant 5) (Wang et al., 2017). Much like caspase-1 mediated pyroptosis, caspase-3 cleavage of GSDME results in an N-terminal fragment that associates with, and permeabilises, the plasma membrane. Neurones express high levels of GSDME but neuronal pyroptosis is yet to be fully described (Zhang et al., 2014, 2016). It is known that caspase-1 activation precedes caspase-3 activity following stroke however (Benchoua et al., 2001).

Of the 5 known inflammasome forming proteins, NLRP1, NLRP3, NLRC4 and AIM2 have been referenced in preclinical stroke literature (Barrington et al., 2017). Inflammasome components are rapidly expressed in several preclinical models of IS and ICH and levels remain high for up to 7 days. NLRP1 was the first inflammasome to be studied in the stroke field where it was found to be expressed in neurones, astrocytes and microglia (Abulafia et al., 2009). Administration of an anti-NLRP1 antibody prevented inflammasome activation but failed to reduce infarct volume in a mouse model of IS. NLRP1 activation can be triggered by intracellular ATP depletion and, with the protein being found in neurones, may instigate neuronal caspase-1 activation during ischaemia.

Anti-NLRP1 antibodies are unlikely to pass the BBB and enter neurones within the 30 minute delay of caspase-1 activation and this may explain the null effect on lesion volume using this method of NLRP1 inhibition. Future studies using small molecule inhibitors or transgenic animals lacking NLRP1 might reveal that this inflammasome complex signals early caspase-1 dependent neuronal death following IS.

AIM2 and NLRC4 contribute to poor neurological outcome in the murine model of MCAO (Denes et al., 2015). Within 24 hours of injury, $AIM2^{-/-}$, $NLRC4^{-/-}$ and $ASC^{-/-}$ mice had fewer activated microglia and an attenuated immune response. AIM2 contributes to sterile inflammatory pathologies through its ability to respond to cytoplasmic DNA. NLRC4, on the other hand, has no known endogenous ligand but, alongside NLRP3, may respond to lysophosphatidylcholine (LPC) (Freeman et al., 2017). LPC is formed through phospholipase A_2 (PLA_2)-catalysed hydrolysis of phosphotidylcholine (Law et al., 2019). LPC levels rise dramatically within infarcted brain tissue and inhibition of the PLA_2 enzyme improves outcome in rodent MCAO (Hoda et al., 2009; Shanta et al., 2012; Mulder et al., 2019). Thus NLRC4 may respond to LPC to trigger NLRC4 activation in IS.

Several studies have now targeted the NLRP3 inflammasome within the stroke field with conflicting outcomes. Antibody targeting, small molecule inhibition and genetic deletion of NLRP3 have all been shown to reduce infarct volume in MCAO models (Yang-Wei Fann et al., 2013; Yang et al., 2014; Ito et al., 2015; Ismael et al., 2018). In contrast however, Denes *et al.*, (2015) found that $NLRP3^{-/-}$ mice were not protected in MCAO. Importantly, neither of the studies using transgenic animals compared $NLRP3^{-/-}$ mice to the correct littermate controls. The genetic composition of transgenic mice is often very different to commercially available mice of the same strain (Holmdahl and Malissen, 2012). Moreover, transgenic mice housed separately to controls are liable to further genetic drift and are exposed to unique environmental stimuli. In line with this, inflammasome-deficient mice have been shown to have changes to the microbiome that are dependent on genetic drift and environmental differences rather than the absence of the gene of interest (Levy et al., 2015; Mamantopoulos et al., 2017). Microbiome changes may be especially important in preclinical stroke studies as altered microflora shape the immune response and can therefore exacerbate or attenuate brain injury (Benakis et al., 2016). In the ICH field, small interfering RNA knockdown and administration of the potent NLRP3 inhibitor, MCC950, attenuates brain injury and brain inflammation in autologous blood and collagenase injection models (Ma et al., 2014; Ren et al., 2018).

Despite the small amount of ICH studies and the conflicting evidence for causal roles of NLRP3 in IS, there are plenty of stroke-relevant NLRP3 activating stimuli. The ischaemic cascade leads to mitochondrial damage, ROS production, lysosomal destabilisation and raised intracellular calcium levels and these have all been shown to activate NLRP3 (Lénárt et al., 2016). Cell swelling has been reported to trigger NLRP3 activation and cytotoxic oedema contributes to cell death in IS and ICH (Compan et al., 2012). One of the best studied NLRP3 activators is ATP which, at high millimolar levels, triggers P2X7R-dependent K^+ efflux (Pelegrin and Surprenant, 2006). Cell death in stroke releases intracellular stores of ATP and inhibition of the P2X7R pathway reduces brain injury in preclinical models of IS and ICH (Cisneros-Mejorado et al., 2015; Feng et al., 2015). Moreover, during ICH the breakdown of RBCs leads to the release of intracellular Hm molecules which have also been shown to trigger NLRP3 activation through the mitochondrial ROS pathway (Dutra et al., 2014). These diverse NLRP3 activating stimuli, along with evidence for its detrimental role in a variety of inflammatory disease, warrant further study into its actions during stroke.

1.8 Summary and aims

Stroke is one of the leading causes of death and disability in the world. Despite progress in designing efficacious therapies for IS, very few patients worldwide have access to licensed procedures and those with haemorrhagic stroke are left without options entirely. The diametrically opposed pathophysiology of the two major stroke subtypes makes universal stroke therapies difficult to design. The acute immune response to both stroke subtypes exacerbates brain injury and thus may represent a potential universal target. There is a convincing amount of data to suggest that the prototypical cytokine IL-1 orchestrates the acute immune response and its downstream detrimental effects in stroke. This makes targeting IL-1, in particular, an attractive therapeutic option. IL-1 biology is rapidly evolving, however, and many timely questions remain unaddressed by current studies.

The overarching aim of this thesis is to investigate the actions of IL-1 in brain haemorrhage and ischaemia using the most relevant preclinical models. This thesis will specifically aim to:

- Develop and optimise the collagenase-induced mouse model of ICH, which will be used for the first time in our laboratory, in order to improve detection power and reduce animal suffering.
- Reveal the pathophysiological consequences of IL-1 signalling during ICH by characterising its expression patterns, in mouse and man, and measuring the effects of its inhibition using relevant pharmacological strategies.
- Determine the relative importance of the NLRP3 inflammasome in the pathogenesis of acute IS using pharmacological and genetic approaches in the clinically relevant clot-forming dMCAO model.

Chapter 2: Refining a murine model of ICH

2.1 Paper title and authors

A refined workflow to detect motor deficits in the collagenase-induced mouse model of intracerebral haemorrhage

Jack Barrington[1], Adrian R. Parry-Jones[1], David Brough[1], Stuart M Allan[1]

[1]Faculty of Biology, Medicine and Health, Manchester Academic Health Science Centre, University of Manchester, AV Hill Building, Oxford Road, Manchester, M13 9PT, U.K.

I designed, implemented and analysed all experiments and wrote the manuscript under guidance from A.P.J, D.B, and S.M.A.

2.2 Abstract

Large attrition rates and variation in brain lesion volumes plague the preclinical stroke field and have led to the biased publication of positive underpowered studies. It is therefore imperative to perform properly powered empirical experiments, yet consideration must also be given to the ethical duty of reducing animal usage and suffering in research. Intracerebral haemorrhage (ICH) is a devastating condition that represents an area of unmet clinical need. In the absence of *in vitro* models able to recapitulate the complex pathophysiology of ICH, animal research is essential. Current animal models of ICH induce large haemorrhages that result in variable haematoma sizes and severe behavioural phenotypes. Using the clinically relevant collagenase-induced mouse model of ICH, we show that haematoma size can be reduced to limit suffering whilst retaining important features of ICH, such as inflammation. We also optimise the accelerating rotarod performance assay to sensitively detect neuromotor impairment in the absence of hemiplegia. We have thus developed a refined workflow to detect changes in blood load and neuromotor injury following ICH using minimal animal numbers and reducing suffering.

2.3 Introduction

Stroke is one of the leading causes of mortality and morbidity worldwide and can present through either occlusion or rupture of cerebral vessels. Intracerebral haemorrhage (ICH) accounts for around 12 % of all stroke cases and occurs when a diseased vessel bleeds into the brain parenchyma[1]. It is estimated that 40 % of patients die within the first month of ICH and, of those that survive, 40 % are left with severe, life-changing, disabilities[2]. There are two distinct waves of neuronal injury following ICH. An initial primary injury is triggered by mass effect of blood accumulating within the cerebral compartment[1]. Following this, a progressive second wave of injury occurs that is defined by a variety of features such as rebleeding, inflammation, red blood cell (RBC) toxicity and oedema[1]. Thus, whilst it is difficult to therapeutically target primary injury during ICH, secondary injury represents a therapeutic window of opportunity. Translational studies must therefore focus on targeting this second wave of injury associated with ICH.

Injection of bacterial collagenase or autologous blood are the two most common inducible models of ICH[3]. Intracerebral collagenase injection results in the breakdown of vascular basal lamina leading to progressive bleeding from small vessels. Autologous blood injection, on the other hand, deposits a RBC mass within the brain causing immediate mechanical disruption of brain tissue. Both models recapitulate clinical features of secondary injury in ICH such as inflammation, RBC toxicity and oedema[3]. Of the two models however, the collagenase injection model mimics more aspects of the clinical condition, such as haematoma expansion and microvascular disruption, driven by continued bleeding from *in situ* vessels[3]. The complex pathophysiology of ICH is currently impossible to recapitulate *in vitro* and *in vivo* models are therefore essential tools for preclinical research in the field.

The preclinical stroke field has been subject to many empirical evaluations of study quality with evidence of excess significance bias. Underlying factors promoting excess significance bias pertain to publication bias and poor study design, including underpowered investigations[4,5]. In result of this, there have been calls to increase the amount of animals used in translational stroke studies to ensure sufficiently powered, although this directly contradicts ethical aspirations to reduce animal usage in research. Current preclinical ICH studies report on severe outcomes such as mortality and hemiplegia, despite the extent of brain damage being dependent on dose of collagenase[6].

Thus, there is the opportunity to reduce animal suffering in ICH research by reducing collagenase dose. Whilst the ischaemic stroke field has paved the way in refining animal models to reduce suffering, there have been no efforts to reduce suffering in preclinical ICH work[7].

One way of overcoming the issue of publishing underpowered studies using severe models is to optimise current protocols to reduce suffering and improve detection power. In preclinical ICH, functional assessments are required to fully elucidate the effects of perturbations but are unfortunately a major source of variation. The most common functional assessments are forelimb placement tests, neurological severity scores and corner turn tests, which all measure severe phenotypes such as hemiplegia[6]. The rotarod assay is used frequently in neurodegenerative conditions that affect motor function. Optimised rotarod protocols can sensitively and robustly detect motor impairment in the absence of outward behavioural phenotypes[8]. To date, few studies have used the rotarod assay as a measure of neuromotor dysfunction following ICH and there are no published studies containing optimised protocols to do so.

2.4 Objectives

The specific objectives of this study are:

- Establish a collagenase dose which promotes consistent haematoma volumes without causing death or substantial distress.
- Identify and subsequently optimise a neuromotor functional assay that can confidently measure motor impairment at the refined collagenase dose.
- Confirm the refined model still produces significant immune cell trafficking to the brain.

Herein we show that an optimised accelerated rotarod assay can be used to sensitively detect motor impairment in ICH, using a dose of collagenase that does not result in hemiplegia but retains important features of secondary injury. We thus provide a workflow to measure functional consequences in the collagenase induced-ICH mouse model that reduces animal suffering and numbers needed to detect statistically significant effects.

2.5 Materials and Methods

Animals

Animal procedures were carried out in accordance with the Animal Scientific Procedures Act (1986) and the European Council Directive 2010/63/EU, and were approved by the Animal Welfare and Ethical Review Body, University of Manchester, UK. Mice had free access to food and water and were housed under light-, humidity- and temperature controlled conditions. Animals were maintained under standard laboratory conditions: ambient temperatures of 21 °C (±2 °C), humidity of 40–50 %, 12 h light cycle, ad libitum access to water and standard rodent chow. Animals were randomised to groups using the research randomizer tool (https://www.randomizer.org/) and groups were concealed from researchers during the sham vs ICH trials. 18 – 24 week old male C57BL/6J mice (Charles River) were used throughout.

Surgery

Mice were induced under anaesthesia using 4 % isoflurane in 70 % N_2O and 30 % O_2 and fur was shaved from the head. Mice were then transferred to a feedback-controlled heating pad set to 37 ˚C, securely fixed to a stereotactic frame (Stoetling), anaesthesia maintained at 1.5-2.0 % isoflurane in 30 % N_2O and 70 % O_2 using a nose cone, and Videne (EcoLab) applied to the scalp. A longitudinal midline incision above the skull was performed and periosteum stripped away from the midline on both sides. A burr-hole was created using a micro-drill and a glass micropipette (BLAUBRAND, pulled at 70 ˚C) inserted at the following co-ordinates from bregma: anterior-posterior 0.0 mm, lateral -2.0 mm, deep -2.7 mm. 0.5 µL of 0.06 units μL^{-1} or 0.09 units μL^{-1} or 0.12 units μL^{-1} of collagenase (C2399, Sigma) dissolved in saline (or saline alone for sham surgeries) was then injected at a rate of 1 µL min^{-1}. The needle was left in situ for 10 minutes before removal and wounds sutured. The scalp was cleaned once more with Videne and a topical analgesia was applied (EMLA cream, AstraZeneca). Mice were given a subcutaneous bolus of saline (10 mL kg^{-1}) and buprenorphine (50 µg kg^{-1}, Vetergesic, UK) before being recovered in 28 ˚C housing. Once recovered, mice were then transferred to ventilated cages suspended over a heating pad with free access to mashed food and water in normal housing conditions.

Neuroscore

Neurological deficits were assessed using the 6-point neuroscore as described previously[10]. Briefly, animals were monitored in an open cage and graded based on the following scale:

0: normal; 1: mild circling behaviour with or without inconsistent rotation when suspended by the tail; 2: mild consistent circling; 3: consistent strong and immediate circling, the mouse holds a rotation position for more than 1-2 seconds; 4: severe rotation or immobility; 5: dead.

Cylinder Test

Mice were placed in an acrylic glass cylinder (diameter: 10 cm; height: 15 cm) and recorded from cameras positioned above the cylinder for a total of 5 min. Scoring was performed as previously described[11]. Mice were monitored for 20 rears and initial paw(s) placed on the cylinder were scored as left, right or both. A laterality index was calculated as follows: (right – left) / (right + left + both). Thus a score of 1 indicates severe left hemiparesis, whereas, a score of 0 indicates no paw preference.

Accelerating rotarod assay

Mice were allowed to habituate to behavioural room and handled for at least one week prior to commencement of training. Mice were trained on consecutive days using the following protocol. Following a 15 second loading period the rotarod was set to accelerate from 4 to 40 rpm over 300 seconds. Each mouse was deemed to have completed the task when it had fallen from the apparatus, accrued 3 passive rotations, or stayed on the apparatus until 300 seconds. The time at which mice completed the task was recorded. Once all animals had finished the run the apparatus was thoroughly cleaned with a 70 % ethanol solution. 3 runs were performed per day with a 15 minute inter-trial interval. On test days following ICH, the same protocol was followed with mice performing 3 runs.

Histology

Mice were transcardially perfused with PBS followed by 4 % paraformaldehyde (PFA). Brains were removed and post-fixed in 4 % PFA for 24 h at 4 ˚C followed by cryoprotection in 20 % sucrose PBS at 4 ˚C for up to 4 days. Cryoprotected brains were then frozen in -50 to -60 ˚C isopentane and 20 µm coronal sections taken every 400 µm using a Leica cryostat. Brain sections were digitally scanned, and regions of interest (ROI) drawn around the haematoma on each section using imageJ. Haematoma volume was calculated by summing the area of all ROIs and multiplying by the inter-section interval (400 µm).

Flow cytometry

Mice were transcardially perfused with PBS and brains isolated, hemisectioned and cerebellums removed. Single cells were isolated from contralateral and ipsilateral hemispheres as described previously[12]. Briefly, hemispheres were sectioned with fine scissors and digested for 30 min at 37 ˚C in a HBSS (with cations) solution containing 2 mg mL^{-1} collagenase D (Sigma), and 28 U mL^{-1} DNAse (Sigma). Digestion was stopped by 40 µL addition of 0.5 mM EDTA and samples were passed through a 70 µm sieve (BD Biosciences) with HBSS containing 3% foetal bovine serum (FBS). Myelin was removed by running pellets through a 37 % (w/v) Percoll (Sigma) at 2000 x*g* for 10 min without brake and aspirating the resultant myelin layer. Cell pellets were washed and RBC lysed (BD Pharmlyse, BD Biosciences) before incubation with the following antibody cocktail: 50 µg mL^{-1} FC block (Clone 93, ebioscience), 1:1000 Zombie NIR (ThermoFisher), 0.2 µg mL^{-1} CD11b-PE (Clone M1/70, BD Bioscience), 2 µg mL^{-1} CD3e-APC (Clone 17A2, Biolegend), 0.67 µg mL^{-1} CD45-PerCP/Cy5.5 (Clone 30-F11, eBioscience), 1 µg mL^{-1} Ly6C-FITC (Clone AL-21, BD Bioscience) and 0.67 µg mL^{-1} Ly6G-ef450 (Clone 1A8, TONBO biosciences). Samples were acquired on a FACs Canto II (Becton Dickenson) using BD FACSDiva software (BD Biosciences). Data was analysed using FlowJo V.10 (Tree Star Inc.) with gates set by fluorescence minus one controls.

Statistical analysis

Data are presented as individual data points with a line at the median (neuroscore), mean or mean ± standard deviation. Wilcoxon signed rank test was used to compare neuroscores to a hypothetical value of 0. One sample t test was used to compare laterality indices to a hypothetical value of 0. Paired or unpaired Student's t tests were used to test for differences between 2 groups. One-way analysis of variance (ANOVA) was used to compare differences between groups of >2 with Tukey's posthoc used for multiple comparisons. Two-way repeated measures ANOVA was used to compare differences in the powered rotarod experiment with Sidak's posthoc used to compare differences between groups on each day. Linear mixed modelling was used to evaluate the effect of baseline inclusion on the modelled data[13]. All factors and interactions were modelled as fixed effects. A within-subject design with random intercepts was used for both models. The significance of inclusion of a dependent variable or interaction terms was evaluated using log-likelihood ratio. Homoscedasticity and normality were evaluated graphically using predicted vs residual and Q-Q plots, respectively. All analyses were performed using GraphPad Prism 7.00 apart from linear mixed modelling which was performed using R

(version 3.3.3). Equal variance and normality were assessed with the Levene's test and the Shapiro–wilk test, respectively, and appropriate transformations were applied when necessary. Accepted levels of significance were *P<0.05, **P<0.01, ***P<0.001.

Blinding

Operator was blinded for experiments contained within Figures 2.1 and 2.4.

2.6 Results

Establishing a collagenase dose with limited mortality and morbidity

The most powerful prognostic factor for outcome in ICH is haematoma volume and in the collagenase-induced mouse model this is determined by dose of collagenase. We thus first aimed to identify the collagenase dose that gave consistent haematoma volumes with limited mortality and suffering. One previous study has directly compared multiple doses of collagenase ranging from 0.030 U to 0.075 U in 0.015 increments. Zhou et al[14] (2013) found that, whilst all doses resulted in a haematoma, only 0.060 U and 0.075 U were associated with mortality (5 % and 17.5% respectively). To limit mortality we therefore used 0.060 U as our greatest dose and compared to 0.030 U and 0.045 U (Figure 2.1). All collagenase doses tested resulted in the development of an intracerebral haematoma. One animal from the 0.060 U group died overnight whilst another was culled after reaching humane endpoints (immobility and laboured breathing). No animals were lost in either of the 0.030 U or 0.045 U groups. We noted that animals in the 0.060 U group had outward signs of distress such as kyphosis, piloerection and orbital tightening, whereas few, if any, in other groups showed these symptoms (data not shown). The 0.045 U injection resulted in significantly less variation in haematoma volume than other groups ($P < 0.003$, Bartlett). As collagenase is an enzyme, we tested the stability of reconstituted 0.045 U solutions stored at – 80 ˚C for either 2 weeks or 9 months (Supplementary Figure 1). Compared to 2 week old solutions of collagenase, 9 month old frozen solutions produced a significantly smaller haematoma volume ($P = 0.002$). Following this discovery we used <6 month old collagenase for subsequent studies. Together these data show that 0.045 U collagenase reduces attrition rates, animal suffering, and the number of animals required to detect statistically significant differences in haematoma volume (Supplementary Figure 2). We next looked to identify neuromotor deficits at this dose.

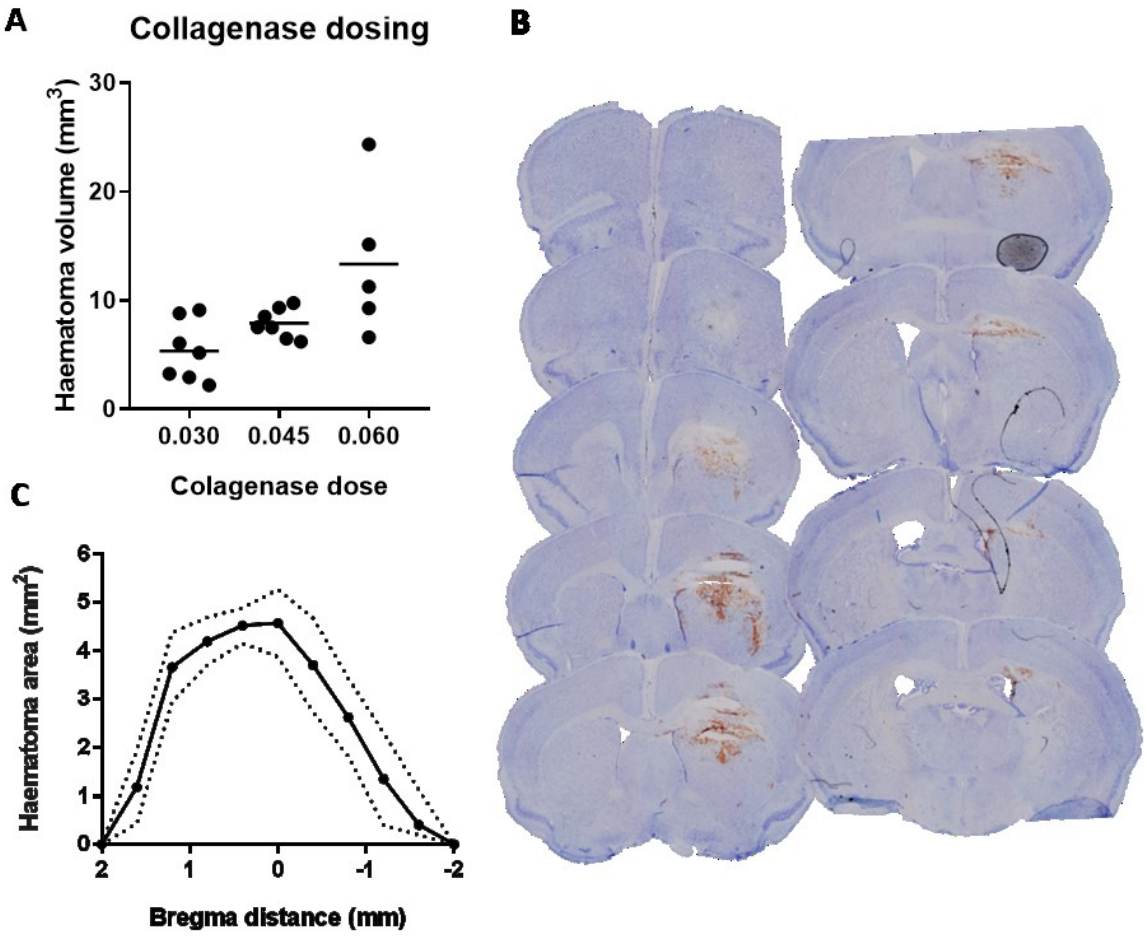

Figure 2.1 0.045 U collagenase injection results in consistent haematoma volumes without mortality.
(A) 7 18 – 24 week old male C57BL/6J mice were intrastriatally injected with 0.030 U, 0.045 U or 0.060 U of collagenase VII-S and brains were taken for histological assessment of haematoma volume. (B) Representative haematoma following 0.045 U collagenase-induced ICH. (C) Haematoma distribution plotted as mean ± SD following 0.045 U collagenase induced ICH.

Identifying a neuromotor assay to detect functional impairment

Behavioural differences were assessed using three neuromotor assays common to the stroke field. The 6-point neuroscore system measures gait changes following stroke ranging from 0 (normal) to 5 (dead/immobile) with midrange numbers grading circling behaviour[10] (see methods). The cylinder test measures forepaw asymmetry when rearing and is converted into a laterality index using right and left forepaw ratios[11]. The accelerating rotarod performance test assesses maximal gait performance by challenging animals to balance on a rotating beam that accelerates over a period of 300 seconds[8]. Following 0.045 U collagenase-induced ICH, all animals curled to one side when suspended by the tail but only 1 animal out of 6 showed mild circling behaviour and scored 1. As all other animals showed no circling tendencies they were subsequently

scored 0 (Figure 2.2A). The group of 6 animals therefore had no significant deficits using the 6-point neuroscore scale. In line with this, we found a spread of laterality indices in the cylinder test (range: -0.75 to 0.78) with a mean of 0.01 that was not significantly different to 0 (Figure 2.2B). Following a 4 day training period to avoid indirect measurement of motor skill learning[8], mice showed a significant reduction in rotarod performance following ICH (217.2 s ± 47.91 vs 119.2 s ± 60.54, P = 0.0005) (Figure 2.2C). Thus, together our data show that, of the three behavioural assays, only the accelerating rotarod performance assay is able to detect statistically significant changes in behaviour following 0.045 U collagenase-induced ICH. We next looked to optimise the training phase of the rotarod in order to reduce animals required to detect statistically significant differences using this assay.

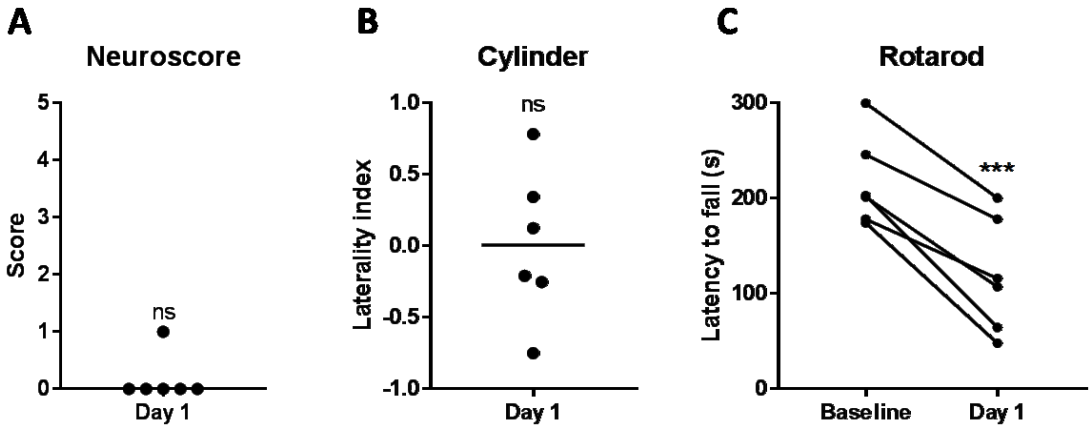

Figure 2.2 The accelerating rotarod assay outperforms other neuromotor tests following 0.045 U collagenase-induced ICH.
(A) ICH was induced in 6 C57BL/6J male mice and 6-point neuroscore, (B) cylinder test and (C) accelerating rotarod assay was used to measure motor deficits. ns = not significant. *** = P<0.001.

Optimising the rotarod assay training phase

Having previously shown that animal performance dropped off beyond 3 days of training (Supplementary Figure 3), we limited the rotarod training phase to 3 days with 3 trials per day. The length of time each mouse was able to balance on the rotating beam significantly improved over time ($F(1.99, 37.82) = 51.33$, $P < 0.0001$) and each days score was significantly greater than the previous (Day 1 vs Day 2, $P < 0.0001$; Day 2 vs Day 3, $P = 0.028$, Sidak) (Figure 2.3A). By graphical assessment we noted a trend whereby latency to fall was substantially quicker in the first run of each day (Figure 2.3B). Comparing standard deviations from 3 trial vs 2 trial averages we found the latter substantially

reduced variation. Thus, training mice for 3 days and using the average score from the final 2 trials is the most statistically powerful rotarod training method (Figure 2.3C). Next, we looked to test our newly developed workflow to detect differences in motor function following murine ICH whilst controlling for surgical intervention.

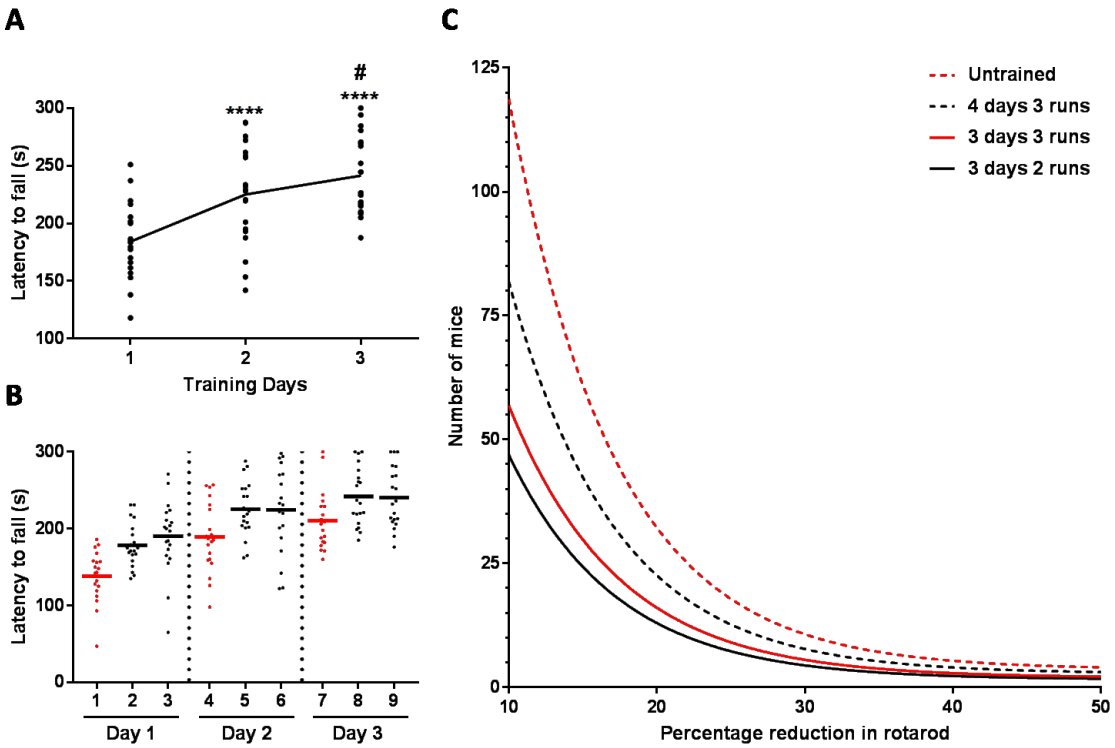

Figure 2.3 An optimised rotarod training phase reduces animals needed to detect differences.
(A) 20 male C57BL/6 mice were trained on the rotarod for 3 consecutive days with 3 runs per day. (B) Mice performed poorly on the first run each day and thus (C) averaging the final two runs reduces animals needed to detect statistically significant effects. **** = P<0.0001 vs day one, # = P<0.05 vs day two.

Testing the reproducibility of the model

In our preliminary behavioural experiment, we found that mice subjected to 0.045 ICH showed a 45 % reduction in maximal gait performance at day one (Figure 2.2C). We therefore powered a study to detect this difference from baseline of our newly optimised rotarod training protocol. In this experiment we also extended the testing period to day 3 to incorporate the period of continued secondary injury in ICH. There was a significant effect of ICH on rotarod performance over the testing period ($F(1, 4) = 17.38$, $P = 0.0140$), no significant main effect of day ($F(1, 4) = 0.8823$, $P = 0.4007$) and no significant interaction ($F(1, 4) = 0.08909$, $P = 0.7802$) (Figure 2.4A). Posthoc analysis identified significant differences between sham and ICH groups at both day 1 ($P = 0.013$, Sidak) and day 3 ($P =$

0.022, Sidak) (Figure 2.4B). We were able to significantly improve the model of our data by including baseline performance as a covariate (AIC 127.89, Pr (>Chisq) : 0.0016 vs AIC 122.50, Pr (>Chisq) : 0.00005) which led to tighter 95% confidence intervals and a greater detectable difference between sham and ICH animals at day 1 (143.7 vs 123.2 mean difference) and day 3 (132.3 vs 111.8 mean difference) (Figure 2.4C-D). Thus, together, our data show that 0.045 U collagenase-induced murine ICH results in a reduction in maximal gait performance that does not improve by day 3, and including baseline scores as a covariate represents the most powerful statistical assessment of this model.

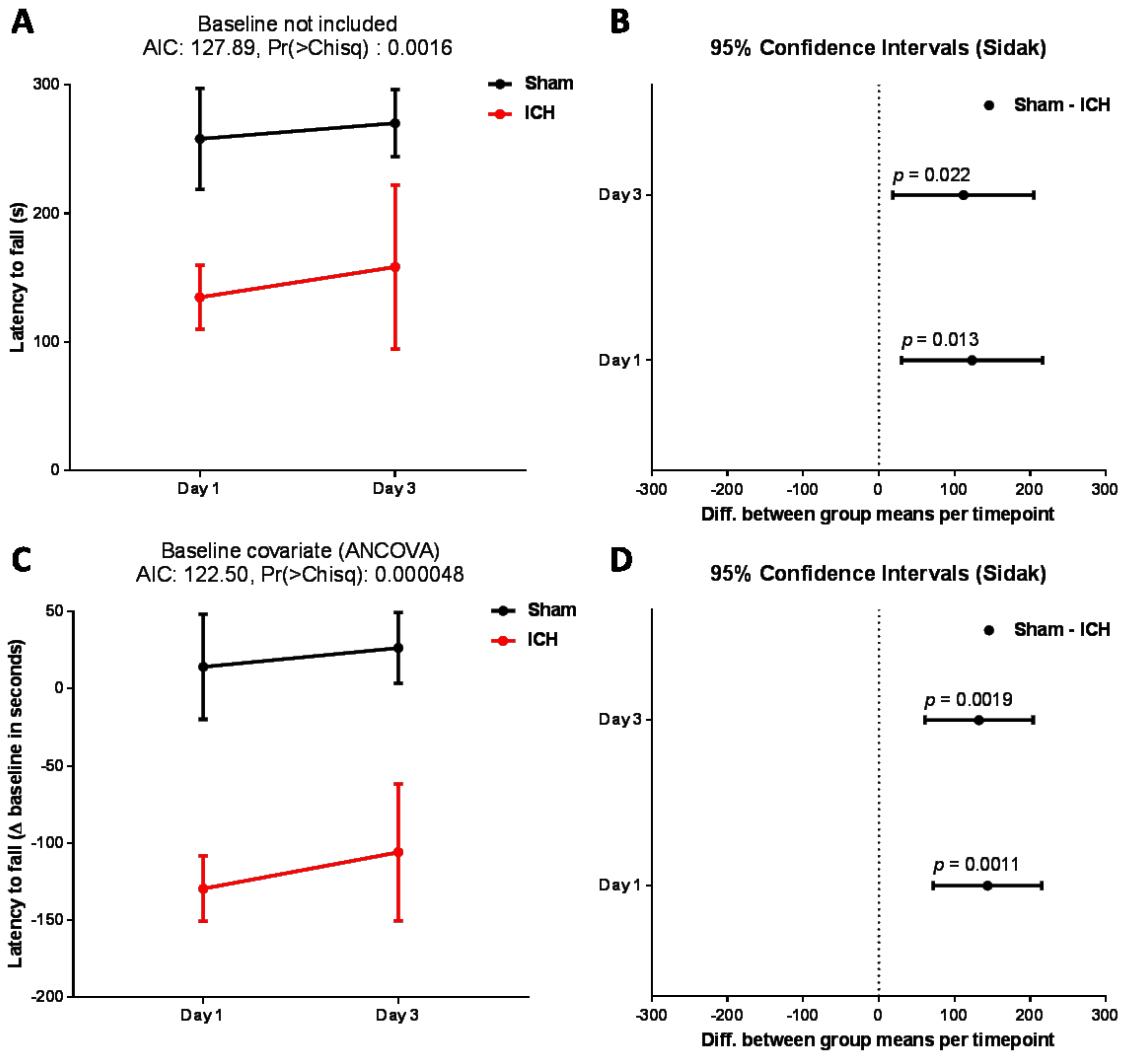

Figure 2.4 Our optimised workflow detects motor impairment in properly powered studies.
3 male C57BL/6 mice per group were required to detect a 45 % difference ($\alpha<0.05$, $\beta<0.2$) based on training data. Significant differences were found between sham and ICH mice at both day 1 and day 3 post-surgery without baseline included (A-B) or with baseline included as a covariate(C-D). The model was improved by analysing data as an analysis of covariance (ANCOVA) using baseline scores as fixed covariates (C). Data expressed as mean ± SD (A,C) or mean ± 95% confidence intervals (B,D). Differences were assessed using a 2-way repeated measures ANOVA and models were compared using linear mixed modelling.

Determining the neuroimmune response to the model

Inflammation is a key driver of ongoing neuronal injury in many diseased brain states. The inflammatory response to ICH has been characterised in many studies and includes trafficking of peripheral immune cells to the brain over the first 72 hours[11]. Markers of inflammation correlate with outcome in the clinical setting and preclinical work has identified immune infiltration as a deleterious feature[1]. Preclinical models of ICH must, therefore, result in brain infiltration of immune cells to have valid translational relevance. Using flow cytometry of single cells isolated from ipsilateral and contralateral hemispheres, we were able to detect changes in the immune landscape of mice subjected to ICH (Figure 6). Compared to contralateral hemisphere 24 hours following ICH, the percentage of microglia in the ipsilateral hemisphere reduced by around 30 % ($P = 0.006$), due to increases in myeloid cells (25.7 % ± 9.6 vs 1.6 % ± 0.7, $P = 0.0004$) and lymphocytes (3.8 % ± 1.3 vs 2.7 % ± 1.3, $P = 0.0025$) (Figure 2.5A). The majority of myeloid cells entering the ipsilateral hemisphere were of the Ly6Chi monocyte domain (12.9 % ± 4.3 vs 0.4 % ± 0.2, $P = 0.0002$), though neutrophils (8.3 % ± 4.4 vs 0.2 % ± 0.1, $P = 0.0006$) and Ly6Clo monocytes/macrophages (2.7 % ± 1.5 vs 0.7 % ± 0.5, $P = 0.0008$) also increased (Figure 2.5B). In contrast, we found no difference in microglia or lymphocyte percentages between hemispheres at 72 h, although we did find elevated levels of myeloid cells in ipsilateral hemispheres (11.1 % ± 3.0 vs 2.9 % ± 1.6, $P = 0.02$) (Figure 2.5C). We again found a percentage increase in Ly6Chi monocytes in ipsilateral hemispheres at 72 h post-ICH (4.3 % ± 0.8 vs 0.4 % ± 0.3, $P = 0.03$), but could not detect significant changes in neutrophils and Ly6Clo monocytes/macrophages at this time (Figure 2.5D). These data show that our refined mouse model of ICH does result in trafficking of immune cells to the ipsilateral hemisphere during the first 72 hours.

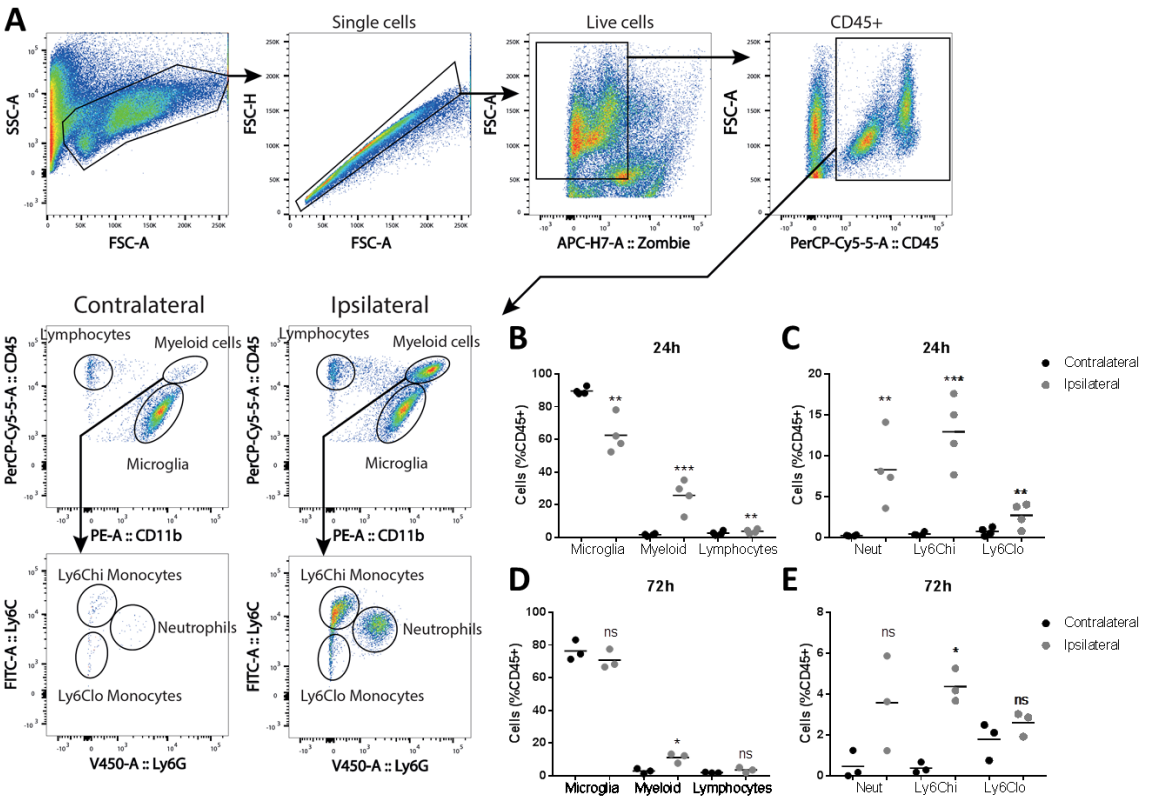

Figure 2.5 0.045 U collagenase-induced murine ICH retains important changes to the cerebral immune landscape.

ICH was induced in male C57BL/6J and flow cytometry performed on single cells isolated from ipsilateral or contralateral hemispheres at day 1 (B-C) or day 3 (D-E) Representative FACs plot showing gating panels (A). Immune cell frequencies were different in all measured populations at 24 h (B-C), whereas only myeloid cells and more specifically Ly6Chi monocytes were different at 72 h (D-E). ns = not significant, * = P<0.05, ** = P<0.01, *** = P<0.001.

2.7 Discussion

ICH is a devastating condition that requires *in vivo* investigations to identify therapeutic targets. Using the clinically relevant collagenase-induced ICH model we have reduced haematoma volume and used an optimised accelerating rotarod protocol to detect motor impairment in the absence of hemiplegia. Meta-analysis of published preclinical ICH studies indicates that a median of 14 rodents per study are used to detect ~25 % effect size[6]. Using our optimised workflow however, only 7 animals are required to confidently detect this effect size ($\alpha<0.05$, $\beta<0.2$, Supplementary figure 5). We have thus developed a refined workflow to detect motor impairment in the mouse model of collagenase-induced ICH that reduces animal usage and suffering.

We found that induction of ICH using 0.06 U collagenase resulted in a haematoma volume of 13.3 ± 6.9 mm^3 and was associated with around 30 % mortality, whereas Zhou et al[14]

(2013) found that 0.060 U collagenase resulted in 32.2 ± 8.2 mm^3 and <10 % mortality rate. This dissimilarity is likely due to a number of methodological differences; including our use of a smaller glass micropipette, older mice with larger brains, maintaining body temperature at 37 ˚C during surgery, and recovering mice in a hotbox following surgery. Issues surrounding maintenance of body temperature are likely to be the major factor in the difference between our results as all collagenase doses resulted in smaller haematoma volumes in our hands, and it is clear that hypothermia aggravates bleeding in the collagenase model[15]. Moreover, mortality rates were lower in the study from Zhou et al (2013) and hypothermia is a well-studied neuroprotective strategy that reduces cell death in models of brain injury. Thus, for future studies using our optimised workflow, it is imperative to control each of these variables.

Preclinical models of neurological disease must include functional outcomes in order to detect differences that are undetectable histologically, such as distal injury and dysfunctional viable circuits. Current animal models of ICH use a variety of neuromotor assays to detect severe phenotypes[6]. In the current study we used the accelerating rotarod performance assay to measure neuromotor impairment following ICH. Whilst we found the rotarod assay to be sensitive and reliable, the procedure is labour intensive and could be causing unnecessary animal distress. There is evidence that a home-cage wheel-running assay can also be a sensitive, yet less intrusive, measure of motor disturbance in mice[16]. However, the home-cage wheel running assay requires more operator time, individual housing, and is predicted to measure a distinct motor deficit compared to rotarod assays[16]. Overall, the rotarod assay equates to the most cost- and time-efficient method to detect motor impairment following intrastriatal ICH. We do recognise, however, that we have not tested for long-term deficits following ICH to which the home-cage wheel-running assay may outperform the rotarod.

Here we have refined the collagenase-induced mouse model of ICH to reduce protocol severity, yet clinically, ICH results in high rates of mortality and morbidity. There are questions whether our refined model has reduced clinical relevance therefore. Low mortality rates are recognised as a species difference in all current animal models of ICH by the Hemorrhagic Stroke Academia Industry (HEADS) Roundtable[17]. Moreover, animal models of disease aim to mimic aspects of the clinical condition to understand pathophysiological processes and inform design of therapies. We note our protocol results in brain haemorrhage in a clinically relevant brain region that causes detectable

neuromotor injury. Moreover, the inflammatory response to ICH contributes to deleterious and pro-reparative processes, and we show here that our model retains changes to the cerebral immune landscape. Thus the strength of this model is to investigate mechanisms underpinning neuromotor injury using few animals, allowing researchers to test more hypotheses and piece together complex pathways, such as those involved in the immune response. In line with HEADS recommendations[17], once important pathways have been identified and targeted in our refined model, researchers must look to confirm findings in other relevant models of ICH and account for important variables such as age, sex, and comorbidities.

In conclusion, it is important to properly power preclinical studies to reduce excess significance bias. Economical, practical and ethical aspirations provide pressure to properly power studies whilst reducing animal usage and suffering. The ischaemic stroke field has provided the framework to reduce animal suffering through refined animal models. The ICH field has yet to do this. We therefore provide the first refined workflow to detect neuromotor impairment in the mouse model of collagenase-induced ICH with finite animal suffering and usage, and provide power analysis based on this workflow for future studies (Supplementary figure 5).

References

1. Qureshi, A. I., Mendelow, a. D. & Hanley, D. F. Intracerebral haemorrhage. *Lancet* **373**, 1632–1644 (2009).

2. van Asch, C. J. J. *et al.* Incidence, case fatality, and functional outcome of intracerebral haemorrhage over time, according to age, sex, and ethnic origin: a systematic review and meta-analysis. *Lancet Neurol.* **9**, 167–176 (2010).

3. Kirkman, M. a, Allan, S. M. & Parry-Jones, A. R. Experimental intracerebral hemorrhage: avoiding pitfalls in translational research. *J. Cereb. Blood Flow Metab.* **31**, 2135–51 (2011).

4. Sena, E. S., van der Worp, H. B., Bath, P. M. W., Howells, D. W. & Macleod, M. R. Publication Bias in Reports of Animal Stroke Studies Leads to Major Overstatement of Efficacy. *PLoS Biol.* **8**, e1000344 (2010).

5. Macleod, M. R., O'Collins, T., Howells, D. W. & Donnan, G. A. Pooling of animal experimental data reveals influence of study design and publication bias. *Stroke* **35**, 1203–8 (2004).

6. Frantzias, J., Sena, E. S., Macleod, M. R. & Salman, R. A.-S. Treatment of intracerebral hemorrhage in animal models: Meta-analysis. *Ann. Neurol.* **69**, 389–399 (2011).

7. Percie du Sert, N. *et al.* The IMPROVE Guidelines (Ischaemia Models: Procedural Refinements Of in Vivo Experiments). *J. Cereb. Blood Flow Metab.* **37**, 3488–3517 (2017).

8. Luh, L. M., Das, I. & Bertolotti, A. qMotor, a set of rules for sensitive, robust and quantitative measurement of motor performance in mice. *Nat. Protoc.* **12**, 1451–1457 (2017).

9. Kilkenny, C., Browne, W. J., Cuthill, I. C., Emerson, M. & Altman, D. G. Improving bioscience research reporting: The arrive guidelines for reporting animal research. *Animals* (2013). doi:10.3390/ani4010035

10. Jiang, S. X. *et al.* Chlortetracycline and demeclocycline inhibit calpains and protect mouse neurons against glutamate toxicity and cerebral ischemia. *J. Biol. Chem.* **280**, 33811–8 (2005).

11. Hammond, M. D. *et al.* CCR2+Ly6Chi Inflammatory Monocyte Recruitment Exacerbates Acute Disability Following Intracerebral Hemorrhage. *J. Neurosci.* (2014). doi:10.1523/JNEUROSCI.4070-13.2014

12. Strangward, P. *et al.* Targeting the IL33–NLRP3 axis improves therapy for experimental cerebral malaria. *Proc. Natl. Acad. Sci.* (2018). doi:10.1073/pnas.1801737115

13. Pinheiro, J., Bates, D. & R-core. Package 'nlme': Linear and Nonlinear Mixed Effects Models. *Cran-R* (2018).

14. Zhou, W. *et al.* Hemostatic therapy in experimental intracerebral hemorrhage associated with rivaroxaban. *Stroke* **44**, 771–8 (2013).

15. John, R. F., Williamson, M. R., Dietrich, K. & Colbourne, F. Localized Hypothermia Aggravates Bleeding in the Collagenase Model of Intracerebral Hemorrhage. *Ther. Hypothermia Temp. Manag.* **5**, 19–25 (2015).

16. Mandillo, S. *et al.* Early motor deficits in mouse disease models are reliably uncovered using an automated home-cage wheel-running system: a cross-laboratory validation. *Dis. Model. Mech.* (2014). doi:10.1242/dmm.013946

17. Hemorrhagic Stroke Academia Industry (HEADS) Roundtable Participants, M. *et al.* Basic and Translational Research in Intracerebral Hemorrhage: Limitations, Priorities, and Recommendations. *Stroke* **49**, 1308–1314 (2018).

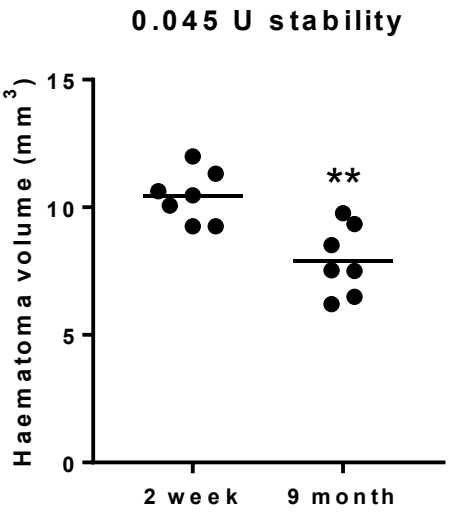

Figure 2.6 Supplementary 1. Collagenase becomes unstable overtime despite storage at -80 ˚C.

ICH was induced in male C57BL/6J mice with either 2 week or 9 month old 0.045 U collagenase. Animals were culled at day 1, brains sectioned and haematoma volumes calculated. ** = P<0.01.

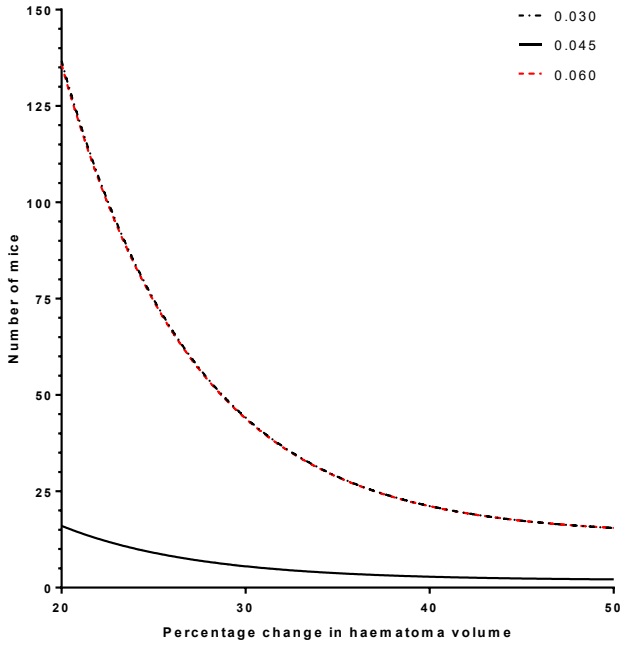

Figure 2.7 Supplementary 2. 0.045 U collagenase produces less variation compared to 0.030 and 0.060 U.

Power analysis based on mean and SD values of haematoma volumes produced by each collagenase dose at day 1 ($\alpha<0.05$, $\beta<0.2$). Graph shows number of mice needed to detect statistically significant changes based on effect sizes stated on the x axis ($\alpha<0.05$, $\beta<0.2$).

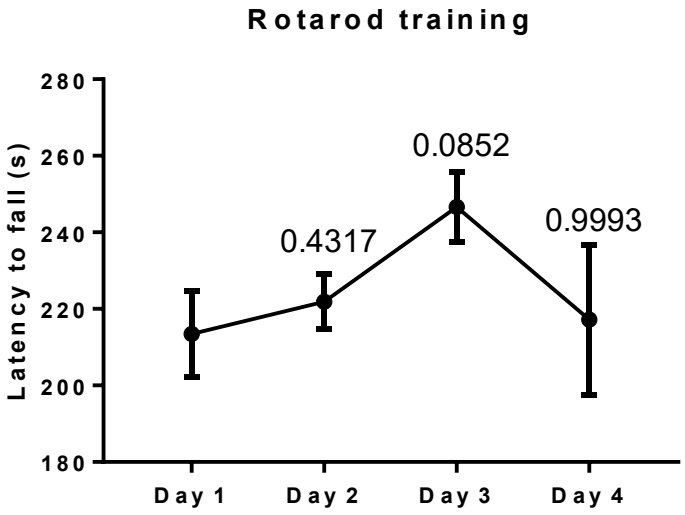

Figure 2.8 Supplementary 3. Rotarod performance increases during training until day 4.
6 male C57BL/6J mice were trained on the accelerating rotarod assay 3 times per day for a total of 4 days. Data expressed as mean ± SD. P values shown refer to Dunnett's post-hoc against day 1 scores following a repeated measures ANOVA.

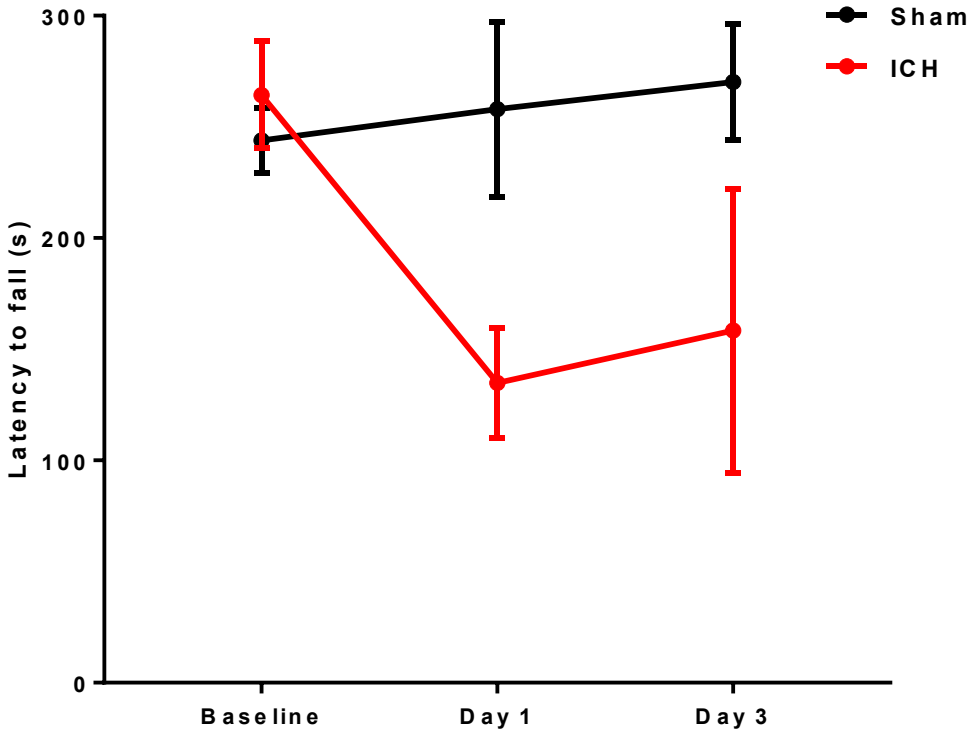

Figure 2.9 Supplementary 4. Rotarod scores from figure 4 of main text this time including baseline set as an average of the final 2 runs from the 3rd training day.
Data expressed as mean ± SD. 3 animals per group.

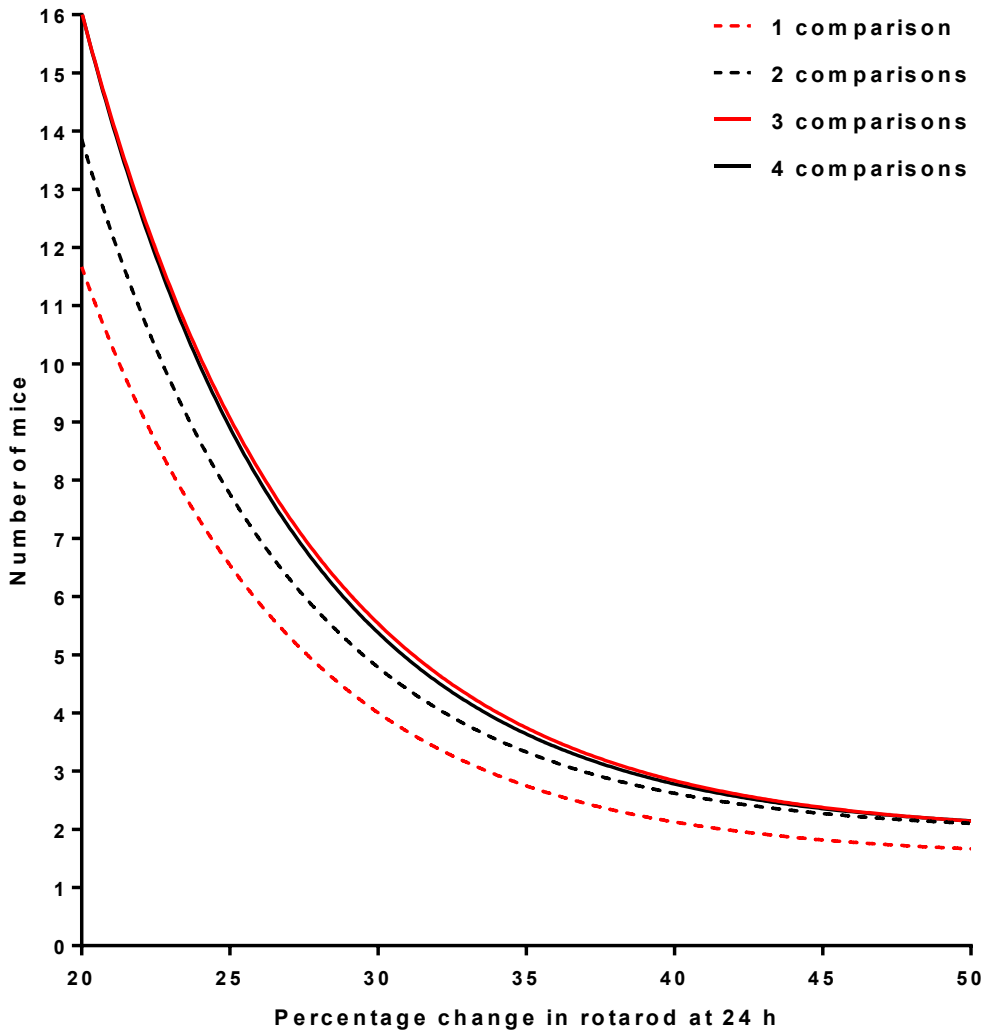

Figure 2.10 Supplementary figure 5. Power analysis based on mean and SD values from ICH animals at day one from figure 4 of main text.

Graph shows number of mice needed to detect statistically significant changes based on effect sizes stated on the x axis ($\alpha<0.05$, $\beta<0.2$).

Chapter 3: IL-1 in brain haemorrhage

3.1 Paper title and authors

Beneficial and detrimental effects of IL-1 in brain haemorrhage; dual regulator of cerebral blood flow and monocyte recruitment

Jack Barrington[1], Jack Rivers-Auty[1,3], Patrick Strangward[1], Sabrina Tamburrano[1], Nikolett Lénárt[2], Eloise Lemarchand[1], Adrian R. Parry-Jones[1], Ádám Dénes[2], David Brough[1]*, Stuart M Allan[1]*

I designed, implemented and performed all experiments apart from SVD patient tissue which was performed by P.S, RNA seq which was analysed by J.R.A, and Figure 5F which was performed by S.T. I also wrote the manuscript and all was performed under the guidance of D.B and S.M.A.

[1]Faculty of Biology, Medicine and Health, Manchester Academic Health Science Centre, University of Manchester, AV Hill Building, Oxford Road, Manchester, M13 9PT, U.K.

[2]Laboratory of Neuroimmunology, Institute of Experimental Medicine of the Hungarian Academy of Sciences, Szigony utca 43, Budapest, HU-1083 Hungary.

[3]School of Medicine, College of Health and Medicine, University of Tasmania, Hobart, Tasmania, Australia

*These authors contributed equally.

3.2 Abstract

Blood leaks into the brain parenchyma in many diseased brain states and can have drastic neurological consequences. Despite this, little is known about the pathological processes which occur following brain haemorrhage but neuroinflammation is thought to contribute considerably. Herein we provide evidence that myeloid cell trafficking to the parenchyma is a conserved feature of brain haemorrhage in clinical and experimental settings. In line with others, we show that monocytes contribute to acute brain damage following collagenase-induced murine brain haemorrhage. Using RNA-seq, we uncover IL-1 as the major upstream regulator of the acute immune response and histological data pinpoints the production of the protein to mononuclear phagocytes in patient and animal tissue. Contrary to others, we found neither depletion of microglia, nor inhibition of the IL-1β processing inflammasomes, prevented recruitment of myeloid cells to the brain. Inhibition of IL-1 receptor 1 (IL-1R1) drastically reduced myeloid recruitment however. To our surprise we discovered that IL-1R1 inhibition worsened neuromotor injury by reducing cerebral blood flow to the affected hemisphere. Thus we reveal novel dichotomous actions of IL-1-dependent inflammation following brain haemorrhage. On the one hand, IL-1 is the dominant regulator of harmful myeloid cell trafficking, whilst on the other, it critically regulates cerebral blood flow.

3.3 Introduction

Intraparenchymal brain haemorrhage, referred to here as brain haemorrhage, is a prominent pathological feature observed in multiple diseased brain states, including acute infections of the central nervous system (CNS)[1], vascular dementia[2], traumatic brain injury[3], and stroke[4]. Brain haemorrhage is associated with neurological symptoms ranging from cognitive decline in microbleeds[2], to paralysis and death in macrobleeds[4]. Despite this, the pathophysiology of brain haemorrhage remains poorly understood and few studies have sought to identify common features of micro- and macrobleeds.

To date, most research regarding brain haemorrhage has focussed on the deadliest form of stroke, intracerebral haemorrhage (ICH). Research in the ICH field indicates that two temporally distinct waves of injury occur[4]. Mass effect, which is driven by intraparenchymal accumulation of blood products, is perceived as the initial driver of neuronal injury that is succeeded by a progressive secondary injury characterised by the

onset of inflammation. Mass effect and inflammation are present in micro- and macrobleeds, however, the former is difficult to target therapeutically due to its rapid onset, whilst the latter occurs in a more clinically relevant time-window. Neuroinflammation is considered a key therapeutic target across a plethora of brain diseases, including acute brain injury[5]. However, there has been strong evolutionary pressure for the immune and coagulation systems to work in unison during bleeding events[6]. Therefore, what is true for inflammatory pathophysiology of some brain diseases may not be true in the case of brain haemorrhage.

In ICH, damage associated molecular patterns (DAMPs) are released that trigger inflammation through toll-like receptor activation[7,8]. TLR signalling (e.g. TLR4) leads to the production of pro-inflammatory cytokines that amplify local inflammation and promote the recruitment of circulating immune cells. Monocyte trafficking to the brain occurs in models of macro- and microbleeds and is a key driver of neuronal injury[9,10]. Vascular inflammation is important in monocyte trafficking during ICH but the factors governing this are poorly understood[11]. Recently the prototypical pro-inflammatory cytokine interleukin-1 (IL-1), a downstream product of TLR-4, has been shown to trigger monocyte recruitment to the brain through actions on the cerebral vasculature[12]. IL-1 promotes myeloid cell infiltration[13], exacerbates excitotoxic damage[14] and contributes to the no-reflow phenomenon[15] during brain ischaemia; however, its influence in brain haemorrhage remains an important open question.

Herein we provide evidence that IL-1 production from mononuclear phagocytes is a conserved feature of brain haemorrhage, and signalling through the type 1 IL-1 receptor (IL-1R1) is the critical mediator of harmful monocyte recruitment. Despite this, and in contrast to findings in other fields, IL-1 inhibition worsened neuromotor dysfunction by preventing reactive vasodilation of cerebral blood vessels, in which cyclooxygenase-2 (COX-2) upregulation by vascular mural cells might play an important role. Thus we reveal a previously unknown aspect of brain haemorrhage where inflammation works to reduce brain damage by increasing blood flow to the affected region.

3.4 Materials and Methods

Immunohistochemistry and immunofluorescence on post-mortem human brain tissue

Small vessel disease and ICH brain tissue samples were acquired from the South West and Edinburgh arms of the Medical Research Council brain banks respectively. Samples were taken from deep brain regions (including basal ganglia and thalamus) of 2 males and 1 female (age range 63 – 86 years) that died within 3 days of ICH and 4 females with diagnosis of dementia and histopathological evidence of SVD and fresh microbleeds (age range 89 – 95).

Brain sections were deparaffinised and rehydrated prior to undergoing relevant heat-mediated antigen retrieval in a water bath set to 97.5 ˚C for 30 min. Antigen retrieval was performed using sodium-citrate pH 6.0 solution for rabbit-anti-CD11b (0.68 - 6.75 µg mL^{-1}, EPR1344, Abcam) or Tris-EDTA pH 9.0 solution for rabbit-anti-Iba1 (2.56 µg mL-1, EPR16588, Abcam) and goat-anti-IL-1β (2.00 µg mL-1, AF-201, RnDSystems). Primary antibodies were incubated overnight at 4 ˚C in primary antibody buffer (1 % BSA, 0.3 % Triton-X-100, 0.05 % sodium azide, PBS), followed by incubation with secondary antibodies for 90 min at RT in secondary antibody buffer (0.1 % bovine serum albumin in tris-buffered saline). The following secondary antibodies were used: donkey-anti-rabbit Alexa Fluor® 647 (10 µg mL^{-1}, Abcam) and donkey-anti-rat Alexa Fluor® 647 (10 µg mL^{-1}, Abcam). In order to amplify low abundance epitopes or overcome red blood cell autofluorescence the Tyramide SuperBoostTM (B40936, ThermoFisher) protocol was followed as per manufacturer's instructions using biotinylated horse-anti-goat IgG (7.5 µg mL^{-1}, BA-9500, Vector) or goat-anti-rat IgG (7.5 µg mL^{-1}, BA-9400, Vector) secondary antibodies. Wash steps were performed throughout using wash buffer (0.1 % tween in Tris-buffered saline).

Animals

Animal procedures were carried out in accordance with the Animal Scientific Procedures Act (1986) and the European Council Directive 2010/63/EU, and were approved by the Animal Welfare and Ethical Review Body, University of Manchester, UK and the Animal Care and Use Committee of the Institute of Experimental Medicine, Budapest, Hungary. Sample size was calculated by power analysis using a significance level of $\alpha = 0.05$ with 80 % power to detect statistical differences. $Ccr2^{-/-}$ animals (originally from The Jackson Laboratory[16]) were bred in-house and shared by J. Grainger (University of Manchester,

Manchester, England, UK), and were backcrossed to a C57BL/6 background for at least 10 generations. For microglia depletion experiments mice were bred at the SPF unit of the Animal Care Unit of the Institute of Experimental Medicine (IEM HAS, Budapest, Hungary). Mice had free access to food and water and were housed under light-, humidity- and temperature controlled conditions. Experiments followed ARRIVE guidelines[17]. Animals were maintained under standard laboratory conditions: ambient temperatures of 21 °C (±2 °C), humidity of 40–50%, 12 h light cycle, ad libitum access to water and standard rodent chow. All surgeries were performed with the surgeon concealed to the treatment and/or genotype, and all behavioural and histological analyses were performed by a blinded observer. Treatments were randomly allocated using the research randomiser tool.

Surgery

We used a model of intraparenchymal brain haemorrhage that creates an active bleed within the brain by using collagenase VII-S (Sigma, C2399) to break down the basal lamina of cerebrovascular beds[18]. To do this, mice were initially induced under anaesthesia using 4 % isoflurane in 70 % N_2O and 30 % O_2 and fur was shaven from the head. Mice were then transferred to a feedback-controlled heating pad set to 37 ˚C, securely fixed to a stereotactic frame (Stoetling), anaesthesia maintained at 1.5-2.0 % isoflurane in 30 % N_2O and 70 % O_2 using a nose cone, and Videne (EcoLab) applied to the scalp. A longitudinal midline incision above the skull was performed and periosteum stripped away from the midline on both sides. A burr-hole was created using a micro-drill and a glass micropipette (BLAUBRAND, pulled at 70 ˚C) inserted at the following co-ordinates from bregma: anterior-posterior 0.0 mm, lateral -2.0 mm, deep -2.7 mm. 0.5 µL of 0.09 units/µL of collagenase (C2399, Sigma) dissolved in saline was then injected at a rate of 1 µL min^{-1}. The needle was left in situ for 10 min before removal and wounds sutured. The scalp was cleaned once more with Videne and a topical analgesia was applied (EMLA cream, AstraZeneca) before animals were given a subcutaneous bolus of saline (10 mL kg^{-1}) and buprenorphine (50 µg kg^{-1}, Vetergesic, UK) before being recovered in 28 ˚C housing. Animals were then transferred to ventilated cages suspended over a heating pad with free access to mashed food and water in normal housing conditions.

Rotarod assay

Mice were allowed to habituate to the behavioural room and handled for at least one week prior to commencement of training. Animals were trained for 3 consecutive days prior to surgery using the following protocol. The rotarod was set to loading phase whilst animals were placed onto the rotarod. Following a 15 s loading period the rotarod was set to accelerate from 4 to 40 rpm over 300 s. An animal was deemed to have completed the task when it had fallen from the apparatus, accrued 3 passive rotations or stayed on the apparatus until 300 s. The time at which an animal completed the task was recorded. Once all animals had finished the run the apparatus was thoroughly cleaned with a 70 % ethanol solution. 3 runs were performed per day with a 15 min inter-trial interval. On the third and final day of training the results from the final 2 runs were averaged and set as the baseline run time for that animal. On test days following ICH the same protocol was followed with animals performing 3 runs and the times from the final 2 runs averaged for the animals score.

Tissue processing and Immunostaining

Mice were transcardially perfused with PBS followed by 4 % paraformaldehyde (PFA) under isoflurane or ketamine-xylazine induced terminal anaesthesia. Brains were removed and post-fixed in 4 % PFA for 24 h at 4 ˚C before being cryoprotected in a 20 % sucrose solution at 4 ˚C for up to 4 days. Brains were then frozen in -50 to -60 ˚C isopentane and 20 µm coronal sections taken every 400 µm using a Leica cryostat.

For immunostains, brain sections were dried for 24 h prior to undergoing relevant heat-mediated antigen retrieval in a water bath set to 97.5 ˚C. Antigen retrieval was performed using Tris-EDTA pH 8.6 solution for 20 min for the following antibodies: rabbit-anti-Iba1 (2.56 µg mL^{-1}, EPR16588, Abcam), goat-anti-IL-1α (1.00 µg mL^{-1}, AF-400, RnDSystems), goat-anti-IL-1β (1.00 µg mL^{-1}, AF-401, RnDSystems), rat-anti-Ly6G (1.25 µg mL^{-1}, 1A8, Biolegend), rabbit-anti-collagen IV (5.00 µg mL^{-1}, EPR16588, Abcam), goat-anti-vascular cell adhesion protein 1 (2.00 µg mL^{-1}, AF643, RnD Systems). Antigen retrieval was performed using sodium-citrate pH 6.0 solution for rabbit-anti-CD11b (2.70 µg mL^{-1}, EPR1344, Abcam). Primary antibodies were incubated overnight at 4 ˚C in primary antibody buffer (1 % BSA, 0.3 % Triton-X-100, 0.05 % sodium azide, PBS), followed by incubation with secondary antibodies for 90 min at RT in secondary antibody buffer (0.1 % bovine serum albumin in tris-buffered saline). The following secondary antibodies were used: donkey-anti-rabbit Alexa Fluor® 647 (10 µg mL^{-1}, Abcam),

donkey-anti-rat Alexa Fluor® 647 (10 µg mL^{-1}, Abcam). In order to amplify low abundance epitopes or overcome red blood cell autofluorescence the Tyramide SuperBoostTM (B40936, ThermoFisher) protocol was followed as per manufacturers instructions using biotinylated horse-anti-goat IgG (7.5 µg mL^{-1}, BA-9500, Vector), goat-anti-rat IgG (7.5 µg mL^{-1}, BA-9400, Vector) or goat-anti-rabbit IgG (7.5 µg mL^{-1}, BA-1000, Vector) secondary antibodies. Wash steps were performed throughout using wash buffer (0.1 % tween in Tris-buffered saline).

Microscopy

Images were collected on a Zeiss Axioimager.D2 or Olympus BX63 upright microscope and captured using a Coolsnap HQ2 camera (Photometrics) or DP80 camera (Olympus) through Micromanager software v1.4.23 or CellSens Dimensions V1.16 (Olympus). Specific band pass filter sets for were used to prevent bleed through from one channel to the next. Images were then processed and analysed using Fiji ImageJ (http://imagej.net/Fiji/Downloads). 4 regions of interest that spanned haematoma and perihaematoma were taken across 4 different brain sections for histological quantification.

Cell isolation

Mice were transcardially perfused with PBS and ipsilateral hemispheres were digested for 60 min at 37 °C with 50 U mL^{-1} Collagenase (17104-019, Gibco), 0.5 U mL^{-1} Dispase II (17105-041, Gibco) and 200 U mL^{-1} DNase I (10104159001, Roche) in Hank's balanced-salt solution containing calcium and magnesium. The tissue was then mechanically dissociated using a dounce homogeniser and myelin removed using a 32 % isotonic percoll solution centrifuged at 2000 x*g* for 10 min at 4 ˚C with brake on 2. When possible cells were kept in ice cold RPMI containing 3% FBS. Following single cell isolation red blood cells were lysed by 3 minute incubation with BD Pharmlyse (555899, BD Bioscience).

Western blot

Following single cell isolation, myeloid cells were purified using CD11b+ magnabeads (130-093-636, Miltenyi) according to manufacturer's protocol. Positive and negative populations were captured and lysed in NP-40 lysis buffer (150 mM NaCl, 50 mM Tris, 1 % NP-40, pH 7.4) supplemented with protease inhibitor cocktail (PIC) (539131, Merck).

Lysates were run on 12 % polyacrylamide gels and transferred onto nitrocellulose membranes using the mixed molecular weight setting of a Trans-Blot Turbo system (Bio-

Rad). Membranes were blocked in 5 % BSA PBS containing 0.1 % Tween-20 (Sigma) (PBST) for 1 hour at room temperature. Following blocking, membranes were incubated (4 ˚C) overnight with goat-anti-mouse IL-1β (100 ng mL^{-1}, RnD Systems) or goat-anti-mouse IL-1α (100 ng mL^{-1}, RnD Systems) in PBST containing 0.1 % BSA. Membranes were then washed and incubated (room temperature) with rabbit anti-goat (550 ng ml^{-1}, DAKO) in 0.1 % BSA PBST. After washing, membranes were incubated in Amersham ECL Western Blotting Detection Reagent (GE Life Sciences) before detection using a G:BOX Chemi XX6 imaging system (Syngene).

Flow cytometry

Isolated single cell pellets were resuspended in FACs staining buffer (PBS with 2mM EDTA) containing a number of the following antibodies. 50 µg mL^{-1} FC block (Clone 93, ebioscience), 1:500 Live/Dead blue (ThermoFisher), 0.4 µg mL^{-1} CD11b-BV786 (Clone M1/70, BD Bioscience), 2 µg mL^{-1} CD3-BV510 (Clone 17A2, Biolegend), 0.67 µg mL^{-1} CX3CR1-PE/Cy7 (Clone SA011F11, Biolegend), 0.67 µg mL^{-1} CD45-PerCP/Cy5.5 (Clone 30-F11, eBioscience), 2 µg mL^{-1} IL-1β-PE (Clone NJTEN3, ThermoFisher), 1 µg mL^{-1} Ly6C-FITC (Clone AL-21, BD Bioscience), 0.67 µg mL^{-1} CD45r-APC/Cy7 (Clone RA3-6B2, Biolegend) and 1 µg mL^{-1} Ly6G-APC (Clone 1A8, TONBO biosciences). 2 µg mL^{-1} Rat/IgG1,kappa-PE (Thermofisher) was used as isotype control for IL-1β and fluorescence minus one controls were used to set gates for all other stains. Cell numbers were quantified using CountBrightTM counting beads (C36950, ThermoFisher). Samples were acquired on a BD LSR II (Becton Dickenson) using BD FACSDiva software (Becton Dickenson). Data was analysed using FlowJo V.10 (Tree Star Inc.).

RNA isolation

Mice were PBS perfused and RNA was isolated from the right hemisphere (ipsilateral in haemorrhaged animals) using the RNeasy lipid tissue mini kit (Qiagen) as per manufacturer's protocol. Brain hemispheres were homogenised using lysing matrix D tubes (MPBio) in a Qiagen Tissue Lyser II.

RNA sequencing

RNA-Seq analysis was performed. RNA samples were assessed for quality and integrity using a 2200 TapeStation (Agilent Technologies) according to the manufacturer's instructions. RNA-Seq libraries were generated using the TruSeq Stranded mRNA assay (Illumina, Inc.) according to the manufacturer's instructions. Briefly, poly-T, oligo-

attached, magnetic beads were used to extract polyadenylated mRNA from 1 μg of total RNA. The mRNA was then fragmented using divalent cations under high temperature and then transcribed into first strand cDNA using random primers. Second strand cDNA was then synthesized using DNA polymerase I and RNase H, and a single "A" base addition was performed. Adapters were then ligated to the cDNA fragments and then purified and enriched by PCR to create the final cDNA library. Adapter indices were used to multiplex libraries, which were pooled prior to cluster generation using a cBot instrument. The loaded flow cell was then pair-end sequenced (101 + 101 cycles, plus indices) on an Illumina HiSeq4000 instrument. Demultiplexing of the output data (allowing one mismatch) and BCL-to-Fastq conversion was performed with CASAVA 1.8.3. Sequencing quality for each sample was determined using the FastQC program. Low-quality sequence data were removed utilizing the trimmomatic program. STAR v2.4.0 was utilized to map the trimmed sequence into the murine genome (mm10 genome with gencode M16 annotation). Raw counts for each sample were generated by the htseq-count program and subsequently normalized relative to respective library sizes using DESeq2 package for the R statistical program. The DESeq2 program was additionally used to plot the PCA with all sample data to visualize different clusters at multiple levels that describes the maximum variance within the data set. Genes of interest were identified by pairwise comparisons. False discovery rate (FDR) adjusted p values were used to evaluate significance.

Functional and Pathway Enrichment Analysis

Genes with an FDR-corrected p value of less than 0.01 were analyzed for transcriptional regulation and cell pathway enrichment utilizing the enrichR package[19] to string search the Enrichr webserver: GO term, PANTHER and Transcriptional Regulatory Relationships Unraveled by Sentence-based Text mining[20] datasets[21,22] on R[23]. Significant features ($p<0.05$) were further probed by cluster analyses utilising Ward's minimum variance method of hierarchical clustering visualised using R package "pheatmaps"[24]. Heatmap, PCA and volcano plots were generated using the R packages "pheatmaps", R version 2.6.1 base and "ggplot2"[25], respectively.

IL-1R1 inhibition

Ubiquitous genetic knockouts can lead to upregulation of compensatory genes and such compensation has been speculated in IL-1R1 knockouts[13]. We thus adopted a pharmacological approach to inhibit IL-1R1. Human IL-1RA (Kineret, SOBI) was

supplied in 10 mM sodium citrate, 140 mM NaCl, 4 μM EDTA, 5.34 μM polysorbate 80, pH 6.5 and further diluted in sterile saline. Placebo controls contained vehicle only. We injected 10 μg of the naturally occurring antagonist IL-1RA intrastriatally (bregma: anterior-posterior 0.0 mm, lateral -2.0 mm, deep -2.7 mm) 10 minutes prior to collagenase injection, followed by a 100 mg kg^{-1} subcutaneous dose. In order to maintain adequate plasma concentrations of IL-1RA a second subcutaneous 100 mg kg^{-1} dose was injected 6 h later[26]. Where animals were kept alive for more than 24 h 100 mg kg^{-1} doses were given subcutaneously morning and evening each day ending in the evening of the second day following surgery. IL-1RA was well tolerated with mice showing no overt signs of physiological illness.

Microglia depletion

PLX5622 was provided by Plexxikon Inc. (Berkeley, USA) and formulated by Research Diets (New Brunswick, USA) into an AIN-76A standard chow in 1200 p.p.m. (1200mg PLX 5622 in 1kg chow) concentration. Mice were fed PLX5622 for 14 days, to eliminate microglia from the brain. We could not observe any sign of physiological illness (alterations in food intake, weight, physical appearance) or behavioural changes (social interactions, exploration) during the diet period, in accordance with other studies[27,28].

Caspase-1 inhibition

To inhibit caspase-1 activation during brain haemorrhage we used the potent caspase-1 inhibitor VX-765 (S2228, Selleckchem) that has recently been shown to be efficacious in mouse models of Alzheimer's disease[29]. We adopted the same dosing regimen used in our IL-1RA model with a single 7.5 μg intrastriatal injection followed by 50 mg/kg subcutaneous doses. VX-765 was diluted in a sterile 5 % Cremophor EL (Sigma), 5 % DMSO (Sigma), 90 % saline mixture. Placebo contained vehicle alone. VX-765 was well tolerated with mice showing no overt signs of physiological illness.

Laser speckle contrast imaging

Mice were anaesthetized and placed in a stereotaxic frame (World Precision Instruments, USA) positioned under a moor FLPI2 Full-Field Perfusion Imager (Moor instruments, UK). Anaesthesia was maintained at 1.50 % isoflurane and body temperature maintained at 37 °C using a feedback-controlled heating pad. A longitudinal midline incision was performed on the scalp to expose the skull. The skull was cleared of any hair and acoustic

gel applied before a glass coverslip was mounted atop. Imaging was conducted for 3 min with a 4 second per image acquisition rate, 20 ms exposure time and 100 frame filter. Mice were imaged 24 h post-haemorrhage and regions of interest drawn around each hemisphere using moor FLPI2 Full-Field Laser Perfusion Imager Review V5.0 software. Flux values were averaged across all timepoints and taken for further analysis.

Bleed size analysis

For histological quanitification of haematoma volume, brains were sectioned at 400 μm intervals, digitally scanned, and regions of interest (ROI) drawn around the haematoma on each section using imageJ. Haematoma volume was calculated by summing the area of all ROIs and multiplying by the inter-section interval (400 μm). For biochemical quantification of blood load, perfused brains were snap frozen before each hemisphere was isolated and lysed on ice in NP-40 lysis buffer containing PIC using a handheld homogeniser. Lysates were centrifuged at 18,000 x*g* for 10 min at 4 °C and supernatants collected and ultracentrifuged at 100,000 x*g* for 30 min at 4 °C. Haemoglobin content of S100 fractions were quantified using a haemoglobin assay kit (Sigma, MAK115-1KT) as per manufacturer's protocol with slight modification to reduce assay volume by 50 %. Samples were run in triplicate at a range of dilution factors and values closest to the standard used in analysis.

hCMEC/D3 (human cerebral microvascular EC line D3) cultures

To investigate the effects of IL-1 on brain endothelial cells, immortalised hCMEC/D3 were grown on collagen I (Sigma, 08-115) coated flasks in EndoGRO-MV Complete Culture Media Kit (Merck, SCME004) until 90 % confluent. Cells were seeded overnight at 80,000 cells well^{-1} and treated the next morning with 10 ng mL^{-1} of IL-1β (RnD systems, 201-LB). 4 h later supernatants were removed and cells were lysedwere lysed in RIPA buffer (150 mM NaCl, 1% (vol/vol) NP-40, 0.5% (wt/vol) sodium deoxycholate, 0.1% (wt/vol) SDS, 50 mM Tris, pH 8), supplemented with a protease inhibitor mixture. Western blots were performed as described earlier using goat-anti-COX-2 (0.20 μg mL^{-1}, RnD systems, AF4198) and rabbit-anti-VCAM-1 (0.44 μg mL^{-1}, ab134047, abcam).

Statistical analyses

Data are presented as individual values ± standard error of the mean (s.e.m) apart from LSCI data which is presented as marginal means ± standard error. For LSCI and

behavioural analyses, linear mixed modelling was used to evaluate the effect of independent factors (treatment and time/hemisphere) on the dependent variable[30]. All factors and interactions were modelled as fixed effects. A within-subject design with random intercepts was used for all models. The significance of inclusion of a dependent variable or interaction terms was evaluated using log-likelihood ratio. Homoscedasticity and normality were evaluated graphically using predicted vs residual and Q-Q plots, respectively. All analyses were performed using R (version 3.3.3). Statistical analyses for everything else were performed using Student's t-tests, one-way analysis of variance (ANOVA) and two-way ANOVA tests with Sidak corrected post hoc. Equal variance and normality were assessed with the Levene's test and the Shapiro–wilk test, respectively, and appropriate transformations were applied when necessary. Accepted levels of significance were *P<0.05, **P<0.01, ***P<0.001, ****P<0.0001. The latter statistical analyses were carried out using GraphPad Prism. Images were processed using Fiji ImageJ49 and analysed by manual counting with experimenter blinded to image identity throughout. Flow cytometry data were analysed and populations quantified using FlowJo V10.

3.5 Results

Intraparenchymal brain haemorrhage results in peripheral immune cell accumulation

We began our investigation, validating the findings of others who showed cerebrovascular rupture results in myeloid cell trafficking to the brain[9,31–33], by examining post-mortem human brain tissue for evidence of CD11b+ myeloid cells. Radiological indications of cerebral microbleeds represent heterogeneous histopathological findings that cause difficulties in estimating actual bleed rates in cerebral small vessel disease (SVD). In our cohort of 36 patients with SVD, 3/36 (8 %) showed evidence of fresh brain haemorrhage but only 2 had parenchymal haemorrhages. Immunostaining of these SVD patients identified extensive infiltration of CD11b+ myeloid cells in parenchymal brain tissue within and around the haematoma (Figure 3.1A). The amount of tissue damage caused by macrobleeds makes it difficult to perform histological analysis on the core of the haematoma. We thus stained perihaematomal regions of acute macrobleeds and CD11b+ cells were evident in this setting too (Figure 3.1A). To further characterise immune cell trafficking to the damaged brain we used a murine model of brain haemorrhage, in which collagenase is injected directly into the brain parenchyma to degrade basal lamina and promote progressive bleeding[18].

Flow cytometry on single cell homogenates of mouse brain tissue was used to characterise immune cell populations in brains of naïve, sham-operated and haemorrhaged mice (Figure 3.1B). Animals with induced brain haemorrhage had more T cells, neutrophils, Ly6Chi and Ly6Clo monocytes/macrophages recruited to the ipsilateral hemisphere one day post-surgery. The greatest effect of haemorrhage was on myeloid cells with both neutrophils and Ly6Chi monocytes increasing ~20-fold compared to sham-operated animals. These data show that myeloid cell trafficking to the brain occurs in both clinical and preclinical brain haemorrhage, with neutrophils and Ly6Chi monocytes predominating.

Monocytes contribute to neuromotor dysfunction following brain haemorrhage

A number of previous studies have shown that preventing Ly6Chi monocyte infiltration improves motor function following brain haemorrhage[9,34]. We looked to validate these findings using CCR2-/- animals, which have fewer Ly6Chi monocytes in circulation due to deficiencies in their release from the bone marrow. Flow cytometry profiling of circulating immune cells established that CCR2-/- animals indeed had ~4-fold reduction in

circulating Ly6Chi monocytes (Figure 3.1Ci-ii). To test whether Ly6Chi monocytes affected neuromotor function following brain haemorrhage, we utilised the rotarod performance test in which animals must balance on an accelerating rotating beam over the course of 300 seconds. On the day following brain haemorrhage induction, CCR2-/- mice performed significantly better on the rotarod assay than wild type littermates (Figure 3.1Ciii). Thus, preventing monocyte trafficking to the haemorrhaged brain limits neuromotor injury. We next looked to identify the upstream mediator of this harmful monocyte recruitment.

IL-1 controls transcriptional changes in the brain following haemorrhage

To identify the factors which control the immune response to brain haemorrhage, we performed RNA-Seq on RNA extracted from the right (ipsilateral) hemisphere of control mice or mice injected with collagenase. Unguided principal component analysis of the data revealed stark differences in the transcriptional landscape of haemorrhage and control animals (Figure 3.2A). Of the 1278 differentially expressed genes, a large proportion of those upregulated following haemorrhage were attributed to inflammation (such as *Ccl2*, *Icam1* and *Il1b*), whereas, those downregulated were linked to neuronal pathways (such as *Bdnf*, *Grin2b* and *Homer2*) (Figure 3.2B). To elucidate the potential processes that are important in the trafficking of harmful monocytes to the brain, enrichment analyses were performed on the data set. Pathway enrichment analysis showed that microglia, complement, coagulation, and multiple chemokine and cytokine pathways were principally upregulated following brain haemorrhage (Figure 3.2D). Many of the differentially expressed genes were transcription factor targets for sensors of IL-1 and IL-6 (NFKB1, JUN, STAT1, STAT3, RELA and FOS). In fact, most of the upregulated inflammatory genes were part of the IL-1 and IL-6 pathway (Figure 3.2C,E). Network analysis further implicated both of these molecules as upstream regulators in the immune response to brain haemorrhage (Figure 3.2F). However, of these molecules, IL-1 was associated with a greater amount (209) of the differentially expressed genes. Moreover, we know from clinical and preclinical evidence that IL-6 sits downstream of IL-1R1 activation[35,36] (Figure 3.2G). These data therefore identify IL-1 as the potential major upstream regulator of brain inflammation following brain haemorrhage.

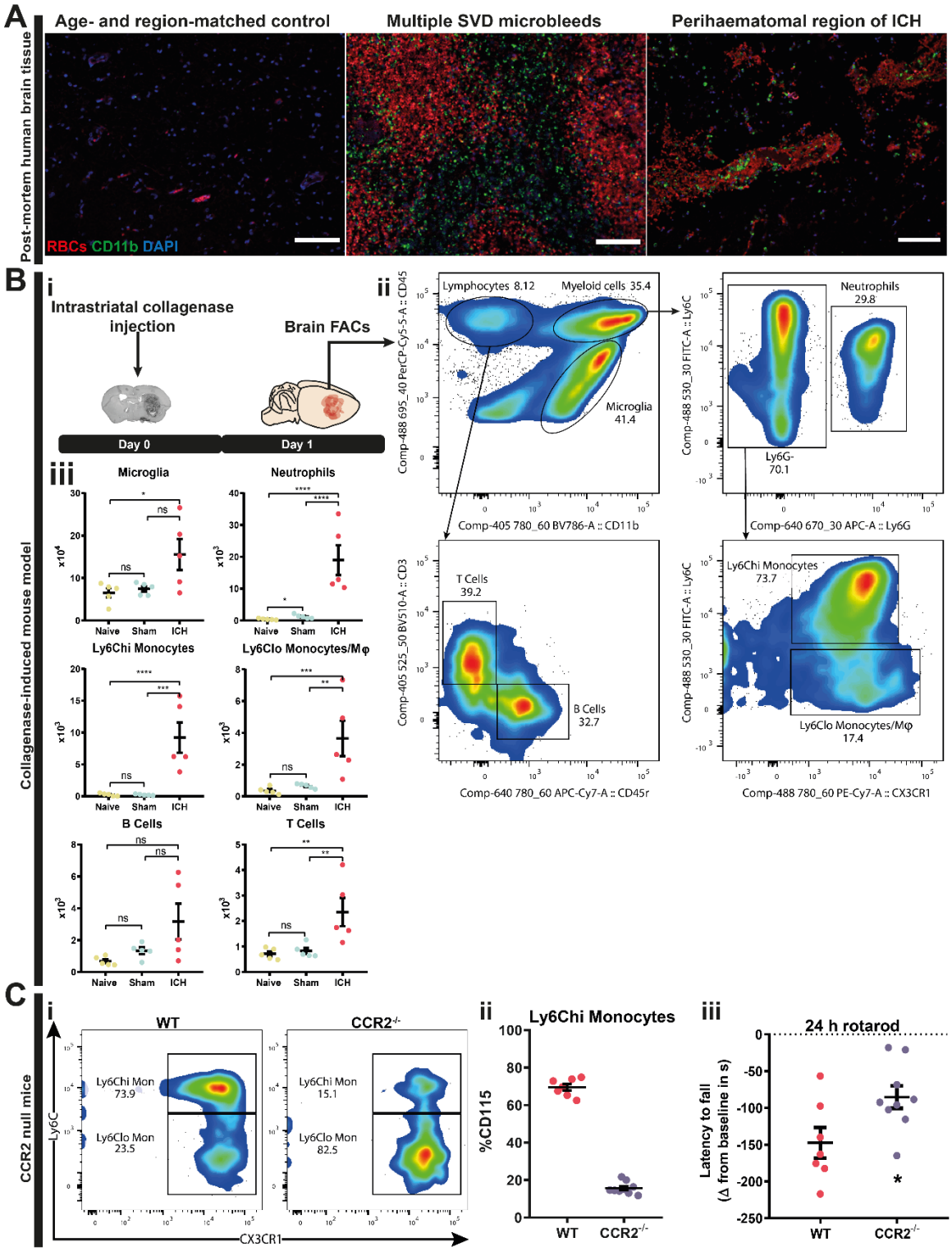

Figure 3.1 Intraparenchymal brain haemorrhage results in detrimental parenchymal accumulation of peripherally derived monocytes.

(A) Formalin-fixed paraffin-embedded post-mortem human brain tissue from age- and region-matched control, microbleed, and macrobleed patients were immunostained for the myeloid cell marker CD11b (green), DAPI (blue) and red blood cell autofluorescence can be seen in red. One representative image from 3 (macro) or 2 (micro) patients per group shown, scale bar 100 µm. (Bi) Single cells were isolated from the right hemisphere of naive, sham-operated, and collagenase-induced intracerebral haemorrhage (ICH) mice 24h post-surgery and immunophenotyped using flow cytometry. (Bii) Gating strategy used during flow cytometry analysis. (Biii) Cell counts are shown from the following populations CD45^{int} CD11b+ microglia, CD45^{hi} CD11b+ Ly6G+ neutrophils, CD45^{hi} CD11b+ Ly6G- Ly6C^{hi} monocytes,

$CD45^{hi}$ CD11b+ Ly6G- $Ly6C^{lo}$ monocyte/macrophage (Mφ), $CD45^{hi}$ CD11b- CD45R+ B cells, and $CD45^{hi}$ CD11b- CD3+ T cells. Data presented as mean + s.e.m, *n* = 5. (C) Ly6Chi monocytes contribute to neuromotor dysfunction following brain haemorrhage. (Ci-ii) White blood cells were isolated from whole blood of wild-type (WT) (*n* = 7) and chemokine receptor 2 (CCR2)-/- (*n* = 9) male littermate mice. (i) Representative FACs plots of the circulating monocyte compartment of each genotype. (ii) Amount of $Ly6C^{hi}$ monocytes as a percentage of total circulating monocytes from each genotype. (iii) Following a 3 day training period on the rotarod assay, WT and CCR2-/- littermates were subjected to collagenase-induced ICH and tested on the rotarod again 24 hours later. Data presented as net difference in latency to fall from baseline performance, *n* = 7-9. . ns = not significant; * = P<0.05; ** = P<0.005; *** = P<0.0005; **** = P<0.0001.

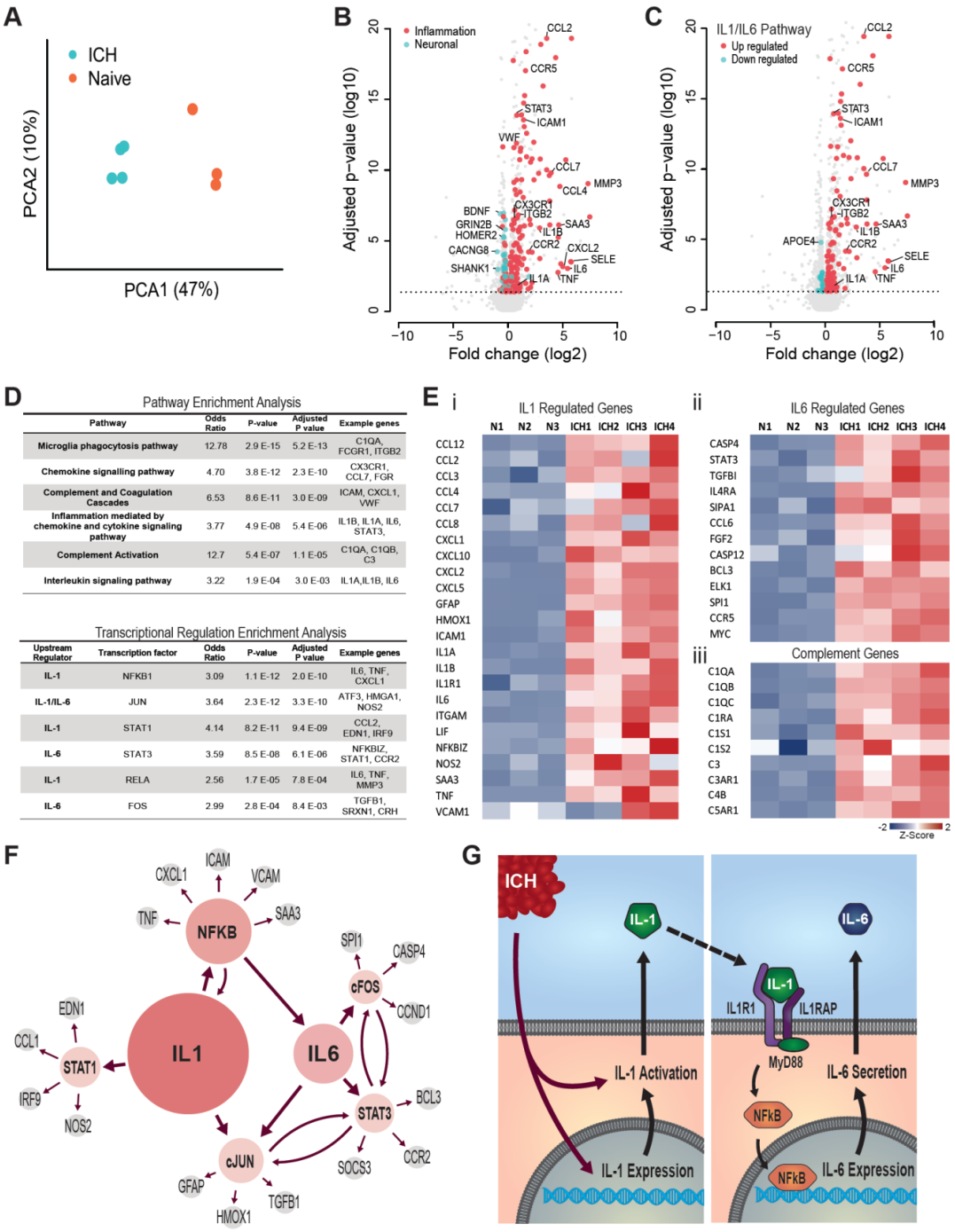

Figure 3.2 Pathway and transcriptional regulation analyses revealed that interleukin (IL)-1 and IL-6 mediated inflammation is a predominate feature of intracerebral haemorrhage (ICH).

Pathway and transcriptional regulation analyses revealed that interleukin (IL)-1 and IL-6 mediated inflammation is a predominate feature of intracerebral haemorrhage (ICH). Whole hemisphere RNA was extracted for RNA sequencing 24h after ICH (n = 4) or no intervention (n = 3) (Naïve). (A) Unguided principal component analysis clearly delineates unique transcriptional profiles of ICH and Naïve animals. (B) A volcano plot with inflammatory genes (red) and neuronal genes (turquoise) identified by PANTHER and GO term string search, demonstrates the predominance of the inflammatory pathway in the transcriptional changes following ICH. (C) A volcano plot of IL-1 and IL-6 networks identified through PANTHER, GO term and TTRUST string searches; illustrating the central role these networks have in ICH induced inflammation. (D) Results from PANTHER and GO term string search pathway enrichment analysis and the TTRUST transcriptional regulation enrichment analysis. (E) Heat maps of the top significant genes identified within the most notable networks; IL-1 (i), IL-6 (ii) and complement (iii). (F) Cluster and pathway analyses identified IL-1β and IL-6 signalling as the predominate pathways regulating inflammation following ICH. Area of the coloured circles are

proportional to the number of significantly upregulated genes identified downstream of the labelled regulator molecule. IL-1 was the dominant signalling pathway identified with 209 downstream genes found to be upregulated. (G) Proposed signalling cascade responsible for the substantial inflammatory response seen following ICH.

Mononuclear phagocytes produce IL-1 in response to brain haemorrhage

IL-1α and IL-1β are part of a highly conserved cytokine pathway that signal through the type 1 IL-1 receptor (IL-1R1) and have important functions in inflammation. In the brain IL-1 has been shown to control monocyte trafficking and directly contribute to deleterious inflammation in sterile injury[12]. A specific role for IL-1 in brain haemorrhage remains undefined however. We therefore continued our investigations by assaying for IL-1 production in brain haemorrhage tissue (Figure 3.3).

We first looked for evidence of IL-1 production in post-mortem human brain tissue. Under steady state conditions microglia, the brain resident mononuclear phagocytes, have a ramified morphology with outstretched processes that carry out important homeostatic functions, including synaptic pruning[37] and neuronal surveillance[38]. In control human brain tissue, age- and region-matched for diseased tissue, microglia stained with Iba1 were ramified and lacked evidence of IL-1 production (Figure 3.3Ai). On the contrary, in acute macrobleed patient samples there was clear evidence of microglia with retracted processes expressing IL-1β in perihaematomal regions (Figure 3.3Aii). Whilst there was also evidence of IL-1β production in microbleed patient tissue, there were far fewer cells producing the molecule in this setting (Supplementary Figure 1). However, the non-fatal nature of microbleeds makes obtaining fresh bleeds difficult and hypertrophic microglial clusters observed in these samples indicated that temporal differences may part explain the reduced levels of IL-1. The inaccessible nature of human brain tissue limits spatiotemporal investigations so in order to fully characterise IL-1 kinetics in response to acute brain haemorrhage, we again turned focus to the murine model.

In line with the findings from human post-mortem brain tissue, IL-1+ perihaematomal microglia were identified in our mouse model of brain haemorrhage (Figure 3.3B). Kinetic mapping of IL-1 production identified two compartmentalised distinct cell types that produced the IL-1 (Figure 3.3B-C). Whilst microglia downregulated IL-1α and IL-1β production after 4h of brain haemorrhage, a number of IL-1β+ Iba1- cells, situated in the haematoma, were seen in the following 20 hours (Figure 3.3C). Single cells from murine brain tissue were isolated and immunoblotting (Figure 3.3D) and flow cytometry (Figure 3.3E) were used to map persistent IL-1β production to CD11b+ mononuclear phagocytes.

In line with transcriptomic analysis, these data indicate that mononuclear phagocytes produce IL-1 proteins in the period preceding and during harmful myeloid cell trafficking to the haemorrhaged brain.

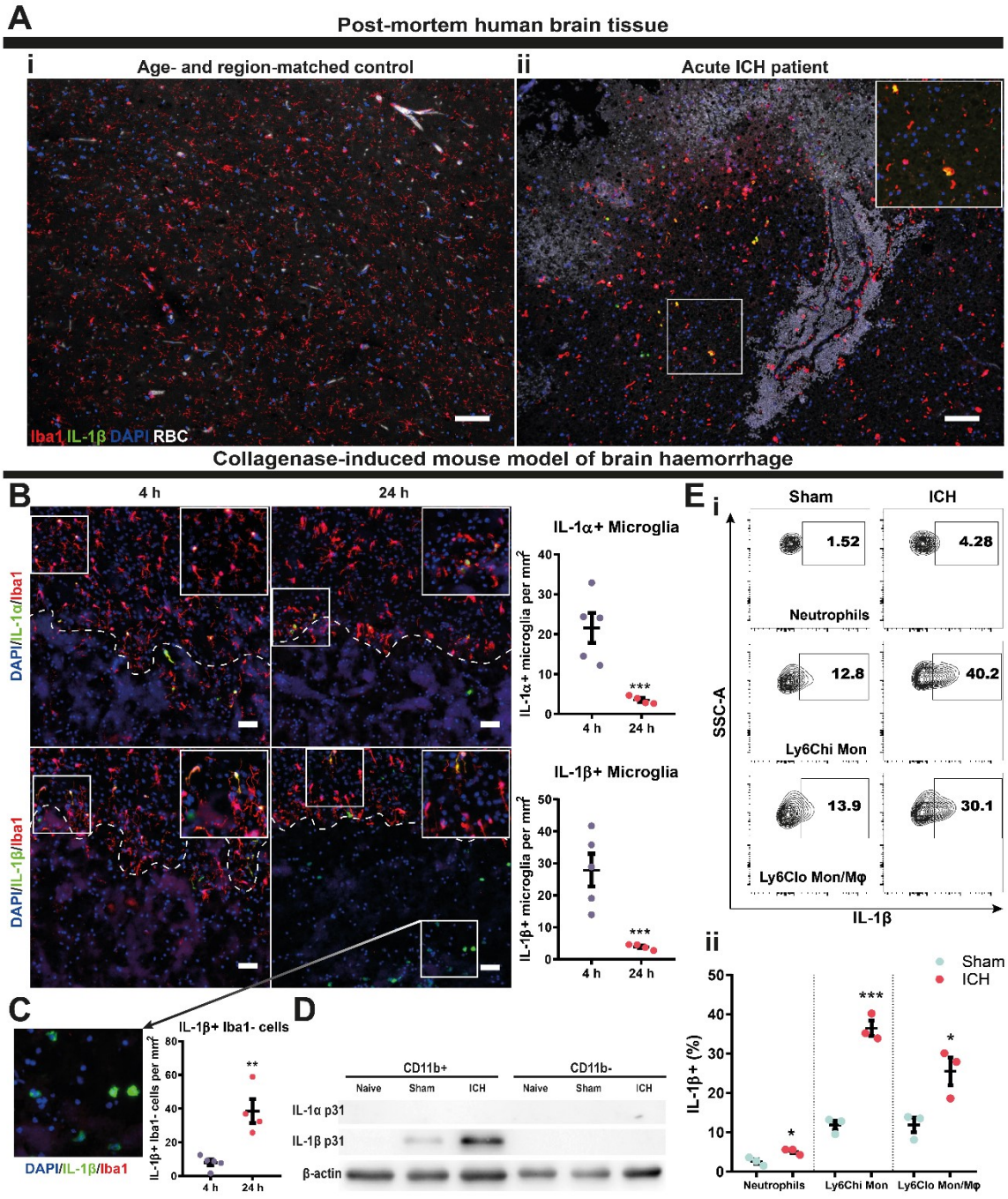

Figure 3.3 IL-1 is produced by mononuclear phagocytes in the acute phase of brain haemorrhage

IL-1 is produced by mononuclear phagocytes in the acute phase of brain haemorrhage. (A) 8 µm sections of formalin-fixed paraffin-embedded post-mortem human brain tissue from age- and region-matched control (Ai) and acute intracerebral haemorrhage (ICH) (Aii) patients were immunostained for Iba1 (red), IL-1β (green) and DAPI (blue). Red blood cell (RBC) autofluorescence can be seen in white. One representative image from 3 patients per group is shown; scale bar 100 µm. Inset is higher magnification image of white box. (B) Mice were subjected to collagenase-induced ICH and culled at 4 and 24 h post-ICH. 20 µm coronal brain sections were immunostained for either IL-1α (green, top) or IL-

1β (green, bottom) together with Iba1 (red) and DAPI (blue). Amount of perihaematomal IL-1 positive microglia were quantified over the two time points. Dotted lines represent haematoma border, insets are higher magnification images of respective white boxes, scale bars are 50 μm. *n* = 4-5. (C) IL-1β+ Iba1- cells were found in the haematoma and quantified at 4 and 24 h post-ICH. *n* = 6. (D) Single cells were isolated from the right hemisphere of naive, sham-operated, and collagenase-induced intracerebral haemorrhage (ICH) mice 24h post-surgery, CD11b+ cells were purified by magnabead separation and CD11b+ and CD11b- lysates immunoblotted for pro-IL-1α (31 kDa), pro-IL-1β (31 kDa) and β-actin (42 kDa). (E) Flow cytometric analysis of IL-1β+ myeloid cells in the brains of sham-operated and haemorrhaged mice 24 h post-surgery. *n* = 3. Data presented as mean + s.e.m. ns = not significant; * = P<0.05; ** = P<0.005; *** = P<0.0005; **** = P<0.0001.

Microglia and caspase-1 are dispensable, but IL-1R1 is essential, for myeloid cell trafficking to the haemorrhaged brain

Using the IL-1 receptor antagonist (IL-1RA) we assessed the functional effects of IL-1 in brain haemorrhage. To block IL-1 from central and peripheral mononuclear phagocyte compartments an intrastriatal bolus of 10 μg IL-1RA was administered immediately before collagenase injection, followed by an immediate sub-cutaneous 100 mg kg^{-1} dose which was repeated 6h later (Figure 3.4A). Using flow cytometry (Figure 4B) and immunohistochemistry (Figure 3.4C), it was discovered that animals injected with IL-1RA had fewer myeloid cells in the brain 24 hours post-haemorrhage. It is hypothesised that IL-1 facilitates myeloid cell trafficking in neuroinflammation by promoting vascular inflammation[12,13]. In line with this, fewer vascular cells expressing the inflammatory adhesion molecule VCAM-1 were observed in the brains of IL-1RA treated mice (Figure 3.4D).

Having established that IL-1 is produced by microglia in the period preceding major myeloid cell recruitment in brain haemorrhage, we subsequently tested whether microglia are the critical source of IL-1 for this recruitment by efficiently depleting them using the specific CSF1R antagonist PLX5622 (Figure 3.4Ei). In microglia depleted animals there were no differences in neutrophil numbers, and increased amounts of IL-1β+ cells could be seen in the brain 24 hours post-haemorrhage (Figure 3.4Eii-iii). These data suggest microglia are not required for neutrophil trafficking and may limit IL-1β+ mononuclear phagocyte entry to the haemorrhaged brain, in contrast to previous studies showing microglia promote myeloid cell trafficking during brain inflammation[33].

Having ruled out microglia, we next turned focus to the molecular processes regulating IL-1 signaling. We previously established that IL-1β was produced early and persisted during the critical myeloid cell recruitment phase. IL-1β is produced as an inactive precursor molecule that is activated upon the formation of macromolecular complexes called inflammasomes, which result in auto-cleavage of the IL-1β activating enzyme caspase-1[39]. The inflammasome field has gained immense traction in recent years because of the

pathological roles inflammasomes have in many diseases. Indeed, some studies suggest inflammasome activation has a causal role in myeloid cell recruitment during brain haemorrhage[40–42]. However, inhibition of caspase-1 using the specific inhibitor VX-765, under the same treatment regimen as for our IL-1RA experiments, had no effect on immune cell trafficking in the first 24 hours of brain haemorrhage (Figure 3.4F). Thus, inflammasomes do not contribute to immune recruitment in the first 24 hours following brain haemorrhage. Overall, these data show that IL-1 signalling through IL-1R1 critically mediates myeloid cell trafficking to the brain following haemorrhage.

IL-1 restricts brain damage by controlling blood flow to sites of brain haemorrhage

Having previously established that monocyte recruitment contributes to neuromotor injury and that IL-1 facilitates monocyte trafficking, we next looked to see whether IL-1 inhibition improved neuromotor outcome in our murine model. To address this question we developed an extended IL-1RA treatment regimen that ended at day 2, in order to limit effects on the published pro-reparative function of monocytes[34] (Figure 3.5A). Using the rotarod assay we found that animals treated with IL-1RA performed worse within 24 hours of brain haemorrhage and did not improve over the 7 day testing period, with weight loss showing a similar trend (Figure 3.5B-C). Whilst IL-1 has important functions in inflammation it is also a pleiotropic cytokine that is proposed to sit at the apex of inflammation and coagulation. We therefore hypothesised that IL-1 inhibition worsened injury in our haemorrhage model by preventing inflammation-coagulation cross-talk resulting in larger bleed volumes. However, histological and biochemical analysis of blood load indicated that IL-1 inhibition did not affect bleed size (Figure 3.5D). IL-1 can also affect vascular tone, where it has been shown to modulate both vasoconstriction and vasodilatation dependent on the signalling niche. To assess potential changes to cerebral blood flow we performed laser speckle contrast imaging on mice subjected to brain haemorrhage. In line with others[43–45], we were able to detect a reduction in cortical CBF following striatal brain haemorrhage. However, the reduction in CBF was exacerbated in mice treated with IL-1RA (Figure 3.5E). Importantly, this was not seen in sham-operated controls (Supplementary Figure 2). Cyclooxygense-2 (COX-2) is a major downstream target of IL-1 that regulates vascular tone during inflammatory conditions by producing various eicosanoids. In line with this, human brain endothelial cells incubated with IL-1β produced COX-2 and VCAM-1 within 4 hours (Figure 3.5E). Moreover, COX-2 was expressed by vascular cells specifically in the ipsilateral hemisphere of haemorrhaged mice

(Figure 3.5G). These data show that, in response to brain haemorrhage, IL-1 modulates vascular tone through COX-2 and this outweighs its function as a facilitator of harmful myeloid cell recruitment.

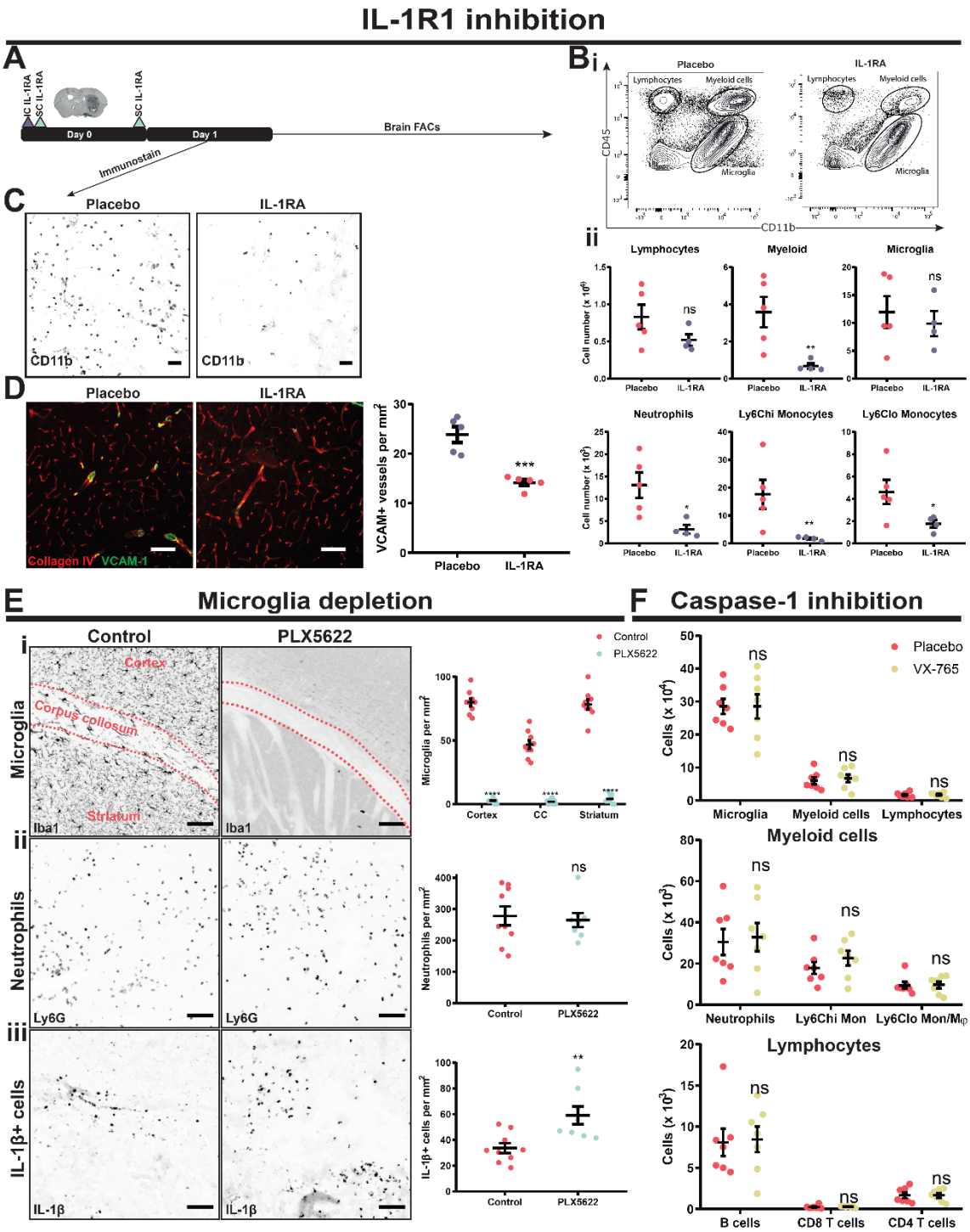

Figure 3.4 IL-1R1 is essential but microglia and caspase-1 are dispensable for myeloid cell trafficking to the brain 24 h following haemorrhage

(A) Experimental design consisted of a placebo or an IL-1 receptor antagonist (IL-1RA) treatment regimen of 10 µg intrastriatal injection followed by a 100 mg kg^{-1} subcutaneous dose, prior to ICH induction, followed by another 100 mg

kg^{-1} subcutaneous dose 6 hours later. (B) (B) Single cells were isolated from the right hemisphere of placebo (n = 5) and IL-1RA (n = 4) treated collagenase-induced haemorrhage mice 24h post-surgery and immunophenotyped using flow cytometry. Gating of lymphocytes, myeloid cells and microglia. (C) Mice were culled at 24 h following haemorrhage and 20 µm coronal brain sections were immunostained for CD11b and images taken of the haematoma. One representative image from 8 biological repeats shown; scale bar 50 µm. (D) 20 µm coronal brain sections were immunostained for collagen IV (red) and VCAM (green) and images taken in the perihaematomal region 24 h post-ICH. Amount of VCAM+ blood vessels were quantified. n = 5, one representative image from each group shown with scale bar 50 µm. (Ei) Mice were fed a control (n = 9) or PLX5622 (CSF1R antagonist; n = 8) containing diet for 14 days prior to collagenase injection and Iba1 was used to quantify microglia in the cortex, corpus collosum (CC) and striatum of brain sections. (Eii) Haematomal neutrophils were quantified using Ly6G and (Eiii) IL-1β+ cells were also measured. One representative image from each group shown with scale bar 50 µm. (F). Mice were intrastriatally and subcutaneously injected with 7.5 µg and 50 mg kg^{-1} of the caspase-1 inhibitor VX-765, respectively, or placebo, prior to collagenase injection, followed by a second subcutaneous 50 mg kg^{-1} dose 6 hours later. Single cells were isolated 24h post-surgery and immunophenotyped using flow cytometry. n = 7. Data presented as mean + s.e.m, ns = not significant; * = P<0.05; ** = P<0.005; *** = P<0.0005; **** = P<0.0001.

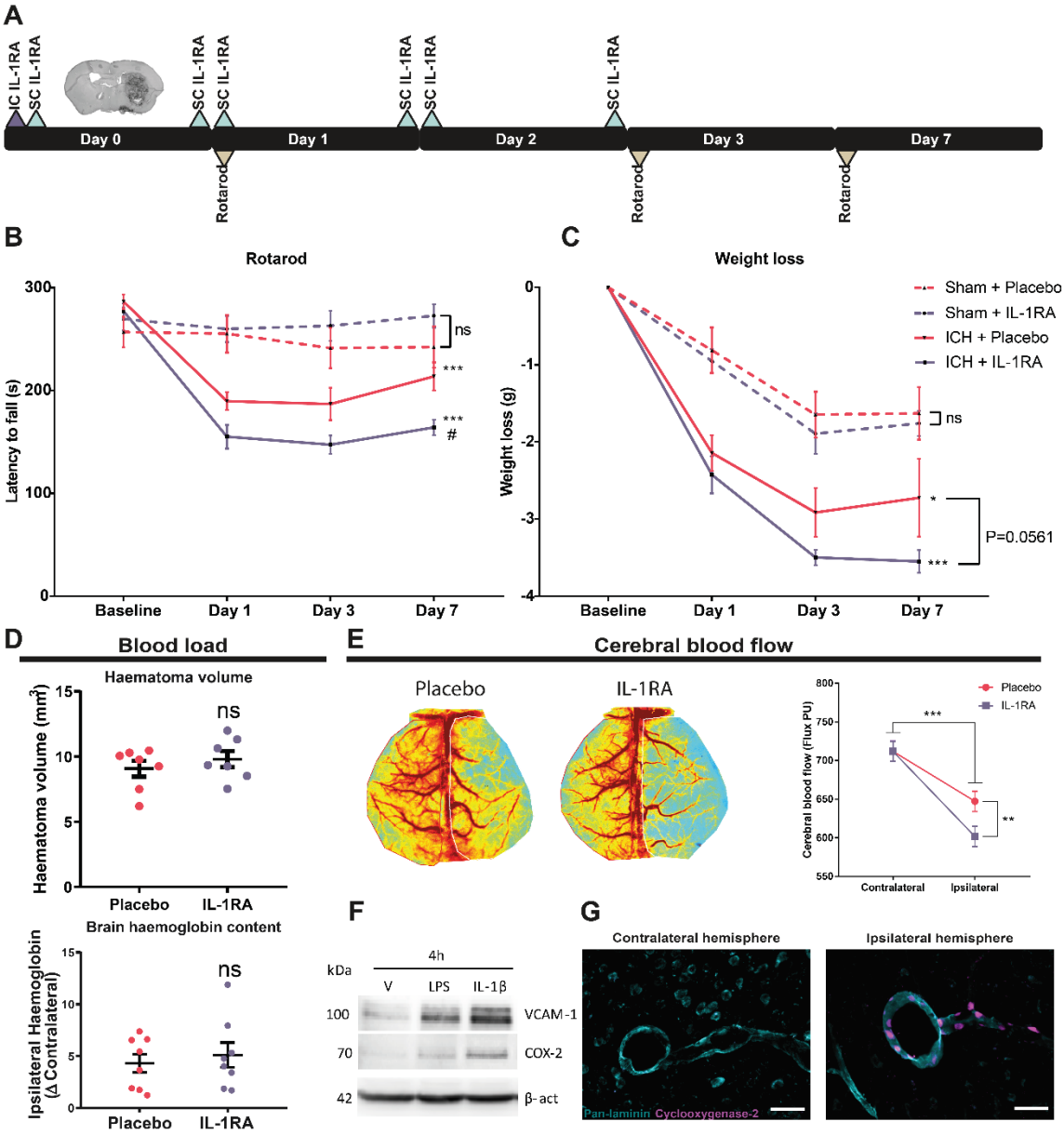

Figure 3.5 IL-1 restricts neuromotor injury by increasing blood flow to sites of brain haemorrhage

(A) Experimental design consisted of a placebo or an IL-1 receptor antagonist (IL-1RA) treatment regimen of 10 µg intrastriatal injection followed by a 100 mg kg-1 subcutaneous dose, prior to ICH induction, followed by another 100 mg

kg-1 subcutaneous dose 6, 24, 30, 48 and 54 hours later. Rotarod performance was also measured at day one, three and seven. (B) Rotarod performance and (C) net weight loss of placebo (n = 7) or IL-1RA (n = 6) treated sham and intracerebral haemorrhage (ICH) mice. ns = not significant; * = P<0.05 compared to relative sham; *** = P<0.0005 compared to relative sham; # = P<0.05 compared to ICH + placebo. (D) Haematoma volume (n = 7) and haemoglobin content (n = 7-8) was assessed using histological and protein analysis of brains. (E) Cerebral blood flow was quantified using laser speckle contrast imaging. (F) Human brain endothelial cells were incubated with 10 ng of IL-1β and western blots were performed for VCAM-1, cyclooxygenase-2 (COX-2) and β actin. One representative blot from 3 independent experiments shown. (G) COX-2 (magenta) is expressed by vascular associated cells in the ipsilateral hemisphere of haemorrhaged mice. Pan-laminin (cyan) was used as a vascular marker. One representative image from 2 animals shown. Scale bar is 50 μm. All data presented as mean ± s.e.m apart from (D) which is presented as marginal means ± standard error. ns = not significant; * = P<0.05; ** = P<0.005; *** = P<0.0005; **** = P<0.0001.

3.6 Discussion

Despite being a prominent feature in many brain diseases, the pathophysiological consequence of brain haemorrhage is poorly understood. Here we present further evidence that brain haemorrhage results in the pathological accumulation of detrimental myeloid cells within the brain. Using RNA-seq, histological analysis, and *in vivo* perturbations, we identify IL-1 as the major upstream regulator of harmful myeloid cell recruitment. However, to our surprise, we found that IL-1 was also required for efficient maintenance of CBF within the affected brain hemisphere. Thus we present first evidence that IL-1 critically controls blood flow to reduce neuromotor damage following brain haemorrhage, and implicate COX-2 in this beneficial role of inflammation.

Intraparenchymal accumulation of blood results in mass effect that is immediate and therefore difficult to treat clinically. We, along with others, have shown that monocytes contribute to injury during acute brain haemorrhage and could thus represent a viable therapeutic target. We used $CCR2^{-/-}$ mice as a model to investigate the contribution of monocytes to brain haemorrhage, however, T cells[46], endothelial cells[47] and brain associated macrophages (BAMs)[48] are also known to express CCR2. T cells are part of the adaptive immune system that requires a period of activation, and CCR2 on BAMs is linked to proliferation and migration in diseased brain states[49]. We report CCR2 effects in the first 24 hours of brain haemorrhage, and this coincides with few T cells in the brain, and precedes brain microglia/macrophage proliferation[50]. It is therefore unlikely that either T-Cells or microglia contribute to our CCR2-dependent effects. Endothelial CCR2, on the other hand, is required for efficient monocyte transmigration and thus is likely to phenocopy monocyte CCR2[47]. Whilst we cannot categorically rule out contribution of T cells and BAMs, we believe the amassed evidence implicating monocytes specifically in the pathophysiology of brain haemorrhage[9,11,34,51], points toward monocyte infiltration being the causative factor in our $CCR2^{-/-}$ results. It is not currently clear how monocytes

contribute to acute neurological injury in mouse models of brain haemorrhage and studies of other acute brain disease paradigms find opposing effects. In mouse models of ischaemic stroke for example, monocytes have been shown to prevent haemorrhagic transformation by maintaining vascular integrity through TGF-β[52], though this has been challenged more recently[53]. The levels of CCL2 in ICH patient plasma correlates with disease severity and one possibility is that monocytes contribute to haematoma expansion, as previous studies have shown delayed haematoma growth in $CCR2^{-/-}$ mice[9,51]. Monocytes enter the brain and over time transition to macrophages that are important in clearance of neurotoxic red blood cells[34]. We chose here to identify the upstream regulator of acute harmful monocyte recruitment.

Monocyte trafficking to inflamed tissue relies on the chemokine CCL2 but here we show that IL-1 critically regulates the recruitment of myeloid cells following brain haemorrhage. Whilst IL-1R1 signalling can result in CCL2 production, it is likely IL-1 sits at the apex of a wide range of inflammatory signalling pathways as we also reveal effects on CCL2-independent neutrophils. Tissue infiltration of myeloid cells requires transmigration through inflamed vasculature and we identified IL-1 specific upregulation of the adhesion molecule VCAM1, which is essential for tethering of immune cells to endothelium during inflammation. VCAM1 directly binds to the very-late antigen 4 complex that is part made up of the α4 integrin, and α4 inhibition has been previously shown to abrogate monocyte infiltration[11,54]. It is likely, therefore, that IL-1 signals to the cerebrovasculature to promote brain trafficking of myeloid cells. Indeed, genetic tools have recently shown activation of brain endothelial specific IL-1R1 facilitates myeloid cell trafficking to the brain and is responsible for neutrophil recruitment in a murine model of ischaemic stroke[12,13].

Here we showed that IL-1 produced by mononuclear phagocytes is responsible for myeloid cell trafficking to the haemorrhaged brain. Previous studies using post-mortem ICH patient tissue provided evidence of IL-1β production but did not identify the cell type responsible[55]. We show that microglia produce IL-1β following clinical ICH and these results validate findings using peri-haematomal resections without the confounding factor of surgical manipulation of the tissue[33]. Both IL-1α and IL-1β signal through IL-1R1 resulting in equivalent downstream signals. We found IL-1α and IL-1β were produced by microglia within 4 hours of collagenase-induced brain haemorrhage whereas monocytes prolong IL-1β production to 24 hours. Although they were the earliest producers of IL-1, depleting microglia had no effect on neutrophil infiltration but increased the amount of IL-

1β positive cells in the brain. Depleting microglia alongside blood brain barrier disruption leads to part-repopulation of the niche by circulating monocytes[56]. The BBB is destroyed during brain haemorrhage and we showed that monocytes produce IL-1β at day one. We speculate that microglia depletion caused a compensatory increase in monocyte trafficking in the first 24 hours of brain haemorrhage and this is in line with results from a reductionist model of brain inflammation[12]. Although, a previous study that depleted microglia using an earlier form of the Plexxikon CSF1R inhibitor did show a reduction in neutrophil recruitment[33]. This discrepancy could be due to the drug used, treatment regimen, or neutrophil quantification methods, as all differed to the current study. We found evidence of persistent IL-1β production in the acute phase of brain haemorrhage. The native 31 kDa IL-1β molecule requires cleavage to adopt a form that can bind and activate IL-1R1. The best studied IL-1β cleaving molecule is caspase-1, which is activated upon multimolecular platforms termed inflammasomes[39]. There are a number of sensor molecules that trigger inflammasome activation upon recognition of DAMPs ranging from ATP to lysophosphotidylcholine[57,58]. There is evidence to show that one such inflammasome sensor molecule, NLRP3, contributes to immune cell trafficking following brain haemorrhage[41]. We previously showed that while inflammasomes do contribute to ischaemic stroke it is independent of NLRP3[59,60]. Here we adopted a strategy to block all inflammasomes in the acute phase of brain haemorrhage by inhibiting caspase-1 and found no effect. Previous studies quantified inflammasome dependent effects on myeloid cell trafficking 3 days post injury, whereas we show no effect at 24 hours. This temporal difference could have a large impact on findings as red blood cells start to lyse at day three resulting in the release of the NLRP3 inflammasome activator haem[61]. Caspase-1 activation also results in cleavage of a plethora of intracellular proteins which may act to oppose IL-1β signalling and therefore muddy our findings[62].

It was initially believed that brain haemorrhage was accompanied by a perihaematomal ischaemic region that could be viewed in the same vein as the ischaemic stroke penumbra. Many studies had identified regions of hypoperfusion in both clinical and preclinical investigations[43–45,63–66]. However, quantification of metabolic function in the hypoperfused region, using the haemodynamic readout of oxygen extraction fraction, could not provide evidence of ischaemia[67]. These findings have led the field to dismiss the importance of changes in CBF following brain haemorrhage, despite evidence that quantitative changes in CBF can predict outcome[65,68]. The brains inability to store energy causes a

disproportionate requirement of blood supply that has resulted in the evolution of multi-level mechanisms of CBF regulation. Disruption to the supply of blood flow in healthy individuals can have profound impacts on cognitive function[69] and pathological reduction of CBF is linked to brain atrophy in clinical[70] and preclinical[71] settings; all in the absence of ischaemia. In line with others we have shown that striatal brain haemorrhage results in reductions in CBF, detectable even in the cortex[43–45]. We have made the novel discovery that inflammation, through the molecule IL-1, helps increase CBF and thus reduces neurological dysfunction following brain haemorrhage. Thus we propose a model whereby an inflammatory reaction to brain haemorrhage forms part of a reactive vasodilatory response. In line with this, previous preclinical studies have noted transient reductions in CBF that normalise once the immune response heightens[10,72]. We hypothesise that IL-1's effect on blood flow is via its common downstream target COX-2. COX-2 is responsible for the conversion of arachidonic acid to prostaglandin H2 which in itself can be converted to any of four further vasoactive prostaglandins by distinct terminal prostaglandin synthases. The five prostaglandins, in turn, can act on a range of receptors leading to spatial and context specific effects. Prostaglandin E_2 (PGE_2), for example, is a potent vasodilator when applied systemically but when applied centrally can be a powerful vasoconstrictor[73]. IL-1 itself has also been shown to have contrasting effects on blood flow. Application of IL-1 into musculoskeletal arteries *in vivo* causes vasodilation, whereas isolation and stimulation of the same arteries *ex vivo* has no effect[74]. IL-1 coupled to acute cerebral ischaemia causes endothelin-1 release leading to reduced haemodynamics[15], however, injections of IL-1 into the basilar artery leads to prostacyclin production and subsequent vasodilation[75]. The vast majority of vascular mural cells express IL-1R1 and the complex actions of IL-1 on vascular tone is likely due to cell-specific effects. Studies are now needed to delineate the cerebral cell-specific actions of IL-1 and COX-2 during steady state and disease. Future studies must also look to place cell-specific actions in to the contexts of biological systems. We hypothesise, for example, that coagulation, without the buffer of IL-1-induced prostaglandins produced by vascular mural cells, skews vascular tone toward vasoconstriction through the large amounts of thromboxane A_2 released from platelets. Studies that test such hypotheses may also provide insights into the mechanisms predisposing brain haemorrhage patients with underlying SVD to secondary ischaemic insults[76].

We currently view micro- and macrobleeds as distinct entities due to the great differences in clinical presentation. Whilst microbleeds do not have such drastic consequences as macrobleeds, it is likely that the acute and chronic pathophysiological consequences share important features. We provide evidence that microglia and peripheral immune cells respond to bleeds independent of size and there is also evidence from mouse models that mass effect and CBF alterations occur in both large and small bleeds[77,78]. Patients with microbleeds are more likely to experience large bleeds and some patients with large bleeds go on to experience cognitive decline that is so often linked to small bleeds[79,80]. More studies are now needed to identify core features of brain haemorrhage that occur independent of size but contribute to its pathogenesis, so that future treatments can target all brain haemorrhage patients.

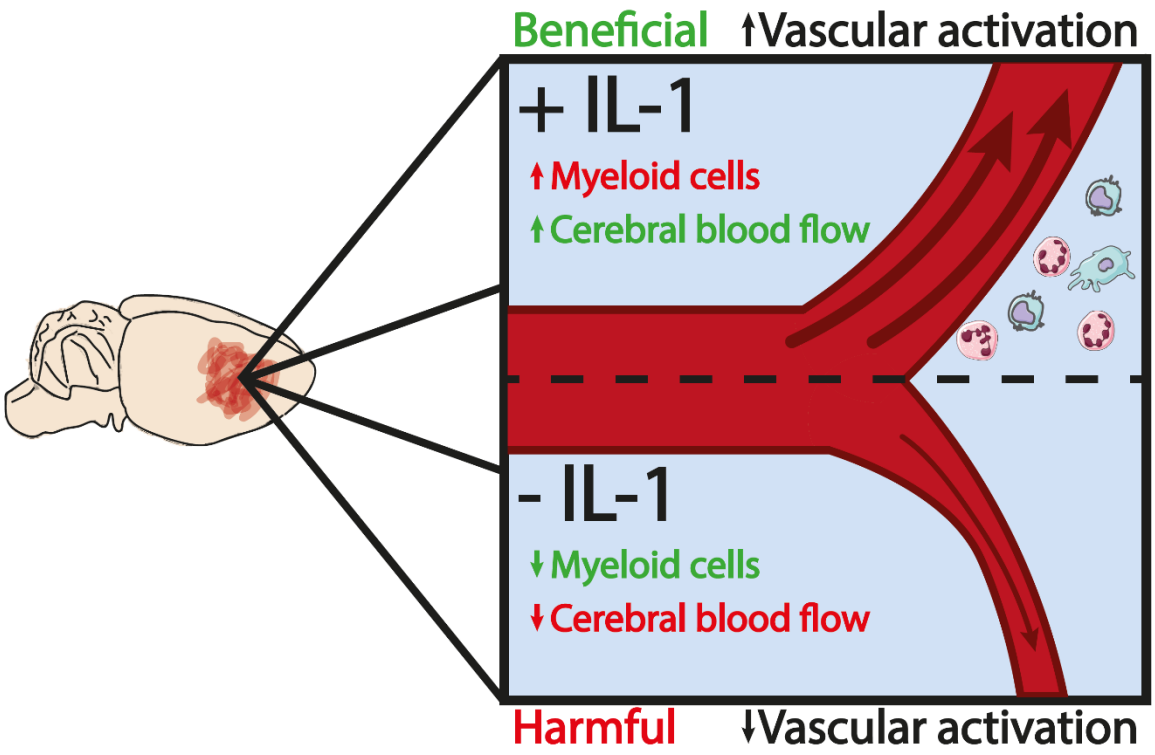

Figure 3.6 Summary diagram highlighting the main findings of this study. Following brain haemorrhage, interleukin-1 (IL-1) has dichotomous functions. On the one hand, IL-1 controls harmful myeloid cell trafficking to the brain, whilst on the other, IL-1 critically regulates cerebral blood flow within the affected hemisphere.

3.7 References

1. Strangward, P. *et al.* A quantitative brain map of experimental cerebral malaria pathology. *PLOS Pathog.* **13**, e1006267 (2017).

2. Ungvari, Z., Tarantini, S., Kirkpatrick, A. C., Csiszar, A. & Prodan, C. I. Cerebral microhemorrhages: mechanisms, consequences, and prevention. *Am. J. Physiol. Circ. Physiol.* **312**, H1128–H1143 (2017).

3. Bruns, J. & Hauser, W. A. The Epidemiology of Traumatic Brain Injury: A Review. *Epilepsia* **44**, 2–10 (2003).

4. Qureshi, A. I., Mendelow, a. D. & Hanley, D. F. Intracerebral haemorrhage. *Lancet* **373**, 1632–1644 (2009).

5. Allan, S. M. & Rothwell, N. J. Inflammation in central nervous system injury. *Philosophical Transactions of the Royal Society B: Biological Sciences* (2003). doi:10.1098/rstb.2003.1358

6. Delvaeye, M. & Conway, E. M. Coagulation and innate immune responses: can we view them separately? *Blood* **114**, 2367–74 (2009).

7. Liesz, A. *et al.* Comparison of humoral neuroinflammation and adhesion molecule expression in two models of experimental intracerebral hemorrhage. *Exp. Transl. Stroke Med.* **3**, 11 (2011).

8. Sansing, L. H. *et al.* Toll-like Receptor 4 Contributes to Poor Outcome after Intracerebral Hemorrhage. *Ann. Neurol.* **70**, 646–656 (2011).

9. Hammond, M. D. *et al.* CCR2+Ly6Chi Inflammatory Monocyte Recruitment Exacerbates Acute Disability Following Intracerebral Hemorrhage. *J. Neurosci.* (2014). doi:10.1523/JNEUROSCI.4070-13.2014

10. Ahn, S. J., Anrather, J., Nishimura, N. & Schaffer, C. B. Diverse Inflammatory Response After Cerebral Microbleeds Includes Coordinated Microglial Migration and Proliferation. *Stroke* **49**, 1719–1726 (2018).

11. Hammond, M. D., Ambler, W. G., Ai, Y. & Sansing, L. H. α4 integrin is a regulator of leukocyte recruitment after experimental intracerebral hemorrhage. *Stroke* **45**, 2485–7 (2014).

12. Liu, X. *et al.* Cell-Type-Specific Interleukin 1 Receptor 1 Signaling in the Brain Regulates Distinct Neuroimmune Activities. *Immunity* **0**, 317-333.e6 (2019).

13. Wong, R. *et al.* Interleukin-1 mediates ischaemic brain injury via distinct actions on endothelial cells and cholinergic neurons. *Brain. Behav. Immun.* **76**, 126–138 (2019).

14. Lawrence, C. B., Allan, S. M. & Rothwell, N. J. Interleukin-1β and the interleukin-1 receptor antagonist act in the striatum to modify excitotoxic brain damage in the rat. *Eur. J. Neurosci.* **10**, 1188–1195 (1998).

15. Murray, K. N. *et al.* Systemic Inflammation Impairs Tissue Reperfusion Through Endothelin-Dependent Mechanisms in Cerebral Ischemia. *Stroke* **45**, 3412–3419 (2014).

16. Boring, L. *et al.* Impaired monocyte migration and reduced type 1 (Th1) cytokine responses in C-C chemokine receptor 2 knockout mice. *J. Clin. Invest.* **100**, 2552–2561 (1997).

17. Kilkenny, C., Browne, W. J., Cuthill, I. C., Emerson, M. & Altman, D. G. Improving bioscience research reporting: The arrive guidelines for reporting animal research. *Animals* (2013). doi:10.3390/ani4010035

18. Kirkman, M. a, Allan, S. M. & Parry-Jones, A. R. Experimental intracerebral hemorrhage: avoiding pitfalls in translational research. *J. Cereb. Blood Flow Metab.* **31**, 2135–51 (2011).

19. Wajid Jawaid. enrichR: Provides an R Interface to 'Enrichr'. (2019).

20. Han, H. *et al.* TRRUST v2: An expanded reference database of human and mouse transcriptional regulatory interactions. *Nucleic Acids Res.* (2018). doi:10.1093/nar/gkx1013

21. Chen, E. Y. *et al.* Enrichr: Interactive and collaborative HTML5 gene list enrichment analysis tool. *BMC Bioinformatics* (2013). doi:10.1186/1471-2105-14-128

22. Kuleshov, M. V. *et al.* Enrichr: a comprehensive gene set enrichment analysis web server 2016 update. *Nucleic Acids Res.* (2016). doi:10.1093/nar/gkw377

23. Team, R. C. R: A Language and Environment for Statistical Computing. *Vienna, Austria* (2019).

24. Kolde, R. pheatmap : Pretty Heatmaps. *R package version 1.0.8* (2015).

25. Wickham, H. Package `ggplot2`: Elegant Graphics for Data Analysis. *Springer-Verlag New York* (2016). doi:10.1093/bioinformatics/btr406

26. Greenhalgh, A. D., Galea, J., Dénes, A., Tyrrell, P. J. & Rothwell, N. J. Rapid brain penetration of interleukin-1 receptor antagonist in rat cerebral ischaemia: Pharmacokinetics, distribution, protection. *Br. J. Pharmacol.* (2010). doi:10.1111/j.1476-5381.2010.00684.x

27. Elmore, M. R. P. *et al.* Colony-stimulating factor 1 receptor signaling is necessary for microglia viability, unmasking a microglia progenitor cell in the adult brain. *Neuron* (2014). doi:10.1016/j.neuron.2014.02.040

28. Fekete, R. *et al.* Microglia control the spread of neurotropic virus infection via P2Y12 signalling and recruit monocytes through P2Y12-independent mechanisms. *Acta Neuropathol.* 1–22 (2018). doi:10.1007/s00401-018-1885-0

29. Flores, J. *et al.* Caspase-1 inhibition alleviates cognitive impairment and neuropathology in an Alzheimer's disease mouse model. *Nat. Commun.* (2018). doi:10.1038/s41467-018-06449-x

30. Pinheiro, J., Bates, D. & R-core. Package 'nlme': Linear and Nonlinear Mixed Effects Models. *Cran-R* (2018).

31. Mracsko, E. *et al.* Leukocyte Invasion of the Brain After Experimental Intracerebral Hemorrhage in Mice. *Stroke* **45**, 2107–2114 (2014).

32. Sansing, L. H., Harris, T. H., Kasner, S. E., Hunter, C. A. & Kariko, K. Neutrophil depletion diminishes monocyte infiltration and improves functional outcome after experimental intracerebral hemorrhage. *Acta Neurochir. Suppl.* **111**, 173–8 (2011).

33. Li, M. *et al.* Colony stimulating factor 1 receptor inhibition eliminates microglia and attenuates brain injury after intracerebral hemorrhage. *J. Cereb. Blood Flow Metab.* **37**, 2383–2395 (2017).

34. Chang, C.-F. *et al.* Erythrocyte efferocytosis modulates macrophages towards recovery after intracerebral hemorrhage. *J. Clin. Invest.* **128**, 607–624 (2018).

35. Lévesque, S. A. *et al.* Myeloid cell transmigration across the CNS vasculature triggers IL-1ß-driven neuroinflammation during autoimmune encephalomyelitis in mice. *J. Exp. Med.* (2016). doi:10.1084/jem.20151437

36. Smith, C. J. *et al.* SCIL-STROKE (Subcutaneous Interleukin-1 Receptor Antagonist in Ischemic Stroke). *Stroke* (2018). doi:10.1161/strokeaha.118.020750

37. Schafer, D. P. *et al.* Microglia Sculpt Postnatal Neural Circuits in an Activity and Complement-Dependent Manner. *Neuron* **74**, 691–705 (2012).

38. Cserép, C. *et al.* Microglia Monitor and Protect Neuronal Function Via Specialized Somatic Purinergic Junctions in an Activity-Dependent Manner. *SSRN Electron. J.* (2019). doi:10.2139/ssrn.3339900

39. Schroder, K. & Tschopp, J. The Inflammasomes. *Cell* **140**, 821–832 (2010).

40. Ma, Q. *et al.* NLRP3 inflammasome contributes to inflammation after intracerebral hemorrhage. *Ann. Neurol.* **75**, 209–219 (2014).

41. Ren, H. *et al.* Selective NLRP3 (pyrin domain-containing protein 3) inflammasome inhibitor reduces brain injury after intracerebral hemorrhage. *Stroke* (2018). doi:10.1161/STROKEAHA.117.018904

42. Barrington, J., Lemarchand, E. & Allan, S. M. S. M. A brain in flame; do inflammasomes and pyroptosis influence stroke pathology? *Brain Pathol.* **27**, (2017).

43. Ropper, A. H. & Zervas, N. T. Cerebral blood flow after experimental basal ganglia hemorrhage. *Ann. Neurol.* **11**, 266–271 (1982).

44. Yang, G.-Y., Betz, A. L., Chenevert, T. L., Brunberg, J. A. & Hoff, J. T. Experimental intracerebral hemorrhage: relationship between brain edema, blood flow, and blood-brain barrier permeability in rats. *J. Neurosurg.* (1994). doi:10.3171/jns.1994.81.1.0093

45. Ke, Z., Ying, M., Li, L., Zhang, S. & Tong, K. Evaluation of transcranial Doppler flow velocity changes in intracerebral hemorrhage rats using ultrasonography. *J. Neurosci. Methods* **210**, 272–280 (2012).

46. Mack, M. *et al.* Expression and characterization of the chemokine receptors CCR2 and CCR5 in mice. *J. Immunol.* **166**, 4697–704 (2001).

47. Dzenko, K., Song, L., Ge, S., Kuziel, W. & Pachter, J. CCR2 expression by brain microvascular endothelial cells is critical for macrophage transendothelial migration in response to CCL2. *Microvasc. Res.* **70**, 53–64 (2005).

48. Van Hove, H. *et al.* A single-cell atlas of mouse brain macrophages reveals unique transcriptional identities shaped by ontogeny and tissue environment. *Nat. Neurosci.* **22**, 1021–1035 (2019).

49. Gómez-Nicola, D., Schetters, S. T. T. & Perry, V. H. Differential role of CCR2 in the dynamics of microglia and perivascular macrophages during prion disease. *Glia* **62**, 1041–52 (2014).

50. Taylor, R. A. & Sansing, L. H. Microglial responses after ischemic stroke and intracerebral hemorrhage. *Clin. Dev. Immunol.* **2013**, 746068 (2013).

51. Yao, Y. & Tsirka, S. E. The CCL2-CCR2 system affects the progression and clearance of intracerebral hemorrhage. *Glia* **60**, 908–918 (2012).

52. Gliem, M. *et al.* Macrophages prevent hemorrhagic infarct transformation in murine stroke models. *Ann. Neurol.* **71**, 743–752 (2012).

53. Schmidt, A. *et al.* Targeting Different Monocyte/Macrophage Subsets Has No Impact on Outcome in Experimental Stroke. *Stroke* **48**, 1061–1069 (2017).

54. Newham, P. *et al.* α4 Integrin binding interfaces on VCAM-1 and MADCAM-1: Integrin binding footprints identify accessory binding sites that play a role in integrin specificity. *J. Biol. Chem.* (1997). doi:10.1074/jbc.272.31.19429

55. Zhang, Z.-L. *et al.* Nuclear factor-κB activation in perihematomal brain tissue correlates with outcome in patients with intracerebral hemorrhage. *J. Neuroinflammation* **12**, 53 (2015).

56. Mildner, A. *et al.* Microglia in the adult brain arise from Ly-6ChiCCR2+ monocytes only under defined host conditions. *Nat. Neurosci.* **10**, 1544–1553 (2007).

57. Broz, P. & Dixit, V. M. Inflammasomes: mechanism of assembly, regulation and signalling. *Nat. Rev. Immunol.* **16**, 407–420 (2016).

58. Freeman, L. *et al.* NLR members NLRC4 and NLRP3 mediate sterile inflammasome activation in microglia and astrocytes. *J. Exp. Med.* (2017). doi:10.1084/jem.20150237

59. Denes, A. *et al.* AIM2 and NLRC4 inflammasomes contribute with ASC to acute brain injury independently of NLRP3. *Proc. Natl. Acad. Sci. U. S. A.* **112**, 4050–5 (2015).

60. Lemarchand, E. *et al.* Extent of Ischemic Brain Injury After Thrombotic Stroke Is Independent of the NLRP3 (NACHT, LRR and PYD Domains-Containing Protein 3) Inflammasome. *Stroke* **50**, (2019).

61. Dutra, F. F. *et al.* Hemolysis-induced lethality involves inflammasome activation by heme. *Proc. Natl. Acad. Sci. U. S. A.* **111**, E4110–E4118 (2014).

62. Denes, A., Lopez-Castejon, G. & Brough, D. Caspase-1: is IL-1 just the tip of the ICEberg? *Cell Death Dis.* **3**, e338 (2012).

63. Nath, F. P. *et al.* Effects of experimental intracerebral hemorrhage on blood flow, capillary permeability, and histochemistry. *J. Neurosurg.* (1987). doi:10.3171/jns.1987.66.4.0555

64. Mayer, S. A. *et al.* Perilesional blood flow and edema formation in acute intracerebral hemorrhage: a SPECT study. *Stroke* **29**, 1791–8 (1998).

65. Tayal, A. H. *et al.* Quantitative Perihematomal Blood Flow in Spontaneous Intracerebral Hemorrhage Predicts In-Hospital Functional Outcome. *Stroke* **38**, 319–324 (2007).

66. Fainardi, E. *et al.* CT perfusion mapping of hemodynamic disturbances associated to acute spontaneous intracerebral hemorrhage. *Neuroradiology* **50**, 729–740 (2008).

67. Zazulia, A. R. *et al.* Hypoperfusion without ischemia surrounding acute intracerebral hemorrhage. *J. Cereb. Blood Flow Metab.* **21**, 804–810 (2001).

68. Chen, W. *et al.* CT Perfusion Imaging Predicts One-Month Outcome in Patients with Acute Spontaneous Hypertensive Intracerebral Hemorrhage. *Adv. Comput. Tomogr.* (2013). doi:10.4236/act.2013.23019

69. Marshall, R. S. *et al.* Recovery of brain function during induced cerebral hypoperfusion. *Brain* **124**, 1208–1217 (2001).

70. Arba, F. *et al.* Cerebral White Matter Hypoperfusion Increases with Small-Vessel Disease Burden. Data From the Third International Stroke Trial. *J. Stroke Cerebrovasc. Dis.* **26**, 1506–1513 (2017).

71. Nishio, K. *et al.* A Mouse Model Characterizing Features of Vascular Dementia With Hippocampal Atrophy. *Stroke* **41**, 1278–1284 (2010).

72. Rosidi, N. L. *et al.* Cortical Microhemorrhages Cause Local Inflammation but Do Not Trigger Widespread Dendrite Degeneration. *PLoS One* **6**, e26612 (2011).

73. Yang, T. & Du, Y. Distinct roles of central and peripheral prostaglandin E2 and EP subtypes in blood pressure regulation. *Am. J. Hypertens.* **25**, 1042–9 (2012).

74. Minghini, A., Britt, L. D. & Hill, M. A. Interleukin-1 and interleukin-6 mediated skeletal muscle arteriolar vasodilation: in vitro versus in vivo studies. *Shock* **9**, 210–5 (1998).

75. Osuka, K. *et al.* Vasodilator Effects on Canine Basilar Artery Induced by Intracisternal Interleukin-1β. *J. Cereb. Blood Flow Metab.* **17**, 1337–1345 (1997).

76. Kang, D.-W. *et al.* New ischemic lesions coexisting with acute intracerebral hemorrhage. *Neurology* **79**, 848–855 (2012).

77. Keep, R. F., Hua, Y. & Xi, G. Intracerebral haemorrhage: Mechanisms of injury and therapeutic targets. *Lancet Neurol.* **11**, 720–731 (2012).

78. Cianchetti, F. A., Kim, D. H., Dimiduk, S., Nishimura, N. & Schaffer, C. B. Stimulus-Evoked Calcium Transients in Somatosensory Cortex Are Temporarily Inhibited by a Nearby Microhemorrhage. *PLoS One* **8**, e65663 (2013).

79. Wilson, D. *et al.* Cerebral microbleeds and stroke risk after ischaemic stroke or transient ischaemic attack: a pooled analysis of individual patient data from cohort studies. *Lancet Neurol.* **0**,

80. Benedictus, M. R. *et al.* Prognostic Factors for Cognitive Decline After Intracerebral Hemorrhage. *Stroke* **46**, 2773–2778 (2015).

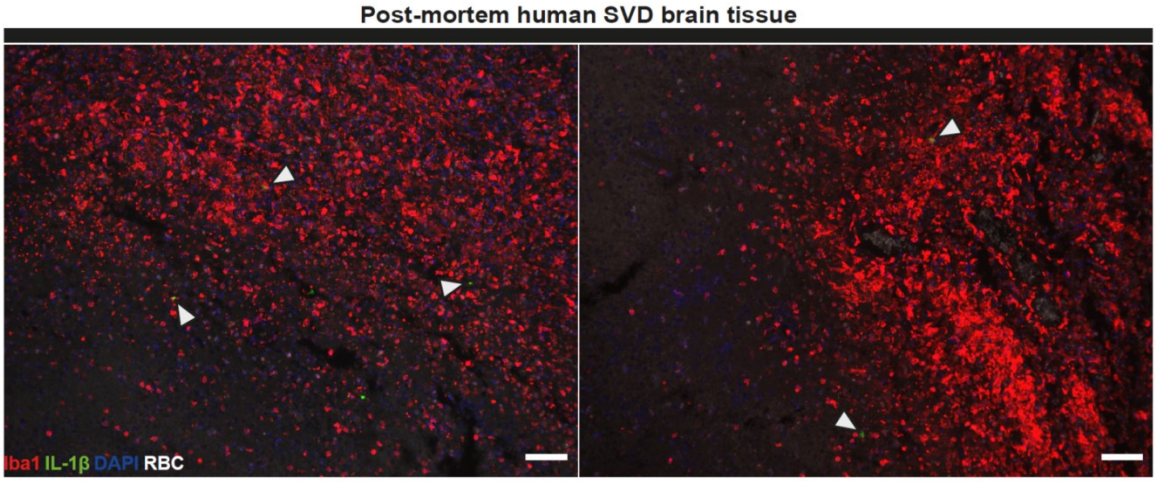

Supplementary Figure 1. IL-1β is expressed in SVD-related microbleeds.

Brain tissue from SVD patients with microbleeds were immunostained for Iba1 (red), IL-1β (green) and DAPI (blue). Red blood cell (RBC) autofluorescence can be seen in white. Two representative image from 3 patients is shown; scale bar 100 µm. Arrows indicate IL-1β+ cells.

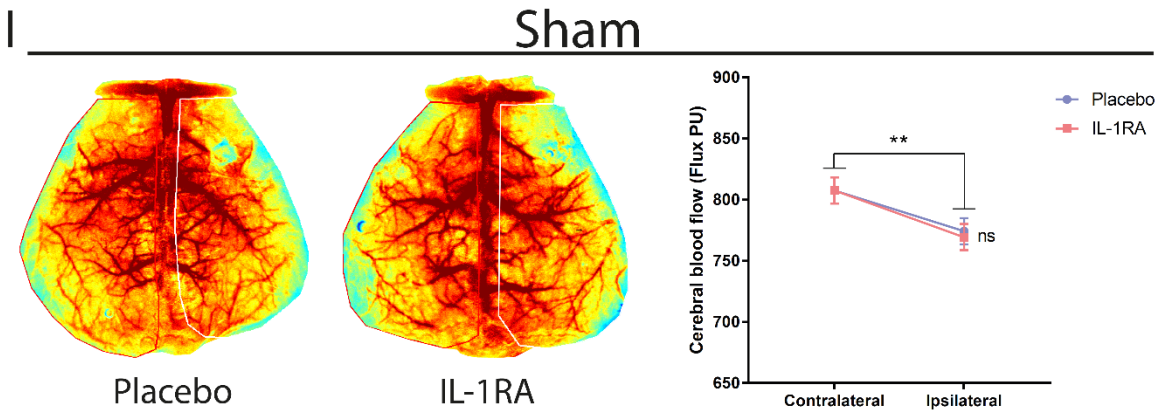

Supplementary Figure 2. IL-1RA does not affect cerebral blood flow in sham-operated animals

Mice were injected with placebo or an IL-1 receptor antagonist (IL-1RA) treatment regimen of 10 µg intrastriatal injection followed by a 100 mg kg-1 subcutaneous dose, prior to ICH induction, followed by another 100 mg kg-1 subcutaneous dose 6, 24, 30, 48 and 54 hours later. Cerebral blood flow was quantified using laser speckle contrast imaging. One representative image from each treatment group shown. Data presented as marginal means ± standard error. ns = not significant, ** = P<0.01.

Chapter 4: NLRP3 in ischaemic stroke

4.1 Paper title and authors

Extent of Ischemic Brain Injury After Thrombotic Stroke Is Independent of the NLRP3 (NACHT, LRR and PYD Domains-Containing Protein 3) Inflammasome

Eloise Lemarchand, PhD[1,3], Jack Barrington BSc[1,3], Alistair Chenery, PhD[2,3], Michael Haley, PhD[2,3], Graham Coutts, PhD[1,3], Judith E. Allen, PhD[2,3], Stuart M. Allan, PhD[1,3,*, #], David Brough, PhD[1,3,*,#]

I designed, implemented and analysed experiments for Figure 3B, 3D and 4C. I also designed the figure layouts and helped write the manuscript alongside E.L. All performed under the guidance of S.M.A and D.B.

[1]Division of Neuroscience and Experimental Psychology

[2]Division of Infection, Immunity & Respiratory Medicine

[3]Lydia Becker Institute of Immunology and Inflammation

School of Biological Sciences, Faculty of Biology, Medicine and Health, Manchester Academic Health Science Centre, University of Manchester, AV Hill Building, Oxford Road, Manchester M13 9PT, UK.

[#]Contributed equally

*Corresponding authors: David Brough, E-mail david.brough@manchester.ac.uk, Tel, +44 (0)161 275 5039, Twitter, @cytobrough; Stuart Allan, E-mail stuart.allan@manchester.ac.uk, Tel, +44 (0)161 275 5255.

Cover title: NLRP3 and ischemic stroke

Figures: 4

Key words: NLRP3 inflammasome, inflammation, cerebral ischemia, cytokine, IL-1

Word count: 4070

4.2 Abstract

Background and Purpose

A major process contributing to cell death in the ischemic brain is inflammation. Inflammasomes are multimolecular protein complexes that drive inflammation through activation of proinflammatory cytokines, such as IL (interleukin)-1β. Preclinical evidence suggests that IL-1β contributes to a worsening of ischemic brain injury.

Methods

Using a mouse middle cerebral artery thrombosis model, we examined the inflammatory response after stroke and the contribution of the NLRP3 (NACHT, LRR and PYD domains-containing protein 3) inflammasome to ischemic injury.

Results

There was a marked inflammatory response after stroke characterized by increased expression of proinflammatory cytokines and NLRP3 and by recruitment of leukocytes to the injured tissue. Targeting NLRP3 with the inhibitor MCC950, or using mice in which NLRP3 was knocked out, had no effect on the extent of injury caused by stroke.

Conclusions

These data suggest that the NLRP3 pathway does not contribute to the inflammation exacerbating ischemic brain damage, contradicting several recent reports to the contrary.

4.3 Introduction

Inflammation is a protective host response required for resistance to infection, though in response to tissue injury inflammation can also contribute to damage[1]. Inflammatory cytokines associated with damaging inflammatory responses include members of the interleukin-1 (IL-1) family, IL-1α and IL-1β[1]. Evidence from pre-clinical models of stroke suggests IL-1 contributes to a worsening of ischemic brain injury[2]. IL-1 activation and release from activated immune cells is regulated by a protein complex called the inflammasome.

Inflammasomes are cytosolic multimeric protein complexes formed in inflammatory cells in response to infection and injury[3]. The most studied inflammasome is composed of the cytosolic pattern recognition receptor (PRR) NACHT, LRR and PYD domains-containing protein 3 (NLRP3). We previously reported ischemic brain injury developed independently of the NLRP3 inflammasome, yet was modified in mice deficient in the PRRs NOD-, LRR- and CARD-containing 4 (NLRC4), absent in melanoma 2 (AIM2), or the inflammasome adaptor molecule apoptosis-associated speck-like protein containing a CARD (ASC)[4]. However, this is controversial and other groups have published correlations and associations with NLRP3 and a worsening of ischemic brain injury[5–8]. Here we sought to definitively determine the importance of NLRP3 to ischemic stroke using $FeCl_3$ to induce thrombi formation in cerebral vessels and cause cerebral ischemia[9], with both genetic and pharmacological approaches to inhibit NLRP3.

4.4 Materials and Methods

The data that support the findings of this study are available from the corresponding author upon reasonable request.

Animals

Experiments were carried out on an in-house colony of 12–16 week old male mice (n = 72) on a C57BL/6 background (WT, $NLRP3^{-/-}$ [10]) at the University of Manchester. The NLRP3 deletion is whole organism rather than cell specific which should be considered when interpreting data in such knockout studies. The experiments were performed on littermate controls except where stated and Supplementary Figure which used mice maintained as homozygotes. Animals were allowed free access to food and water and maintained under temperature-, humidity-, and light-controlled conditions. All animal

procedures adhered to the UK Animals (Scientific Procedures) Act (1986), and experiments were performed in accordance with ARRIVE guidelines, with researchers blinded to treatment or genotype.

Model of thrombotic stroke

Thrombi formation and cerebral ischemia was performed using the $FeCl_3$ method as described previously[9]. Mice were anesthetized with 5% isoflurane, placed in a stereotaxic device, and maintained under anaesthesia with 2.5% isoflurane in a 70%:30% mixture of N_2O/O_2. A small craniotomy (1 mm diameter) was performed on the parietal bone to expose the right middle cerebral artery (MCA). A Whatman filter paper strip soaked in $FeCl_3$ (30%, Sigma) was placed on the dura mater on top of the MCA for 5 min[9]. Cerebral blood flow (CBF) in the MCA territory was measured continuously by laser Doppler flowmetry (Oxford Optronix).

Pharmacological treatment

MCC950 (Sigma) or saline were injected 30 min after onset of artery occlusion. Injections were intraperitoneal (100 µL, 50 mg/kg) or intra-cerebroventricular (1 µL, 10 µg) at the following stereotaxic coordinates: Bregma 0, lateral: -1 mm, dorso-ventral: -1.8 mm.

RT-qPCR

Total RNAs were extracted from samples with TRIzol Reagent (ThermoFisher) according to the manufacturer. RNA (1 µg) was converted to cDNA using M-MLV Reverse Transcriptase (ThermoFisher). qPCR was performed using Power SYBR® Green PCR Master Mix (ThermoFisher) in 384-well format using an 7900HT Fast Real-Time PCR System (Applied Biosystems). 3 µL of 1:50 diluted cDNA was loaded with 200 mmol/L of primers in triplicate. Data were normalized to the expression of the housekeeping gene *Hmbs*. Specific primers were designed by using Primer3Plus software (http://www.bioinformatics.nl/cgi-bin/primer3plus/primer3plus.cgi). Primers used were: *Nlrp3* Forward – GCCCAAGGAGGAAGAAGAAG, *Nlrp3* Reverse – TCCGGTTGGTGCTTAGACTT, *Aim2* Forward – AAGAGAGCCAGGGAAACTCC, *Aim2* Reverse – CACCTCCATTGTCCCTGTTT, *Nlrc4* Forward – GTGACAGGCCTCCAGAACTT, *Nlrc4* Reverse – CCAAGCTGTCAATCAGACCA, *Pycard* Forward – TGCTTAGAGACATGGGCTTACA, *Pycard* Reverse – ACTCTGAGCAGGGACACTGG, *Casp1* Forward – CATTTGTAATGAAGACTGCTACCTG, *Casp1* Reverse –

GATGTCCTCCTTTAGAATCTTCTGT, *Gsdmd* Forward – TGCAGATCACTGAGGTCCAC, *Gsdmd* Reverse – GCCTTCACCCTTCAAGCATA, *Il1b* Forward – AACCTGCTGGTGTGTGACGTTC, *Il1b* Reverse – CAGCACGAGGCTTTTTTGTTGT, *Il18* Forward – GACTCTTGCGTCAACTTCAAGG, *Il18* Reverse – CAGGCTGTCTTTTGTCAACGA, *Tnfa* Forward – GCCTCTTCTCATTCCTGCTTG, *Tnfa* Reverse – CTGATGAGAGGGAGGCCATT, *Il1a* Forward - TCTCAGATTCACAACTGTTCGTG, *Il1a* Reverse - AGAAAATGAGGTCGGTCTCACTA. Expression levels of genes of interest were computed as follows: relative mRNA expression = $E^{-(Ct\ of\ gene\ of\ interest)}$/ $E^{-(Ct\ of\ housekeeping\ gene)}$, where Ct is the threshold cycle value and E is efficiency.

Flow cytometry

Single-cell suspensions were prepared by digestion of brain tissue for 45 min at 37 °C with 50 U/mL Collagenase (Gibco), 0.5 U/mL Dispase II (Gibco) and 200 U/ml DNase I (Roche) in Hank's balanced-salt solution and red blood cells were lysed (Sigma). Myelin was removed by centrifugation in a 30% percoll solution (GE Healthcare). Cells were incubated with Fc block (anti-CD16/CD32 and rat serum) and surface-stained with fluorescence-conjugated anti-CD11b (M1/70), anti-Ly6G (1A8), anti-CD45.2 (104), and anti-CD64 (X54-5/7.1). Cells were then fixed (20 min, 4 °C) with IC fixation buffer (eBioscience) prior to staining with APC-eFluor780-conjugated antibody to mouse IL-1β (NJTEN3), or APC-eFluor780-conjugated Rat IgG1κ antibody (isotype- control), in permeabilization buffer (eBioscience) before acquisition. Live/Dead Aqua (Life Technologies) was used for exclusion of dead cells from analysis. Samples were analyzed by flow cytometry with an LSR II (Becton-Dickinson) and cells were characterized with FlowJo software. Cells were identified by expression of surface markers as follows: neutrophils - $CD45^{hi}/CD11b^{hi}/Ly6G^{hi}$, monocytes - $CD45^{hi}/CD11b^{hi}/Ly6C^{hi}$, and macrophages/microglia - $CD45^{int\text{-}hi}/CD11b^{hi}/Ly6G^{-}/Ly6C^{-}/CD64^{+}$.

Tissue processing and measurement of infarct volumes

Anesthetized mice were transcardially perfused with cold heparinized saline followed by 100 mL of fixative (PBS 0.1 mol/L, pH 7.4 containing 4% paraformaldehyde). Brains were removed, post-fixed (24 hours) and cryoprotected (sucrose 20% in PBS; 24 hours) before freezing in optimal cutting temperature compound (PFM Medical UK Ltd). Cryostat-cut sections (10 μm) were stained with Cresyl violet. Lesion volume was analysed using

ImageJ and calculated as the sum of every lesion area multiplied by the distance between each section (0.4 mm).

Immunohistochemistry

For immunostains, brain sections from littermate WT, NLRP3-/-, and MCC950 treated WT mice perfused fixed as above were dried for 24 h prior to undergoing heat-mediated antigen retrieval in Tris-EDTA pH 8.6 solution for 20 min in a water bath set to 97.5 ˚C. Sections were then incubated with rat-anti-Ly6G (1.25 μg/mL, 1A8, Biolegend) and goat-anti-IL-1β (1 μg/mL, AF-401-NA, RnDSystems) antibodies overnight at 4˚C. Ly6G was labelled using donkey-anti-rat Alexa Fluor® 647 (10 μg/mL, Abcam), IL-1β signal was amplified with Tyramide SuperBoostTM (ThermoFisher) using biotinylated horse-anti-goat IgG (7.5 μg/mL, BA-9500, Vector) secondary antibody. Cellular IL-1β signal likely represents pro-IL-1β. Low magnification images were collected on an Olympus BX63 upright microscope and high magnification images were taken on an Axio Imager.M2 Upright [Zeiss] microscope. Quantitative analysis was performed on 3 low magnification images of the lesion taken from 3 different coronal brain slices. Images were processed using ImageJ. The cells were then were counted using the analyse particles function and colocalisation analysis performed using the DiAna plugin[11].

Western blotting of isolated CD11b positive cells

Littermate WT and NLRP3−/− mice were transcardially perfused with saline 24 h after stroke. Brains were then removed and digested into a single-cell suspension and myelin removed (as described above), and cells were isolated by magnetic-activated cell sorting using CD11b+ magnetic beads (Miltenyi). Positive and Negative CD11b+ cells were lysed in Tris-Triton buffer [150 mM NaCl, 1% (vol/vol) Triton X-100, 50 mM Tris, pH 7.5], supplemented with a protease inhibitor mixture. Cell lysates were separated by Tris-glycine SDS/PAGE and then transferred onto PVDF membranes at 25 V using a semi-dry Trans-Blot Turbo system (Bio-Rad). Membranes were blocked in 2.5% (wt/vol) BSA in PBS,1% (vol/vol) Tween 20 (PBST) before being incubated with indicated primary antibodies at 4°C overnight. Membranes were then labelled with HRP-tagged secondary antibodies and visualized with Amersham ECL detection reagent (GE Healthcare). Western blot images were captured digitally using a G:Box Chemi XX6 (Syngene). Specific antibodies were used targeting mouse IL-1β (AF-401, R&D), ASC (D2W8U, Cell Signalling Technology), caspase-1 p10 (EPR16883, abcam), and β-actin (Sigma).

Statistical analysis

Data are presented as mean values ± standard error of the mean (s.e.m) overlaid with individual data points. Sample size was calculated by power analysis using a significance level of α=0.05 with 80% power to detect statistical differences. Levels of significance were $P < 0.05$ (*), $P < 0.01$ (**), $P < 0.001$ (***). Statistical analyses were carried out using GraphPad Prism (version 7). qPCR data were analysed using a one-way ANOVA with Tukey's post-hoc comparisons. Flow cytometry and lesion volumes were analysed using two-tailed t-test.

4.5 Results

Using the $FeCl_3$ model of ischemia mice were subjected to stroke, brains were removed 24 hours after stroke and infarct, peri-infarct and contralateral areas dissected and analysed for gene expression by RT-qPCR (Figure 4.1). A significant increase in the expression of *Nlrp3*, *Gsdmd*, *Il1b*, *Il1a*, and *Tnfa* were measured in infarcted tissue (Figure 4.1). No differences were observed for *Aim2*, *Nlrc4*, *Pycard* (ASC), *Casp1*, or *Il18* expression. These data are consistent with previous reports showing increased expression of the NLRP3 system and other markers of inflammation in the injured tissue[5,6,12,13].

Activated microglia/macrophages and infiltrating immune cells (i.e. monocytes and neutrophils) are present in the infarct and in the peri-infarct area after ischemic stroke[14]. Previous research showed microglial IL-1β expression 24 hours after stroke[13]. NLRP3 is also described to be expressed in infiltrating cells at a similar time-point[12]. To further characterise the inflammatory response occurring after ischemia we utilised flow cytometry of brain homogenates to measure microglia and immune cell infiltrates. We identified defined cellular subsets based upon specific epitope expression and quantified infiltrating neutrophils ($CD45^{hi}/CD11b^{hi}/Ly6G^{hi}$), monocytes ($CD45^{hi}/CD11b^{hi}/Ly6C^{hi}$) and macrophages/microglia ($CD45^{int\text{-}hi}/CD11b^{hi}/CD64^{hi}$) (Figure 4.2A). There were no increases in numbers of macrophages/microglia in the injured ipsilateral hemisphere when measured as a percentage of total immune cells (i), or when analysed as total cell number (ii) (Figure 4.2B). However, increases in monocytes and neutrophils were measured in the ipsilateral hemisphere after stroke (Figure 4.2Bi, ii). IL-1β expressing cell populations were measured by flow cytometry (Figure 4.2C). Here, there was significantly increased IL-1β expression in macrophages/microglia, monocytes, and neutrophils (Figure 4.2D). Given that the expressed IL-1β was cellular it was most likely pro-IL-1β. Together these

data show a marked inflammatory response in the brain following ischemia and significant upregulation of the NLRP3 system.

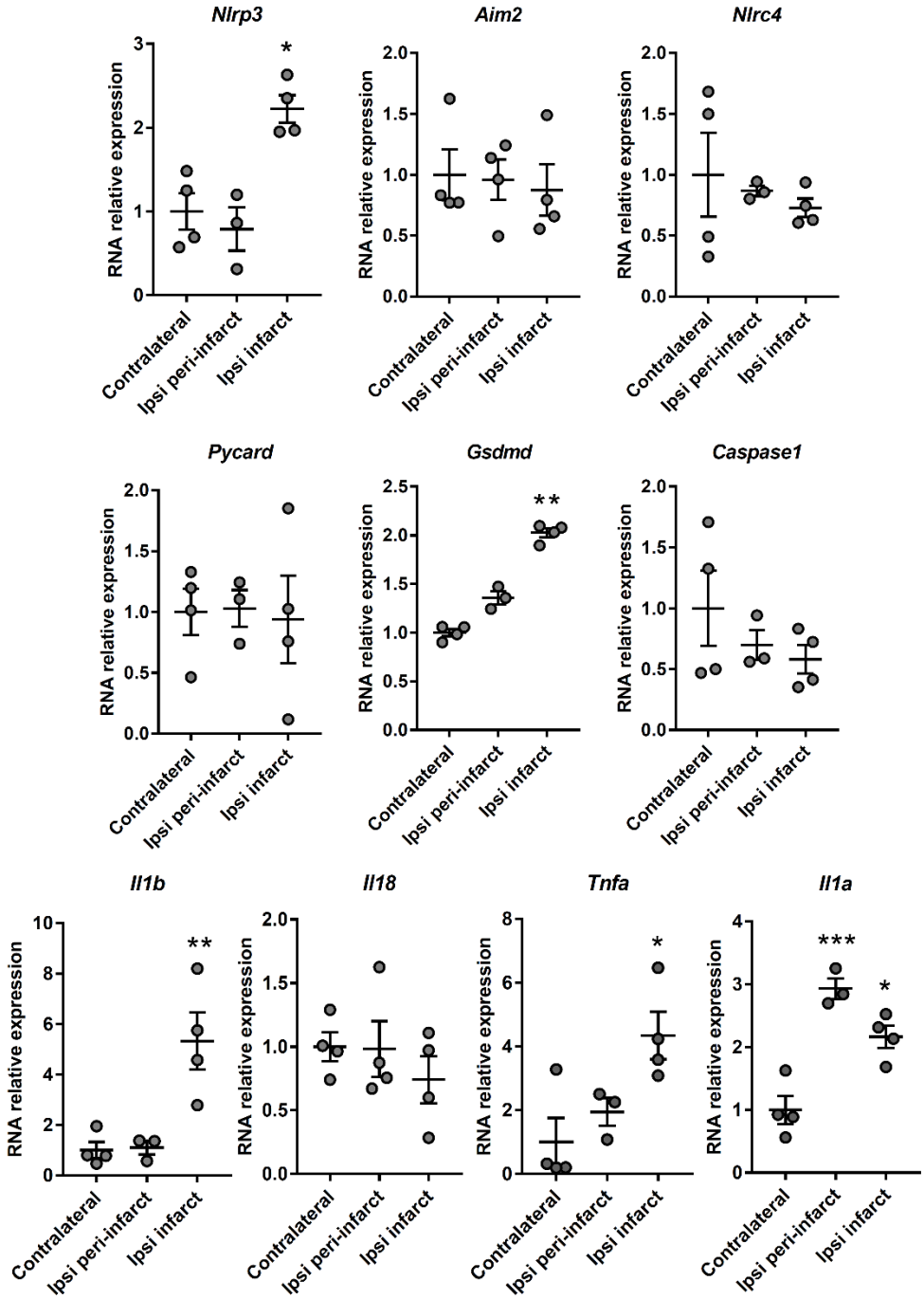

Figure 4.1 Inflammasome and cytokine expression 24 hours after stroke.
mRNA levels (normalised to contralateral tissue) of inflammasome components and cytokines in the contralateral, peri-infarct and infarct areas at 24 hours (n=3/4 mice, *p<0.05, **p,0.01, ***p<0.001, one-way ANOVA followed by Tukey's post hoc test).

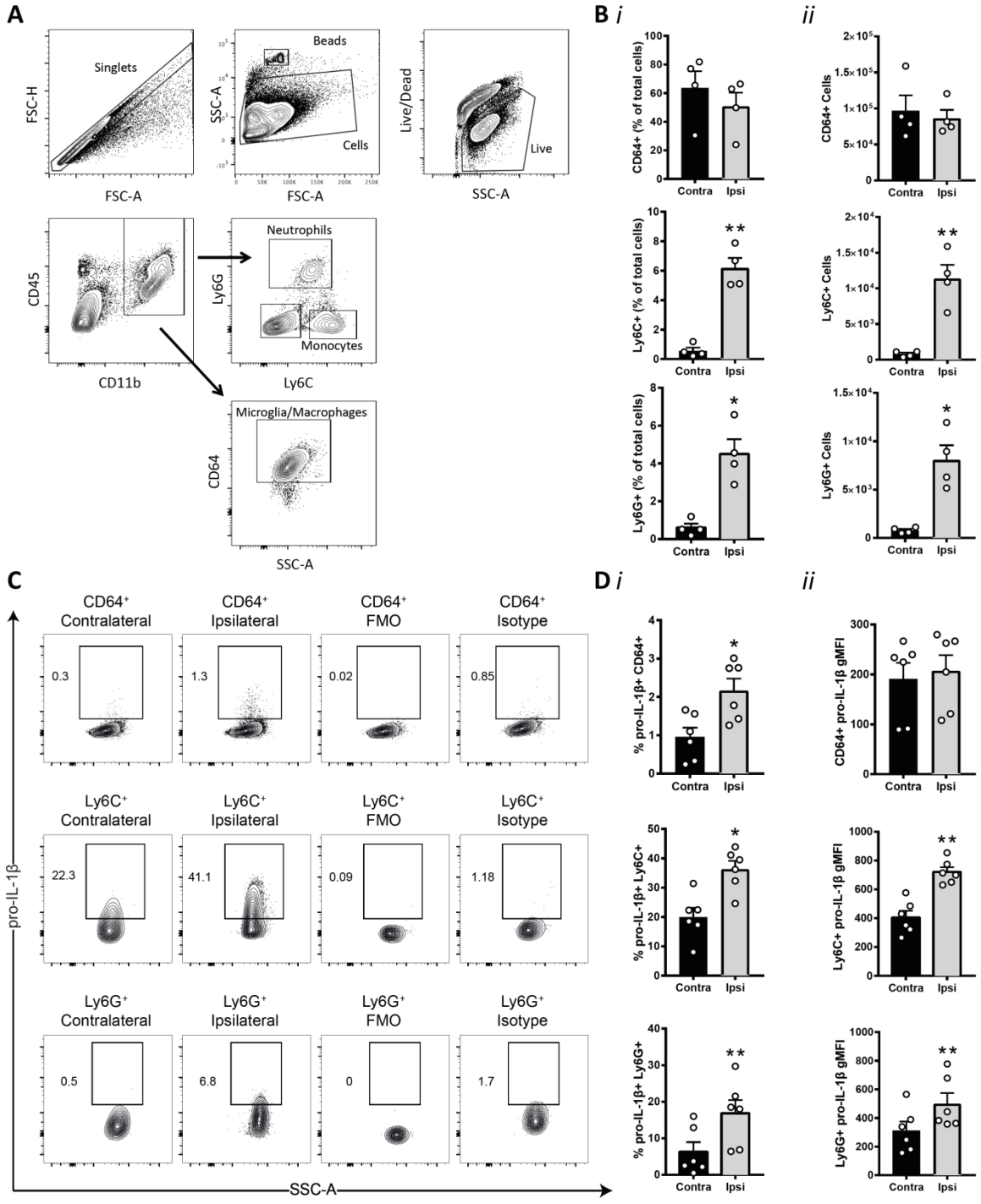

Figure 4.2 Immune cell recruitment and pro-IL-1β expression in immune cells 24 hours after stroke.

(A) Gating strategy and flow cytometry analysis of microglia/macrophages CD45^{int-hi}/CD11b^{hi}/CD64^{hi}, monocytes CD45^{hi}/CD11b^{hi}/Ly6C^{hi} and neutrophils CD45^{hi}/CD11b^{hi}/Ly6G^{hi} in the ipsilateral hemisphere. (Bi) Percentage of microglia/macrophages, monocytes and neutrophils vs the total number of live cells in the contralateral and ipsilateral hemisphere. (Bii) Absolute number of microglia/macrophages, monocytes and neutrophils in the contralateral and ipsilateral hemisphere (n=4 mice, *p<0.05, **p<0.01, analysed by two-tailed paired t-test). (C) Gating strategy analysis and flow cytometry analysis of pro-IL-1β 24 hours after stroke. (Di) Percentage of pro-IL-1β positive cells and (Dii) geometric mean fluorescence intensity of pro-IL-1β staining in microglia/macrophages, monocytes and neutrophils (n=6 mice, *p<0.05, **p<0.01, analysed by two-tailed paired t-test).

We recently evaluated a panel of the best literature compounds for their effects on inhibition of ASC speck formation and IL-1β release, hallmarks of NLRP3 inflammasome activation[15]. The sulfonylurea containing MCC950 was the most potent and selective inhibitor of NLRP3, and retained its inhibitory activity in primary adult microglia[15]. MCC950 delivered intraperitoneally did not affect lesion volume following thrombotic stroke (Figure 4.3A). MCC950 also failed to inhibit the recruitment of neutrophils, IL-1β expression, or neutrophil IL-1β expression as measured by immunohistochemistry (Figure 4.3B). To ensure that MCC950 reached the required site of action an additional experiment with central (lateral ventricle) injection of MCC950 was performed. Again, ischemic brain injury was unaffected by MCC950 treatment (Figure 4.3C). As with peripheral MCC950 administration, central administration of MCC950 had no effect on the recruitment of neutrophils, IL-1β expression, or neutrophil IL-1β expression as measured by immunohistochemistry (Figure 4.3D). To validate these pharmacologic data, thrombotic stroke was first induced in NLRP3-/- mice that were maintained as a homozygote colony, and age and sex matched C57BL/6 mice. Unexpectedly infarct volume was significantly enhanced in the NLRP3-/- mice (maintained as homozygotes) compared to WT (Figure 4.4A). RNA-seq analysis of isolated adult microglia from these WT and NLRP3-/- mice showed that, at baseline, there were over 700 differentially expressed genes (Supplementary Figure) suggesting that maintenance as a homozygote colony of the mice resulted in genetic drift. We therefore repeated the experiment using littermate WT and NLRP3-/- mice bred from heterozygote breeding pairs. In this experiment there was no difference in ischemic brain injury between WT and NLRP3-/- mice (Figure 4.4B). These data are consistent with our previous work in the filament MCAo model[4], and provide robust evidence for a lack of involvement of the NLRP3 inflammasome in ischemic brain injury, contrary to other recently published data[5–8], and highlight the pitfalls of using homozygote KO mouse colonies. Analysis of neutrophil recruitment and IL-1β expression in the brains of WT versus littermate NLRP3-/- mice revealed no difference in the recruitment of neutrophils, IL-1β expression, or neutrophil IL-1β expression consistent with the MCC950 experiments presented in Figure 4.3 (Figure 4.4C). Magnetic bead separation of myeloid and non-myeloid cell populations from the ipsi- and contralateral hemispheres of WT and littermate NLRP3-/- mice followed by western blotting revealed that only the myeloid cell population expressed detectable inflammasome adaptor protein ASC and caspase-1, and only myeloid cells isolated from the injured ipsilateral hemisphere

expressed pro-IL-1β, and this was unchanged between WT and NLRP3-/- mice (Figure 4.4D).

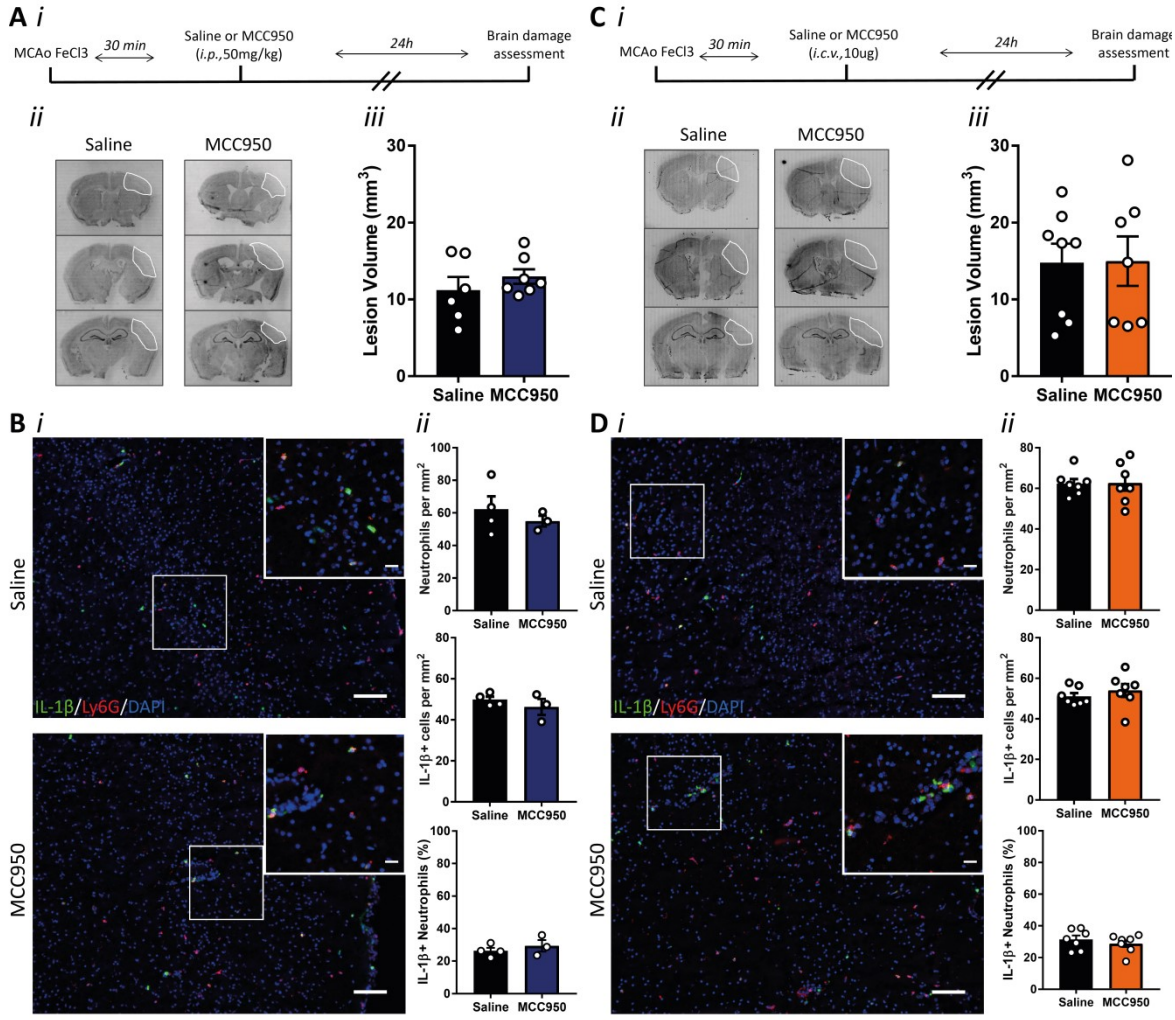

Figure 4.3 Influence of NLRP3 inhibition on brain damage after stroke.
(Aii) representative cresyl violet staining, and (Aiii) lesion volume quantification 24 hours after stroke in mice treated with MCC950 (50 mg/kg) or saline by intraperitoneal injection 30 minutes after the stroke onset (n=6/group). (Bi) Representative immunostaining of IL-1β (green), neutrophils (Ly6G, red) and DAPI (blue) in the infarct 24 hours after stroke (Scale bar in the large image is 100 μm, and in the inset is 20 μm). (Bii) Numbers of neutrophils and IL-1β positive cells per mm^2, and % IL-1β positive neutrophils in the infarct 24 hours after stroke plus and minus intraperitoneal MCC950 (n=3-4/group). (Ci) Schematic representation of the experiment. (Cii) representative cresyl violet staining and (Ciii) lesion volume quantification 24 hours after stroke in mice treated with MCC950 (10 μg) or saline by intracerebroventricular injection 30 minutes after stroke onset (n=7-8/group). (Di) Representative immunostaining of IL-1β (green), neutrophils (Ly6G, red) and DAPI (blue) in the infarct 24 hours after stroke (Scale bar in the large image is 100 μm, and in the inset is 20 μm). (Dii) Numbers of neutrophils and IL-1β positive cells per mm^2, and % IL-1β positive neutrophils in the infarct 24 hours after stroke plus and minus intracerebroventricular MCC950 (n=7/group).

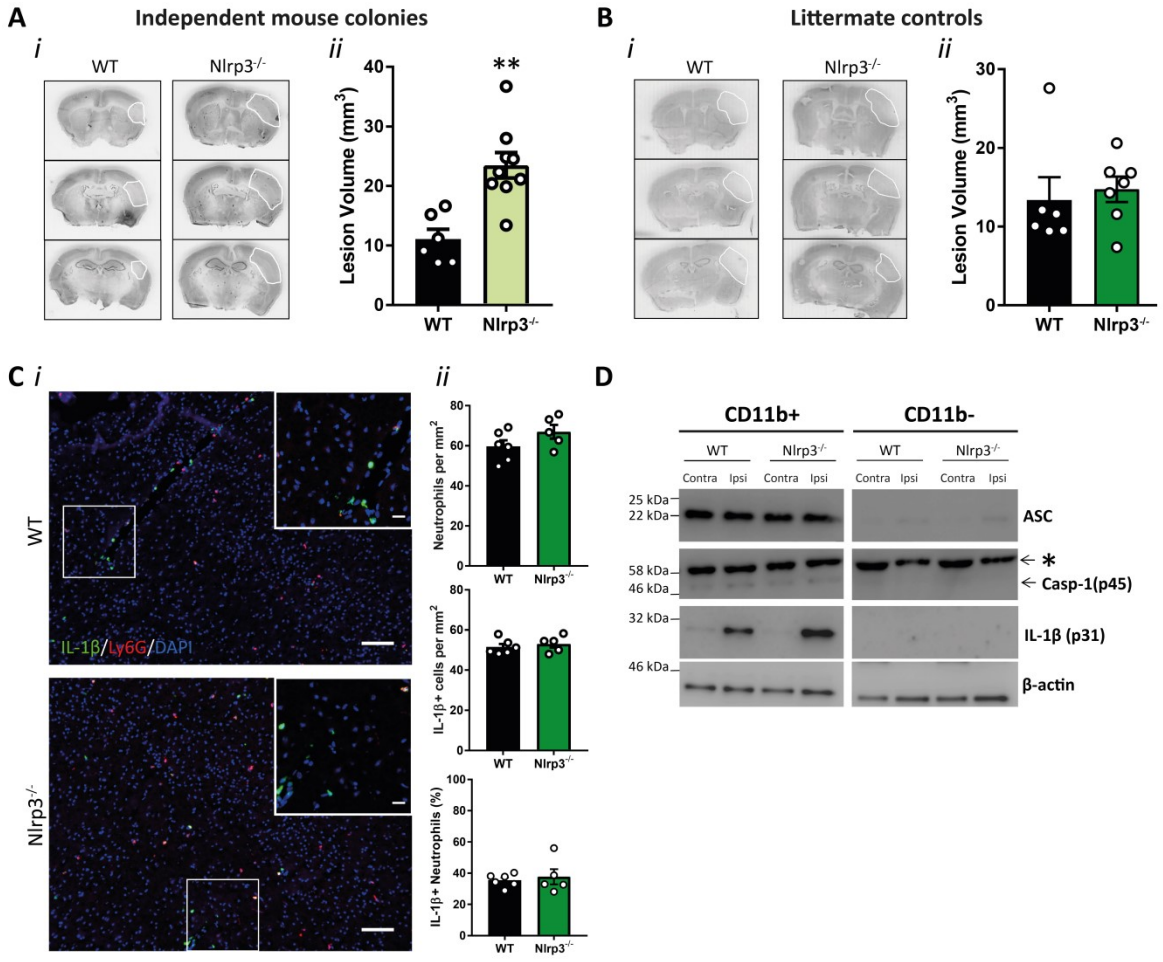

Figure 4.4 Influence of NLRP3 gene deletion on brain damage after stroke.
(Ai) Representative cresyl violet staining and (Aii) lesion volume quantification 24 hours after stroke in WT and non-littermate NLRP3-/- mice (n=6-9/group) (**p< 0.01, analysed by two-tailed unpaired t-test). (Bi) Representative cresyl violet staining and (Bii) lesion volume quantification 24 hours after stroke in WT and littermate NLRP3-/- mice (n=6-7/group) (ns=non-significant, analysed by two-tailed unpaired t-test). (Ci) Representative immunostaining of IL-1β (green), neutrophils (Ly6G, red) and DAPI (blue) in the infarct 24 hours after stroke (scale bar in the large image is 100 μm, and in the inset is 20 μm) (Cii) Numbers of neutrophils and IL-1β positive cells per mm^2, and % IL-1β positive neutrophils in the infarct 24 hours after stroke in WT and littermate NLRP3-/- mice (n=5-6/group). (D) ASC, Caspase-1, IL-1β and β-actin western blot of cell lysates from magnetic bead cell isolation of myeloid cells (CD11b+) and non-myeloid cells (CD11b-) from the ipsi- and contralateral hemisphere 24 hours after stroke (n=3). *Is a non-specific band.

4.6 Discussion

Here we report that ischemic brain injury was not reduced by specific inhibition of NLRP3 with MCC950 or in NLRP3-/- mice. These data provide evidence that NLRP3, the canonical sensor of sterile injury, is not involved in the acute phase of ischemic stroke.

NLRP3 has been described to be involved in sterile brain injury and diseases such as Alzheimer's disease, multiple sclerosis, and traumatic brain injury[16]. However, in the context of stroke, there is some controversy over its involvement in increasing infarct volume. Previous studies have shown that mice deficient in NLRP3 have a reduction in brain damage[6], or that NLRP3 inhibition with an antibody[5] or with MCC950[8] is protective.

In contrast, we previously reported mice deficient in NLRP3 had no reduction in brain injury caused by the filament model of MCAo[4]. The involvement of inflammation in ischemic injury, and in particular IL-1-dependent inflammation is less equivocal with studies reporting that genetic deletion of IL-1, or blocking the IL-1 receptor with the naturally occurring IL-1 receptor antagonist (IL-1Ra) is protective[17,18]. In this study, we chose to use a more clinically relevant model of stroke using $FeCl_3$ to induce thrombosis of the MCA[9]. Whilst there was a marked increase in inflammation using the $FeCl_3$ model, there was no reduction in ischemic damage using the specific and potent NLRP3 inhibitor MCC950, or in the littermate NLRP3-/- experiment, confirming our previous report that NLRP3 does not contribute to ischemic brain injury[4]. Expression of IL-1β and myeloid cell recruitment was also independent of NLRP3. However, we do not exclude the likelihood that NLRP3 contributes to other cardiovascular events. The positive result of the CANTOS trial (Canakinumab Anti-Inflammatory Thrombosis Outcomes Study) highlights the importance of IL-1β in the risk of recurrent cardiovascular events[19]. Moreover, NLRP3 has been demonstrated to contribute to the vascular inflammatory response driving atherosclerosis[20], suggesting that NLRP3 could contribute to an increased risk of ischemic stroke.

These data also highlight a cautionary note for using homozygote KO mouse colonies. We observed significant genetic changes in pure microglia isolated from age and sex matched, co-housed, adult WT and NLRP3-/- mice which may explain the observed increase in infarct volume. In studies using non-littermate NLRP6 and ASC KO animals NLRP6 and ASC were reported to be regulators of the gut microbiome and influence the severity of colitis[21]. However, subsequent studies using littermate controls find that NLRP6 and ASC do not regulate the composition of gut microbiota and that maternal inheritance and long-term separate housing are the biggest non-genetic confounders when studying the microbiome[22,23]. These studies[22,23] and our own argue the necessity of litter-mate controlled experiments when studying mechanisms of innate immunity.

Summary

In summary, this study suggests that while there is a marked inflammatory response after ischemic stroke, NLRP3-dependent inflammation is not involved in exacerbation of the injury and thus does not represent a therapeutic target for ischemic brain injury.

Acknowledgments

We are grateful to Genentech for the NLRP3-/- mice. We are also grateful to Jack Rivers-Auty (University of Manchester) who advised on the statistical analysis. Thanks also to the core-facility service at the University of Manchester; Biological Services Facility, Genomic Technologies Facility, Bioimaging Facility and Histology Facility for expert guidance and use of facilities.

Sources of Funding

This work was funded by the MRC (grant number MR/N003586/1 to D.B., S.M.A., and E.L.; MC_PC_16033 to D.B., and M.J.H.) and Wellcome Trust to J. A. (106898/A/15/Z).

Disclosures: None

4.7 References

1. Rock KL, Latz E, Ontiveros F, Kono H. The Sterile Inflammatory Response. *Annu. Rev. Immunol.* 2010;28:321–342.

2. Murray KN, Parry-Jones AR, Allan SM. Interleukin-1 and acute brain injury. *Front. Cell. Neurosci.* 2015;9:18.

3. Broz P, Dixit VM. Inflammasomes: mechanism of assembly, regulation and signalling. *Nat. Rev. Immunol.* 2016;16:407–420.

4. Denes A, Coutts G, Lénárt N, Cruickshank SM, Pelegrin P, Skinner J, et al. AIM2 and NLRC4 inflammasomes contribute with ASC to acute brain injury independently of NLRP3. *Proc. Natl. Acad. Sci. U. S. A.* 2015;112:4050–4055.

5. Fann DY-W, Lee SY, Manzanero S, Tang SC, Gelderblom M, Chunduri P, et al. Intravenous immunoglobulin suppresses NLRP1 and NLRP3 inflammasome-mediated neuronal death in ischemic stroke. *Cell Death Dis.* 2013;4:e790.

6. Yang F, Wang Z, Wei X, Han H, Meng X, Zhang Y, et al. NLRP3 deficiency ameliorates neurovascular damage in experimental ischemic stroke. *J. Cereb. Blood Flow Metab.* 2014;34:660–667.

7. Ye X, Shen T, Hu J, Zhang L, Zhang Y, Bao L, et al. Purinergic 2X7 receptor/NLRP3 pathway triggers neuronal apoptosis after ischemic stroke in the mouse. *Exp. Neurol.* 2017;292:46–55.

8. Ismael S, Zhao L, Nasoohi S, Ishrat T. Inhibition of the NLRP3-inflammasome as a potential approach for neuroprotection after stroke. *Sci. Rep.* 2018;8:5971.

9. Le Behot A, Gauberti M, De Lizarrondo SM, Montagne A, Lemarchand E, Repesse Y, et al. GpIbα-VWF blockade restores vessel patency by dissolving platelet aggregates formed under very high shear rate in mice. *Blood.* 2014;123:3354–3363.

10. Mariathasan S, Weiss DS, Newton K, McBride J, O'Rourke K, Roose-Girma M, et al. Cryopyrin activates the inflammasome in response to toxins and ATP. *Nature*. 2006;440:228–232.

11. Gilles J-F, Dos Santos M, Boudier T, Bolte S, Heck N. DiAna, an ImageJ tool for object-based 3D co-localization and distance analysis. *Methods*. 2017;115:55–64.

12. Ito M, Shichita T, Okada M, Komine R, Noguchi Y, Yoshimura A, et al. Bruton's tyrosine kinase is essential for NLRP3 inflammasome activation and contributes to ischaemic brain injury. *Nat. Commun.* 2015;6:7360.

13. Luheshi NM, Kovács KJ, Lopez-Castejon G, Brough D, Denes A. Interleukin-1α expression precedes IL-1β after ischemic brain injury and is localised to areas of focal neuronal loss and penumbral tissues. *J. Neuroinflammation*. 2011;8:186.

14. Benakis C, Garcia-Bonilla L, Iadecola C, Anrather J. The role of microglia and myeloid immune cells in acute cerebral ischemia. *Front. Cell. Neurosci.* 2014;8:461.

15. Redondo-Castro E, Faust D, Fox S, Baldwin AG, Osborne S, Haley MJ, et al. Development of a characterised tool kit for the interrogation of NLRP3 inflammasome-dependent responses. *Sci. Rep.* 2018;8:5667.

16. Lénárt N, Brough D, Dénes Á. Inflammasomes link vascular disease with neuroinflammation and brain disorders. *J. Cereb. Blood Flow Metab.* 2016;30:1668–1685.

17. Boutin H, LeFeuvre RA, Horai R, Asano M, Iwakura Y, Rothwell NJ. Role of IL-1alpha and IL-1beta in ischemic brain damage. *J. Neurosci.* 2001;21:5528–5534.

18. Mulcahy NJ, Ross J, Rothwell NJ, Loddick SA. Delayed administration of interleukin-1 receptor antagonist protects against transient cerebral ischaemia in the rat. *Br. J. Pharmacol.* 2003;140:471–476.

19. Ridker PM, Everett BM, Thuren T, MacFadyen JG, Chang WH, Ballantyne C, et al. Antiinflammatory Therapy with Canakinumab for Atherosclerotic Disease. *N. Engl. J. Med.* 2017;377:1119–1131.

20. Grebe A, Hoss F, Latz E. NLRP3 Inflammasome and the IL-1 Pathway in Atherosclerosis. *Circ. Res.* 2018;122:1722–1740.

21. Elinav E, Strowig T, Kau AL, Henao-Mejia J, Thaiss CA, Booth CJ, et al. NLRP6 Inflammasome Regulates Colonic Microbial Ecology and Risk for Colitis. *Cell*. 2011;145:745–757.

22. Mamantopoulos M, Ronchi F, Van Hauwermeiren F, Vieira-Silva S, Yilmaz B, Martens L, et al. Nlrp6- and ASC-Dependent Inflammasomes Do Not Shape the Commensal Gut Microbiota Composition. *Immunity*. 2017;47:339–348.

23. Mamantopoulos M, Ronchi F, McCoy KD, Wullaert A. Inflammasomes make the case for littermate-controlled experimental design in studying host-microbiota interactions. *Gut Microbes*. 2018;1–8.

4.8 Supplemental Methods

RNA-seq analysis of isolated microglia

Mice (NLRP3−/− bred as homozygotes, and wild type, with both genotypes co-housed) were transcardially perfused with ice-cold Hank's balanced-salt solution. Brains were then digested into a single-cell suspension and myelin removed (as described above), and microglia isolated by magnetic-activated cell sorting using Cd11b+ magnetics beads (Miltenyi). RNA was isolated using a Qiagen RNeasy Micro Kit. After confirming RNA integrity, RNA was sequenced on an Illumina HiSeq2500. The sequenced data was then trimmed using FastQC, and mapped into the murine genome. Raw count data was normalised in DESeq2, and corrected counts of genes compared pairwise between genotypes, with a correction for false discovery rate.

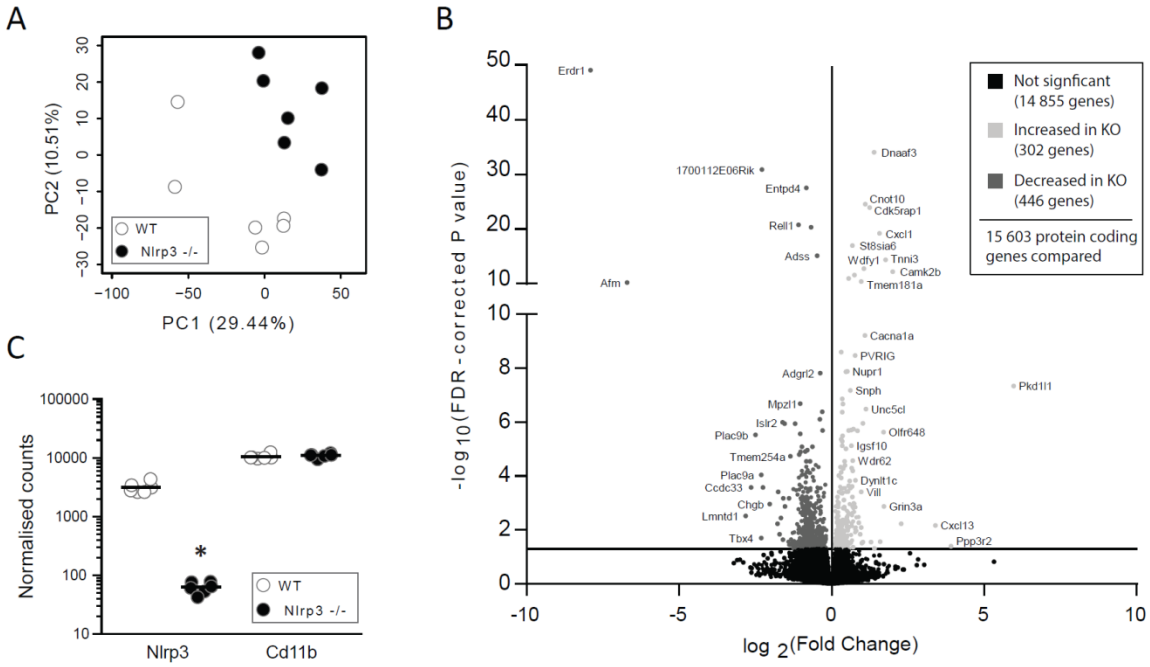

Figure 4.5 Supplemental Figure. Differentially expressed genes in microglia from non-littermate mouse colonies.

(A) Clear clustering of genotypes can be seen by principal components analysis. (B) Of the 22561 genes identified, 15603 were protein coding, with 708 of these differentially expressed between genotype. (C) NLRP3 knock out was confirmed, and cd11b (used to isolate microglia) was not differentially expressed (n=6 mice/genotype, differentially expressed genes identified by pair-wise comparison with correction for falsediscovery rate).

Chapter 5: Discussion

5.1 Summary

Stroke is a devastating condition to which treatment options are severely limited. The diametrically opposed pathophysiology of the two major subtypes of stroke makes targeting both with the same therapy extremely difficult. There are currently 2 licenced therapies for IS which are only available to a small fraction of patients and require rapid diagnosis to be effective, since both involve reperfusion. It is therefore difficult for LMICs to incorporate these 2 IS therapies. Moreover, no licensed therapies are available for the most devastating stroke subtype; ICH, which disproportionately affects LMICs. The immune response to IS and ICH exacerbates brain injury and is currently perceived to progress in a similar pattern. Importantly, the prototypical cytokine IL-1 sits at the apex of many inflammatory processes and has salient actions in acute sterile brain inflammation. Thus, targeting IL-1 may have therapeutic potential in treating both stroke subtypes. This thesis therefore aimed to address the most pertinent questions regarding IL-1 in IS and ICH with the following specific aims:

- Develop and optimise the collagenase-induced mouse model of ICH, which will be used for the first time in our laboratory, in order to improve detection power and reduce animal suffering.

- Reveal the pathophysiological consequences of IL-1 signalling during ICH by characterising its expression patterns, in mouse and man, and measuring the effects of its inhibition using relevant pharmacological strategies.

- Determine the relative importance of the NLRP3 inflammasome in the pathogenesis of acute IS using pharmacological and genetic approaches in the clinically relevant clot-forming dMCAO model.

To address the first aim, the collagenase-induced mouse model of ICH was characterised and refined in a step-wise process. First, the dose of collagenase was titrated to induce a haematoma volume with limited variability and outcome severity. Second, the accelerating rotarod performance assay was first identified and subsequently optimised to detect motor deficits at this refined collagenase dose. Finally, evidence that the cerebral immune response occurs in this refined model was presented alongside power calculations based on haematoma volume and rotarod performance. Together this represents the first report of an

optimised ICH model, with limited animal suffering and usage, which retains important clinical features such as brain inflammation.

The optimised ICH model was then used to address the second aim of this thesis and revealed novel roles for IL-1 in ICH and brain haemorrhage in general. Confirming previous work, a rapid immune response was observed following ICH that was characterised by detrimental monocyte trafficking to the brain. Using RNA sequencing we identified IL-1 as the major upstream regulator of brain inflammation and harmful monocyte recruitment. IL-1 production was mapped to mononuclear phagocytes, in clinical and preclinical brain tissue, and signalling through IL-1R1 was essential for myeloid cell trafficking to the brain. Contrary to previous reports, caspase-1 and microglia were not required for immune recruitment and despite IL-1RA preventing the entry of harmful monocytes, it worsened functional outcome. IL-1 was not required for sufficient haemostasis but instead was required to regulate CBF in the affected hemisphere. We have thus revealed novel dichotomous actions of IL-1 following brain haemorrhage where the molecule mediates detrimental myeloid cell recruitment and beneficial CBF regulation.

The third and final aim of this thesis was completed by measuring the effect of NLRP3 on infarct volume in the $FeCl_3$-induced dMCAO mouse model of IS. Despite a large induction of NLRP3, GSDMD and IL-1 expression within the infarct, neither genetic deletion nor pharmacological inhibition of the NLRP3 inflammasome affected lesion volume in this model. Moreover, NLRP3 was not necessary for neutrophil trafficking to the ischaemic brain. These results contradict some existing findings in the literature and we suggest the lack of littermate controls in previous studies as an important factor to consider. Overall this data builds on previous findings from our lab in finding no role for NLRP3 in IS pathogenesis.

Overall, the results of this thesis present further evidence that refined animal models can be used to establish brain inflammation as a canonical feature of stroke of either subtype. However, the role IL-1 has in the pathogenesis of these diseases is more complex than currently perceived and more work is required to tease apart its complex biology in stroke.

5.2 General discussion

5.2.1 Improving animal research in stroke

The stroke field has been subject to many reviews and criticisms regarding failures in the translation of preclinical findings and the apparent unnecessary animal suffering required to achieve such failures. For almost three decades preclinical stroke researchers have been working toward improving upon these failures by increasing reporting transparency, reducing bias, and refining animal models. This thesis makes important contributions toward achieving each of these goals.

Across the globe, animal researchers are under ethical pressure to reduce the degree of animal suffering in the search of new discoveries. The UK government has even established a scientific organisation to promote the discovery of new applications and approaches to replace, reduce and refine the use of animals for scientific purposes (Prescott and Lidster, 2017). Whilst these issues are not limited to the stroke field, stroke does have a catastrophic clinical presentation and an equally severe phenotype when modelled in rodents. The preclinical stroke field is thus under pressure to reduce the severity of current rodent models of stroke whilst retaining disease relevance. There is abundant evidence that preclinical IS procedures are being refined to reduce animal suffering, most notably with the publishing of the Ischaemia Models: Procedural Refinements Of in Vivo Experiments (IMPROVE) guidelines (Percie du Sert et al., 2017). The IMPROVE guidelines challenge researchers to adopt the best model to answer their research question whilst keeping animal suffering to a minimum. In Chapter 4 of this thesis a preclinical investigation was performed into the role of NLRP3 in IS pathogenesis using the dMCAO model. In contrast to the most commonly used filament MCAO models, the dMCAO model spares subcortical tissue and is therefore not associated with mortality and induces minor functional deficits (McCabe et al., 2018). Moreover, in Chapter 2 of this thesis the collagenase-induced mouse model of ICH was successfully refined to reduce animal suffering. Most preclinical studies currently rely on behavioural assessments that measure severe phenotypes such as hemiplegia, despite the degree of such phenotypes being dependent on haematoma volume and therefore being under the control of the surgeon (Frantzias et al., 2011). To the best of my knowledge, there are no publications that have attempted to reduce animal suffering in preclinical ICH models. The optimisation of the rotarod performance assay to detect neurological deficits in the absence of

hemiplegia therefore represents a significant contribution to reduced suffering in preclinical ICH work.

In 2016, a survey of 1,576 scientists was conducted to uncover the magnitude of reproducibility issues in science. Over 70% of responders had tried and failed to reproduce the findings of others and over 50% had failed to reproduce their own findings (Baker, 2016). The 3 leading contributing factors to this irreproducibility crisis were reported as publication bias, pressure to publish and poor statistical power. Not only do these factors affect the progress made in academic endeavours but they also have grand effects on translation of new therapies to the clinic (O'Collins et al., 2006). In the IS field, attempts to identify important components underpinning extremely poor translatability of preclinical findings have been ongoing since 1999 (Stroke Therapy Academic Industry Roundtable (STAIR), 1999). The result of such discussions has been the advent of stringent study reporting guidelines aimed at improving transparency within *in vivo* research (Kilkenny et al., 2013). At the heart of reporting guidelines and discussions to reduce bias in animal research is the necessity to perform properly powered experiments. Statistical power relies on the signal to noise ratio of the effects being measured and the variability of the measurement. Therefore, in the absence of optimised workflows, *in vivo* biologists find themselves juxtaposed between the pressures to increase animal usage to perform properly powered experiments (to improve reproducibility and translatability) and those to reduce animal usage altogether (from the ethical standpoint). Chapter 2 of this works towards overcoming this juxtaposition in ICH research by first optimising the collagenase dose to reduce variability in haematoma volume, followed by the optimisation of rotarod training phases. We also show that accounting for baseline rotarod performance as a covariate (or nuisance variable) in data analysis of rotarod scores improves statistical power. Thus we provide the first preclinical ICH refined workflow to detect histological and motor outcomes with minimal animal suffering and usage. Moreover, the major finding in Chapter 3 was that IL-1RA administration worsened functional performance using the optimised collagenase-induced murine ICH protocol from Chapter 2. The experiment depicted in Figure 3.5B was in fact powered from a preliminary experiment utilising the same methods (see Appendix Figure 6.1). Thus Chapter 2 and 3 together provide evidence of the robustness and reliability of the refined ICH protocol in detecting consistent biologically relevant changes. The major limitation to this argument is that I am the only person to have performed the refined protocol and thus researcher-researcher

variability is currently unaccounted for. If the consistency of the model is retained in the presence of researcher-researcher variation, Chapter 2 provides future researchers with a workflow to confidently assess effects of interventions on histological and functional outcomes in properly powered experiments with limited animal usage and suffering. The absence of such data for the $FeCl_3$ dMCAO model led to reliance on Cohen's estimates to power animal studies in Chapter 4 of this thesis. However, Chapter 4 also represents significant advances toward scientific integrity through the publishing of accepted null hypotheses and emphasising the importance of littermate controls in preclinical work.

Publication bias, that is the propensity for the field of scientific and medical research to publish positive results over negative ones, is a complex matter that has been part of discussion since 1959 (Sterling, 1959). In the simplest yet most extreme terms, publication bias can be summarised as the "file drawer problem", in which 95 % of studies reporting on null results are filed away, whereas, the 5 % of falsely significant results are published (Rosenthal, 1979). In lieu of a full representation of their respective field, expert reviewers then come to erroneous conclusions and contribute to self-fulfilling prophecies and overstate the efficacy of tested therapies. In the preclinical stroke field, almost 14 % of neuroprotection studies are predicted to remain unpublished and the loss of such studies results in overestimation of the efficacy of interventions by around a third (Sena et al., 2010). It is highly likely that publication bias in the stroke field has directly contributed to the translational roadblock and it is, therefore, imperative to publish robust results that reject *or* accept the null hypothesis. In Chapter 4 of this thesis the NLRP3 inflammasome was shown to have no effect on acute IS pathogenesis using the $FeCl_3$-induced dMCAO model. This is an important finding as a considerable amount of previous studies allude to the NLRP3 inflammasome as a promising therapeutic target (Barrington et al., 2017). However, only three previous studies have directly targeted NLRP3 and assessed outcome in animal models of IS. Of these, two genetic deletion studies arrive at incongruous conclusions, whereas, the third study administered MCC950 and showed improvement (Yang et al., 2014; Denes et al., 2015; Ismael et al., 2018). In our hands, central or peripheral administration of MCC950 did not affect lesion volume nor did genetic deletion of NLRP3. Thus, together with previous findings, these results suggest NLRP3 does not show benefit in preclinical IS models overall. There is of course between-establishment variability in experimental protocols that could explain the aforementioned contradictory findings through scientific reasoning, which will be discussed in section 5.2.3. Although

we point toward the lack of littermate-controls in previous studies as being an important contributing factor. We found that NLRP3 KO mice had a 2-fold increase in ischaemic damage compared to non-littermate WT mice and this effect disappeared when mice were backcrossed. Separately maintained mouse colonies are subject to environmental differences and genetic drift which contribute to phenotypic changes (Holmdahl and Malissen, 2012; Mamantopoulos et al., 2017). In our own separately maintained NLRP3 KO colony we found that isolated microglia had >700 differentially expressed transcripts compared to cohoused non-littermate controls. Although not directly tested, we hypothesise that these genetic/epigenetic changes contributed toward greater ischaemic damage seen in the separately housed NLRP3 colony. Thus we present evidence of the importance of littermate-controlled experiments in preclinical stroke research.

5.2.2 The complex actions of IL-1 in stroke

IL-1 sits at the apex of many inflammatory processes. In the brain, IL-1 injection promotes neuroinflammation, BBB breakdown, neuronal death and alters CBF (Andersson et al., 1992; Anthony et al., 1997, 1998; Minghetti et al., 1999; Blamire et al., 2000; Bernardes-Silva et al., 2001). Genetic and pharmacological targeting of the IL-1 pathway has produced unequivocal evidence that it contributes to brain damage following IS (Murray et al., 2015). However, very little is known about the actions of IL-1 in ICH. Chapter 3 of this thesis shows, for the first time, that IL-1 orchestrates the immune response but also critically regulates CBF in the collagenase-induced mouse model of ICH. Surprisingly, inhibition of IL-1 worsened outcome from as early as 24 hours post-ICH. These results are in stark contrast to those from the IS field and those from an earlier preclinical ICH study. In their study, Masada et al., (2001) modelled ICH in rats using the autologous blood injection method and showed that overexpression of IL-1RA reduced oedema in the ipsilateral basal ganglia at 3 days.

One notable difference between the collagenase-induced ICH model and both the autologous blood model and IS, is the former specifically results in active bleeding from *in situ* vessels. Therefore, interactions may occur between the coagulation cascade and IL-1 during collagenase-induced ICH, that do not occur in IS or in the study from Masada et al., (2001). It is important to test effects of IL-1 in the context of bleeding vessels due to its ability to promote coagulation and shape the immune response in such circumstances (Jansen et al., 1995; Yang et al., 2013; Burzynski et al., 2019). Inflammation is known to promote coagulation, in part through the upregulation and delivery of tissue factor to the

site of haemorrhage, although, we found no evidence that IL-1 contributes to limiting haematoma volume during ICH (Foley and Conway, 2016). Instead, we found that IL-1 controls myeloid cell recruitment and blood flow to the affected hemisphere.

In line with various published studies, monocytes were found to exacerbate acute ICH injury in Chapter 3. IL-1 was the critical mediator of this harmful monocyte recruitment but the upstream origin and downstream effector of the IL-1 signal remain undetermined. Similarly to IS, microglia rapidly produce IL-1 following ICH but trafficking monocytes (seen in Chapter 4 for IS) also produce the potent cytokine (Luheshi et al., 2011). Although microglia are the primary source of IL-1 in both ICH and IS, they are not essential for its downstream effects. In Chapter 3, the depletion of microglia represents a crude method to conclude that microglial IL-1 is not necessary for IL-1R1 activation as monocytes can enter the brain in their absence (Cronk et al., 2018). A better method would be to generate IL-1α/β KO chimeras to compare the effects of mice with and without the capacity to produce these molecules in microglia specifically. Denes et al., (2013) adopted this strategy to show that microglial and haematopoietic IL-1 contribute to IS pathogenesis. However, the authors performed whole-body irradiation in the absence of head-shielding which is known to cause BBB breakdown and facilitate monocyte entry to the brain (Mildner et al., 2007). Thus more studies are required to account for this caveat before the findings can be completely interpreted. Nevertheless, it is unlikely that the identification of the origin of IL-1 will significantly advance the field considering that IL-1α and IL-1β act through the same receptor to have multiple effects following ICH. Focus is best turned to identifying the critical mediator of said effects.

A recent study using an elegant knock in reporter system revealed that neurones, astrocytes, endothelial cells and cells of the choroid plexus all express IL-1R1 (Liu et al., 2019). This study, along with recent findings from our lab, identified endothelial cells as a major downstream target of IL-1 through which the molecule facilitates myeloid cell recruitment (Wong et al., 2019). Amongst endothelial subsets, venous endothelial cells have the greatest amount of IL-1R1 mRNA and it is widely stated that post-capillary venules are the major site of immune cell trafficking during neuroinflammation (Wolburg et al., 2005; Bechmann et al., 2007; Vanlandewijck et al., 2018). In response to IL-1, endothelial cells upregulate important adhesion molecules, such as VCAM-1, which are essential for immune cell entry into tissues. In Chapter 3, IL-1RA reduced the amount of VCAM-1 positive vessels in the brain following ICH, thus suggesting IL-1 does signal

through endothelial cells in this setting. Therefore, it seems likely that the IL-1-endothelial cell pathway has an important role in myeloid cell trafficking during ICH. I attempted to test the hypothesis that endothelial IL-1R1 was the major driver of myeloid cell trafficking following ICH by using a tamoxifen inducible brain endothelial-specific IL-1R1$^{-/-}$ (BER1KO) mouse line (seen in Wong et al., 2019). Following a five day tamoxifen treatment regimen, WT and BER1KO mice underwent ICH induction and single cells were isolated from brain homogenates 24 hours later (see Appendix Figure 6.2). Analysis based on genotype showed no significant differences existed in the immune cell landscape of the brain. However, immunofluorescence analysis of vascular brain smears highlighted a mismatch between genotype and phenotype. When flow cytometry results were stratified based on phenotype there was a significant reduction in Ly6Chi monocytes and CD8 T cells in the brain of animals lacking endothelial IL-1R1. It is unclear how such a genotype/phenotype mismatch may occur but the tamoxifen-inducible Cre system is known to spontaneously activate *in vivo* (Kristianto et al., 2017). Interestingly however, the α4 integrin is highly expressed by Ly6Chi monocytes and CD8 T cells and is required for their recruitment to the brain during ICH (Hammond et al., 2014). α4 binds VCAM-1 on the endothelium to facilitate cell diapedeses and thus BER1KO data, alongside evidence of IL-1 dependent VCAM-1 expression from Chapter 3, points toward endothelial IL-1R1 as the critical mediator of harmful monocyte recruitment following ICH. However, the data presented in Figure 6.2 are very preliminary and fraught with technical issues and thus much more work is required to validate such claims.

IL-1 reduces CBF during IS (Parry-Jones et al., 2008; Murray et al., 2014; Wong et al., 2019). The results of Chapter 3 show that IL-1 increases CBF in the collagenase-induced mouse model of ICH and this is similar to what is seen in naïve states (Blamire et al., 2000). Quite how IL-1 has opposing effects on CBF in the two stroke subtypes is unresolved but again might be due to cell-specific effects.

There are three distinct cells of the vascular unit that are closely tied to CBF control. Endothelial cells and SMCs are the most widely appreciated modulators of blood flow, however, in the brain, it is suspected that CBF is chiefly regulated at the level of capillaries by contractile cells known as pericytes (although this is debated by Hill et al., (2015)) (Peppiatt et al., 2006; Hall et al., 2014). A recent paper utilising cutting edge single cell RNA sequencing has revealed that each of these cell types express IL-1R1 (see Appendix Figure 6.3) (Vanlandewijck et al., 2018). Importantly, pericytes and SMCs die during IS

and, in doing so, constrict to close off blood supply and contribute to the no-reflow phenomenon (Hall et al., 2014; Hill et al., 2015). Endothelial cells, on the other hand, remain alive and deletion of IL-1R1 from these cells improves CBF following IS (Wong et al., 2019). Moreover, administration of IL-1 to endothelial cells *in vitro* triggers the production of the potent vasoconstrictor endothelin-1 (Yoshizumi et al., 1990). In fact, systemically administered IL-1 reduces CBF following IS through an endothelin-1-dependent mechanism (Murray et al., 2014). Thus during IS, IL-1 signals through endothelial cells to produce endothelin-1 and reduce CBF. In contrast, IL-1 can reduce vascular tone by directly preventing SMC constriction (Beasley et al., 1989, 1991). Moreover, COX-2 is a common downstream target of IL-1 and produces potent vasoactive eicosanoids such as PGE_2 which can modify SMC and pericyte function (Parfenova et al., 2002). IL-1 facilitates pericyte relaxation in a COX-2 dependent fashion and we found evidence of COX-2 expression on perivascular cells in Chapter 3 (Kerkar et al., 2006). Very little is known about SMC and pericyte biology in ICH and investigations into the actions of IL-1 on these cells may reveal important roles in CBF regulation. Transgenic animals in which the IL-1R1 gene is deleted specifically on pericytes or SMCs will provide the best tools to investigate IL-1 biology on these cell types. Although, identification of specific promoters for brain resident SMCs and pericytes (which are required to develop transgenic KOs) is proving difficult (Hartmann et al., 2015).

IL-1 effects on vascular tone are complex and this complexity is compounded by the finding that distinct tissue sites respond to IL-1 in an individual manner (Robert et al., 1993). Considering how important IL-1 and CBF are in the pathogenesis of diseases such as stroke, more studies are required to reveal the interactions between the two systems.

5.2.3 Do inflammasomes affect stroke pathophysiology?

The inflammasome field has gained immense traction in recent years. The findings of the CANTOS trial directly implicate inflammasomes, as IL-1 activating machinery, in the onset of vascular disease and many preclinical studies allude to inflammasomes as therapeutic targets in post-stroke brain damage (Barrington et al., 2017; Ridker et al., 2017). However, the findings of Chapter 3 and 4 from this thesis suggest that inflammasomes may not have therapeutic potential in stroke.

Following ICH, multiple inflammasome genes (such as NLRP3 and AIM2) were upregulated in the ipsilateral brain hemisphere. Yet, despite IL-1 controlling myeloid cell

recruitment, caspase-1 inhibition had no effect on immune cell trafficking to the brain. No previous studies have directly inhibited caspase-1 and measured immune cell recruitment following ICH. Although, two published studies indicate that NLRP3 activation does directly promote myeloid cell trafficking (Ma et al., 2014; Ren et al., 2018). These discrepancies may be part explained by methodological differences as one study measured neutrophil recruitment by histological means (Ma et al., 2014), whilst the other quantified immune cells 3 days following ICH (Ren et al., 2018), compared to 1 day in Chapter 3. The temporal difference may be most pertinent as we found that, whilst IL-1α levels decreased, IL-1β production was highest at 24 hours. Therefore, inflammasome activation may occur from day one onwards and reflect the dominant IL-1 processing signal at this time point. Nevertheless, previous studies do indicate that caspase-1 and NLRP3 contribute to neuronal injury and neurological deficits and neither have been tested in this thesis (Wu et al., 2010; Ma et al., 2014; Ren et al., 2018). Therefore, important next steps are to assess whether delayed NLRP3 activation contributes to neurological injury as this could represent a viable therapeutic target. No role could be found for NLRP3 in neuronal injury following IS however.

Similarly to ICH, inflammasome genes were found upregulated within the brain following IS. Although, in this setting only NLRP3 was specifically induced by stroke. In contrast to others, we found that genetic or pharmacological inhibition of NLRP3 did not affect immune cell recruitment or neuronal death (Yang et al., 2014; Ismael et al., 2018). A major limitation of our study in Chapter 4 is the lack of functional assessments as it is clear that functional deficits may occur in the absence of overt histological changes (Lyeth et al., 1990; Harris et al., 2016). However, an important limitation of the study in Chapter 4 is how poorly it may reflect the clinical condition, in that co-morbid conditions are absent.

There is unequivocal evidence that humans adopt a pro-inflammatory physiological state over the course of their lifetime in a process known as “inflammaging” (Franceschi et al., 2006). The mechanisms underpinning the inflammaging process are unclear but the innate immune system and poor diet have been strongly implicated (Salminen et al., 2008; Netea et al., 2016). As a member of the innate immune system, NLRP3 can respond to a wide variety of stimuli and evolutionary pressure to fine-tune its activation has brought about an initial priming step as an important checkpoint (Swanson et al., 2019). Many different stimuli can trigger NLRP3 priming but perhaps the most relevant are those linked to chronic stresses associated with non-communicable diseases such as OxLDL (Stewart et

al., 2010; Robbins et al., 2014). Importantly, NLRP3 is known to contribute toward a pro-inflammatory state induced by a western diet (causing hypercholesterolemia), which may place the inflammasome at the heart of the inflammaging process (Christ et al., 2018). In Chapter 4, as is often the case in most preclinical stroke studies, stroke was induced in young naïve mice that have not been party to the inflammaging process. The use of young mice is therefore likely to reduce the amount of NLRP3 priming experienced in the laboratory setting, compared to that seen in humans. IS has consistently been shown to worsen when comorbidities are modelled in animals through an IL-1 dependent pathway (Murray et al., 2015). For example, in obese mice, which will have raised OxLDL and therefore likely primed NLRP3, neurological deficits are far worse than non-obese counterparts following IS (Haley and Lawrence, 2016). An important future direction is therefore to assess whether NLRP3 contributes to stroke injury in animals with a primed immune system.

5.2.4 The outlook for stroke therapies

Overall the results of this thesis may cause one to reassess the inflammatory response as a therapeutic target in stroke. Raised inflammatory biomarkers have been consistently linked to poor outcome in stroke patients but the immune response is likely to increase proportionally with the amount of damage suffered. We therefore rely on empirical preclinical studies to differentiate correlation from causation.

Since its inception by Celsus, inflammation has stood out mainly as a pathological process in medical doctrine, despite beneficial effects of inflammation being demonstrated since the writings of John Hunter in 1794 (Muir, 1909; Turk, 1994). These contrasting roles of inflammation are said to occur in a somewhat temporally evolving mutually exclusive manner (acutely damaging but chronically beneficial). Yet, as science evolves, so does our appreciation of incomplete truths. It is now evident that immune cells can promote tissue homeostasis (Nimmerjahn et al., 2005; Schafer et al., 2012), limit bleeding (Burzynski et al., 2019), reduce acute tissue damage (Uderhardt et al., 2019) and even inform cognitive processes (Kipnis et al., 2012). Should we, therefore, continue to view the immune response to stroke as something that must be completely nullified? Or should we instead work to reveal the complex actions of the immune system in order to design bespoke therapies to specifically prevent deleterious processes and promote beneficial ones? We have a long way to go in achieving such aims as the complexity of the immune response often results in the same cell or process having advantageous and detrimental actions. For

example, in Chapter 3 of this thesis, we found that monocytes exacerbate acute neurological injury in ICH. However, previous studies have shown that these same cells contribute to tissue resolution and functional recovery from day 3 onwards (Chang et al., 2018). Complete inhibition of monocyte entry to the brain therefore may not be the best strategy to adopt. Instead we should be looking to identify the exact mechanism by which monocytes damage the brain at acute timepoints, whilst facilitating their beneficial actions later on. In a surprising finding, we also showed that inhibition of IL-1 (the major inflammatory mediator) worsened outcome in ICH and point toward a novel acute beneficial immunovascular reaction governing this response. Yet conversely, IL-1 was necessary for harmful monocyte recruitment. These dichotomous actions of IL-1 in ICH, therefore, exemplify the need to further our understanding before therapeutically targeting the immune response in disease. Examples do not come only from this thesis however. As mentioned in section 1.5.2, microglia were initially believed to be responsible for all deleterious inflammatory reactions in stroke, yet now we are aware that these cells regulate neuronal firing to limit excitotoxicity and prevent harmful neutrophil entry to the brain following IS (Szalay et al., 2016; Otxoa-de-Amezaga et al., 2019).

So what about the overwhelming evidence that acute inflammation is pathological in the stroke setting? First it is important to note that, compared to IS, relatively little has been investigated in preclinical models of ICH (see Appendix Figure 6.4) and less still is known about the comparability of the immune response between the two major stroke subtypes. When we consider the diametrically opposed pathophysiology of the two stroke subtypes, it seems naïve to transpose ideas from the IS field directly to ICH, as so often happens. It is also important to appreciate the evolution of scientific rigour that has occurred over the past twenty years and how this may affect the field of stroke research. As recently as 2009, a survey into the quality of published animal research studies found that nearly 90% of papers failed to impose important measures to reduce internal bias such as blinding and randomisation (Kilkenny et al., 2009). Such poor study quality has been shown to increase the reported effect size of interventions tested in published studies (O'Collins et al., 2006) On top of this, evidence of considerable publication bias contributes to an incomplete interpretation of the preclinical stroke field at large (Macleod et al., 2004; Sena et al., 2010). IL-1RA, for example, has been predicted to have an over-statement of efficacy of up to 50 % due to publication bias alone (Sena et al., 2010) (though this was later amended to 40 % by McCann et al., 2016). In the recent phase II clinical trial IL-1RA successfully

reduced IL-6 levels and thus reduced inflammation (Smith et al., 2018). However, no benefit was found in patient outcome, which may have indirectly revealed that inflammation is not detrimental in acute IS. This would not be the first time such a surprising conclusion has been made from a clinical trial built on sound scientific theory. For many years, corticosteroids were administered to traumatic brain injury patients under the premise they would reduce inflammation and lower ICP. However, a large multi-centre randomised controlled trial revealed that corticosteroids actually increased the absolute risk of death (Olldashi et al., 2004). This study highlighted the importance of performing such large and rigorous trials before interpreting the effects of treatments. So far, IL-1RA has only been tested in small clinical trials, thus larger studies are required before confident conclusions can be made. There is currently a phase 2 clinical trial ongoing testing the effects of IL-1RA in ICH patients (NCT03737344) that may cause alarm upon reading the findings from Chapter 3 of this thesis. However, it is important to understand that we have not tested the therapeutic potential of IL-1RA, instead we asked the question of what role does IL-1 play from the onset of ICH. An immediate aim should therefore be to test the effects IL-1RA has on neurological function when administered in a delayed fashion, in order to mimic the clinical situation more appropriately. Yet, the question still remains as to whether inflammation is the most pertinent therapeutic target for ICH. Should we now look to treat inflammation as any other physiological parameter in stroke patients and aim to prevent it reaching extremes?

Current licensed IS therapies aim to reduce the loss of salvageable tissue by dislodging the occluding clot, but it is unclear whether such salvageable tissue exists in haemorrhage. Up to 30 % of ICH patients experience extensive haematoma expansion but attempts to treat persistent bleeding by promoting haemostasis have failed (Mayer et al., 2005, 2008; Baharoglu et al., 2016; Law et al., 2018). It is not clear how the brain continues to bleed during ICH but the hypothesis most widely appreciated was proposed by Fisher in 1971. In his histopathological investigation, Fisher described the appearance of multiple bleed sites that lacked obvious cellular or pathological changes and, thus, attributed the onset of bleeds from these sites to mechanical disruption by the expanding haematoma (often referred to as “Fisher’s avalanche model”). However, despite resulting in mass effect, neither autologous blood injection nor microballoon inflation have been reported to cause *in situ* bleeding. It is therefore unlikely that mass effect alone causes persistent bleeding following ICH. In patients, coagulation parameters are not associated with markers of

ongoing bleeding but high BP is (Becker et al., 1999). Post hoc analysis of a large clinical trial showed that patients that were treated to intensively lower BP had decreased haematoma expansion (Leasure et al., 2019). This data may implicate loss of vascular autoregulation in continuous bleeding as it is known that (i) ICH patients have disruptions to cerebral autoregulation, (ii) blood pressure that exceeds autoregulation leads to vascular leakage, and (iii) vascular leakage precedes brain haemorrhage in spSHRs (Hatashita et al., 1986; Lee et al., 2007; Cipolla, 2009; Minhas et al., 2019). Therefore, disruptions to myogenic tone in arteries nearby the haematoma might be the key feature leading to haematoma expansion following ICH. Interestingly, there might also be evidence that all ICH patients experience persistent bleeding. When blood is injected into cadavers, or as part of the autologous blood model, haematoma volume decreases over the course of a day due to clot retraction (Lei et al., 2014; Majidi et al., 2016; Sobowale, 2018). In contrast, haematoma volume remains somewhat stable or even increases in ICH patients (Ovesen et al., 2014). Therefore, any therapies designed to treat persistent bleeding might show benefit to all ICH patients. Before then however, we must first look to reveal the mechanisms leading to secondary vascular breakdown.

5.3 Concluding remarks

The acute immune response is said to be a promising therapeutic target in both stroke subtypes. Yet, whilst the inflammatory response to IS is well characterised, relatively little is known about inflammation in ICH. The work contained within this thesis provides novel insights into fundamental processes of the inflammatory response to brain ischaemia and haemorrhage. Importantly, we identify IL-1 as the conserved master regulator of brain inflammation during stroke. However, divergent downstream actions result in IL-1 triggering beneficial events in ICH as well as pathological ones similar to those seen in IS. We also report that IL-1β processing inflammasomes may be redundant in driving brain inflammation when stroke is modelled in young naïve mice. Overall, the fundamental findings of this thesis serve to add further complexity to our understanding of inflammation in stroke. We thus provide future researchers with a refined ICH model that can be used to decipher the described dichotomous effects of inflammation in a timely fashion. It is now imperative to perform further comparative studies of stroke subtypes to identify universal therapeutic targets to treat this devastating condition.

Bibliography

Abid, K. A., Sobowale, O. A., Parkes, L. M., Naish, J., Parker, G. J. M., du Plessis, D., Brough, D., Barrington, J., Allan, S. M., Hinz, R. and Parry-Jones, A. R. (2018). Assessing Inflammation in Acute Intracerebral Hemorrhage with PK11195 PET and Dynamic Contrast-Enhanced MRI. *Journal of Neuroimaging*, 28(2), 158–161.

Abulafia, D. P., Vaccari, J. P. de R., Lozano, J. D., Lotocki, G., Keane, R. W. and Dietrich, W. D. (2009). Inhibition of the inflammasome complex reduces the inflammatory response after thromboembolic stroke in mice. *Journal of Cerebral Blood Flow and Metabolism*, 29(3), 534–544.

Afonina, I. S., Müller, C., Martin, S. J. and Beyaert, R. (2015). Proteolytic Processing of Interleukin-1 Family Cytokines: Variations on a Common Theme. *Immunity* 991–1004.

Afonina, I. S., Tynan, G. A., Logue, S. E., Cullen, S. P., Bots, M., Lüthi, A. U., Reeves, E. P., McElvaney, N. G., Medema, J. P., Lavelle, E. C. and Martin, S. J. (2011). Granzyme B-dependent proteolysis acts as a switch to enhance the proinflammatory activity of IL-1α. *Molecular Cell*, 44(2), 265–278.

Aganna, E., Martinon, F., Hawkins, P. N., Ross, J. B., Swan, D. C., Booth, D. R., Lachmann, H. J., Gaudet, R., Woo, P., Feighery, C., Cotter, F. E., Thome, M., Hitman, G. A., Tschopp, J. and McDermott, M. F. (2002). Association of mutations in the NALP3/CIAS1/PYPAF1 gene with a broad phenotype including recurrent fever, cold sensitivity, sensorineural deafness, and AA amyloidosis. *Arthritis and Rheumatism*, 46(9), 2445–2452.

Agard, N. J., Maltby, D. and Wells, J. A. (2010). Inflammatory stimuli regulate caspase substrate profiles. *Molecular and Cellular Proteomics*, 9(5), 880–893.

Aksentijevich, I., Nowak, M., Mallah, M., Chae, J. J., Watford, W. T., Hofmann, S. R., Stein, L., Russo, R., Goldsmith, D., Dent, P., Rosenberg, H. F., Austin, F., Remmers, E. F., Balow, J. E., … Goldbach-Mansky, R. (2002). De novo CIAS1 mutations, cytokine activation, and evidence for genetic heterogeneity in patients with neonatal-onset multisystem inflammatory disease (NOMID): A new member of the expanding family of pyrin-associated autoinflammatory diseases. *Arthritis and Rheumatism*, 46(12), 3340–3348.

Alfaidi, M., Wilson, H., Daigneault, M., Burnett, A., Ridger, V., Chamberlain, J. and Francis, S. (2015). Neutrophil elastase promotes interleukin-1β secretion from human coronary endothelium. *Journal of Biological Chemistry*, 290(40), 24067–24078.

Alharbi, B. M., Tso, M. K. and Macdonald, R. L. (2016). Animal models of spontaneous intracerebral hemorrhage. *Neurological Research*, 38(5), 448–455.

Allan, S. M., Tyrrell, P. J. and Rothwell, N. J. (2005). Interleukin-1 and neuronal injury. *Nature Reviews Immunology*, 5(8), 629–640.

Allen, C., Thornton, P., Denes, A., McColl, B. W., Pierozynski, A., Monestier, M., Pinteaux, E., Rothwell, N. J. and Allan, S. M. (2012). Neutrophil Cerebrovascular Transmigration Triggers Rapid Neurotoxicity through Release of Proteases Associated with Decondensed DNA. *The Journal of Immunology*, 189(1), 381–392.

Andersson, P. B., Perry, V. H. and Gordon, S. (1992). Intracerebral injection of proinflammatory cytokines or leukocyte chemotaxins induces minimal myelomonocytic cell recruitment to the parenchyma of the central nervous system. *Journal of Experimental Medicine*, 176(1), 255–259.

Anrather, J. and Iadecola, C. (2016). Inflammation and Stroke: An Overview. *Neurotherapeutics*, 13(4), 661–670.

Anthony, D. C., Bolton, S. J., Fearn, S. and Perry, V. H. (1997). Age-related effects of interleukin-1β on polymorphonuclear neutrophil-dependent increases in blood-brain barrier permeability in rats. *Brain*, 120(3), 435–444.

Anthony, D., Dempster, R., Fearn, S., Clements, J., Wells, G., Perry, V. H. and Walker, K. (1998). CXC chemokines generate age-related increases in neutrophilmediated brain inflammation and blood-brain barrier breakdown. *Current Biology*, 8(16), 923–927.

Aronowski, J. and Zhao, X. R. (2011). Molecular Pathophysiology of Cerebral Hemorrhage Secondary Brain Injury. *Stroke*, 42(6), 1781–1786.

Askenase, M. H. and Sansing, L. H. (2016). Stages of the Inflammatory Response in Pathology and Tissue Repair after Intracerebral Hemorrhage. *Seminars in neurology*, 36(3), 288–97.

Aslam, M., Ahmad, N., Srivastava, R. and Hemmer, B. (2012). TNF-alpha induced NFκB signaling and p65 (RelA)

overexpression repress Cldn5 promoter in mouse brain endothelial cells. *Cytokine*, 57(2), 269–275.

Attems, J., Lauda, F. and Jellinger, K. A. (2008). Unexpectedly low prevalence of intracerebral hemorrhages in sporadic cerebral amyloid angiopathy - An autopsy study. *Journal of Neurology*, 255(1), 70–76.

Auffray, C., Fogg, D., Garfa, M., Elain, G., Join-Lambert, O., Kayal, S., Sarnacki, S., Cumano, A., Lauvau, G. and Geissmann, F. (2007). Monitoring of blood vessels and tissues by a population of monocytes with patrolling behavior. *Science*, 317(5838), 666–670.

Avital, A., Goshen, I., Kamsler, A., Segal, M., Iverfeldt, K., Richter-Levin, G. and Yirmiya, R. (2003). Impaired interleukin-1 signaling is associated with deficits in hippocampal memory processes and neural plasticity. *Hippocampus*, 13(7), 826–834.

Baeten, K. M. and Akassoglou, K. (2011). Extracellular matrix and matrix receptors in blood-brain barrier formation and stroke. *Developmental Neurobiology*, 71(11), 1018–1039.

Baharoglu, M. I., Cordonnier, C., Salman, R. A. S., de Gans, K., Koopman, M. M., Brand, A., Majoie, C. B., Beenen, L. F., Marquering, H. A., Vermeulen, M., Nederkoorn, P. J., de Haan, R. J. and Roos, Y. B. (2016). Platelet transfusion versus standard care after acute stroke due to spontaneous cerebral haemorrhage associated with antiplatelet therapy (PATCH): a randomised, open-label, phase 3 trial. *The Lancet*, 387(10038), 2605–2613.

Bailey, E. L., Smith, C., Sudlow, C. L. M. and Wardlaw, J. M. (2011). Is the spontaneously hypertensive stroke prone rat a pertinent model of sub cortical ischemic stroke? A systematic review. *International Journal of Stroke* 434–444.

Baker, M. and Penny, D. (2016). Is there a reproducibility crisis? *Nature*, 533(7604), 452–454.

Ballou, L. R., Chao, C. P., Holness, M. A., Barker, S. C. and Ragshow, R. (1992). Interleukin-1-mediated PGE2 production and sphingomyelin metabolism. *J. Biol. Chem.*, 267(28), 20044–20050.

Banerjee, C. and Chimowitz, M. I. (2017). Stroke Caused by Atherosclerosis of the Major Intracranial Arteries. *Circulation Research* 502–513.

Barrington, J., Lemarchand, E. and Allan, S. M. (2017). A brain in flame; do inflammasomes and pyroptosis influence stroke pathology? *Brain Pathology*, 27(2), 205–212.

Beasley, D., Cohen, R. A. and Levinsky, N. G. (1989). Interleukin 1 inhibits contraction of vascular smooth muscle. *Journal of Clinical Investigation*, 83(1), 331–335.

Beasley, D., Schwartz, J. H. and Brenner, B. M. (1991). Interleukin 1 induces prolonged L-arginine-dependent cyclic guanosine monophosphate and nitrite production in rat vascular smooth muscle cells. *Journal of Clinical Investigation*, 87(2), 602–608.

Bechmann, I., Galea, I. and Perry, V. H. (2007). What is the blood-brain barrier (not)? *Trends in Immunology*, 28(1), 5–11.

Becker, K. J., Baxter, A. B., Bybee, H. M., Tirschwell, D. L., Abouelsaad, T. and Cohen, W. A. (1999). Extravasation of radiographic contrast is an independent predictor of death in primary intracerebral hemorrhage. *Stroke*, 30(10), 2025–2032.

Benakis, C., Brea, D., Caballero, S., Faraco, G., Moore, J., Murphy, M., Sita, G., Racchumi, G., Ling, L., Pamer, E. G., Iadecola, C. and Anrather, J. (2016). Commensal microbiota affects ischemic stroke outcome by regulating intestinal γδ T cells. *Nature Medicine*, 22(5), 516–523.

Benchoua, A., Guégan, C., Couriaud, C., Hosseini, H., Sampaïo, N., Morin, D. and Onténiente, B. (2001). Specific caspase pathways are activated in the two stages of cerebral infarction. *The Journal of Neuroscience*, 21(18), 7127–7134.

Bernardes-Silva, M., Anthony, D. C., Issekutz, A. C. and Perry, V. H. (2001). Recruitment of neutrophils across the blood-brain barrier: The role of E- and P-selectins. *Journal of Cerebral Blood Flow and Metabolism*, 21(9), 1115–1124.

Blamire, A. M., Anthony, D. C., Rajagopalan, B., Sibson, N. R., Perry, V. H. and Styles, P. (2000). Interleukin-1β-induced changes in blood-brain barrier permeability, apparent diffusion coefficient, and cerebral blood volume in the rat brain: A magnetic resonance study. *Journal of Neuroscience*, 20(21), 8153–8159.

Bonaventura, C., Henkens, R., Alayash, A. I., Banerjee, S. and Crumbliss, A. L. (2013). Molecular Controls of the Oxygenation and Redox Reactions of Hemoglobin. *Antioxidants & Redox Signaling*, 18(17), 2298–2313.

Boucher, D., Monteleone, M., Coll, R. C., Chen, K. W., Ross, C. M., Teo, J. L., Gomez, G. A., Holley, C. L., Bierschenk, D., Stacey, K. J., Yap, A. S., Bezbradica, J. S. and Schroder, K. (2018). Caspase-1 self-cleavage is an

intrinsic mechanism to terminate inflammasome activity. *Journal of Experimental Medicine*, 215(3), 827–840.

Boutin, H., LeFeuvre, R. A., Horai, R., Asano, M., Iwakura, Y. and Rothwell, N. J. (2001). Role of IL-1α and IL-1β in ischemic brain damage. *Journal of Neuroscience*, 21(15), 5528–5534.

Brennan, A. M., Won Suh, S., Joon Won, S., Narasimhan, P., Kauppinen, T. M., Lee, H., Edling, Y., Chan, P. H. and Swanson, R. A. (2009). NADPH oxidase is the primary source of superoxide induced by NMDA receptor activation. *Nature Neuroscience*, 12(7), 857–863.

Brinkmann, V., Reichard, U., Goosmann, C., Fauler, B., Uhlemann, Y., Weiss, D. S., Weinrauch, Y. and Zychlinsky, A. (2004). Neutrophil Extracellular Traps Kill Bacteria. *Science*, 303(5663), 1532–1535.

Brouns, R. and De Deyn, P. P. (2009). The complexity of neurobiological processes in acute ischemic stroke. *Clinical Neurology and Neurosurgery* 483–495.

Buryskova, M., Pospisek, M., Grothey, A., Simmet, T. and Burysek, L. (2004). Intracellular Interleukin-1α Functionally Interacts with Histone Acetyltransferase Complexes. *Journal of Biological Chemistry*, 279(6), 4017–4026.

Burzynski, L. C., Humphry, M., Pyrillou, K., Wiggins, K. A., Chan, J. N. E., Figg, N., Kitt, L. L., Summers, C., Tatham, K. C., Martin, P. B., Bennett, M. R. and Clarke, M. C. H. (2019). The Coagulation and Immune Systems Are Directly Linked through the Activation of Interleukin-1α by Thrombin. *Immunity*, 50(4), 1033–1042.e6.

Cai, W., Liu, S., Hu, M., Huang, F., Zhu, Q., Qiu, W., Hu, X., Colello, J., Zheng, S. G. and Lu, Z. (2019). Functional Dynamics of Neutrophils After Ischemic Stroke. *Translational Stroke Research*, 11(1), 108–121.

Chan, J., Atianand, M., Jiang, Z., Carpenter, S., Aiello, D., Elling, R., Fitzgerald, K. A. and Caffrey, D. R. (2015). Cutting Edge: A Natural Antisense Transcript, AS-IL1α, Controls Inducible Transcription of the Proinflammatory Cytokine IL-1α. *The Journal of Immunology*, 195(4), 1359–1363.

Chang, C. F., Goods, B. A., Askenase, M. H., Hammond, M. D., Renfroe, S. C., Steinschneider, A. F., Landreneau, M. J., Ai, Y., Beatty, H. E., Da Costa, L. H. A., Mack, M., Sheth, K. N., Greer, D. M., Huttner, A., … Sansing, L. H. (2018). Erythrocyte efferocytosis modulates macrophages towards recovery after intracerebral hemorrhage. *Journal of Clinical Investigation*, 128(2), 607–624.

Chen, C. J., Kono, H., Golenbock, D., Reed, G., Akira, S. and Rock, K. L. (2007). Identification of a key pathway required for the sterile inflammatory response triggered by dying cells. *Nature Medicine*, 13(7), 851–856.

Chen, J. and Chen, Z. J. (2018). PtdIns4P on dispersed trans-Golgi network mediates NLRP3 inflammasome activation. *Nature*, 564(7734), 71–76.

Christ, A., Günther, P., Lauterbach, M. A. R., Duewell, P., Biswas, D., Pelka, K., Scholz, C. J., Oosting, M., Haendler, K., Baßler, K., Klee, K., Schulte-Schrepping, J., Ulas, T., Moorlag, S. J. C. F. M., … Latz, E. (2018). Western Diet Triggers NLRP3-Dependent Innate Immune Reprogramming. *Cell*, 172(1–2), 162–175.e14.

Cipolla, M. (2009). Chapter 5 Control of Cerebral Blood Flow Autoregulation of Cerebral Blood Flow. *In The Cerebral Circulation*, pp. 69–71.

Cisneros-Mejorado, A., Gottlieb, M., Cavaliere, F., Magnus, T., Koch-Nolte, F., Scemes, E., Pérez-Samartín, A. and Matute, C. (2015). Blockade of P2X7 receptors or pannexin-1 channels similarly attenuates postischemic damage. *Journal of Cerebral Blood Flow and Metabolism*, 35(5), 843–850.

Clancy, D. M., Sullivan, G. P., Moran, H. B. T., Henry, C. M., Reeves, E. P., McElvaney, N. G., Lavelle, E. C. and Martin, S. J. (2018). Extracellular Neutrophil Proteases Are Efficient Regulators of IL-1, IL-33, and IL-36 Cytokine Activity but Poor Effectors of Microbial Killing. *Cell Reports*, 22(11), 2937–2950.

Cohen, I., Rider, P., Carmi, Y., Braiman, A., Dotan, S., White, M. R., Voronov, E., Martin, M. U., Dinarello, C. A. and Apte, R. N. (2010). Differential release of chromatin-bound IL-1α discriminates between necrotic and apoptotic cell death by the ability to induce sterile inflammation. *Proceedings of the National Academy of Sciences of the United States of America*, 107(6), 2574–2579.

Compan, V., Baroja-Mazo, A., L??pez-Castej??n, G., Gomez, A. I. I., Mart??nez, C. M., Angosto, D., Montero, M. T. M. T., Herranz, A. S. S., Baz??n, E., Reimers, D., Mulero, V., Pelegr??n, P., López-Castejón, G., Gomez, A. I. I., … Pelegrín, P. (2012). Cell Volume Regulation Modulates NLRP3 Inflammasome Activation. *Immunity*, 37(3), 487–500.

Cook, D. N., Pisetsky, D. S. and Schwartz, D. A. (2004). Toll-like receptors in the pathogenesis of human disease. *Nature Immunology* 975–979.

Cookson, B. T. and Brennan, M. A. (2001). Pro-inflammatory programmed cell death [2]. *Trends in Microbiology*, 9(3),

113–114.

Corbyn, Z. (2014). Statistics: A growing global burden. *Nature*, 510(7506 SUPPL.), S2–S3.

Cronk, J. C., Filiano, A. J., Louveau, A., Marin, I., Marsh, R., Ji, E., Goldman, D. H., Smirnov, I., Geraci, N., Acton, S., Overall, C. C. and Kipnis, J. (2018). Peripherally derived macrophages can engraft the brain independent of irradiation and maintain an identity distinct from microglia. *The Journal of experimental medicine*, 215(6), 1627–1647.

Cruz Hernández, J. C., Bracko, O., Kersbergen, C. J., Muse, V., Haft-Javaherian, M., Berg, M., Park, L., Vinarcsik, L. K., Ivasyk, I., Rivera, D. A., Kang, Y., Cortes-Canteli, M., Peyrounette, M., Doyeux, V., … Schaffer, C. B. (2019). Neutrophil adhesion in brain capillaries reduces cortical blood flow and impairs memory function in Alzheimer's disease mouse models. *Nature Neuroscience*, 22(3), 413–420.

Cuartero, M. I., Ballesteros, I., Moraga, A., Nombela, F., Vivancos, J., Hamilton, J. A., Corbí, Á. L., Lizasoain, I. and Moro, M. A. (2013). N2 neutrophils, novel players in brain inflammation after stroke: Modulation by the ppary agonist rosiglitazone. *Stroke*, 44(12), 3498–3508.

Cui, G. Y., Gao, X. M., Qi, S. H., Gillani, A., Gao, L., Shen, X. and Zhang, Y. D. (2011). The action of thrombin in intracerebral hemorrhage induced brain damage is mediated via PKCα/PKCδ signaling. *Brain Research*, 1398 86–93.

Cunningham, D. D. (1997). Thrombin induces apoptosis in cultured neurons and astrocytes via a pathway requiring tyrosine kinase and RhoA activities. *Journal of Neuroscience*, 17(14), 5316–5326.

Daniels, M. J. D., Adamson, A. D., Humphreys, N. and Brough, D. (2017). CRISPR/Cas9 mediated mutation of mouse IL-1α nuclear localisation sequence abolishes expression. *Scientific Reports*, 7(1), 17077.

Daniels, M. J. D. and Brough, D. (2017). Unconventional pathways of secretion contribute to inflammation. *International Journal of Molecular Sciences*, 18(1), pii: E102.

Davis, C. N., Tabarean, I., Gaidarova, S., Behrens, M. M. and Bartfai, T. (2006). IL-1β induces a MyD88-dependent and ceramide-mediated activation of Src in anterior hypothalamic neurons. *Journal of Neurochemistry*, 98(5), 1379–1389.

Davis, S. M., Broderick, J., Hennerici, M., Brun, N. C., Diringer, M. N., Mayer, S. A., Begtrup, K., Steiner, T. and Recombinant Activated Factor, V. I. I. (2006). Hematoma growth is a determinant of mortality and poor outcome after intracerebral hemorrhage. *Neurology*, 66(8), 1175–1181.

Deinsberger, W., Vogel, J., Kuschinsky, W., Auer, L. M. and Böker, D. K. (1996). Experimental intracerebral hemorrhage: Description of a double injection model in rats. *Neurological Research*, 18(5), 475–477.

Denes, A., Coutts, G., Lenart, N., Cruickshank, S. M., Pelegrin, P., Skinner, J., Rothwell, N., Allan, S. M., Brough, D., Lénárt, N., Cruickshank, S. M., Pelegrin, P., Skinner, J., Rothwell, N., … Brough, D. (2015). AIM2 and NLRC4 inflammasomes contribute with ASC to acute brain injury independently of NLRP3. *Proceedings of the National Academy of Sciences of the United States of America*, 112(13), 4050–5.

Denes, A., Vidyasagar, R., Feng, J., Narvainen, J., McColl, B. W., Kauppinen, R. A. and Allan, S. M. (2007). Proliferating resident microglia after focal cerebral ischaemia in mice. *Journal of Cerebral Blood Flow and Metabolism*, 27(12), 1941–1953.

Denes, A., Wilkinson, F., Bigger, B., Chu, M., Rothwell, N. J. and Allan, S. M. (2013). Central and haematopoietic interleukin-1 both contribute to ischaemic brain injury in mice. *DMM Disease Models and Mechanisms*, 6(4), 1043–1048.

Dimitrijevic, O. B., Stamatovic, S. M., Keep, R. F. and Andjelkovic, A. V. (2007). Absence of the chemokine receptor CCR2 protects against cerebral ischemia/reperfusion injury in mice. *Stroke*, 38(4), 1345–1353.

Ding, J., Wang, K., Liu, W., She, Y., Sun, Q., Shi, J., Sun, H., Wang, D. and Shao, F. (2016). Pore-forming activity and structural autoinhibition of the gasdermin family. *Nature*, 535(7610), 111–116.

Dirnagl, U., Iadecola, C. and Moskowitz, M. A. (1999). Pathobiology of ischaemic stroke: an integrated view. *Trends in Neurosciences*, 22(9), 391–397.

Doyle, K. P., Quach, L. N., Solé, M., Axtell, R. C., Nguyen, T. V. V., Soler-Llavina, G. J., Jurado, S., Han, J., Steinman, L., Longo, F. M., Schneider, J. A., Malenka, R. C. and Buckwalter, M. S. (2015). B-lymphocyte-mediated delayed cognitive impairment following stroke. *Journal of Neuroscience*, 35(5), 2133–2145.

Ducroux, C., Di Meglio, L., Loyau, S., Delbosc, S., Boisseau, W., Deschildre, C., Maacha, M. Ben, Blanc, R., Redjem, H., Ciccio, G., Smajda, S., Fahed, R., Michel, J. B., Piotin, M., … Desilles, J. P. (2018). Thrombus neutrophil extracellular traps content impair tPA-induced thrombolysis in acute ischemic stroke. *Stroke*, 49(3), 754–757.

Ducruet, A. F., Zacharia, B. E., Hickman, Z. L., Grobelny, B. T., Yeh, M. L., Sosunov, S. a., Connolly, E. S. and Connolly E. Sander, J. (2009). The complement cascade as a therapeutic target in intracerebral hemorrhage. *Experimental Neurology*, 219(2), 398–403.

Duewell, P., Kono, H., Rayner, K. J., Sirois, C. M., Vladimer, G., Bauernfeind, F. G., Abela, G. S., Franchi, L., Nũez, G., Schnurr, M., Espevik, T., Lien, E., Fitzgerald, K. A., Rock, K. L., … Latz, E. (2010). NLRP3 inflammasomes are required for atherogenesis and activated by cholesterol crystals. *Nature*, 464(7293), 1357–1361.

Dutra, F. F., Alves, L. S., Rodrigues, D., Fernandez, P. L., de Oliveira, R. B., Golenbock, D. T., Zamboni, D. S. and Bozza, M. T. (2014). Hemolysis-induced lethality involves inflammasome activation by heme. *Proceedings of the National Academy of Sciences of the United States of America*, 111(39), E4110–E4118.

Eigenbrod, T., Park, J.-H., Harder, J., Iwakura, Y. and Núñez, G. (2008). Cutting Edge: Critical Role for Mesothelial Cells in Necrosis-Induced Inflammation through the Recognition of IL-1α Released from Dying Cells. *The Journal of Immunology*, 181(12), 8194–8198.

El-Brolosy, M. A. and Stainier, D. Y. R. (2017). Genetic compensation: A phenomenon in search of mechanisms. *PLoS Genetics* e1006780.

Elmore, M. R. P., Najafi, A. R., Koike, M. A., Dagher, N. N., Spangenberg, E. E., Rice, R. A., Kitazawa, M., Matusow, B., Nguyen, H., West, B. L. and Green, K. N. (2014). Colony-stimulating factor 1 receptor signaling is necessary for microglia viability, unmasking a microglia progenitor cell in the adult brain. *Neuron*, 82(2), 380–397.

Elmore, S. (2007). Apoptosis: A Review of Programmed Cell Death. *Toxicologic Pathology* 495–516.

Emsley, H. C. A., Smith, C. J., Georgiou, R. F., Vail, A., Hopkins, S. J., Rothwell, N. J., Tyrrell, P. J. and Investigators, I. L.-1ra A. S. (2005). A randomised phase II study of interleukin-1 receptor antagonist in acute stroke patients. *Journal of Neurology Neurosurgery and Psychiatry*, 76(10), 1366–1372.

England, H., Summersgill, H. R., Edye, M. E., Rothwell, N. J. and Brough, D. (2014). Release of Interleukin-1 alpha or Interleukin-1 beta Depends on Mechanism of Cell Death. *Journal of Biological Chemistry*, 289(23), 15942–15950.

Erridge, C. (2010). Endogenous ligands of TLR2 and TLR4: agonists or assistants? *Journal of Leukocyte Biology*, 87(6), 989–999.

Evers, S. M. A. A., Struijs, J. N., Ament, A. J. H. A., Van Genugten, M. L. L., Jager, J. C. and Van Den Bos, G. A. M. (2004). International comparison of stroke cost studies. *Stroke*, 35(5), 1209–1215.

Fang, J., Wang, Y. and Krueger, J. M. (1998). Effects of interleukin-1β on sleep are mediated by the type I receptor. *American Journal of Physiology - Regulatory Integrative and Comparative Physiology*, 274(3 43-3),.

Feigin, V. L., Forouzanfar, M. H., Krishnamurthi, R., Mensah, G. a., Connor, M., Bennett, D. a., Moran, A. E., Sacco, R. L., Anderson, L., Truelsen, T., O'Donnell, M., Venketasubramanian, N., Barker-Collo, S., Lawes, C. M. M., … Grp, G. B. D. S. E. (2014). Global and regional burden of stroke during 1990-2010: Findings from the Global Burden of Disease Study 2010. *The Lancet*, 383(9913), 245–255.

Feigin, V. L., Nichols, E., Alam, T., Bannick, M. S., Beghi, E., Blake, N., Culpepper, W. J., Dorsey, E. R., Elbaz, A., Ellenbogen, R. G., Fisher, J. L., Fitzmaurice, C., Giussani, G., Glennie, L., … Vos, T. (2019). Global, regional, and national burden of neurological disorders, 1990–2016: a systematic analysis for the Global Burden of Disease Study 2016. *The Lancet Neurology*, 18(5), 459–480.

Feigin, V. L., Norrving, B. and Mensah, G. A. (2017). Global Burden of Stroke. *Circulation Research*, 120(3), 439–448.

Feng, L., Chen, Y., Ding, R., Fu, Z., Yang, S., Deng, X. and Zeng, J. (2015). P2X7R blockade prevents NLRP3 inflammasome activation and brain injury in a rat model of intracerebral hemorrhage: involvement of peroxynitrite. *Journal of neuroinflammation*, 12 190.

Fernandes, H. M., Siddique, S., Banister, K., Chambers, I., Wooldridge, T., Gregson, B. and Mendelow, A. D. (2000). Continuous monitoring of ICP and CPP following ICH and its relationship to clinical, radiological and surgical parameters. *Acta neurochirurgica. Supplement*, 76 463–466.

Fisher, C. M. (1971). Pathological observations in hypertensive cerebral hemorrhage. *Journal of Neuropathology and Experimental Neurology*, 30(3), 536–550.

Foley, J. H. and Conway, E. M. (2016). Cross Talk Pathways between Coagulation and Inflammation. *Circulation Research* 1392–1408.

Francheschi, C., Bonafe, M., Valensin, S., Olivieri, F., De Luca, M., Ottavani, E. and De Benedictus, G. (2006).

Inflamm-aging: An Evolutionary Perspective on Immunosenescence. *Annals of the New York Academy of Sciences*, 908(1), 244–254.

Franchi, L., Eigenbrod, T. and Núñez, G. (2009). Cutting Edge: TNF-α Mediates Sensitization to ATP and Silica via the NLRP3 Inflammasome in the Absence of Microbial Stimulation. *The Journal of Immunology*, 183(2), 792–796.

Frantzias, J., Sena, E. S., MacLeod, M. R. and Salman, R. A. S. (2011). Treatment of intracerebral hemorrhage in animal models: Meta-analysis. *Annals of Neurology*, 69(2), 389–399.

Freeman, L., Guo, H., David, C. N., Brickey, W. J., Jha, S. and Ting, J. P. Y. (2017). NLR members NLRC4 and NLRP3 mediate sterile inflammasome activation in microglia and astrocytes. *Journal of Experimental Medicine*, 214(5), 1351–1370.

Friedlander, R. M., Gagliardini, V., Hara, H., Fink, K. B., Li, W., MacDonald, G., Fishman, M. C., Greenberg, A. H., Moskowitz, M. A. and Yuan, J. (1997). Expression of a dominant negative mutant of interleukin-1β converting enzyme in transgenic mice prevents neuronal cell death induced by trophic factor withdrawal and ischemic brain injury. *Journal of Experimental Medicine*, 185(5), 933–940.

Gaidt, M. M., Ebert, T. S., Chauhan, D., Schmidt, T., Schmid-Burgk, J. L., Rapino, F., Robertson, A. A. B., Cooper, M. A., Graf, T. and Hornung, V. (2016). Human Monocytes Engage an Alternative Inflammasome Pathway. *Immunity*, 44(4), 833–846.

Garlanda, C., Dinarello, C. A. and Mantovani, A. (2013). The Interleukin-1 Family: Back to the Future. *Immunity*, 39(6), 1003–1018.

Gelderblom, M., Leypoldt, F., Steinbach, K., Behrens, D., Choe, C. U., Siler, D. A., Arumugam, T. V., Orthey, E., Gerloff, C., Tolosa, E. and Magnus, T. (2009). Temporal and spatial dynamics of cerebral immune cell accumulation in stroke. *Stroke*, 40(5), 1849–1857.

Giles, J. A., Greenhalgh, A. D., Davies, C. L., Denes, A., Shaw, T., Coutts, G., Rothwell, N. J., McColl, B. W. and Allan, S. M. (2015). Requirement for interleukin-1 to drive brain inflammation reveals tissue-specific mechanisms of innate immunity. *Eur J Immunol*, 45(2), 525–530.

Ginhoux, F., Greter, M., Leboeuf, M., Nandi, S., See, P., Gokhan, S., Mehler, M. F., Conway, S. J., Ng, L. G., Stanley, E. R., Samokhvalov, I. M. and Merad, M. (2010). Fate mapping analysis reveals that adult microglia derive from primitive macrophages. *Science*, 330(6005), 841–845.

Giulian, D. and Lachman, L. B. (1985). Interleukin-1 stimulation of astroglial proliferation after brain injury. *Science*, 228(4698), 497–499.

Giulian, D., Woodward, J., Young, D. G., Krebs, J. F. and Lachman, L. B. (1988). Interleukin-1 injected into mammalian brain stimulates astrogliosis and neovascularization. *Journal of Neuroscience*, 8(7), 2485–2490.

Gliem, M., Mausberg, A. K., Lee, J. I., Simiantonakis, I., Van Rooijen, N., Hartung, H. P. and Jander, S. (2012). Macrophages prevent hemorrhagic infarct transformation in murine stroke models. *Annals of Neurology*, 71(6), 743–752.

Goyal, M., Menon, B. K., Van Zwam, W. H., Dippel, D. W. J., Mitchell, P. J., Demchuk, A. M., Dávalos, A., Majoie, C. B. L. M., Van Der Lugt, A., De Miquel, M. A., Donnan, G. A., Roos, Y. B. W. E. M., Bonafe, A., Jahan, R., … Jovin, T. G. (2016). Endovascular thrombectomy after large-vessel ischaemic stroke: A meta-analysis of individual patient data from five randomised trials. *The Lancet*, 387(10029), 1723–1731.

Green, J. P., Yu, S., Martín-Sánchez, F., Pelegrin, P., Lopez-Castejon, G., Lawrence, C. B. and Brough, D. (2018). Chloride regulates dynamic NLRP3-dependent ASC oligomerization and inflammasome priming. *Proceedings of the National Academy of Sciences of the United States of America*, 115(40), E9371–E9380.

Groß, C. J., Mishra, R., Schneider, K. S., Médard, G., Wettmarshausen, J., Dittlein, D. C., Shi, H., Gorka, O., Koenig, P. A., Fromm, S., Magnani, G., Ćiković, T., Hartjes, L., Smollich, J., … Groß, O. (2016). K+ Efflux-Independent NLRP3 Inflammasome Activation by Small Molecules Targeting Mitochondria. *Immunity*, 45(4), 761–773.

Groß, O., Yazdi, A. S., Thomas, C. J., Masin, M., Heinz, L. X., Guarda, G., Quadroni, M., Drexler, S. K. and Tschopp, J. (2012). Inflammasome Activators Induce Interleukin-1α Secretion via Distinct Pathways with Differential Requirement for the Protease Function of Caspase-1. *Immunity*, 36(3), 388–400.

Hacke, W., Kaste, M., Bluhmki, E., Brozman, M., Dávalos, A., Guidetti, D., Larrue, V., Lees, K. R., Medeghri, Z., Machnig, T., Schneider, D., Von Kummer, R., Wahlgren, N. and Toni, D. (2008). Thrombolysis with alteplase 3 to 4.5 hours after acute ischemic stroke. *New England Journal of Medicine*, 359(13), 1317–1329.

Haley, M. J. and Lawrence, C. B. (2016). Obesity and stroke: Can we translate from rodents to patients? *Journal of*

Cerebral Blood Flow and Metabolism 2007–2021.

Hall, C. N., Reynell, C., Gesslein, B., Hamilton, N. B., Mishra, A., Sutherland, B. A., Oâ Farrell, F. M., Buchan, A. M., Lauritzen, M. and Attwell, D. (2014). Capillary pericytes regulate cerebral blood flow in health and disease. *Nature*, 508(1), 55–60.

Hammond, M. D., Ambler, W. G., Ai, Y. and Sansing, L. H. (2014). α4 integrin is a regulator of leukocyte recruitment after experimental intracerebral hemorrhage. *Stroke*, 45(8), 2485–7.

Hammond, M. D., Taylor, R. A., Mullen, M. T., Ai, Y., Aguila, H. L., Mack, M., Kasner, S. E., McCullough, L. D. and Sansing, L. H. (2014). CCR2+Ly6Chi inflammatory monocyte recruitment exacerbates acute disability following intracerebral hemorrhage. *Journal of Neuroscience*, 34(11), 3901–3909.

Hanley, D. F., Thompson, R. E., Rosenblum, M., Yenokyan, G., Lane, K., McBee, N., Mayo, S. W., Bistran-Hall, A. J., Gandhi, D., Mould, W. A., Ullman, N., Ali, H., Carhuapoma, J. R., Kase, C. S., … Zomorodi, A. (2019). Efficacy and safety of minimally invasive surgery with thrombolysis in intracerebral haemorrhage evacuation (MISTIE III): a randomised, controlled, open-label, blinded endpoint phase 3 trial. *The Lancet*, 393(10175), 1021–1032.

Hara, H., Friedlander, R. M., Gagliardini, V., Ayata, C., Fink, K., Huang, Z., Shimizu-Sasamata, M., Yuan, J. and Moskowitz, M. a. (1997). Inhibition of interleukin 1beta converting enzyme family proteases reduces ischemic and excitotoxic neuronal damage. *Proceedings of the national academy of sciences of the United States of America*, 94(5), 2007–12.

Harris, N. M., Ritzel, R., Mancini, N., Jiang, Y., Yi, X., Manickam, D. S., Banks, W. A., Kabanov, A. V., McCullough, L. D. and Verma, R. (2016). Nano-particle delivery of brain derived neurotrophic factor after focal cerebral ischemia reduces tissue injury and enhances behavioral recovery. *Pharmacology Biochemistry and Behavior*, 150–151 48–56.

Hartmann, D. A., Underly, R. G., Watson, A. N. and Shih, A. Y. (2015). A murine toolbox for imaging the neurovascular unit. *Microcirculation* 168–182.

Hatashita, S., Hoff, J. T. and Ishii, S. (1986). Focal brain edema associated with acute arterial hypertension. *Journal of Neurosurgery*, 64(4), 643–649.

He, W., Wan, H., Hu, L., Chen, P., Wang, X., Huang, Z., Yang, Z.-H., Zhong, C.-Q. and Han, J. (2015). Gasdermin D is an executor of pyroptosis and required for interleukin-1β secretion, 25, December, 1285–1298.

Heiss, W. D. (2000). Ischemic penumbra: Evidence from functional imaging in man. *Journal of Cerebral Blood Flow and Metabolism* 1276–1293.

Hill, R. A., Tong, L., Yuan, P., Murikinati, S., Gupta, S. and Grutzendler, J. (2015). Regional Blood Flow in the Normal and Ischemic Brain Is Controlled by Arteriolar Smooth Muscle Cell Contractility and Not by Capillary Pericytes. *Neuron*, 87(1), 95–110.

Hiscott, J., Marois, J., Garoufalis, J., D'Addario, M., Roulston, A., Kwan, I., Pepin, N., Lacoste, J., Nguyen, H. and Bensi, G. (1993). Characterization of a functional NF-kappa B site in the human interleukin 1 beta promoter: evidence for a positive autoregulatory loop. *Molecular and Cellular Biology*, 13(10), 6231–6240.

Hoda, M. N., Singh, I., Singh, A. K. and Khan, M. (2009). Reduction of lipoxidative load by secretory phospholipase A2 inhibition protects against neurovascular injury following experimental stroke in rat. *Journal of Neuroinflammation*, 6 21.

Hoffman, H. M., Mueller, J. L., Broide, D. H., Wanderer, A. A. and Kolodner, R. D. (2001). Mutation of a new gene encoding a putative pyrin-like protein causes familial cold autoinflammatory syndrome and Muckle-Wells syndrome. *Nature Genetics*, 29(3), 301–305.

Holmdahl, R. and Malissen, B. (2012). The need for littermate controls. *European Journal of Immunology* 45–47.

Holmin, S. and Mathiesen, T. (2000). Intracerebral administration of interleukin-1 β and induction of inflammation, apoptosis, and vasogenic edema. *Journal of Neurosurgery*, 92(1), 108–120.

Hornung, V., Ablasser, A., Charrel-Dennis, M., Bauernfeind, F., Horvath, G., Caffrey, D. R., Latz, E. and Fitzgerald, K. A. (2009). AIM2 recognizes cytosolic dsDNA and forms a caspase-1-activating inflammasome with ASC. *Nature*, 458(7237), 514–518.

Hoss, F., Rodriguez-Alcazar, J. F. and Latz, E. (2017). Assembly and regulation of ASC specks. *Cellular and Molecular Life Sciences* 1211–1229.

Hossmann, K. -A (1994). Viability thresholds and the penumbra of focal ischemia. *Annals of Neurology*, 36(4), 557–565.

Hossmann, K. A. (2012). The two pathophysiologies of focal brain ischemia: Implications for translational stroke research. *Journal of Cerebral Blood Flow and Metabolism* 1310–1316.

Van Hove, H., Martens, L., Scheyltjens, I., De Vlaminck, K., Pombo Antunes, A. R., De Prijck, S., Vandamme, N., De Schepper, S., Van Isterdael, G., Scott, C. L., Aerts, J., Berx, G., Boeckxstaens, G. E., Vandenbroucke, R. E., … Movahedi, K. (2019). A single-cell atlas of mouse brain macrophages reveals unique transcriptional identities shaped by ontogeny and tissue environment. *Nature Neuroscience*, 22(6), 1021–1035.

Howells, D. W., Porritt, M. J., Rewell, S. S. J., O'Collins, V., Sena, E. S., Van Der Worp, H. B., Traystman, R. J. and MacLeod, M. R. (2010). Different strokes for different folks: The rich diversity of animal models of focal cerebral ischemia. *Journal of Cerebral Blood Flow and Metabolism* 1412–1431.

Hu, X., Michael De Silva, T., Chen, J. and Faraci, F. M. (2017). Cerebral Vascular Disease and Neurovascular Injury in Ischemic Stroke. *Circulation Research* 449–471.

Hua, Y., Schallert, T., Keep, R. F., Wu, J. M., Hoff, J. T. and Xi, G. H. (2002). Behavioral tests after intracerebral hemorrhage in the rat. *Stroke*, 33(10), 2478–2484.

Huang, Q., Yang, J., Lin, Y., Walker, C., Cheng, J., Liu, Z. G. and Su, B. (2004). Differential regulation of interleukin 1 receptor and toll-like receptor signaling by MEKK3. *Nature Immunology*, 5(1), 98–103.

Hunter, J. and Hunter, J. (2015). a Treatise on the Blood, Inflammation, and Gun-Shot Wounds. *The Works of John Hunter, F.R.S.* vii–viii.

Iida, S., Baumbach, G. L., Lavoie, J. L., Faraci, F. M., Sigmund, C. D. and Heistad, D. D. (2005). Spontaneous stroke in a genetic model of hypertension in mice. *Stroke*, 36(6), 1253–1258.

Ishii, H. and Yoshida, M. (2010). Inflammatory cytokines. *Nippon rinsho. Japanese journal of clinical medicine* 819–822.

Ismael, S., Zhao, L., Nasoohi, S. and Ishrat, T. (2018). Inhibition of the NLRP3-inflammasome as a potential approach for neuroprotection after stroke. *Scientific Reports*, 8(1), 5971.

Ito, M., Shichita, T., Okada, M., Komine, R., Noguchi, Y., Yoshimura, A. and Morita, R. (2015). Bruton's tyrosine kinase is essential for NLRP3 inflammasome activation and contributes to ischaemic brain injury. *Nature Communications*, 10(6), 7360.

Jackson, C. A. and Sudlow, C. L. M. (2006). Is hypertension a more frequent risk factor for deep than for lobar supratentorial intracerebral haemorrhage? *Journal of Neurology Neurosurgery and Psychiatry*, 77(11), 1244–1252.

Jaitin, D. A., Adlung, L., Thaiss, C. A., Weiner, A., Li, B., Descamps, H., Lundgren, P., Bleriot, C., Liu, Z., Deczkowska, A., Keren-Shaul, H., David, E., Zmora, N., Eldar, S. M., … Amit, I. (2019). Lipid-Associated Macrophages Control Metabolic Homeostasis in a Trem2-Dependent Manner. *Cell*, 178(3), 686–698.e14.

Janeway, C. A. and Medzhitov, R. (2002). I Nnate I Mmune R Ecognition . *Annual Review of Immunology*, 20(1), 197–216.

Jansen, P. M., Boermeester, M. A., Fischer, E., De Jong, I. W., Van der Poll, T., Moldawer, L. L., Hack, C. E. and Lowry, S. F. (1995). Contribution of interleukin-1 to activation of coagulation and fibrinolysis, neutrophil degranulation, and the release of secretory-type phospholipase A2 in sepsis: Studies in nonhuman primates after interleukin- 1α administration and during lethal bacteremia. *Blood*, 86(3), 1027–1034.

Jeanne, M., Jorgensen, J. and Gould, D. B. (2015). Molecular and genetic analyses of collagen type IV mutant mouse models of spontaneous intracerebral hemorrhage identify mechanisms for stroke prevention. *Circulation*, 131(18), 1555–1565.

Jin, W. N., Shi, S. X. Y., Li, Z., Li, M., Wood, K., Gonzales, R. J. and Liu, Q. (2017). Depletion of microglia exacerbates postischemic inflammation and brain injury. *Journal of Cerebral Blood Flow and Metabolism*, 37(6), 2224–2236.

Johnson, W., Onuma, O., Owolabi, M. and Sachdev, S. (2016). Stroke: A global response is needed. *Bulletin of the World Health Organization*, p. 634A–635A.

Kamel, H. and Healey, J. S. (2017). Cardioembolic Stroke. *Circulation Research*, 120(3), 514–526.

Karatas, H., Erdener, S. E., Gursoy-Ozdemir, Y., Gurer, G., Soylemezoglu, F., Dunn, A. K. and Dalkara, T. (2011). Thrombotic distal middle cerebral artery occlusion produced by topical FeCl 3 application: A novel model suitable for intravital microscopy and thrombolysis studies. *Journal of Cerebral Blood Flow and Metabolism*, 31(6), 1452–1460.

Kaur, P., Kwatra, G., Kaur, R. and Pandian, J. D. (2014). Cost of stroke in low and middle income countries: A systematic review. *International Journal of Stroke* 678–682.

Kayagaki, N., Stowe, I. B., Lee, B. L., O'Rourke, K., Anderson, K., Warming, S., Cuellar, T., Haley, B., Roose-Girma, M., Phung, Q. T., Liu, P. S., Lill, J. R., Li, H., Wu, J., … Dixit, V. M. (2015). Caspase-11 cleaves gasdermin D for non-canonical inflammasome signalling. *Nature*, 526(7575), 666–671.

Kayagaki, N., Warming, S., Lamkanfi, M., Walle, L. Vande, Louie, S., Dong, J., Newton, K., Qu, Y., Liu, J., Heldens, S., Zhang, J., Lee, W. P., Roose-Girma, M. and Dixit, V. M. (2011). Non-canonical inflammasome activation targets caspase-11. *Nature*, 479(7371), 117–121.

Kayagaki, N., Wong, M. T., Stowe, I. B., Ramani, S. R., Gonzalez, L. C., Akashi-Takamura, S., Miyake, K., Zhang, J., Lee, W. P., Muszyński, A., Forsberg, L. S., Carlson, R. W. and Dixit, V. M. (2013). Noncanonical inflammasome activation by intracellular LPS independent of TLR4. *Science (New York, N.Y.)*, 341(6151), 1246–9.

Kearney, C. J. and Martin, S. J. (2017). An Inflammatory Perspective on Necroptosis. *Molecular Cell* 965–973.

Keep, R. F., Hua, Y. and Xi, G. (2012). Intracerebral haemorrhage: Mechanisms of injury and therapeutic targets. *The Lancet Neurology*, 11(8), 720–731.

Keep, R. F., Zhou, N., Xiang, J., Andjelkovic, A. V, Hua, Y. and Xi, G. (2014). Vascular disruption and blood-brain barrier dysfunction in intracerebral hemorrhage. *Fluids and barriers of the CNS*, 11 18.

Kerkar, S., Williams, M., Blocksom, J. M., Wilson, R. F., Tyburski, J. G. and Steffes, C. P. (2006). TNF-α and IL-1β Increase Pericyte/Endothelial Cell Co-Culture Permeability. *Journal of Surgical Research*, 132(1), 40–45.

Kilkenny, C., Browne, W. J., Cuthill, I. C., Emerson, M. and Altman, D. G. (2013). Improving bioscience research reporting: The arrive guidelines for reporting animal research. *Animals*, 4(1), 35–44.

Kilkenny, C., Parsons, N., Kadyszewski, E., Festing, M. F. W., Cuthill, I. C., Fry, D., Hutton, J. and Altman, D. G. (2009). Survey of the Quality of Experimental Design, Statistical Analysis and Reporting of Research Using Animals. *PLoS ONE*, 4(11),.

Kim, S. K., Yoon, W., Kim, T. S., Kim, H. S., Heo, T. W. and Park, M. S. (2015). Histologic analysis of retrieved clots in acute ischemic stroke: Correlation with stroke etiology and gradient-echo MRI. *American Journal of Neuroradiology*, 36(9), 1756–1762.

Kim, S. W., Lee, H., Lee, H. K., Kim, I. D. and Lee, J. K. (2019). Neutrophil extracellular trap induced by HMGB1 exacerbates damages in the ischemic brain. *Acta neuropathologica communications*, 7(1), 11.

Kipnis, J., Gadani, S. and Derecki, N. C. (2012). Pro-cognitive properties of T cells. *Nature Reviews Immunology* 663–669.

Kirkman, M. a, Allan, S. M. and Parry-Jones, A. R. (2011). Experimental intracerebral hemorrhage: avoiding pitfalls in translational research. *Journal of cerebral blood flow and metabolism : official journal of the International Society of Cerebral Blood Flow and Metabolism*, 31(11), 2135–51.

Kleinschnitz, C., Schwab, N., Kraft, P., Hagedorn, I., Dreykluft, A., Schwarz, T., Austinat, M., Nieswandt, B., Wiendl, H. and Stoll, G. (2010). Early detrimental T-cell effects in experimental cerebral ischemia are neither related to adaptive immunity nor thrombus formation. *Blood*, 115(18), 3835–3842.

Kofoed, E. M. and Vance, R. E. (2011). Innate immune recognition of bacterial ligands by NAIPs determines inflammasome specificity. *Nature*, 477(7366), 592–597.

Koizumi J, Yoshida Y, Nakazawa T, O. G. (1986). Experimental studies of ischemic brain edema. I. A new experimental model of cerebral embolism in rats in which. *Jpn J Stroke*, 8(8), 1–8.

Kominato, Y., Galson, D., Waterman, W. R., Webb, A. C. and Auron, P. E. (1995). Monocyte expression of the human prointerleukin 1 beta gene (IL1B) is dependent on promoter sequences which bind the hematopoietic transcription factor Spi-1/PU.1. *Molecular and Cellular Biology*, 15(1), 59–68.

Kong, J., Grando, S. A. and Li, Y. C. (2006). Regulation of IL-1 Family Cytokines IL-1α, IL-1 Receptor Antagonist, and IL-18 by 1,25-Dihydroxyvitamin D 3 in Primary Keratinocytes . *The Journal of Immunology*, 176(6), 3780–3787.

Kono, H. and Rock, K. L. (2008). How dying cells alert the immune system to danger. *Nature Reviews Immunology* 279–289.

Kostura, M. J., Tocci, M. J., Limjuco, G., Chin, J., Cameron, P., Hillman, A. G., Chartrain, N. A. and Schmidt, J. A.

(1989). Identification of a monocyte specific pre-interleukin 1β convertase activity. *Proceedings of the National Academy of Sciences of the United States of America*, 86(14), 5227–5231.

Kremer, P. H. C., Jolink, W. M. T., Kappelle, L. J., Algra, A., Klijn, C. J. M., Groups, S., Study, E., Van Der Graaf, Y., Grobbee, D. E., Rutten, G. E. H. M., Visseren, F. L. J., Moll, F. L., Kappelle, L. J., Mali, W. P. T. M., … Koudstaal, P. J. (2015). Risk factors for lobar and non-lobar intracerebral hemorrhage in patients with vascular disease. *PLoS ONE*, 10(11), 1–10.

Kristianto, J., Johnson, M. G., Zastrow, R. K., Radcliff, A. B. and Blank, R. D. (2017). Spontaneous recombinase activity of Cre–ERT2 in vivo. *Transgenic Research*, 26(3), 411–417.

Kurisu, K., Zheng, Z., Kim, J. Y., Shi, J., Kanoke, A., Liu, J., Hsieh, C. L. and Yenari, M. A. (2019). Triggering receptor expressed on myeloid cells-2 expression in the brain is required for maximal phagocytic activity and improved neurological outcomes following experimental stroke. *Journal of Cerebral Blood Flow and Metabolism*, 39(10), 1906–1918.

Labat-gest, V. and Tomasi, S. (2013). Photothrombotic ischemia: a minimally invasive and reproducible photochemical cortical lesion model for mouse stroke studies. *Journal of visualized experiments : JoVE*, (76).

Lamkanfi, M. and Dixit, V. M. (2012). Inflammasomes and Their Roles in Health and Disease. *Annual Review of Cell and Developmental Biology*, 28(1), 137–161.

Lammie, G. A. (2002). Hypertensive cerebral small vessel disease and stroke. *Brain pathology (Zurich, Switzerland)*, 12(3), 358–70.

Lan, X., Han, X., Li, Q., Yang, Q. W. and Wang, J. (2017). Modulators of microglial activation and polarization after intracerebral haemorrhage. *Nature Reviews Neurology* 420–433.

Laridan, E., Denorme, F., Desender, L., François, O., Andersson, T., Deckmyn, H., Vanhoorelbeke, K. and De Meyer, S. F. (2017). Neutrophil extracellular traps in ischemic stroke thrombi. *Annals of Neurology*, 82(2), 223–232.

Law, S. H., Chan, M. L., Marathe, G. K., Parveen, F., Chen, C. H. and Ke, L. Y. (2019). An updated review of lysophosphatidylcholine metabolism in human diseases. *International Journal of Molecular Sciences* 1149.

Law, Z. K., Salman, R. A. S., Bath, P. M., Steiner, T. and Sprigg, N. (2018). Hemostatic Therapies For Acute Spontaneous Intracerebral Hemorrhage. *Stroke*, 49(8), e271–e272.

Leasure, A. C., Qureshi, A. I., Murthy, S. B., Kamel, H., Goldstein, J. N., Woo, D., Ziai, W. C., Hanley, D. F., Al-Shahi Salman, R., Matouk, C. C., Sansing, L. H., Sheth, K. N. and Falcone, G. J. (2019). Association of Intensive Blood Pressure Reduction with Risk of Hematoma Expansion in Patients with Deep Intracerebral Hemorrhage. *JAMA Neurology*, 76(8), 949–955.

Lee, J. M., Zhai, G., Liu, Q., Gonzales, E. R., Yin, K., Yan, P., Hsu, C. Y., Vo, K. D. and Lin, W. (2007). Vascular permeability precedes spontaneous intracerebral hemorrhage in stroke-prone spontaneously hypertensive rats. *Stroke*, 38(12), 3289–3291.

Lee, K. R., Kawai, N., Kim, S., Sagher, O. and Hoff, J. T. (1997). Mechanisms of edema formation after intracerebral hemorrhage: Effects of thrombin on cerebral blood flow, blood-brain barrier permeability, and cell survival in a rat model. *Journal of Neurosurgery*, 86(2), 272–278.

Lei, B., Sheng, H., Wang, H., Lascola, C. D., Warner, D. S., Laskowitz, D. T. and James, M. L. (2014). Intrastriatal injection of autologous blood or clostridial collagenase as murine models of intracerebral hemorrhage. *Journal of Visualized Experiments*, (89).

Lénárt, N., Brough, D. and Dénes, Á. (2016). Inflammasomes link vascular disease with neuroinflammation and brain disorders. *Journal of Cerebral Blood Flow and Metabolism* 1668–1685.

Lévesque, S. A., Paré, A., Mailhot, B., Bellver-Landete, V., Kébir, H., Lécuyer, M. A., Alvarez, J. I., Prat, A., de Rivero Vaccari, J. P., Keane, R. W. and Lacroix, S. (2016). Myeloid cell transmigration across the CNS vasculature triggers IL-1ß-driven neuroinflammation during autoimmune encephalomyelitis in mice. *Journal of Experimental Medicine*, 213(6), 929–949.

Levy, M., Thaiss, C. A., Zeevi, D., Dohnalová, L., Zilberman-Schapira, G., Mahdi, J. A., David, E., Savidor, A., Korem, T., Herzig, Y., Pevsner-Fischer, M., Shapiro, H., Christ, A., Harmelin, A., … Elinav, E. (2015). Microbiota-Modulated Metabolites Shape the Intestinal Microenvironment by Regulating NLRP6 Inflammasome Signaling. *Cell*, 163(6), 1428–1443.

Ley, K., Laudanna, C., Cybulsky, M. I. and Nourshargh, S. (2007). Getting to the site of inflammation: The leukocyte

adhesion cascade updated. *Nature Reviews Immunology*, 7(9), 678–689.

Li, M., Li, Z., Ren, H., Jin, W. N., Wood, K., Liu, Q., Sheth, K. N. and Shi, F. D. (2017). Colony stimulating factor 1 receptor inhibition eliminates microglia and attenuates brain injury after intracerebral hemorrhage. *Journal of Cerebral Blood Flow and Metabolism*, 37(7), 2383–2395.

Li, Q. fen, Decker-Rockefeller, B., Bajaj, A. and Pumiglia, K. (2018). Activation of Ras in the Vascular Endothelium Induces Brain Vascular Malformations and Hemorrhagic Stroke. *Cell Reports*, 24(11), 2869–2882.

Liberale, L., Diaz-Cañestro, C., Bonetti, N. R., Paneni, F., Akhmedov, A., Beer, J. H., Montecucco, F., Lüscher, T. F. and Camici, G. G. (2018). Post-ischaemic administration of the murine Canakinumab-surrogate antibody improves outcome in experimental stroke. *European Heart Journal*, 39(38), 3511–3517.

Libermann, T. A. and Baltimore, D. (1990). Activation of interleukin-6 gene expression through the NF-kappa B transcription factor. *Molecular and Cellular Biology*, 10(5), 2327–2334.

Liesz, A., Middelhoff, M., Zhou, W., Karcher, S., Illanes, S. and Veltkamp, R. (2011). Comparison of humoral neuroinflammation and adhesion molecule expression in two models of experimental intracerebral hemorrhage. *Experimental & Translational Stroke Medicine*, 3(1), 11.

Liesz, A., Suri-Payer, E., Veltkamp, C., Doerr, H., Sommer, C., Rivest, S., Giese, T. and Veltkamp, R. (2009). Regulatory T cells are key cerebroprotective immunomodulators in acute experimental stroke. *Nature Medicine*, 15(2), 192–199.

Liesz, A., Zhou, W., Mracskó, É., Karcher, S., Bauer, H., Schwarting, S., Sun, L., Bruder, D., Stegemann, S., Cerwenka, A., Sommer, C., Dalpke, A. H. and Veltkamp, R. (2011). Inhibition of lymphocyte trafficking shields the brain against deleterious neuroinflammation after stroke. *Brain*, 134(3), 704–720.

Liu, X., Nemeth, D. P., McKim, D. B., Zhu, L., DiSabato, D. J., Berdysz, O., Gorantla, G., Oliver, B., Witcher, K. G., Wang, Y., Negray, C. E., Vegesna, R. S., Sheridan, J. F., Godbout, J. P., … Quan, N. (2019). Cell-Type-Specific Interleukin 1 Receptor 1 Signaling in the Brain Regulates Distinct Neuroimmune Activities. *Immunity*, 50(2), 317–333.e6.

Llovera, G., Roth, S., Plesnila, N., Veltkamp, R. and Liesz, A. (2014). Modeling stroke in mice: Permanent coagulation of the distal middle cerebral artery. *Journal of Visualized Experiments*, (89).

Lo, E. H., Dalkara, T. and Moskowitz, M. A. (2003). Neurological diseases: Mechanisms, challenges and opportunities in stroke. *Nature Reviews Neuroscience*, 4(5), 399–414.

Locatelli, G., Theodorou, D., Kendirli, A., Jordão, M. J. C., Staszewski, O., Phulphagar, K., Cantuti-Castelvetri, L., Dagkalis, A., Bessis, A., Simons, M., Meissner, F., Prinz, M. and Kerschensteiner, M. (2018). Mononuclear phagocytes locally specify and adapt their phenotype in a multiple sclerosis model. *Nature Neuroscience*, 21(9), 1196–1208.

Lord, A. S., Langefeld, C. D., Sekar, P., Moomaw, C. J., Badjatia, N., Vashkevich, A., Rosand, J., Osborne, J., Woo, D. and Elkind, M. S. V. (2014). Infection after intracerebral hemorrhage: Risk factors and association with outcomes in the ethnic/racial variations of intracerebral hemorrhage study. *Stroke*, 45(12), 3535–3542.

Love, B. B. and Bendixen, B. H. (1993). Classification of subtype of acute ischemic stroke definitions for use in a multicenter clinical trial. *Stroke*, 24(1), 35–41.

Lu, A., Tang, Y., Ran, R., Ardizzone, T. L., Wagner, K. R. and Sharp, F. R. (2006). Brain genomics of intracerebral hemorrhage. *Journal of Cerebral Blood Flow and Metabolism*, 26(2), 230–252.

Luheshi, N. M., Kovács, K. J., Lopez-Castejon, G., Brough, D. and Denes, A. (2011). Interleukin-1α expression precedes IL-1β after ischemic brain injury and is localised to areas of focal neuronal loss and penumbral tissues. *Journal of Neuroinflammation*, 8.

Luheshi, N. M., McColl, B. W. and Brough, D. (2009). Nuclear retention of IL-1α by necrotic cells: A mechanism to dampen sterile inflammation. *European Journal of Immunology*, 39(11), 2973–2980.

Lusis, A. J. (2000). Atherosclerosis. *Nature*, 407(6801), 233–241.

Lyeth, B. G., Jenkins, L. W., Hamm, R. J., Dixon, C. E., Phillips, L. L., Clifton, G. L., Young, H. F. and Hayes, R. L. (1990). Prolonged memory impairment in the absence of hippocampal cell death following traumatic brain injury in the rat. *Brain Research*, 526(2), 249–258.

Ma, Q., Chen, S., Hu, Q., Feng, H., Zhang, J. H. and Tang, J. (2014). NLRP3 inflammasome contributes to inflammation after intracerebral hemorrhage. *Annals of Neurology*, 75(2), 209–219.

Ma, Q., Khatibi, N. H., Chen, H., Tang, J. and Zhang, J. H. (2011). History of preclinical models of intracerebral hemorrhage. *In Acta Neurochirurgica, Supplementum*, pp. 3–8.

Macleod, M. R., O'Collins, T., Howells, D. W. and Donnan, G. A. (2004). Pooling of animal experimental data reveals influence of study design and publication bias. *Stroke*, 35(5), 1203–1208.

Majidi, S., Rahim, B., Gilani, S. I., Gilani, W. I., Adil, M. M. and Qureshi, A. I. (2016). CT Evolution of Hematoma and Surrounding Hypodensity in a Cadaveric Model of Intracerebral Hemorrhage. *Journal of Neuroimaging*, 26(3), 346–350.

Mamantopoulos, M., Ronchi, F., Van Hauwermeiren, F., Vieira-Silva, S., Yilmaz, B., Martens, L., Saeys, Y., Drexler, S. K., Yazdi, A. S., Raes, J., Lamkanfi, M., McCoy, K. D. and Wullaert, A. (2017). Nlrp6- and ASC-Dependent Inflammasomes Do Not Shape the Commensal Gut Microbiota Composition. *Immunity*, 47(2), 339–348.e4.

Mangan, M. S. J., Olhava, E. J., Roush, W. R., Seidel, H. M., Glick, G. D. and Latz, E. (2018). Targeting the NLRP3 inflammasome in inflammatory diseases. *Nature Reviews Drug Discovery* 588–606.

Mantovani, A., Dinarello, C. A., Molgora, M. and Garlanda, C. (2019). Interleukin-1 and Related Cytokines in the Regulation of Inflammation and Immunity. *Immunity* 778–795.

Mariathasan, S., Newton, K., Monack, D. M., Vucic, D., French, D. M., Lee, W. P., Roose-Girma, M., Erickson, S. and Dixit, V. M. (2004). Differential activation of the inflammasome by caspase-1 adaptors ASC and Ipaf. *Nature*, 430(6996), 213–218.

Martin, S. J. (2016). Cell death and inflammation: the case for IL-1 family cytokines as the canonical DAMPs of the immune system. *FEBS J.*

Martinod, K. and Wagner, D. D. (2014). Thrombosis: Tangled up in NETs. *Blood*, 123(18), 2768–2776.

Martinon, F., Burns, K. and Tschopp, J. (2002). The Inflammasome: A molecular platform triggering activation of inflammatory caspases and processing of proIL-β. *Molecular Cell*, 10(2), 417–426.

Masada, T., Hua, Y., Xi, G. H., Yang, G. Y., Hoff, J. T. and Keep, R. F. (2001). Attenuation of intracerebral hemorrhage and thrombin-induced brain edema by overexpression of interleukin-1 receptor antagonist. *Journal of Neurosurgery*, 95(4), 680–686.

Masamune, A., Igarashi, Y. and Hakomori, S. I. (1996). Regulatory role of ceramide in interleukin (IL)-1B-induced E-selectin expression in human umbilical vein endothelial cells: Ceramide enhances IL-1B action, but is not sufficient for E-selectin expression. *Journal of Biological Chemistry*, 271(16), 9368–9375.

Mayer, S. A., Brun, N. C., Begtrup, K., Broderick, J., Davis, S., Diringer, M. N., Skolnick, B. E., Steiner, T. and Investigators, F. T. (2008). Efficacy and safety of recombinant activated factor VII for acute intracerebral hemorrhage. *New England Journal of Medicine*, 358(20), 2127–2137.

Mayer, S. A., Brun, N. C., Begtrup, K., Broderick, J., Davis, S., Diringer, M. N., Skolnick, B. E., Steiner, T. and Recombinant Activated Factor, V. A. (2005). Recombinant activated factor VII for acute intracerebral hemorrhage. *New England Journal of Medicine*, 352(8), 777–785.

Maysami, S., Wong, R., Pradillo, J. M., Denes, A., Dhungana, H., Malm, T., Koistinaho, J., Orset, C., Rahman, M., Rubio, M., Schwaninger, M., Vivien, D., Bath, P. M., Rothwell, N. J. and Allan, S. M. (2016). A cross-laboratory preclinical study on the effectiveness of interleukin-1 receptor antagonist in stroke. *Journal of Cerebral Blood Flow & Metabolism*, 36(3), 596–605.

McCabe, C., Arroja, M. M., Reid, E. and Macrae, I. M. (2018). Animal models of ischaemic stroke and characterisation of the ischaemic penumbra. *Neuropharmacology* 169–177.

McCann, S. K., Cramond, F., Macleod, M. R. and Sena, E. S. (2016). Systematic Review and Meta-Analysis of the Efficacy of Interleukin-1 Receptor Antagonist in Animal Models of Stroke: an Update. *Translational Stroke Research*, 7(5), 395–406.

McColl, B. W., Carswell, H. V., McCulloch, J. and Horsburgh, K. (2004). Extension of cerebral hypoperfusion and ischaemic pathology beyond MCA territory after intraluminal filament occlusion in C57Bl/6J mice. *Brain Research*, 997(1), 15–23.

McColl, B. W., Rothwell, N. J. and Allan, S. M. (2007). Systemic inflammatory stimulus potentiates the acute phase and CXC chemokine responses to experimental stroke and exacerbates brain damage via interleukin-1- and neutrophil-dependent mechanisms. *Journal of Neuroscience*, 27(16), 4403–4412.

McMeekin, P., White, P., James, M. A., Price, C. I., Flynn, D. and Ford, G. A. (2017). Estimating the number of UK

stroke patients eligible for endovascular thrombectomy. *European Stroke Journal*, 2(4), 319–326.

Menon, R. S., Burgess, R. E., Wing, J. J., Gibbons, M. C., Shara, N. M., Fernandez, S., Jayam-Trouth, A., German, L., Sobotka, I., Edwards, D. and Kidwell, C. S. (2012). Predictors of highly prevalent brain ischemia in intracerebral hemorrhage. *Annals of Neurology*, 71(2), 199–205.

Mertens, M. and Singh, J. A. (2009). Anakinra for rheumatoid arthritis: A systematic review. *Journal of Rheumatology*, 36(6), 1118–1125.

Mildner, A., Schmidt, H., Nitsche, M., Merkler, D., Hanisch, U. K., Mack, M., Heikenwalder, M., Brück, W., Priller, J. and Prinz, M. (2007). Microglia in the adult brain arise from Ly-6ChiCCR2+ monocytes only under defined host conditions. *Nature Neuroscience*, 10(12), 1544–1553.

Minghetti, L., Walsh, D. T., Levi, G. and Perry, V. H. (1999). In vivo expression of cyclooxygenase-2 in rat brain following intraparenchymal injection of bacterial endotoxin and inflammatory cytokines. *Journal of Neuropathology and Experimental Neurology*, 58(11), 1184–1191.

Minhas, J. S., Panerai, R. B., Ghaly, G., Divall, P. and Robinson, T. G. (2019). Cerebral autoregulation in hemorrhagic stroke: A systematic review and meta-analysis of transcranial Doppler ultrasonography studies. *Journal of Clinical Ultrasound*, 47(1), 14–21.

Mizutani, H., Schechter, N., Lazarus, G., Black, R. A. and Kupper, T. S. (1991). Rapid and Specific Conversion of Precursor Interleukin 1β (IL-1β) to an Active IL-1 Species by Human Mast Cell Chymase. *Journal of Experimental Medicine*, 174(4), 821–825.

Morris, G. P., Wright, A. L., Tan, R. P., Gladbach, A., Ittner, L. M. and Vissel, B. (2016). A comparative study of variables influencing ischemic injury in the longa and koizumi methods of intraluminal filament middle cerebral artery occlusion in mice. *PLoS ONE*, 11(2),.

Moskowitz, M. A., Lo, E. H. and Iadecola, C. (2010). The science of stroke: Mechanisms in search of treatments. *Neuron* 181–198.

Mosley, B., Urdal, D. L. and Prickett, K. S. (1987). The interleukin-1 receptor binds the human interleukin-1α precursor but not the interleukin-1β precursor. *Journal of Biological Chemistry*, 262(7), 2941–2944.

Moxon-Emre, I. and Schlichter, L. C. (2011). Neutrophil Depletion Reduces Blood-Brain Barrier Breakdown, Axon Injury, and Inflammation After Intracerebral Hemorrhage. *Journal of Neuropathology & Experimental Neurology*, 70(3), 218–235.

Mracsko, E., Javidi, E., Na, S.-Y., Kahn, A., Liesz, A. and Veltkamp, R. (2014). Leukocyte Invasion of the Brain After Experimental Intracerebral Hemorrhage in Mice. *Stroke*, 45(7), 2107–2114.

Mracsko, E. and Veltkamp, R. (2014). Neuroinflammation after intracerebral hemorrhage. *Frontiers in cellular neuroscience*, 8(November), 388.

Mrdjen, D., Pavlovic, A., Hartmann, F. J., Schreiner, B., Utz, S. G., Leung, B. P., Lelios, I., Heppner, F. L., Kipnis, J., Merkler, D., Greter, M. and Becher, B. (2018). High-Dimensional Single-Cell Mapping of Central Nervous System Immune Cells Reveals Distinct Myeloid Subsets in Health, Aging, and Disease. *Immunity*, 48(2), 380–395.e6.

Muir, R. (1909). The Doctrine of Inflammation. *Glasgow medical journal*, 72(5), 321–338.

Mulder, I. A., Ogrinc Potočnik, N., Broos, L. A. M., Prop, A., Wermer, M. J. H., Heeren, R. M. A. and van den Maagdenberg, A. M. J. M. (2019). Distinguishing core from penumbra by lipid profiles using Mass Spectrometry Imaging in a transgenic mouse model of ischemic stroke. *Scientific Reports*, 9(1), 1090.

Muñoz-Planillo, R., Kuffa, P., Martínez-Colón, G., Smith, B. L., Rajendiran, T. M. and Núñez, G. (2013). K+ Efflux Is the Common Trigger of NLRP3 Inflammasome Activation by Bacterial Toxins and Particulate Matter. *Immunity*, 38(6), 1142–1153.

Murray, K. N., Girard, S., Holmes, W. M., Parkes, L. M., Williams, S. R., Parry-Jones, A. R. and Allan, S. M. (2014). Systemic inflammation impairs tissue reperfusion through endothelin-dependent mechanisms in cerebral ischemia. *Stroke*, 45(11), 3412–3419.

Murray, K. N., Parry-Jones, A. R. and Allan, S. M. (2015). Interleukin-1 and acute brain injury. *Frontiers in Cellular Neuroscience*, 9, February, 18.

Netea, M. G., Joosten, L. A. B., Latz, E., Mills, K. H. G., Natoli, G., Stunnenberg, H. G., O'Neill, L. A. J. and Xavier, R. J. (2016). Trained immunity: A program of innate immune memory in health and disease. *Science* 427.

Neumann, J., Riek-Burchardt, M., Herz, J., Doeppner, T. R., König, R., Hütten, H., Etemire, E., Männ, L., Klingberg, A., Fischer, T., Görtler, M. W., Heinze, H. J., Reichardt, P., Schraven, B., … Gunzer, M. (2015). Very-late-antigen-4 (VLA-4)-mediated brain invasion by neutrophils leads to interactions with microglia, increased ischemic injury and impaired behavior in experimental stroke. *Acta Neuropathologica*, 129(2), 259–277.

Ng, Y. S., Stein, J., Ning, M. M. and Black-Schaffer, R. M. (2007). Comparison of clinical characteristics and functional outcomes of ischemic stroke in different vascular territories. *Stroke*, 38(8), 2309–2314.

NHS England (2018). *Clinical Commissioning Policy: Mechanical thrombectomy for acute ischaemic stroke (all ages)*. Clinical Commissioning Policy: Mechanical thrombectomy for acute ischaemic stroke (all ages). [Online] [Accessed on 6th August 2019] https://www.england.nhs.uk/wp-content/uploads/2019/05/Mechanical-thrombectomy-for-acute-ischaemic-stroke-ERRATA-29-05-19.pdf.

Nimmerjahn, A., Kirchhoff, F. and Helmchen, F. (2005). Neuroscience: Resting microglial cells are highly dynamic surveillants of brain parenchyma in vivo. *Science*, 308(5726), 1314–1318.

O'Collins, V. E., Macleod, M. R., Donnan, G. A., Horky, L. L., Van Der Worp, B. H. and Howells, D. W. (2006). 1,026 Experimental treatments in acute stroke. *Annals of Neurology*, 59(3), 467–477.

O'Donnell, M. J., Chin, S. L., Rangarajan, S., Xavier, D., Liu, L., Zhang, H., Rao-Melacini, P., Zhang, X., Pais, P., Agapay, S., Lopez-Jaramillo, P., Damasceno, A., Langhorne, P., McQueen, M. J., … Yusuf, S. (2016). Global and regional effects of potentially modifiable risk factors associated with acute stroke in 32 countries (INTERSTROKE): a case-control study. *The Lancet*, 388(10046), 761–775.

Olldashi, F., Muzha, I., Filipi, N., Lede, R., Copertari, P., Traverso, C., Copertari, A., Vergara, E. A., Montenegro, C., De Huidobro, R. R., Surt, K., Cialzeta, J., Lazzeri, S., Piñero, G., … Muñoz-Sánchez, A. (2004). Effect of intravenous corticosteroids on death within 14 days in 10008 adults with clinically significant head injury (MRC CRASH trial): Randomised placebo-controlled trial. *The Lancet*, 364(9442), 1321–1328.

Ornello, R., Degan, D., Tiseo, C., Di Carmine, C., Perciballi, L., Pistoia, F., Carolei, A. and Sacco, S. (2018). Distribution and temporal trends from 1993 to 2015 of ischemic stroke subtypes a systematic review and meta-analysis. *Stroke*, 49(4), 814–819.

Orset, C., Macrez, R., Young, A. R., Panthou, D., Angles-Cano, E., Maubert, E., Agin, V. and Vivien, D. (2007). Mouse model of in situ thromboembolic stroke and reperfusion. *Stroke*, 38(10), 2771–2778.

Otxoa-de-Amezaga, A., Miró-Mur, F., Pedragosa, J., Gallizioli, M., Justicia, C., Gaja-Capdevila, N., Ruíz-Jaen, F., Salas-Perdomo, A., Bosch, A., Calvo, M., Márquez-Kisinousky, L., Denes, A., Gunzer, M. and Planas, A. M. (2019). Microglial cell loss after ischemic stroke favors brain neutrophil accumulation. *Acta Neuropathologica*, 137(2), 321–341.

Ovesen, C., Christensen, A. F., Krieger, D. W., Rosenbaum, S., Havsteen, I. and Christensen, H. (2014). Time course of early postadmission hematoma expansion in spontaneous intracerebral hemorrhage. *Stroke*, 45(4), 994–999.

Parfenova, H., Levine, V., Gunther, W. M., Pourcyrous, M. and Leffler, C. W. (2002). COX-1 and COX-2 Contributions to Basal and IL-1β-Stimulated Prostanoid Synthesis in Human Neonatal Cerebral Microvascular Endothelial Cells. *Pediatric Research*, 52(3), 342–348.

Park, Y. H., Wood, G., Kastner, D. L. and Chae, J. J. (2016). Pyrin inflammasome activation and RhoA signaling in the autoinflammatory diseases FMF and HIDS. *Nature Immunology*, 17(8), 914–921.

Parry-Jones, A. R., Liimatainen, T., Kauppinen, R. A., Gröhn, O. H. J. and Rothwell, N. J. (2008). Interleukin-1 exacerbates focal cerebral ischemia and reduces ischemic brain temperature in the rat. *Magnetic Resonance in Medicine*, 59(6), 1239–1249.

Parry-Jones, A. R., Sammut-Powell, C., Paroutoglou, K., Birleson, E., Rowland, J., Lee, S., Cecchini, L., Massyn, M., Emsley, R., Bray, B. and Patel, H. (2019). An Intracerebral Hemorrhage Care Bundle Is Associated with Lower Case Fatality. *Annals of Neurology*, 86(4), 495–503.

Patel, A., Berdunov, V., King, D., Quayyum, Z., Wittenberg, R. and Knapp, M. (2017). Current, future and avoidable costs of stroke in the UK, Executive summary Part 2. *Stroke Association* 12.

Pelegrin, P. and Surprenant, A. (2006). Pannexin-1 mediates large pore formation and interleukin-1β release by the ATP-gated P2X7 receptor. *EMBO Journal*, 25(21), 5071–5082.

Peppiatt, C. M., Howarth, C., Mobbs, P. and Attwell, D. (2006). Bidirectional control of CNS capillary diameter by pericytes. *Nature*, 443(7112), 700–704.

Percie du Sert, N., Alfieri, A., Allan, S. M., Carswell, H. V. O., Deuchar, G. A., Farr, T. D., Flecknell, P., Gallagher, L.,

Gibson, C. L., Haley, M. J., Macleod, M. R., McColl, B. W., McCabe, C., Morancho, A., … Macrae, I. M. (2017). The IMPROVE Guidelines (Ischaemia Models: Procedural Refinements Of in Vivo Experiments). *Journal of Cerebral Blood Flow and Metabolism*, 37(11), 3488–3517.

Perez-de-Puig, I., Miró-Mur, F., Ferrer-Ferrer, M., Gelpi, E., Pedragosa, J., Justicia, C., Urra, X., Chamorro, A. and Planas, A. M. (2015). Neutrophil recruitment to the brain in mouse and human ischemic stroke. *Acta Neuropathologica*, 129(2), 239–257.

Pober, J. S. and Sessa, W. C. (2015). Inflammation and the blood microvascular system. *Cold Spring Harbor Perspectives in Biology*, 7(1),.

Prescott, M. J. and Lidster, K. (2017). Improving quality of science through better animal welfare: The NC3Rs strategy. *Lab Animal* 152–156.

Qian, J., Zhu, L., Li, Q., Belevych, N., Chen, Q., Zhao, F., Herness, S. and Quan, N. (2012). Interleukin-1R3 mediates interleukin-1-induced potassium current increase through fast activation of Akt kinase. *Proceedings of the National Academy of Sciences of the United States of America*, 109(30), 12189–12194.

Qureshi, A. I., Mendelow, a. D. and Hanley, D. F. (2009). Intracerebral haemorrhage. *Lancet*, 373(9675), 1632–1644.

Rabuffetti, M., Sciorati, C., Tarozzo, G., Clementi, E., Manfredi, a a and Beltramo, M. (2000). Inhibition of caspase-1-like activity by Ac-Tyr-Val-Ala-Asp-chloromethyl ketone induces long-lasting neuroprotection in cerebral ischemia through apoptosis reduction and decrease of proinflammatory cytokines. *J Neurosci*, 20(12), 4398–4404.

Rannikmäe, K., Woodfield, R., Anderson, C. S., Charidimou, A., Chiewvit, P., Greenberg, S. M., Jeng, J. S., Meretoja, A., Palm, F., Putaala, J., Rinkel, G. J. E., Rosand, J., Rost, N. S., Strbian, D., … Sudlow, C. L. M. (2016). Reliability of intracerebral hemorrhage classification systems: A systematic review. *International Journal of Stroke* 626–636.

Ransohoff, R. M. (2016). A polarizing question: Do M1 and M2 microglia exist. *Nature Neuroscience* 987–991.

Relton, J. K. and Rothwell, N. J. (1992). Interleukin-1 receptor antagonist inhibits ischaemic and excitotoxic neuronal damage in the rat. *Brain Research Bulletin*, 29(2), 243–246.

Ren, H., Kong, Y., Liu, Z., Zang, D., Yang, X., Wood, K., Li, M. and Liu, Q. (2018). Selective NLRP3 (pyrin domain-containing protein 3) inflammasome inhibitor reduces brain injury after intracerebral hemorrhage. *Stroke*, 49(1), 184–192.

Ren, X., Akiyoshi, K., Dziennis, S., Vandenbark, A. A., Herson, P. S., Hurn, P. D. and Offner, H. (2011). Regulatory B cells limit CNS inflammation and neurologic deficits in murine experimental stroke. *Journal of Neuroscience*, 31(23), 8556–8563.

Reuter, B., Venus, A., Heiler, P., Schad, L., Ebert, A., Hennerici, M. G., Grudzenski, S. and Fatar, M. (2016). Development of cerebral microbleeds in the APP23-transgenic mouse model of cerebral amyloid angiopathy-a 9.4 tesla MRI study. *Frontiers in Aging Neuroscience*, 8(JUN),.

Ridker, P. M., Everett, B. M., Thuren, T., MacFadyen, J. G., Chang, W. H., Ballantyne, C., Fonseca, F., Nicolau, J., Koenig, W., Anker, S. D., Kastelein, J. J. P., Cornel, J. H., Pais, P., Pella, D., … Zineldine, A. (2017). Antiinflammatory therapy with canakinumab for atherosclerotic disease. *New England Journal of Medicine*, 377(12), 1119–1131.

Rivers-Auty, J., Daniels, M. J. D., Colliver, I., Robertson, D. L. and Brough, D. (2018). Redefining the ancestral origins of the interleukin-1 superfamily. *Nature Communications*, 9(1), 1156.

Robbins, G. R., Wen, H. and Ting, J. P. Y. (2014). Inflammasomes and metabolic disorders: Old genes in modern diseases. *Molecular Cell* 297–308.

Robert, R., Chapelain, B. and Neliat, G. (1993). Different effects of interleukin-1 on reactivity of arterial vessels isolated from various vascular beds in the rabbit. *Circulatory Shock*, 40(2), 139–143.

Roman, J., Ritzenthaler, J. D., Fenton, M. J., Roser, S. and Schuyler, W. (2000). Transcriptional regulation of the human interleukin 1β gene by fibronectin: Role of protein kinase C and activator protein 1 (AP-1). *Cytokine*, 12(11), 1581–1596.

Ropper, A. H. and Zervas, N. T. (1982). Cerebral blood flow after experimental basal ganglia hemorrhage. *Annals of Neurology*, 11(3), 266–271.

Rosenberg, G. A., Mun-Bryce, S., Wesley, M. and Komfeld, M. (1990). Collagenase-induced intracerebral hemorrhage in rats. *Stroke*, 21(5), 801–807.

Rosenthal, R. (1979). The file drawer problem and tolerance for null results. *Psychological Bulletin*, 86(3), 638–641.

Rosidi, N. L., Zhou, J., Pattanaik, S., Wang, P., Jin, W., Brophy, M., Olbricht, W. L., Nishimura, N. and Schaffer, C. B. (2011). Cortical microhemorrhages cause local inflammation but do not trigger widespread dendrite degeneration. Block, M. L. (ed.) *PLoS ONE*, 6(10), e26612.

Ross, J., Brough, D., Gibson, R. M., Loddick, S. A. and Rothwell, N. J. (2007). A selective, non-peptide caspase-1 inhibitor, VRT-018858, markedly reduces brain damage induced by transient ischemia in the rat. *Neuropharmacology*, 53(5), 638–642.

Rouhiainen, A., Kuja-Panula, J., Tumova, S. and Rauvala, H. (2013). RAGE-mediated cell signaling. *In Methods in Molecular Biology*, pp. 239–263.

Royal College of Physicians (2013). *Sentinel Stroke National Audit Programme (SSNAP): Clinical audit first pilot public report*. Sentinel Stroke National Audit Programme (SSNAP) Clinical Audit April 2013 - March 2018. [Online] [Accessed on 6th August 2019] https://www.strokeaudit.org/Documents/National/Clinical/Apr2017Mar2018/Apr2017Mar2018-AnnualReport.aspx.

Salminen, A., Huuskonen, J., Ojala, J., Kauppinen, A., Kaarniranta, K. and Suuronen, T. (2008). Activation of innate immunity system during aging: NF-kB signaling is the molecular culprit of inflamm-aging. *Ageing Research Reviews* 83–105.

Samarasekera, N., Fonville, A., Lerpiniere, C., Farrall, A. J., Wardlaw, J. M., White, P. M., Smith, C., Al-Shahi Salman, R., Addison, A., Ahmad, K., Alhadad, S., Andrews, P., Bisset, E., Bodkin, P., … Todd, I. (2015). Influence of intracerebral hemorrhage location on incidence, characteristics, and outcome: Population-based study. *Stroke*, 46(2), 361–368.

Sandstrom, A., Mitchell, P. S., Goers, L., Mu, E. W., Lesser, C. F. and Vance, R. E. (2019). Functional degradation: A mechanism of NLRP1 inflammasome activation by diverse pathogen enzymes. *Science*, 364(6435),.

Sansing, L. H., Harris, T. H., Kasner, S. E., Hunter, C. A. and Kariko, K. (2011). Neutrophil depletion diminishes monocyte infiltration and improves functional outcome after experimental intracerebral hemorrhage. *Acta Neurochirurgica, Supplementum*, 111(111), 173–178.

Sansing, L. H., Kasner, S. E., McCullough, L., Agarwal, P., Welsh, F. A. and Kariko, K. (2011). Autologous Blood Injection to Model Spontaneous Intracerebral Hemorrhage in Mice. *Journal of Visualized Experiments*, (54).

Savage, C. D., Lopez-Castejon, G., Denes, A. and Brough, D. (2012). NLRP3-inflammasome activating DAMPs stimulate an inflammatory response in glia in the absence of priming which contributes to brain inflammation after injury. *Frontiers in Immunology*, 18(3), 288.

Sborgi, L., Rühl, S., Mulvihill, E., Pipercevic, J., Heilig, R., Stahlberg, H., Farady, C. J., Müller, D. J., Broz, P. and Hiller, S. (2016). GSDMD membrane pore formation constitutes the mechanism of pyroptotic cell death . *The EMBO Journal*, 35(16), 1766–1778.

Schafer, D. P., Lehrman, E. K., Kautzman, A. G., Koyama, R., Mardinly, A. R., Yamasaki, R., Ransohoff, R. M., Greenberg, M. E., Barres, B. A. and Stevens, B. (2012). Microglia Sculpt Postnatal Neural Circuits in an Activity and Complement-Dependent Manner. *Neuron*, 74(4), 691–705.

Schielke, G. P., Yang, G. Y., Shivers, B. D. and Betz, A. L. (1998). Reduced ischemic brain injury in interleukin-1 beta converting enzyme-deficient mice. *Journal of cerebral blood flow and metabolism*, 18(2), 180–5.

Schilling, M., Besselmann, M., Leonhard, C., Mueller, M., Ringelstein, E. B. and Kiefer, R. (2003). Microglial activation precedes and predominates over macrophage infiltration in transient focal cerebral ischemia: a study in green fluorescent protein transgenic bone marrow chimeric mice. *Experimental Neurology*, 183(1), 25–33.

Schmidt, A., Strecker, J. K., Hucke, S., Bruckmann, N. M., Herold, M., MacK, M., Diederich, K., Schäbitz, W. R., Wiendl, H., Klotz, L. and Minnerup, J. (2017). Targeting Different Monocyte/Macrophage Subsets Has No Impact on Outcome in Experimental Stroke. *Stroke*, 48(4), 1061–1069.

Schneider, H., Pitossi, F., Balschun, D., Wagner, A., Del Rey, A. and Besedovsky, H. O. (1998). A neuromodulatory role of interleukin-1β in the hippocampus. *Proceedings of the National Academy of Sciences of the United States of America*, 95(13), 7778–7783.

Schroder, K. and Tschopp, J. (2010). The Inflammasomes. *Cell*, 140(6), 821–832.

Sena, E. S., Bart van der Worp, H., Bath, P. M. W., Howells, D. W. and Macleod, M. R. (2010). Publication bias in reports of animal stroke studies leads to major overstatement of efficacy. Roberts, I. (ed.) *PLoS Biology*, 8(3), e1000344.

Shanta, S. R., Choi, C. S., Lee, J. H., Shin, C. Y., Kim, Y. J., Kim, K. H. and Kim, K. P. (2012). Global changes in

phospholipids identified by MALDI MS in rats with focal cerebral ischemia. *Journal of Lipid Research*, 53(9), 1823–1831.

Shi, J., Zhao, Y., Wang, K., Shi, X., Wang, Y., Huang, H., Zhuang, Y., Cai, T., Wang, F. and Shao, F. (2015). Cleavage of GSDMD by inflammatory caspases determines pyroptotic cell death. *Nature*, 526(7575), 660–665.

Shi, J., Zhao, Y., Wang, Y., Gao, W., Ding, J., Li, P., Hu, L. and Shao, F. (2014). Inflammatory caspases are innate immune receptors for intracellular LPS. *Nature*, 514(7521), 187–192.

Shichita, T., Sugiyama, Y., Ooboshi, H., Sugimori, H., Nakagawa, R., Takada, I., Iwaki, T., Okada, Y., Iida, M., Cua, D. J., Iwakura, Y. and Yoshimura, A. (2009). Pivotal role of cerebral interleukin-17-producing T cells in the delayed phase of ischemic brain injury. *Nature Medicine*, 15(8), 946–950.

Shirakawa, F., Saito, K., Bonagura, C. A., Galson, D. L., Fenton, M. J., Webb, A. C. and Auron, P. E. (1993). The human prointerleukin 1 beta gene requires DNA sequences both proximal and distal to the transcription start site for tissue-specific induction. *Molecular and Cellular Biology*, 13(3), 1332–1344.

Sinar, E. J., Mendelow, A. D., Graham, D. I. and Teasdale, G. M. (1987). Experimental intracerebral hemorrhage: Effects of a temporary mass lesion. *Journal of Neurosurgery*, 66(4), 568–576.

Smith, A. and McCulloh, R. J. (2015). Hemopexin and haptoglobin: Allies against heme toxicity from hemoglobin not contenders. *Frontiers in Physiology*, 30(6), 187.

Smith, C. J., Hulme, S., Vail, A., Heal, C., Parry-Jones, A. R., Scarth, S., Hopkins, K., Hoadley, M., Allan, S. M., Rothwell, N. J., Hopkins, S. J. and Tyrrell, P. J. (2018). SCIL-STROKE (subcutaneous interleukin-1 receptor antagonist in ischemic stroke): A randomized controlled phase 2 trial. *Stroke*, 49(5), 1210–1216.

Smith, D. E., Lipsky, B. P., Russell, C., Ketchem, R. R., Kirchner, J., Hensley, K., Huang, Y., Friedman, W. J., Boissonneault, V., Plante, M. M., Rivest, S. and Sims, J. E. (2009). A Central Nervous System-Restricted Isoform of the Interleukin-1 Receptor Accessory Protein Modulates Neuronal Responses to Interleukin-1. *Immunity*, 30(6), 817–831.

Sobowale, O. A. (2018). *Intracerebral Haemorrhage and Inflammation*.

Sobowale, O. A., Parry-Jones, A. R., Smith, C. J., Tyrrell, P. J., Rothwell, N. J. and Allan, S. M. (2016). Interleukin-1 in Stroke: From Bench to Bedside. *Stroke*, 47(8), 2160–2167.

Sommer, C. J. (2017). Ischemic stroke: experimental models and reality. *Acta Neuropathologica* 245–261.

Spangenberg, E., Severson, P. L., Hohsfield, L. A., Crapser, J., Zhang, J., Burton, E. A., Zhang, Y., Spevak, W., Lin, J., Phan, N. Y., Habets, G., Rymar, A., Tsang, G., Walters, J., … Green, K. N. (2019). Sustained microglial depletion with CSF1R inhibitor impairs parenchymal plaque development in an Alzheimer's disease model. *Nature Communications*, 10(1), 3758.

Sporns, P. B., Hanning, U., Schwindt, W., Velasco, A., Minnerup, J., Zoubi, T., Heindel, W., Jeibmann, A. and Niederstadt, T. U. (2017). Ischemic Stroke: What Does the Histological Composition Tell Us about the Origin of the Thrombus? *Stroke*, 48(8), 2206–2210.

Sterling, T. D. (1959). Publication Decisions and their Possible Effects on Inferences Drawn from Tests of Significance—or Vice Versa. *Journal of the American Statistical Association*, 54(285), 30–34.

Stewart, C. R., Stuart, L. M., Wilkinson, K., van Gils, J. M., Deng, J., Halle, A., Rayner, K. J., Boyer, L., Zhong, R., Frazier, W. A., Lacy-Hulbert, A., El Khoury, J., Golenbock, D. T. and Moore, K. J. (2010). CD36 ligands promote sterile inflammation through assembly of a Toll-like receptor 4 and 6 heterodimer. *Nature Immunology*, 11(2), 155-U75.

Stroemer, R. P. and Rothwell, N. J. (1998). Exacerbation of Ischemic Brain Damage by Localized Striatal Injection of Interleukin-1β in the Rat. *Journal of Cerebral Blood Flow & Metabolism*, 18(8), 833–839.

Stroke Therapy Academic Industry Roundtable (STAIR) (1999). Recommendations for standards regarding preclinical neuroprotective and restorative drug development. *Stroke*, 30(12), 2752–8.

Sutherland, G. R. and Auer, R. N. (2006). Primary intracerebral hemorrhage. *Journal of Clinical Neuroscience*, 13(5), 511–517.

Swanson, K. V., Deng, M. and Ting, J. P. Y. (2019). The NLRP3 inflammasome: molecular activation and regulation to therapeutics. *Nature Reviews Immunology* 477–489.

Szalay, G., Martinecz, B., Lénárt, N., Környei, Z., Orsolits, B., Judák, L., Császár, E., Fekete, R., West, B. L., Katona, G., Rózsa, B. and Dénes, Á. (2016). Microglia protect against brain injury and their selective elimination dysregulates

neuronal network activity after stroke. *Nature Communications*, 7, May, 11499.

Tannahill, G. M., Curtis, A. M., Adamik, J., Palsson-Mcdermott, E. M., McGettrick, A. F., Goel, G., Frezza, C., Bernard, N. J., Kelly, B., Foley, N. H., Zheng, L., Gardet, A., Tong, Z., Jany, S. S., … O'Neill, L. A. J. (2013). Succinate is an inflammatory signal that induces IL-1β through HIF-1α. *Nature*, 496(7444), 238–242.

Tapia, V. S., Daniels, M. J. D., Palazón-Riquelme, P., Dewhurst, M., Luheshi, N. M., Rivers-Auty, J., Green, J., Redondo-Castro, E., Kaldis, P., Lopez-Castejon, G. and Brough, D. (2019). The three cytokines IL-1β, IL-18, and IL-1α share related but distinct secretory routes. *Journal of Biological Chemistry*, 294(21), 8325–8335.

Taylor, R. A., Chang, C. F., Goods, B. A., Hammond, M. D., Grory, B. Mac, Ai, Y., Steinschneider, A. F., Renfroe, S. C., Askenase, M. H., Mccullough, L. D., Kasner, S. E., Mullen, M. T., Hafler, D. A., Love, J. C. and Sansing, L. H. (2017). TGF-β1 modulates microglial phenotype and promotes recovery after intracerebral hemorrhage. *Journal of Clinical Investigation*, 127(1), 280–292.

Thornberry, N. A., Bull, H. G., Calaycay, J. R., Chapman, K. T., Howard, A. D., Kostura, M. J., Miller, D. K., Molineaux, S. M., Weidner, J. R., Aunins, J., Elliston, K. O., Ayala, J. M., Casano, F. J., Chin, J., … Tocci, M. J. (1992). A novel heterodimeric cysteine protease is required for interleukin-1βprocessing in monocytes. *Nature*, 356(6372), 768–774.

Touzani, O., Boutin, H., Lefeuvre, R., Parker, L., Miller, A., Luheshi, G. and Rothwell, N. (2002). Interleukin-1 influences ischemic brain damage in the mouse independently of the interleukin-1 type I receptor. *Journal of Neuroscience*, 22(1), 38–43.

Tsuchiya, K., Nakajima, S., Hosojima, S., Thi Nguyen, D., Hattori, T., Manh Le, T., Hori, O., Mahib, M. R., Yamaguchi, Y., Miura, M., Kinoshita, T., Kushiyama, H., Sakurai, M., Shiroishi, T. and Suda, T. (2019). Caspase-1 initiates apoptosis in the absence of gasdermin D. *Nature Communications*, 10(1), 2091.

Tsukada, J., Saito, K., Waterman, W. R., Webb, A. C. and Auron, P. E. (1994). Transcription factors NF-IL6 and CREB recognize a common essential site in the human prointerleukin 1 beta gene. *Molecular and Cellular Biology*, 14(11), 7285–7297.

Uderhardt, S., Martins, A. J., Tsang, J. S., Lämmermann, T. and Germain, R. N. (2019). Resident Macrophages Cloak Tissue Microlesions to Prevent Neutrophil-Driven Inflammatory Damage. *Cell*, 177(3), 541–555.e17.

Urday, S., Kimberly, W. T., Beslow, L. A., Vortmeyer, A. O., Selim, M. H., Rosand, J., Simard, J. M. and Sheth, K. N. (2015). Targeting secondary injury in intracerebral haemorrhage--perihaematomal oedema. *Nature reviews. Neurology*, 11(2), 111–22.

Vanlandewijck, M., He, L., Mäe, M. A., Andrae, J., Ando, K., Del Gaudio, F., Nahar, K., Lebouvier, T., Laviña, B., Gouveia, L., Sun, Y., Raschperger, E., Räsänen, M., Zarb, Y., … Betsholtz, C. (2018). A molecular atlas of cell types and zonation in the brain vasculature. *Nature*, 554(7693), 475–480.

de Vasconcelos, N. M., Van Opdenbosch, N., Van Gorp, H., Parthoens, E. and Lamkanfi, M. (2019). Single-cell analysis of pyroptosis dynamics reveals conserved GSDMD-mediated subcellular events that precede plasma membrane rupture. *Cell Death and Differentiation*, 26(1), 146–161.

Wagner, K. R., Beiler, S., Beiler, C., Kirkman, J., Casey, K., Robinson, T., Larnard, D., De Courten-Myers, G. M., Linke, M. J. and Zuccarello, M. (2006). Delayed profound local brain hypothermia markedly reduces interleukin-1β gene expression and vasogenic edema development in a porcine model of intracerebral hemorrhage. *Acta Neurochirurgica, Supplementum*.

Wakisaka, Y., Chu, Y., Miller, J. D., Rosenberg, G. A. and Heistad, D. D. (2010). Spontaneous intracerebral hemorrhage during acute and chronic hypertension in mice. *Journal of Cerebral Blood Flow and Metabolism*, 30(1), 56–69.

Wang, J. and Tsirka, S. E. (2005). Neuroprotection by inhibition of matrix metalloproteinases in a mouse model of intracerebral haemorrhage. *Brain*, 128(7), 1622–1633.

Wang, Y., Cella, M., Mallinson, K., Ulrich, J. D., Young, K. L., Robinette, M. L., Gilfillan, S., Krishnan, G. M., Sudhakar, S., Zinselmeyer, B. H., Holtzman, D. M., Cirrito, J. R. and Colonna, M. (2015). TREM2 lipid sensing sustains the microglial response in an Alzheimer's disease model. *Cell*, 160(6), 1061–1071.

Wang, Y., Gao, W., Shi, X., Ding, J., Liu, W., He, H., Wang, K. and Shao, F. (2017). Chemotherapy drugs induce pyroptosis through caspase-3 cleavage of a gasdermin. *Nature*, 547(7661), 99–103.

Wardlaw, J. M., Smith, C. and Dichgans, M. (2019). Small vessel disease: mechanisms and clinical implications. *The Lancet Neurology* 684–696.

Wasserman, J. K., Zhu, X. and Schlichter, L. C. (2007). Evolution of the inflammatory response in the brain following intracerebral hemorrhage and effects of delayed minocycline treatment. *Brain Research*, 1180, November, 140–154.

Weber, A., Wasiliew, P. and Kracht, M. (2010). Interleukin-1 (IL-1) pathway. *Science Signaling* cm1.

Weng, Y. C., Sonni, A., Labelle-Dumais, C., De Leau, M., Kauffman, W. B., Jeanne, M., Biffi, A., Greenberg, S. M., Rosand, J. and Gould, D. B. (2012). COL4A1 mutations in patients with sporadic late-onset intracerebral hemorrhage. *Annals of Neurology*, 71(4), 470–477.

Werman, A., Werman-Venkert, R., White, R., Lee, J. K., Werman, B., Krelin, Y., Voronov, E., Dinarello, C. A. and Apte, R. N. (2004). The precursor form of IL-1α is an intracrine proinflammatory activator of transcription. *Proceedings of the National Academy of Sciences of the United States of America*, 101(8), 2434–2439.

Wheeler, R. D., Boutin, H., Touzani, O., Luheshi, G. N., Takeda, K. and Rothwell, N. J. (2003). No role for interleukin-18 in acute murine stroke-induced brain injury. *Journal of Cerebral Blood Flow and Metabolism*, 23(5), 531–535.

Wilson, H. L., Varcoe, R. W., Stokes, L., Holland, K. L., Francis, S. E., Dower, S. K., Surprenant, A. and Crossman, D. C. (2007). P2X receptor characterization and IL-1/IL-1Ra release from human endothelial cells. *British Journal of Pharmacology*, 151(1), 96–108.

Wilson, K. P., Black, J. A. F., Thomson, J. A., Kim, E. E., Griffith, J. P., Navia, M. A., Murcko, M. A., Chambers, S. P., Aldape, R. A., Raybuck, S. A. and Livingston, D. J. (1994). Structure and mechanism of interleukin-lβ converting enzyme. *Nature*, 370(6487), 270–275.

Winkler, D. T., Bondolfi, L., Herzig, M. C., Jann, L., Calhoun, M. E., Wiederhold, K. H., Tolnay, M., Staufenbiel, M. and Jucker, M. (2001). Spontaneous hemorrhagic stroke in a mouse model of cerebral amyloid angiopathy. *Journal of Neuroscience*, 21(5), 1619–1627.

Wolburg, H., Wolburg-Buchholz, K. and Engelhardt, B. (2005). Diapedesis of mononuclear cells across cerebral venules during experimental autoimmune encephalomyelitis leaves tight junctions intact. *Acta Neuropathologica*, 109(2), 181–190.

Wolf, A. J., Reyes, C. N., Liang, W., Becker, C., Shimada, K., Wheeler, M. L., Cho, H. C., Popescu, N. I., Coggeshall, K. M., Arditi, M. and Underhill, D. M. (2016). Hexokinase Is an Innate Immune Receptor for the Detection of Bacterial Peptidoglycan. *Cell*, 166(3), 624–636.

Wong, R., Lénárt, N., Hill, L., Toms, L., Coutts, G., Martinecz, B., Császár, E., Nyiri, G., Papaemmanouil, A., Waisman, A., Müller, W., Schwaninger, M., Rothwell, N., Francis, S., … Allan, S. M. (2019). Interleukin-1 mediates ischaemic brain injury via distinct actions on endothelial cells and cholinergic neurons. *Brain, Behavior, and Immunity*, 76, February, 126–138.

Worcester, R. (1995). New Perspectives on Britain. *New Political Science*, 17(1–2), 309–311.

Wu, B., Ma, Q., Khatibi, N., Chen, W., Sozen, T., Cheng, O. and Tang, J. (2010). Ac-YVAD-CMK Decreases Blood-Brain Barrier Degradation by Inhibiting Caspase-1 Activation of Interleukin-1β in Intracerebral Hemorrhage Mouse Model. *Translational Stroke Research*, 1(1), 57–64.

Xi, G. H., Keep, R. F. and Hoff, J. T. (1998). Erythrocytes and delayed brain edema formation following intracerebral hemorrhage in rats. *Journal of Neurosurgery*, 89(6), 991–996.

Xi, G. H., Reiser, G. and Keep, R. F. (2003). The role of thrombin and thrombin receptors in ischemic, hemorrhagic and traumatic brain injury: deleterious or protective? *Journal of Neurochemistry*, 84(1), 3–9.

Xue, M. and Del Bigio, M. R. (2000). Intracerebral injection of autologous whole blood in rats: Time course of inflammation and cell death. *Neuroscience Letters*, 283(3), 230–232.

Xue, M. and Del Bigio, M. R. (2003). Comparison of brain cell death and inflammatory reaction in three models of intracerebral hemorrhage in adult rats. *Journal of Stroke and Cerebrovascular Diseases*, 12(3), 152–159.

Yamada, M. (2015). Cerebral Amyloid Angiopathy: Emerging Concepts. *Journal of Stroke*, 17(1), 17–30.

Yamaguchi, H., Yamazaki, T., Lemere, C. A., Frosch, M. P. and Selkoe, D. J. (1992). Beta amyloid is focally deposited within the outer basement membrane in the amyloid angiopathy of Alzheimer's disease: An immunoelectron microscopic study. *American Journal of Pathology*, 141(1), 249–259.

Yamasaki, Y., Matsuura, N., Shozuhara, H., Onodera, H., Itoyama, Y. and Kogure, K. (1995). Interleukin-1 as a pathogenetic mediator of ischemic brain damage in rats. *Stroke*, 26(4), 676–680.

Yang-Wei Fann, D., Lee, S.-Y., Manzanero, S., Tang, S.-C., Gelderblom, M., Chunduri, P., Bernreuther, C., Glatzel, M., Cheng, Y.-L., Thundyil, J., Widiapradja, A., Lok, K.-Z., Foo, S. L., Wang, Y.-C., … Arumugam, T. V (2013). Intravenous immunoglobulin suppresses NLRP1 and NLRP3 inflammasome-mediated neuronal death in ischemic stroke. *Cell Death and Disease*, 4(9), e790.

Yang, F., Wang, Z. Y., Wei, X. B., Han, H. R., Meng, X. F., Zhang, Y., Shi, W. C., Li, F. L., Xin, T., Pang, Q. and Yi, F. (2014). NLRP3 deficiency ameliorates neurovascular damage in experimental ischemic stroke. *Journal of Cerebral Blood Flow and Metabolism*, 34(4), 660–667.

Yang, H., Ko, H. J., Yang, J. Y., Kim, J. J., Seo, S. U., Park, S. G., Choi, S. S., Seong, J. K. and Kweon, M. N. (2013). Interleukin-1 promotes coagulation, which is necessary for protective immunity in the lung against streptococcus pneumoniae infection. *Journal of Infectious Diseases*, 207(1), 50–60.

Yilmaz, G., Arumugam, T. V., Stokes, K. Y. and Granger, D. N. (2006). Role of T lymphocytes and interferon-γ in ischemic stroke. *Circulation*, 113(17), 2105–2112.

Yong, V. W., Power, C. and Edwards, D. R. (2001). Metalloproteinases in biology and pathology of the nervous system. *Nature Reviews Neuroscience*, 2(7), 502–511.

Yoshizumi, M., Kurihara, H., Morita, T., Yamashita, T., Oh-hashi, Y., Sugiyama, T., Takaku, F., Yanagisawa, M., Masaki, T. and Yazaki, Y. (1990). Interleukin 1 increases the production of endothelin-1 by cultured endothelial cells. *Biochemical and Biophysical Research Communications*, 166(1), 324–329.

Zazulia, A. R., Diringer, M. N., Videen, T. O., Adams, R. E., Yundt, K., Aiyagari, V., Grubb, R. L. and Powers, W. J. (2001). Hypoperfusion without ischemia surrounding acute intracerebral hemorrhage. *Journal of Cerebral Blood Flow and Metabolism*, 21(7), 804–810.

Zhang, W. H., Wang, X., Narayanan, M., Zhang, Y., Huo, C., Reed, J. C. and Friedlander, R. M. (2003). Fundamental role of the Rip2/caspase-1 pathway in hypoxia and ischemia-induced neuronal cell death. *Proceedings of the National Academy of Sciences of the United States of America*, 100(26), 16012–16017.

Zhang, X., Liu, W., Yuan, J., Zhu, H., Yang, Y., Wen, Z., Chen, Y., Li, L., Lin, J. and Feng, H. (2017). T lymphocytes infiltration promotes blood-brain barrier injury after experimental intracerebral hemorrhage. *Brain Research*, 1670 96–105.

Zhang, Y., Chen, K., Sloan, S. A., Bennett, M. L., Scholze, A. R., O'Keeffe, S., Phatnani, H. P., Guarnieri, P., Caneda, C., Ruderisch, N., Deng, S., Liddelow, S. A., Zhang, C., Daneman, R., … Wu, J. Q. (2014). An RNA-sequencing transcriptome and splicing database of glia, neurons, and vascular cells of the cerebral cortex. *Journal of Neuroscience*, 34(36), 11929–11947.

Zhang, Y., Sloan, S. A., Clarke, L. E., Caneda, C., Plaza, C. A., Blumenthal, P. D., Vogel, H., Steinberg, G. K., Edwards, M. S. B., Li, G., Duncan, J. A., Cheshier, S. H., Shuer, L. M., Chang, E. F., … Barres, B. A. (2016). Purification and Characterization of Progenitor and Mature Human Astrocytes Reveals Transcriptional and Functional Differences with Mouse. *Neuron*, 89(1), 37–53.

Zhao, X. R., Song, S., Sun, G. H., Strong, R., Zhang, J., Grotta, J. C. and Aronowski, J. (2009). Neuroprotective Role of Haptoglobin after Intracerebral Hemorrhage. *Journal of Neuroscience*, 29(50), 15819–15827.

Zhao, X., Ting, S. M., Liu, C. H., Sun, G., Kruzel, M., Roy-O'Reilly, M. and Aronowski, J. (2017). Neutrophil polarization by IL-27 as a therapeutic target for intracerebral hemorrhage. *Nature Communications*, 8(1), 602.

Zhong, Z., Liang, S., Sanchez-Lopez, E., He, F., Shalapour, S., Lin, X. jia, Wong, J., Ding, S., Seki, E., Schnabl, B., Hevener, A. L., Greenberg, H. B., Kisseleva, T. and Karin, M. (2018). New mitochondrial DNA synthesis enables NLRP3 inflammasome activation. *Nature*, 560(7717), 198–203.

Zhou, K., Zhong, Q., Wang, Y. C., Xiong, X. Y., Meng, Z. Y., Zhao, T., Zhu, W. Y., Liao, M. F., Wu, L. R., Yang, Y. R., Liu, J., Duan, C. M., Li, J., Gong, Q. W., … Yang, Q. W. (2017). Regulatory T cells ameliorate intracerebral hemorrhage-induced inflammatory injury by modulating microglia/macrophage polarization through the IL-10/GSK3β/PTEN axis. *Journal of Cerebral Blood Flow and Metabolism*, 37(3), 967–979.

Zhou, R., Yazdi, A. S., Menu, P. and Tschopp, J. (2011). A role for mitochondria in NLRP3 inflammasome activation. *Nature*, 469(7329), 221–226.

Zhou, Y., Wang, Y., Wang, J., Stetler, R. A., Yang, Q.-W. W., Anne Stetler, R. and Yang, Q.-W. W. (2014). Inflammation in intracerebral hemorrhage: From mechanisms to clinical translation. *Progress in Neurobiology*, 115(183), 25–44.

del Zoppo, G. J., Schmid-Schönbein, G. W., Mori, E., Copeland, B. R. and Chang, C. M. (1991). Polymorphonuclear

leukocytes occlude capillaries following middle cerebral artery occlusion and reperfusion in baboons. *Stroke*, 22(10), 1276–1283.

Zychlinsky, A., Prevost, M. C. and Sansonetti, P. J. (1992). Shigella flexneri induces apoptosis in infected macrophages. *Nature*, 358(6382), 167–169.

Appendix

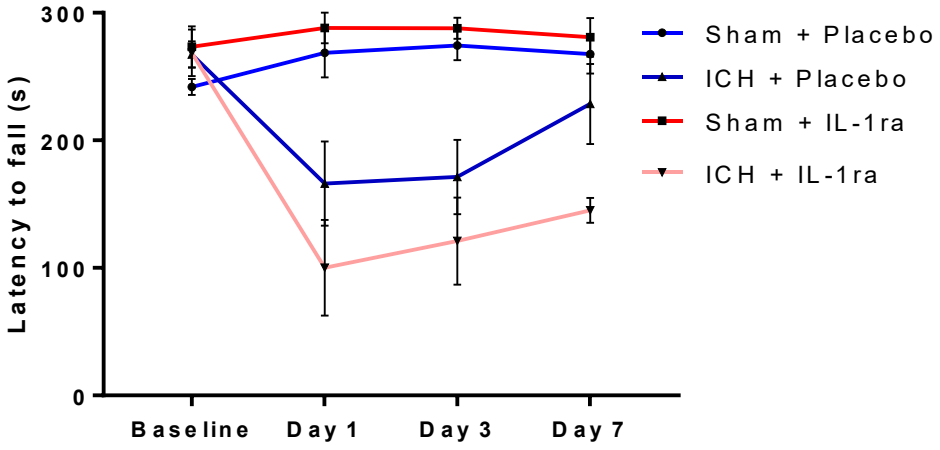

Figure 5.1 Preliminary IL-1RA experiment.
Mice were injected with placebo or 10 µg of IL-1RA intrastriatally and 100 mg kg^{-1} subcutaneously, as detailed in Chapter 3, and rotarod was performed over a 7 day period. $n = 4$ per group.

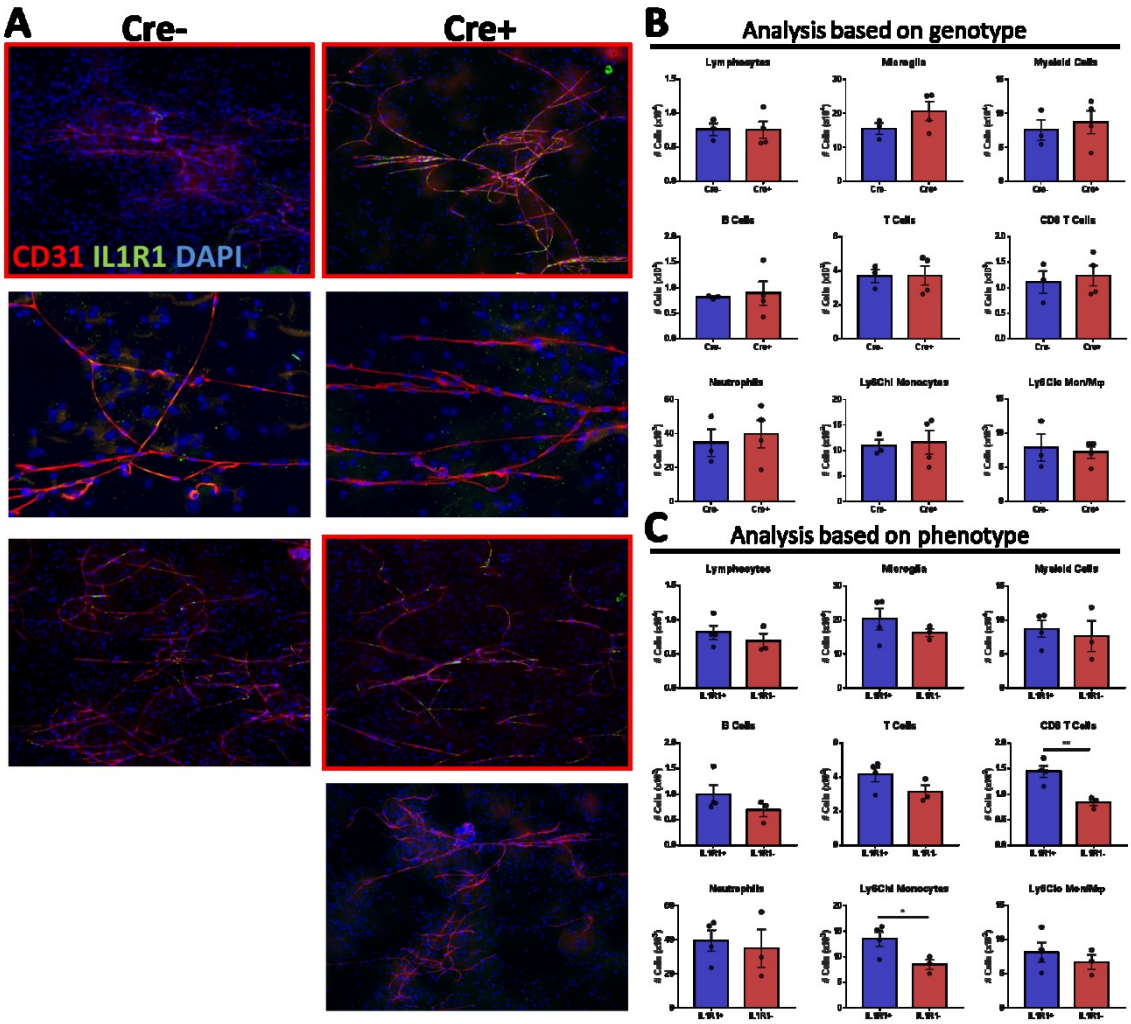

Figure 5.2 Depletion of brain endothelial IL-1R1 may affect the immune response to ICH
IL-1R1 floxed mice expressing tamoxifen-inducible Cre-recombinase under the Slco1c1 promoter or Cre- controls were treated with tamoxifen and subjected to collagenase induced ICH. (A) brain smears were made from contralateral hemispheres and stained for IL-1R1 (green), the endothelial marker CD31 (red) and DAPI (blue). Genotype and phenotype mismatch is highlighted in red. (B) Flow cytometry of single cells isolated from brain homogenates 24 h post ICH found no differences. (C) Flow cytometry analysis based on phenotype found differences in CD8 T cells and Ly6Chi monocytes. Statistical analysis performed using Students 2-sample t-test, * = P<0.05.

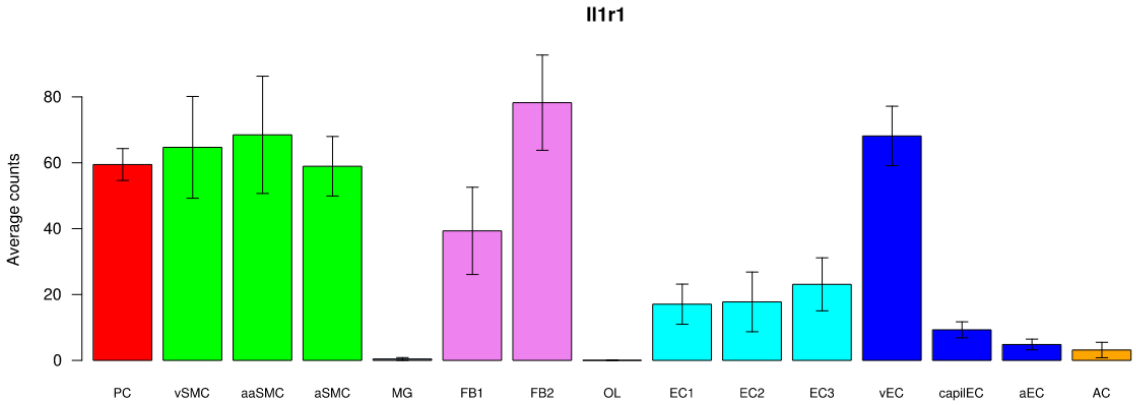

Figure 5.3 Expression of *Il1r1* mRNA on cells of the cerebrovasculature.
Single cell RNA sequencing analysis of *Il1r1*expression by cells of the cerebrovasculature taken from (Vanlandewijck et al., 2018). PC (Pericyte), SMC (Smooth muscle cell), MG (Microglia), FB (Fibroblast), OL (Oligodendrocyte), EC (Endothelial cell), AC (Astrocyte). v = venous, capil = capillary, aa = arteriolar, a = arterial. 1,2,3 = subtypes.

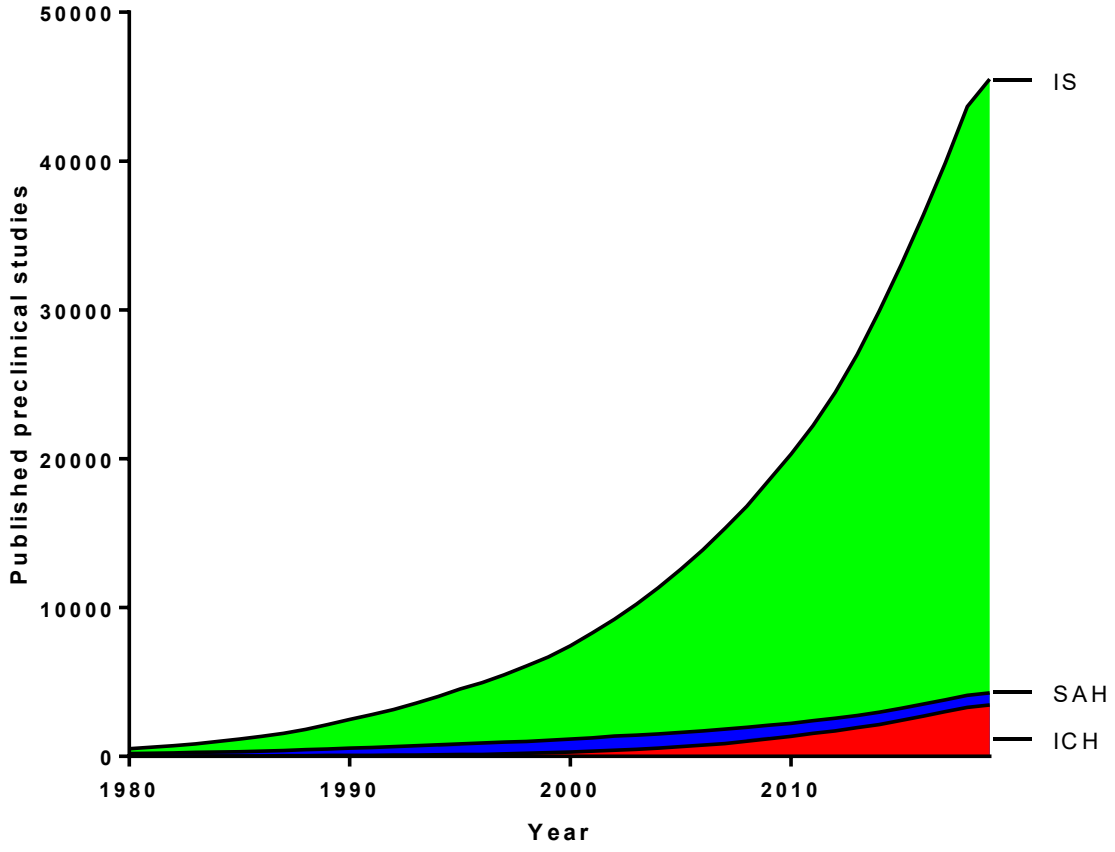

Figure 5.4 Cumulative amount of published preclinical studies into each stroke subtype since 1980.
IS = Ischaemic stroke, SAH = Subarachnoid haemorrhage, ICH = Intracerebral haemorrhage.

Ischaemic stroke search terms

"experimental" or "preclinical" or "model" or "animal" and ("stroke"[All Fields]) NOT ("intracerebral haemorrhage"[All Fields] OR "intracerebral hemorrhage"[All Fields] OR "ICH"[All Fields] OR "subarachnoid haemorrhage"[All Fields] OR "subarachnoid hemorrhage"[All Fields] OR "SAH"[All Fields])

Intracerebral haemorrhage search terms

"experimental" or "preclinical" or "model" or "animal" and ("intracerebral haemorrhage"[All Fields] OR "intracerebral hemorrhage"[All Fields] OR "ICH"[All Fields])

Subarachnoid haemorrhage search terms

"experimental" or "preclinical" or "model" or "animal" and ("subarachnoid haemorrhage"[All Fields] OR "subarachnoid hemorrhage"[All Fields] OR "SAH"[All Fields])